Universidade de Lisboa
Faculdade de Medicina

Do Neurotrophins Play a Role in Adult Neurogenesis?

Rui Galvão

Doutoramento em Ciências Biomédicas

Especialidade · Neurociências Básicas

Lisboa · 2008

Tese orientada pelos Prof. Doutores

Arturo Alvarez-Buylla (UCSF, USA)

e Domingos Henrique (FMUL, Portugal)

As opiniões expressas nesta publicação são da exclusiva responsabilidade do seu autor

The opinions expressed in this publication are the sole responsibility of its author

A impressão desta dissertação foi aprovada pela

Comissão Coordenadora do Conselho Científico da Faculdade de Medicina de Lisboa em reunião de 20 de Maio de 2008.

Acknowledgements

Though the cover of this thesis will only bear my name, there are a number of people whithout whom my work would not have been possible. First and foremost, I want to thank my advisor, Arturo Alvarez-Buylla, for his inexorable creativity, openness, support and guidance. You are truly an example worth following and you have made me a better (aspiring) scientist. I also thank Domingos Henrique, my advisor during my college days, my doctoral days and hopefully for many years to come. I must also thank José Manuel Garcia-Verdugo, a long-time collaborator of the Alvarez-Buylla lab, who made the electron microscopy work in this thesis possible and to whom I owe all I know about electron microscopy. I am especially grateful to Minoree Kohwi for her constant support and advice on all aspects of this study, as well as for our collaborative effort in developing the single cell RT-PCR methods. Your energy is contagious and has kept me going through stressful times. I am also grateful to all other members of the Alvarez-Buylla lab, past and present, from whom I have had the pleasure of learning. Among them, Ricardo Romero has been especially helpful, assisting me with perfusions and histology. Lily Edmondson also provided crucial technical assistance with quantitative RT-PCR experiments. In addition, all members of the Rowitch lab, Kriegstein lab, Reiter lab and Ramalho-Santos lab were great neighbors and provided a truly stimulating environment. I would like to thank Dr. Louis Reichardt, Dr. Moses Chao and Dr. Steven Goldman for helpful discussions and for providing various reagents to this project, including the conditional $TrkB^{lox/lox}$ mice (Louis Reichardt) and antibodies against p75 receptor (Louis Reichardt and Moses Chao). For several years, I was financially supported by the Fundação para a Ciência e Tecnologia. This work was also supported by the NIH grant HD 32116 and by a gift from Frances and John Bowes.

Last but not least, I thank my parents, my sister and my grandparents for always being there for me.

Table of Contents

List of Figures and Tables

Abbreviations

AOB: Accessory Olfactory Bulb
AP: Alkaline Phosphatase
AraC: Cytosine-β-D-Arabinofuranoside
BDNF: Brain-Derived Neurotrophic Factor
BFCN: Basal Forebrain Cholinergic Neuron
β-Gal: β-Galactosidase
BMP: Bone Morphogenetic Protein
BrdU: Bromo-deoxy-Uridine
CalB: Calbindin
CNS: Central Nervous System
CNTF: Ciliary Neurotrophic Factor
CSF: Cerebral Spinal Fluid
DNA: Deoxyribonucleic Acid
Dopa: Dopamine
d.p.c.: days *post coitus*
DRG: Dorsal Root Ganglia
EGF: Epidermal Growth Factor
Epi: Epinephrine
EPL: External Plexiform Layer
EPO: Erythropoietin
FACS: Fluorescence-Activated Cell Sorting
FGF: Fibroblast Growth Factor
GABA: Gamma-Aminobutyric Acid
GAPDH: Glyceraldehyde 3-phosphate dehydrogenase
GCL: Granular Cell Layer
GDP: Guanosine Diphosphate
GFAP: Glial Fibrillary Acidic Protein
GFP: Green Fluorescent Protein
GL: Glomerular Layer
GTP: Guanosine Triphosphate
HSV-TK: Herpes Simplex Virus Thymidine Kinase
HVC: High Vocal Center
KO: Knock-Out
LGE: Lateral Ganglionic Eminence
LTD: Long-Term Depression
LTP: Long-Term Potentiation
MAG: Myelin-Associated Glycoprotein
MCL: Mitral Cell Layer
MGE: Medial Ganglionic Eminence
M/T: Mitral/Tufted cells
NGF: Nerve Growth Factor
NMDA: N-Methyl-D-Aspartic acid
NO: Nitric Oxide
NOS: Nitric Oxide Synthase

NT: Neurotrophin
OB: Olfactory Bulb
OMgP: Oligodendrocyte Myelin Glycoprotein
ORN: Olfactory Receptor Neuron
PCR: Polymerase Chain Reaction
PDGF: Platelet-Derived Growth Factor
pH3: phosphorylated histone H3
PKC: Protein Kinase C
PLC: Phospholipase C
PNS: Peripheral Nervous System
PRL: Prolactin
PSA-NCAM: Polysialic Acid-Neural Cell Adhesion Molecule
pTrkB: phosphorylated TrkB
RMS: Rostral Migratory Stream
RT-PCR: Reverse Transcription-PCR
SC-RT-PCR: Single Cell-RT-PCR
SGZ: Subgranular Zone
Shh: Sonic Hedgehog
Smo: Smoothened
SVZ: Subventricular Zone
TGF: Transforming Growth Factor
TH: Tyrosine Hydroxilase
TK: Thymidine Kinase
TPA: phorbol 12-myristate 13-acetate
TrkB-FL: TrkB-Full Length
TrkB-TR: TrkB-Truncated
TUNEL: Terminal dUTP Nick-End Labeling
WT: Wild Type

Resumo

O processo de neurogénese continua activo ao longo da vida adulta em mamíferos graças a células estaminais em determinadas zonas do cérebro. Esta capacidade representa um importante potencial para terapias regenerativas. Em roedores, a zona subventricular (SVZ) gera milhares de neuroblastos diáriamente, os quais migram para o bolbo olfactivo (OB) e se diferenciam em interneurónios. Descobertas recentes indicam que a neurotrofina Brain-Derived Neurotrophic Factor (BDNF) estimula a neurogénese adulta na SVZ, mas o mecanismo pelo qual actua é desconhecido. Na minha tese, analizei a função de BDNF e do seu receptor TrkB na neurogénese adulta da SVZ. Descobri que a proteína BDNF está presente na SVZ e que TrkB é o receptor de neurotrofinas mais abundante nessa zona do cérebro, mas apenas foi detectada a forma truncada deste receptor (TrkB-TR). TrkB-TR é expresso em células ependimais e astrócitos da SVZ, mas não em neuroblastos. Embora mutantes TrkB exibam proliferação e sobrevivência reduzida na SVZ e tenham menos neurónios novos no OB, células da SVZ knockout para TrkB (TrkB-KO) transplantadas para a SVZ de um cérebro normal (wild type, WT) são capazes de produzir neuroblastos que migram para o OB. Com a excepção de células periglomerulares dopaminérgicas, interneurónios do OB derivados de transplantes de TrkB-KO e WT exibiram propriedades moleculares, morfológicas e de sobrevivência semelhantes. Para estudar o efeito de BDNF na neurogénese da SVZ, infundi esta neurotrofina no ventrículo lateral de ratazanas e ratos adultos. Após 14 dias de infusão, registei uma redução de proliferação na SVZ de ambas as espécies. No entanto, a produção de neurónios foi afectada diferencialmente: infusões de BDNF reduziram o número de novos neurónios no OB de ratazanas mas não tiveram efeito no de ratos. Interessantemente, ratazanas e ratos também diferem na expressão do receptor de neurotrofinas p75. Em ratazanas, detectei p75 em muitas células tipo C (progenitores intermediários da SVZ) e em alguns neuroblastos, enquanto que muito poucas células $p75^{+}$ foram detectadas na SVZ de ratos. Este é o primeiro estudo a encontrar tais efeitos, uma vez que outros laboratórios relataram um aumento de neurogénese após tratamento com BDNF. Globalmente, os meus resultados indicam que TrkB não é essencial para a produção e diferenciação da maioria dos interneurónios derivados da SVZ e não

confirmam a actual visão de que administração de BDNF à SVZ aumenta a neurogénese adulta. Pelo contrário, é possível que TrkB-TR em células ependimais e astrócitos da SVZ sirva para formar uma barreira, protegendo progenitores e neuroblastos da SVZ dos efeitos de uma eventual activação de p75 por BDNF. O meu trabalho deverá promover novos estudos sobre a regulação de neurogénese adulta antes que utilizações terapêuticas sejam possíveis.

Para além dos estudos acima descritos, desenvolvi também técnicas para o estudo de expressão genética da SVZ ao nível unicelular baseadas em transcripção reversa e reacção em cadeia de polimerase (RT-PCR). Relato nesta tese resultados preliminares encorajadores, demonstrando que é possível detectar expressão de múltiplos genes em uma única célula da SVZ. No futuro, este método poderá ser usado para caracterizar a heterogeneidade molecular dentro de cada tipo celular da SVZ (astrócitos tipo B, células tipo C e neuroblastos tipo A). Este tipo de análise deverá revelar mais subclasses dentro das células B, C e A, e ajudar a caracterizar as diferenças entre astrócitos neurogénicos e não-neurogénicos bem como entre células de zonas diferentes da SVZ.

Abstract

Neurogenesis continues throughout adulthood in the vertebrate brain. New neurons originate from endogenous neural stem cells which could have important applications for brain repair. In rodents, the adult subventricular zone (SVZ) generates thousands of neuroblasts daily, which migrate to the olfactory bulb (OB) and differentiate into interneurons. Recent findings indicate that the neurotrophin Brain-Derived Neurotrophic Factor (BDNF) can enhance adult SVZ neurogenesis, but the mechanism by which it acts is unknown. In my thesis, I analyzed the role of BDNF and its receptor TrkB in adult SVZ neurogenesis. I found that BDNF protein is present and that TrkB is the most prominent neurotrophin receptor in the mouse SVZ, though only the truncated, kinase-negative isoform (TrkB-TR) was detected. TrkB-TR is expressed in SVZ astrocytes and ependymal cells, but not in neuroblasts. Though TrkB mutants have reduced SVZ proliferation and survival and fewer new OB neurons, grafting SVZ cells from TrkB knockout mice (TrkB-KO) into the SVZ of wild-type mice (WT) showed that neuroblasts are generated and migrate to the OB in the absence of TrkB. With the exception of dopaminergic periglomerular cells, OB interneurons derived from TrkB-KO and WT grafts displayed similar survival, molecular and morphological properties. To study the effect of BDNF on SVZ neurogenesis, I infused this neurotrophin into the lateral ventricle of adult rats and mice. After 14 days of infusion, SVZ proliferation was reduced in both species. However, the neuronal output of the SVZ was differentially affected: BDNF infusions decreased the number of new neurons in the rat OB but had no effect in the mouse. Interestingly, rats and mice also differ in their expression of the neurotrophin receptor, p75. In the rat, I detected p75 receptor in many putative type C cells (SVZ intermediate progenitors) and in some neuroblasts, whereas mice had very few $p75^{+}$ cells. This is the first study to report such effects, as other laboratories had reported that BDNF increased SVZ neurogenesis. Overall, my results indicate that TrkB is not essential for the production and maturation of most SVZ interneurons and do not support the current view that delivering BDNF to the SVZ can enhance adult neurogenesis. Rather, TrkB-TR in ependyma and glial tubes may form a protective barrier, shielding SVZ progenitors and neuroblasts from an activation of p75 by BDNF. My work should promote new

studies on how neurotrophins affect adult neurogenesis and the survival of new neurons before therapeutic applications can be designed.

In addition to the research described above, I developed techniques based on reverse transcription and polymerase chain reaction (RT-PCR) to study gene expression in single SVZ cells. I report on encouraging preliminary results, showing that it is possible to detect multiple gene products from a single cell. In the future, this method can be applied to characterize molecular heterogeneity within each cell type of the SVZ (type B astrocytes, type C intermediate progenitors and type A neuroblasts). This type of analysis will likely reveal more subclasses within type B, C and A cells, and will help to characterize differences between neurogenic and non-neurogenic astrocytes and between cells of different regions of the SVZ.

Chapter One: General Introduction

One of the greatest challenges for medicine in the near future will be to treat diseases and repair injuries in the nervous system, particularly the central nervous system, which has a very limited capacity for regeneration. Many organs, such as the skin and digestive system, are constantly regenerating themselves and repairing injuries, yet this does not occur in the brain. For this reason, neurodegenerative disorders such as Alzheimer's, Parkinson's, Huntington's chorea and multiple sclerosis as well as injuries such as those caused by stroke or mechanical traumas, all of which can cause substantial loss of neurons, are particularly devastastating to patients suffering from them. Until recently, it was thought that neurogenesis, the production of neurons, stopped entirely shortly after birth in the mammalian brain, which would thus be left with the same set of neurons for the remainder of its life. In recent years, the discovery of neural progenitors that continue to produce neurons throughout life in the adult mammalian brain has revolutionized the way we think about this organ and how to heal it. In particular, the existence of adult neural stem cells can help circumvent ethical and availability issues associated with the use of embryonic stem cells and fetal tissue for therapeutic purposes. Though adult progenitors are much less abundant and are thought to have more limited proliferative and differentiation potential, they offer the attractive possibility of self-repair. The largest neurogenic region of the adult mammalian brain is the subventricular zone (SVZ) lining the lateral walls of the lateral ventricles. Importantly, the SVZ seems to respond to injury and participates in brain repair, though this natural response is not sufficient to regenerate lost cells and recover function. Further understanding of how to enhance SVZ responses to injury, direct migration of new cells to desired locations and induce differentiation of specific cell types from adult neural progenitors could bring significant progress to brain repair. From a biological perspective, it is also intriguing that neurogenesis, a widespread phenomenon in the developing and early postnatal brain, is quickly shut down after these stages with the exception of small "resisting pockets", called stem cell niches. What makes these regions special? What mechanisms allow embryonic processes to continue throughout adult life when everywhere else they have been lost?

For my thesis, I studied the effects of a secreted factor, the neurotrophin Brain-Derived Neurotrophic Factor (BDNF), on progenitors of the rodent SVZ. BDNF is known to regulate neuronal survival and differentiation and has recently been involved in modulating postnatal neurogenesis. BDNF was thus an excellent candidate to both improve the regenerative potential of the SVZ and to discover important physiological mechanisms by which adult neurogenesis is made possible.

1.1 Historic overview

It is now well established that restricted regions of the adult vertebrate brain continue to generate new neurons. Joseph Altman's work during the 1960's was first to suggest that new neurons continue to be added to the olfactory bulb (OB) and hippocampus in the adult rodent brain (Altman and Das, 1965; Altman, 1969a, b). Similar suggestions that neurogenesis also continues in the adult cerebral cortex remain highly controversial (Gould et al., 1999; Kornack and Rakic, 2001; Koketsu et al., 2003; Dayer et al., 2005). Perhaps, because of these controversies or because the earlier work did not demonstrate conclusively that the new cells were in fact neurons, the process of adult neurogenesis did not become fully accepted for almost two more decades. Working with adult songbirds, the laboratory of Fernando Nottebohm used electrophysiology, ultrastructure and retrograde axonal labeling to provide firm evidence for adult neurogenesis (Goldman and Nottebohm, 1983; Paton et al., 1986). Work in songbirds also showed that adult neurogenesis is part of an ongoing process of neuronal replacement likely linked to song plasticity (Nottebohm, 1991; Wilbrecht and Kirn, 2004). It was also work in songbirds that provided some of the first clues on the identity of primary precursors and on mechanisms of neuronal birth, migration and integration in an adult brain (Alvarez-Buylla and Nottebohm, 1988; Alvarez-Buylla et al., 1990).

The discovery of adult neurogenesis was followed by the breakthrough observation that cells taken from the adult mammalian brain could self-renew in culture under the influence of growth factors (Reynolds and Weiss, 1992). In addition to their ability to self-renew, these cells could also generate neurons and glia upon removal of the growth factors, all of which are properties of neural stem cells. The fact that such multipotent

progenitors could be isolated not just from postnatal but also adult brains and greatly expanded *in vitro* sparked a new series of studies on the possible use of these *in vitro* neural stem cells for brain repair (Weiss et al., 1996; Tai and Svendsen, 2004).

1.2 Adult neurogenesis

In rodents, there are 2 known adult neurogenic regions: the subventricular zone (SVZ) of the lateral ventricles (Fig. 1.1A-C) and the subgranular zone (SGZ) of the hippocampal dentate gyrus (Fig. 1.1D, E). The experiments in this thesis were focused on SVZ neurogenesis, the largest adult germinal zone. Therefore, I will not describe hippocampal neurogenesis in detail, though several good reviews are available (Gage et al., 1998; Kempermann and Gage, 2000; Ming and Song, 2005; Christie and Cameron, 2006).

Organization of the adult brain SVZ

The SVZ is located in the lateral walls of the lateral ventricles (Fig. 1.1A). Persistent cell proliferation in these walls was discovered almost a century ago by Allen (1912). The cellular composition and organization of the SVZ has been described in detail in rodents (Alvarez-Buylla and Garcia-Verdugo, 2002). The rodent SVZ is composed of three main cell types that are in close proximity with each other residing right next to the ependymal layer lining the lateral ventricles (Fig. 1.1B). Elongated clusters of small cells, called chains, correspond to young neurons that retain some proliferative capacity. These neuroblasts are also referred to as type A cells. Two other cell types surround type A cells: type B and type C cells. Type B cells have multiple characteristics that identify them as astrocytes, including multiple processes and bundles of intermediate filaments containing glial fibrillary acidic protein (GFAP). Type B cells interact closely with ependymal cells and all other major cell types in the SVZ. Interestingly, a thin process has been observed in these cells that intercalates between ependymal cells and reaches the ventricle. On this apical surface, B cells exhibit a single short cilium contacting the ventricular lumen (Doetsch et al., 1999a). Markers of cell division indicate that type B cells have some level of proliferation. Type C cells have a more undifferentiated appearance, are more globular and are highly mitotic. These cells express the proneural gene Mash1 and the homeobox gene Dlx2 (Doetsch et al., 2002; Parras et al., 2004).

Figure 1.1: Neurogenic lineages of the adult brain. ***A***, coronal section of the mouse brain at the level of the anterior SVZ. ***B***, close-up view of boxed area in A, showing cell composition and organization of the adult SVZ. Multiciliated ependymal cells (gray) line the ventricular walls (LV: lateral ventricle). Directly underneath lie the SVZ type B astrocytes (blue), type C transient amplifying cells (green) and type A neuroblasts (red). Some type B cells contact the ventricle lumen into which they extend a primary cilium. ***C***, neurogenic lineage of the SVZ. Type B cells act as neural stem cells, dividing to give rise to more type B cells (self-renewal) as well as to highly proliferative type C cells, which then become type A migratory neuroblasts. ***D***, coronal section of the mouse brain at the level of the hippocampus. ***E***, close-up view of boxed area in D, showing cell composition and organization of the adult dentate gyrus (DG), where neurogenesis also occurs. Radial astrocytes (blue) with their cell bodies in the subgranular zone (SGZ) of the dentate gyrus extend a radial process through the DG granular layer (composed of densely packed granular neurons). Here too, astrocytes play the role of stem cells, giving rise to a transient amplifying cell type (green), which becomes a migratory neuroblast (red). These cells follow the astrocytes' radial process into the granular layer, where they differentiate into granular neurons. ***F***, coronal section of the human brain. Neural stem cells can be isolated from several areas of the human brain, including (yellow): the lateral walls of the lateral (LV) and temporal horn ventricles, as well as the hippocampal dentate gyrus (DG).

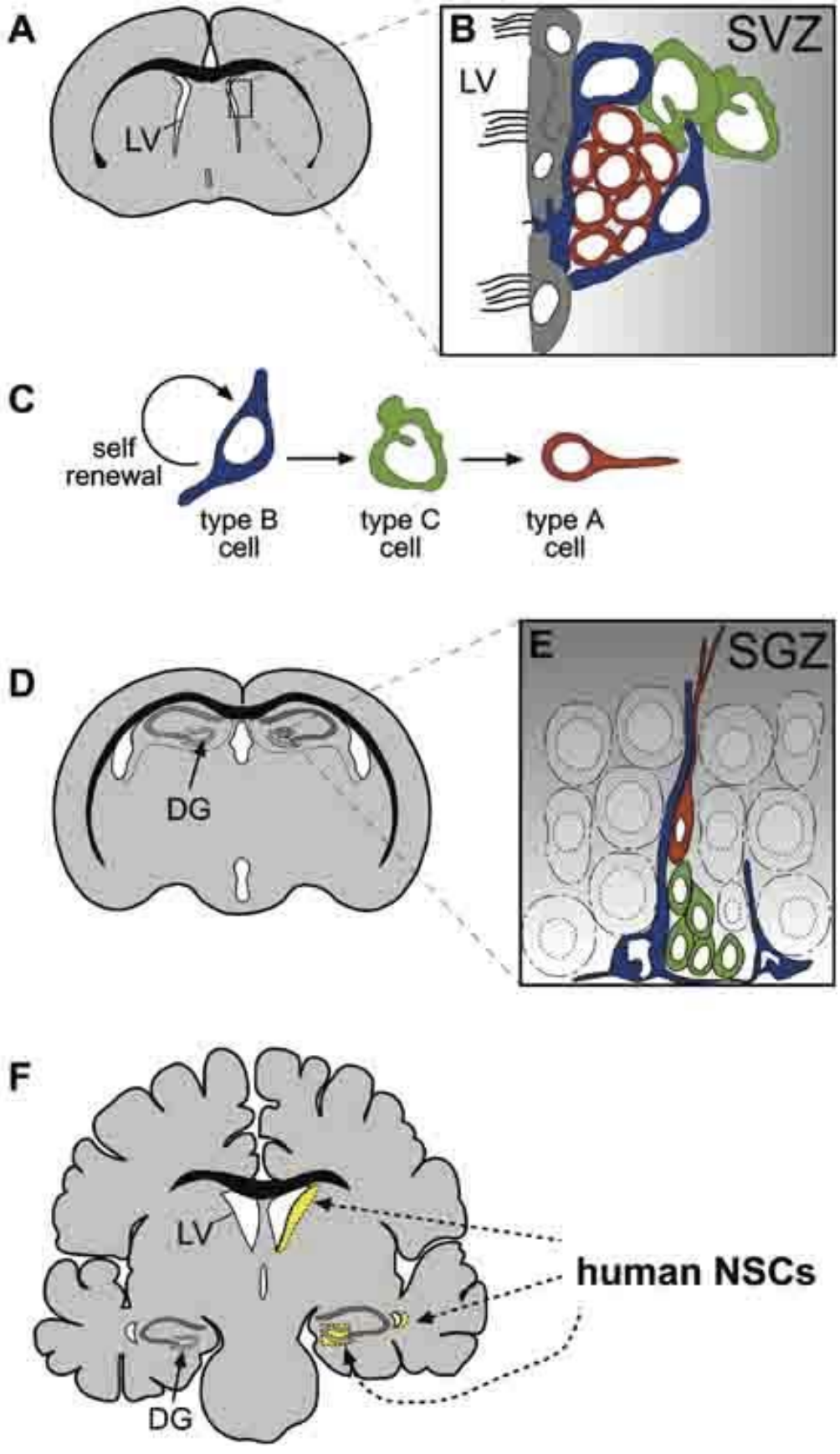
A
LV
B
SVZ
LV
C
self
renewal
type B
cell
type C
cell
type A
cell
D
DG
E
SGZ
F
LV
human NSCs
DG

Neurogenesis in the adult SVZ

The function of the adult SVZ and destiny of its proliferating cells was highly controversial for many years. Most work suggested that the primary function of the adult SVZ was the generation of glial cells (Committee, 1970). Other studies suggested that most of the proliferation in the SVZ was offset by cell death (Morshead and Van der Kooy, 1992). However, more recent work indicates that the primary function of the SVZ in the early postnatal and adult rodent brain, and possibly in other mammals, is the generation of neurons (Luskin, 1993; Lois and Alvarez-Buylla, 1994).

Young neurons born in the SVZ migrate in chains (Fig. 1.2A, B), elongated structures formed by cells sliding over each other (Jankovski and Sotelo, 1996; Lois et al., 1996; Peretto et al., 1997; Wichterle et al., 1997). This process was first described in the RMS, but more recent work shows that the entire SVZ is the site of birth of neurons and glial cells (Doetsch and Alvarez-Buylla, 1996; Doetsch et al., 1997). The young neurons in the SVZ form a complex network of interconnected pathways used for chain migration (Fig. 1.2B) (Doetsch and Alvarez-Buylla, 1996). The orientation of chains within the SVZ parallels the flow of cerebrospinal fluid (CSF) within the ventricles (Sawamoto et al., 2006). It has been hypothesized that chemorepellents secreted by the choroid plexus are deposited in a gradient in the SVZ, aided by the organized flow of CSF close to the ventricle walls due to the coordinated beating of long motile ependymal cilia. In addition to chemorepellents it has been suggested that chemoattractants are secreted in the OB (Astic et al., 2002; Murase and Horwitz, 2002; Liu and Rao, 2003; Ng et al., 2005). Therefore, a combination of repulsive and attractant molecules may help organize the complex journey of SVZ young neurons. While very interesting insights into the mechanism of neuroblast orientation have recently emerged, there is much to be learned about the identity and origin of attractive and repulsive cues responsible for guiding neuroblasts born throughout the SVZ rostrally towards the OB.

Figure 1.2: Neuroblast migration to the olfactory bulb (OB) and OB cellular organization. ***A***, saggital representation of a rodent head, illustrating the brain (white) and skull (brown). Migratory neuroblasts produced in the SVZ (red) form chains throughout the lateral wall of the lateral ventricle (LV, gray), then converge onto the rostral migratory stream (RMS), moving towards the OB. There, neuroblasts migrate radially (dotted arrows) into the OB layers. OE, olfactory epithelium; CC, corpus callosum; CX, cortex; CB, cerebellum. ***B***, diagram of the boxed area in A, showing the network of PSA-NCAM$^+$ (red) neuroblast chains. ***C***, diagram of the second boxed area in A, showing the layered organization of the OB and the main cell types composing the OB circuit. Olfactory receptor neurons (ORN) of the olfactory epithelium bind directly to odorants, leading to the generation of action potentials. These signals are transmitted into the OB via the ORN axons, which contact the OB projection neurons (mitral, M, tufted, T, cells) at the glomerular layer (GL), forming multiple glomeruli (dotted circles). Type A neuroblasts arrive in the OB through the RMS at the core of the OB. Neuroblasts migrate radially into the granular cell layer (GCL) and the GL, where they differentiate into several subtypes of granular (blue, purple) and periglomerular (green, red) interneurons. Deep granular cells (blue) preferentially contact the dendrites of M cells, whereas superficial granular cells (purple) preferentially contact the dendrites of T cells. ***D***, Nissl stained section of the OB, showing the different cell layers. EPL, external plexiform layer; MCL, mitral cell layer. Scale bar: 100 μm (***B***).

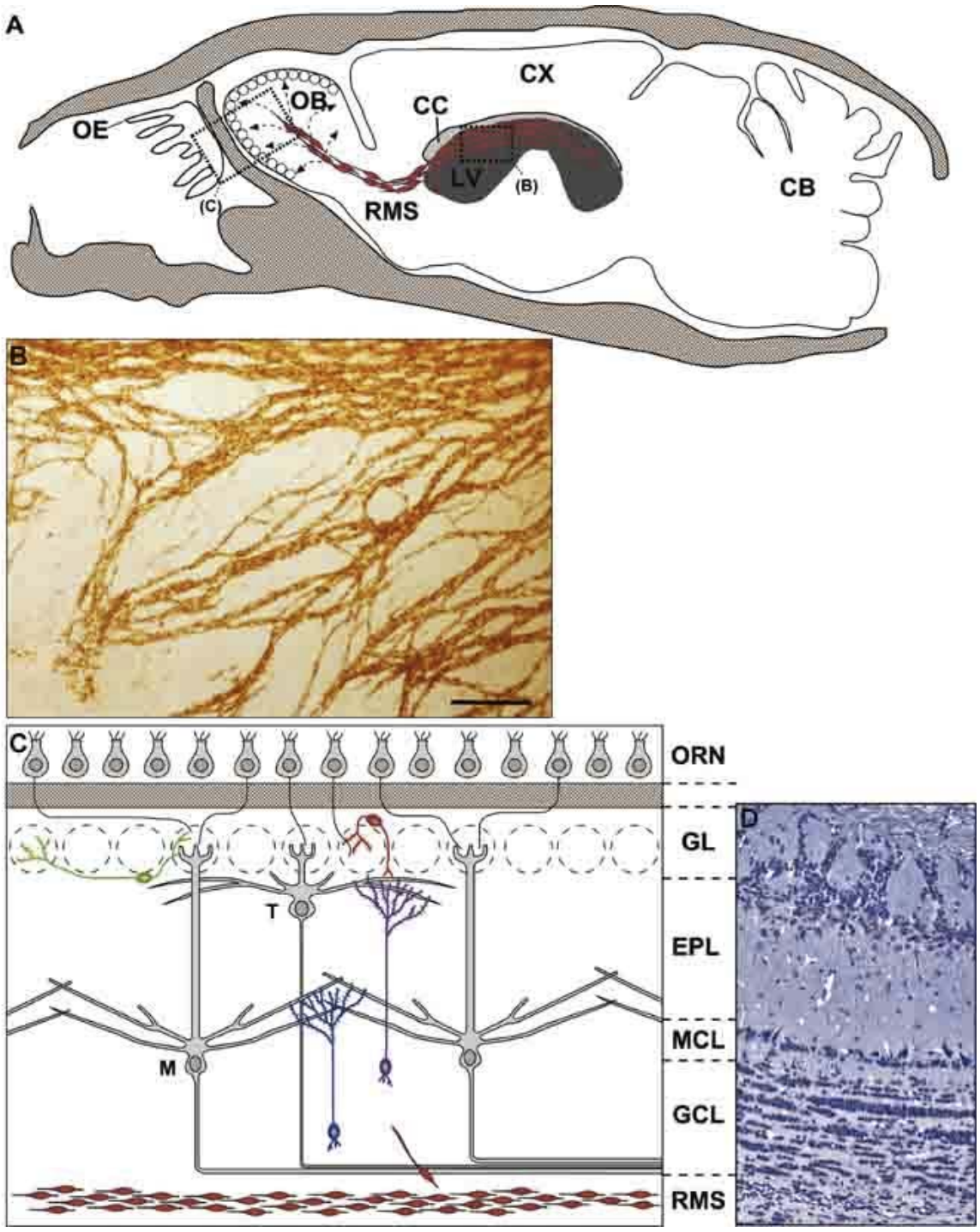
A
CX
OB
CC
OE
LV
(B)
CB
(C)
RMS
B
C
ORN
GL
D
T
EPL
MCL
M
GCL
RMS

Astrocytes as SVZ adult stem cells

A recent important advancement in the understanding of SVZ neurogenesis has been the identification of the stem cells within this structure. As indicated above, type C cells are actively proliferating and frequently labeled by injections of [^{3}H]-thymidine or BrdU (Doetsch et al., 1997), both of which are thymidine analogs that incorporate into DNA during S phase of the cell cycle. Type C cells have an undifferentiated appearance and it was possible that these cells corresponded to the primary progenitors that generate new neurons. However, as explained below, type C cells turned out to be secondary precursors that function as transient amplifying cells. Type B and A cells also undergo cell division but to a lesser degree than type C cells.

Because type A cells divide (Menezes et al., 1995; Lois et al., 1996), it was possible that self-renewal of this cell population could directly generate more A cells. However, purified A cells in culture are not self-renewing, indicating that these cells are derived from an earlier progenitor. Treating the brain with antimitotic drugs for 6 days results in the elimination of type A and C cells from the SVZ, yet the SVZ readily regenerates following this antimitotic treatment. This result shows that type A or C cells are not the primary precursors of the new neurons (Doetsch et al., 1999b). Instead, multiple lines of experimentation point to type B cells as the primary progenitors for the new SVZ neurons (Fig. 1.1C). This was fully unexpected, as type B cells had been previously catalogued as terminally differentiated astrocytes (Privat and Leblond, 1972). Experiments using transgenic mice expressing the receptor for an avian retrovirus under the control of the GFAP promoter (Holland and Varmus, 1998) allowed specific labeling of SVZ type B cells and their progeny. This experiment provided direct evidence that SVZ astrocytes can function as neuronal precursors (Doetsch et al., 1999b). Consistently, following ablation of type C and A cells with the antimitotic treatment mentioned above, a subpopulation of surviving SVZ astrocytes begins to divide to give rise to new C cells and then to A cells (Doetsch et al., 1999b). Thus, under normal conditions as well as during SVZ regeneration, type B cells function as the primary precursors of new neurons destined for the olfactory bulb.

In contrast to A, B and C cells, ependymal cells do not divide *in vivo* (Doetsch et al., 1999b; Spassky et al., 2005), suggesting that these multiciliated cells do not function as neural stem cells as previously suggested (Johansson et al., 1999). Several other lines of evidence also indicate that ependymal cells do not function as progenitors of new neurons in the adult brain (Chiasson et al., 1999; Doetsch et al., 1999b; Rietze et al., 2001). Yet, the controversy over whether ependymal cells can function as stem cells continues. New experiments suggest that, under normal conditions, ependymal cells do not divide, but that these cells may be activated during injury to begin proliferating and function as progenitor cells (Zhang et al., 2007). Given that some type B cells normally touch the ventricle through a thin process (Doetsch et al., 1999a), it is possible that, following injury, some of these cells expand this apical process and become more exposed to the ventricle. In fact, several experimental manipulations that activate neuronal stem cells in the SVZ lead to a significant increase in the number and extent to which type B cells contact the ventricle (Conover et al., 2000; Doetsch et al., 2002). These astrocytes might have been mistaken for ependymal cells in previous experiments, thereby explaining the contradictory results surrounding the "stemness" of ependymal cells.

Several recent studies support the conclusion that some SVZ cells previously considered part of a differentiated astroglial lineage are in fact neural progenitor cells. Laywell et al. (2000) observed that mouse GFAP-expressing astrocytes isolated from cortex, cerebellum, and spinal cord in animals younger than 2 weeks of age can, *in vitro*, behave as stem cells. Interestingly, they found that astrocytes isolated from the SVZ throughout life can generate neural stem cells *in vitro*. Imura et al. (2003) used a different approach to test whether astrocytes within adult germinal layers work as neuronal precursors. In this study, dividing GFAP-positive SVZ cells were eliminated using mice that express herpes simplex virus thymidine kinase (HSV-TK) under the control of the GFAP promoter (GFAP-TK). In these mice, dividing GFAP- positive cells are selectively killed by treatment with ganciclovir. They show that very few neurospheres, if any, can be made after the ganciclovir treatment in the adult brain. The authors also observed that progenitors isolated from GFAP-TK mouse embryos generated neurospheres even in the presence of ganciclovir, indicating that neural stem cells at this

early age do not express GFAP. Ganciclovir treatment of adult transgenic mice expressing HSV-TK under the GFAP promoter also resulted in a severe reduction of the generation of new olfactory bulb neurons (Garcia et al., 2004). In conclusion, multiple lines of evidence support the interpretation that primary precursors for the generation of new neurons in the adult brain SVZ correspond to astroglial cells expressing GFAP.

Astrocytes as SGZ adult stem cells

In addition to the SVZ, neurogenesis continues in the subgranular zone (SGZ) of the dentate gyrus in the adult brain (Altman and Das, 1965; Cameron et al., 1993; Eriksson et al., 1998; Gage, 2000) (Fig. 1.1D, E). Here too, recent work suggests that the primary precursors for the new neurons correspond to cells previously identified as astrocytes (Seri et al., 2001; Filippov et al., 2003; Fukuda et al., 2003). These primary precursors of adult hippocampal neurons also express GFAP. These cells are quite elaborate and have a large radial process that traverses the granule cells layer. Interestingly, selective killing of dividing radial astrocytes using the GFAP-TK mice mentioned above also results in a dramatic reduction in the production of new granule neurons (Garcia et al., 2004).

Therefore, studies in both adult germinal layers indicate that GFAP-expressing cells with astroglial structural properties function as primary progenitors in the generation of new neurons.

Glial lineage of neural stem cells

Just as astrocytes are now known to be the primary neural stem cell in the adult SVZ, recent reseach has led to the discovery that another glial cell can function as a neural progenitor during development. Radial glia are a prominent cell type in the embryonic brain, appearing as early as E10.5 and remaining in the brain until the first postnatal week. Their cell bodies reside in the germinal ventricular zone, near the cerebral ventricles, but their processes span the entire thickness of the brain, contacting both the ventricular lumen and the pial surface of the brain (Fig. 1.3B, C). Radial glia have long been known to serve as scaffolds for the radial migration of cortical projection neurons (Rakic, 1988, 1995), but it was recently discovered that not only do they direct the

Figure 1.3: Glial lineage of stem cells. ***A***, cellular organization of the forebrain germinal zone at an early stage of development. Neuroepithelial cells divide to generate more neuroepithelial cells (expansion of the progenitor pool) and some early-born neurons. ***B***, cellular organization of the lateral wall of the lateral ventricle at a later embryonic stage (~ E14). Radial glia, presumably derived from neuroepithelial cells, maintain their cell body in the ventricular zone (VZ) while contacting the pial surface of the brain via a long radial process. Radial glia divide to give rise to progeny either directly or through intermediate progenitors (green), which will divide further in the SVZ. Neuroblasts (red) generated by radial glia migrate radially in close contact with the stem cell's process. At this time, radial glia of the lateral ventricle generate both striatal (ST) neurons and oligodendrocytes. ***C***, in the neonatal brain, radial glia are still present in the lateral wall of the lateral ventricles, and continue to generate progenitors. Some migrate tangentially and will become olfactory bulb interneurons (pink), others will become oligodendrocytes, astrocytes or ependymal cells. ***D***, ultimately, radial glia themselves transform into astrocytes, some of which will reside in the SVZ and will continue to function as stem cells throughout adulthood (blue). At this stage, SVZ stem cells generate almost exclusively neuroblasts for the olfactory bulb (red), though some oligodendrocytes are also produced. A feature common to neuroepithelial cells, radial glia and at least some SVZ astrocytes, is the direct contact with the ventricular lumen through an apical projection, extending a primary cilium into the ventricle.

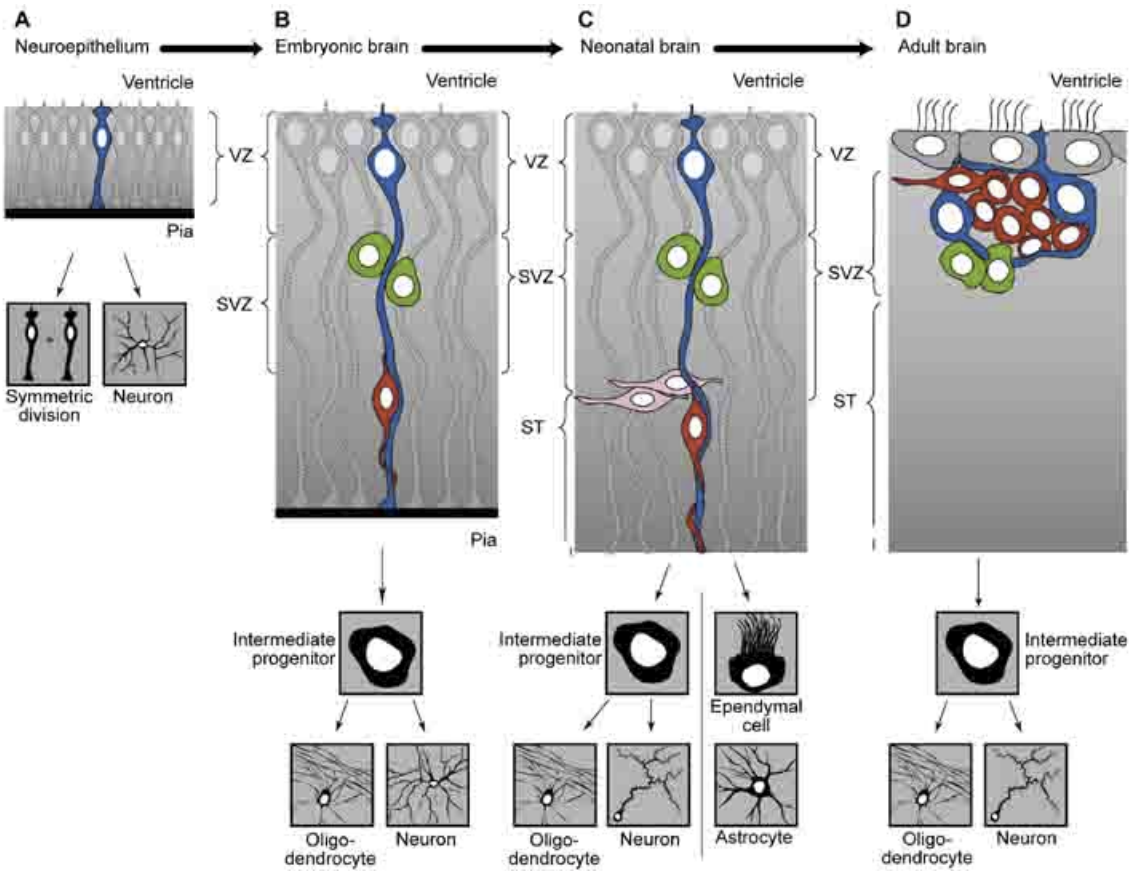
A
Neuroepithelium
B
Embryonic brain
C
Neonatal brain
D
Adult brain
Ventricle
Pia
VZ
SVZ
ST
Symmetric division
Neuron
Intermediate progenitor
Oligo-dendrocyte
Ependymal cell
Astrocyte

migration of new neurons, they are actually the source of those very same neurons (Malatesta et al., 2000; Miyata et al., 2001; Noctor et al., 2001; Tamamaki et al., 2001). Radial glia divide asimetrically, giving rise to progeny that remains associated with their long radial process. This new cell then migrates along the radial process away from the ventricle and either divides again in the deeper subventricular zone, or differentiates directly into a neuron (Noctor et al., 2004) (Fig. 1.3B, C). Radial glia seem to be the main neural stem cell during brain development, not only for the cerebral cortex, but for most regions of the central nervous system (CNS) (Anthony et al., 2004).

Embryonic radial glia and post-natal SVZ astrocytes have several properties in common: both are glial cells and both divide to generate neurons. Additionally, both cell types are located near the ventricular walls, and even though in the adult, SVZ astrocytes are separated from the ventricular surface by the ependymal layer, many still contact the ventricle through thin processes intercalating between ependymal cells. At the location where they contact the ventricle, both radial glia and SVZ astrocytes extend a single primary cilium, which could be an important structure for the maintenance of stem cell properties by these cells. Importantly, after the neurogenic phase is complete, radial glia give rise to astrocytes (Schmechel and Rakic, 1979; Voigt, 1989; Gaiano et al., 2000) and disappear from the brain. It was therefore possible that the neurogenic astrocytes found in the post-natal SVZ were direct descendants of radial glia. This hypothesis has been confirmed experimentally (Merkle et al., 2004) and we can now trace the lineage of neural stem cells from embryonic to adult stages. It is likely that this lineage begins with the neuroepithelial cells that compose the ealy neural tube, though that has not yet been confirmed. The complete neural stem cell lineage would thus begin with neuroepithelial cells, which progressively become radial glia, which in turn give rise to the post-natal astrocytic SVZ stem cells (Fig. 1.3).

Just as primary neural progenitors change over time, so does their potential to generate different cell types. In cortical development, neural progenitors give rise to different types of neurons at different time. Cajal-Retzius neurons are generated first, then deeper cortical layers 6 and 5 neurons, followed by those destined for the more superficial layers. Importantly, as development progresses, neural progenitors seem to lose the

ability to generate the earlier-born cell types (Desai and McConnell, 2000; Pearson and Doe, 2004; Shen et al., 2006). How progenitor potential changes with time on the lateral wall of the lateral ventricle, ultimately giving rise to the adult SVZ, remains largely unknown. In the embryo, radial glia of this lateral wall produce many oligodendrocytes and striatal projection neurons. At later stages, radial glia of the lateral ventricles no longer produce striatal neurons, but give rise to olfactory bulb neurons, ependymal cells and astrocytes. In the adult, SVZ stem cells produce mainly OB interneurons and some oligodendrocytes. Likely, the specific cell types produced within each of these categories change over time as well, as has recently been suggested for the OB interneurons (De Marchis et al., 2007).

Stem cells in the postnatal SVZ are also spatially heterogeneous: progenitors in dorsal regions of the SVZ mainly give rise to superficial granular OB interneurons, whereas progenitors in the ventral SVZ mainly give rise to deep granular interneurons. Periglomerular OB interneurons are generated mainly from the anterior SVZ and different subclasses of these cells originate from dorsal and ventral SVZ (Merkle et al., 2007) (see next section for details on OB interneuron subtypes). It will be important in the future to further understand the temporal and spatial differences of neural stem cells' potential, both to expand our basic understanding of brain development as well as to effectively use neural stem cells for therapy.

1.3 Olfactory Bulb Structure and Function

Under normal conditions, the final destination of most, if not all, young neurons generated in the SVZ is the OB, the most rostral structure of the mouse brain (Fig. 1.2).

Circuitry of the OB

The OB, a highly laminated structure (Fig. 1.2C, D), receives input directly from the olfactory epithelium and is the first processing stage of olfactory information (reviewed in Shepherd, 1972; Shepherd and Greer, 1998). It is composed of two main cell types: the principal, or output neurons and the local interneurons. The output neurons are the mitral and tufted cells (collectively called M/T cells). Both send dendrites to the surface of the

OB, where they contact the axons of olfactory receptor neurons (ORNs) from the olfactory epithelium. These connections form a spherical neuropil structure called a glomerulus. Each glomerulus receives axons from a single type of ORN, and each M/T cell contacts only one glomerulus. This organization is responsible for most of the odor specificity in the activation of M/T cells. M/T cells then project their axons to the pyriform and entorhinal (main and accessory olfactory) cortex, where a second level of information processing occurs. The OB circuitry and processing capability is, however, not limited to the relay of neuronal excitation between ORNs and M/T cells. The majority of neurons in the OB are inhibitory interneurons: the periglomerular and granular cells. Periglomerular cells are located around glomeruli and establish contacts with ORN axon terminals and between different glomeruli. Granular cells, by far the most numerous, are in the deepest layer of the OB (the granular cell layer, GCL) and project dendrites into the external plexiform layer (EPL). There they establish bidirectional, dendro-dendritic synapses with several M/T cells (Rall et al., 1966; Nicoll, 1969; Shepherd, 1972; Woolf et al., 1991). When M/T cells receive input from ORNs, they release the excitatory neurotransmitter glutamate onto granular cell dendrites. Granular cells respond by releasing the inhibitory neurotransmitter GABA onto the M/T cells that excited them as well as other neighboring M/T cells (Isaacson and Strowbridge, 1998; Chen et al., 2000). This inhibitory feedback system is thought to be important for the fine tuning of olfactory information in the OB circuit before that information is relayed, via M/T cell axons, to pyriform and entorhinal cortex for further processing.

Role of OB interneurons in information processing

It has been suggested that the function of the modulation of M/T cell excitation by OB interneurons is to maximize the differences between the patterns of neuronal activation elicited by different odorants (which can differ by as little as chirality of the molecule) before this information is sent to the olfactory cortex for further processing. Exactly how that is achieved is not certain. Because of OB interneurons, activation of M/T cells results in feedback inhibition as well as lateral inhibition of neighboring M/T cells (Rall and Shepherd, 1968; Nicoll, 1969; Yokoi et al., 1995). Akin to what occurs in the visual or auditory systems, local inhibitory interneurons may therefore sharpen sensory responses,

silencing neighboring neurons that are less strongly activated by the afferent stimulus (Yokoi et al., 1995; Mori et al., 1999). Other models have been proposed. Any odor leads to the activation of a variety of ORNs, which is translated in the OB into activation of multiple glomeruli often located all over the OB's surface. Closely related odors evoke activation patterns that are initially very similar. However, due to the interactions mediated by interneurons between M/T cells, these patterns evolve over ~800ms, becoming increasingly dissimilar. It is believed that this change in patterns is used by the OB to sharpen odor discrimination (Friedrich and Laurent, 2001; Laurent et al., 2001). Another mechanism used by the OB to enhance odor detection and perhaps identification is an oscillatory synchronization of M/T cell firing. These oscillations are believed to synchronize M/T cells responding to the same odor to render transmission of information to the olfactory cortex more efficient (Stopfer et al., 1997; MacLeod et al., 1998; Schoppa and Westbrook, 1999). OB interneurons are thought to be essential for all of these mechanisms.

Neuronal replacement in the adult OB

Unlike most neurons in the adult CNS, OB interneurons undergo continuous cell death (Kaplan et al., 1985). At the same time, thousands of neuroblasts produced in the distant SVZ arrive daily in the OB via the RMS, at the core of the OB. They then migrate radially to more superficial layers of the OB. As this occurs, these cells undergo a progressive maturation process that will transform them into fully functional interneurons. Migrating neuroblasts in the RMS already express GABA, GABA receptors, AMPA glutamate receptors (Carleton et al., 2003; Wang et al., 2003) and NMDA glutamate receptors (Platel et al., 2008) (Angelique Bordey unpublished observations). Even before they stop migrating, the new neurons begin receiving synaptic inputs. Interestingly, the last neuronal property to arise seems to be the ability to fire action potentials (Carleton et al., 2003). This entire process takes 15-30 days, though periglomerular cells may take longer to mature (Winner et al., 2002; Kohwi et al., 2007). Once maturation is complete, new granular neurons exhibit morphological and electrophysiological properties identical to that of other granular neurons and become fully integrated in the OB circuit (Belluzzi et al., 2003; Carleton et al., 2003).

Some neuroblasts are destined towards the outermost cellular layer of the OB and become periglomerular interneurons, but most integrate into the deeper layers of the OB and differentiate into granular interneurons (Figure 1.2C). Periglomerular and granular cells can be further divided into multiple subtypes based on the expression of various molecular markers and on their connectivities, which suggest distinct roles in olfactory information processing. There are many types of periglomerular interneurons, either based on their expression of molecular markers (the dopamine-producing enzyme TH, the calcium-binding proteins Calbindin and Calretinin) or on their connectivities (contacting ORNs and M/T cells, M/T cells only, connecting different glomeruli or restricted to one glomerulus) (Kosaka and Kosaka, 2005; Parrish-Aungst et al., 2007). Based on molecular markers alone, the SVZ is known to contribute new neurons that become dopaminergic TH^+, as well as $Calbindin^+$ and $Calretinin^+$ periglomerular cells (Beech et al., 2004; De Marchis et al., 2007; Kohwi et al., 2007). Granular interneurons can be broadly subdivided into deep cells, many of which express the transcription factor Er81 and preferentially contact mitral cells, and superficial cells, many of which express the transcription factor Pax6 and preferentially contact tufted cells (Orona et al., 1983; Stenman et al., 2003; Kohwi et al., 2005). The SVZ continuously generates large numbers of both deep and superficial granular cells. It is not yet known how or when SVZ neuroblasts become commited to one of the many interneuron types that are generated in the adult.

Role of OB interneuron replacement

What could be the advantage of a continuous removal and addition of OB interneurons for the organism's sense of smell? Several studies have suggested that adult neurogenesis can enhance olfactory discrimination (Gheusi et al., 2000; Cecchi et al., 2001; Rochefort et al., 2002; Alonso et al., 2006; Bath et al., 2008).

Neuroblasts are produced in excess by the SVZ and migrate to the OB, where they arrive 3 to 5 days later. However, only a fraction of these cells survive: approximately 50% of the new neurons are eliminated between 15 and 45 days after they are born in the SVZ (Petreanu and Alvarez-Buylla, 2002). The exact mechanisms responsible for this selection process are not understood, though it is known that incoming activity from

ORNs of the olfactory epithelium plays an important part (Petreanu and Alvarez-Buylla, 2002). Neurons that overcome this initial period become stable components of the OB circuit and may survive for months or years, though as a population, they are still subject to a slow, continuous turnover.

Based on this information and on the knowledge of the general pattern of OB connectivity, a mathematical model was constructed to study how adult neurogenesis could affect olfactory processing (Cecchi et al., 2001). In this model, granular cells are added randomly to the network and selected based on activity: cells with higher levels of activity are kept and those with lower levels are eliminated. After a number of iterations (or "trainings"), the system becomes capable of optimally discriminating the 10 odors for which it was trained and the network is stable (no more granular cells are added or lost). However, if the odors are changed, the network cannot adapt to achieve maximal performance again. To do so, an additional rule must be added to the model. There must be not only an initial activity-dependent selection of incoming granular cells but also a random, slow elimination of pre-existing granular cells from the circuit. In this model, this elimination creates vacancies that allow for the incorporation of new neurons. With these rules, the system can now readjust itself to accommodate new odors. According to this model, a continual replacement of these interneurons is necessary for maximal discrimination of odors in an olfactory environment that is constantly changing.

A series of experimental observations are consistent with the predictions of this model. Mice subjected to an odor-enriched environment show marked increases in the number of new OB interneurons, correlating with enhanced olfactory performance (Rochefort et al., 2002). Conversely, reduced survival of granular cells caused by olfactory deprivation disrupts the representation of odors by M/T cells (Guthrie et al., 1990). NCAM mutant mice, in which migration of neuroblasts to the OB is reduced, have greater difficulty in discriminating different odors (Gheusi et al., 2000), suggesting that production of new neurons is necessary to maintain a functional olfactory system. However, this study does not directly address the role of neuronal replacement in odor discrimination, as these animals only have a deficit in the addition of new neurons to the OB. It would be important to study the consequences on olfactory performance of simultaneously blocking the arrival of new cells and preventing the death of older cells in the OB.

Neurogenesis might continue throughout life in brain regions that receive inputs with a high statistical variability that preclude the predetermined assembly of a unique optimal circuit. As the olfactory environment changes, it may become necessary to change the wiring of OB interneurons to different combinations of M/T cells. This type of change may be too drastic to be accommodated by synaptic plasticity alone. The elimination of old neurons and incorporation of new ones would thus provide a means by which this type of plasticity could be attained (Nottebohm, 2002b, a). Additionally, young neurons may have an enhanced potential for synaptic plasticity (Schmidt-Hieber et al., 2004). The incorporation of new neurons in the OB would then enable the brain to accommodate changes in the environment. Hippocampal neurogenesis may serve a similar function (Kempermann, 2002).

1.4 Stem cell niche within the adult SVZ

It is striking that neurogenesis, which occurs throughout the entire CNS during development, becomes restricted to very specific regions in adulthood. It is not yet clear why neurogenesis continues in these regions but it is believed that a combination of cell signaling molecules and cellular interactions, broadly defined as the stem cell niche, must be available (Fig. 1.4). In fact, if cells are grafted from a neurogenic niche into non-neurogenic regions of the brain, they stop producing neurons and become postmitotic glia (Herrera et al., 1999), demonstrating that stem cells need a supportive environment to self-renew and generate neurons. In the SVZ, some of the neurogenic niche components have been identified.

Extrinsic cues

The transmembrane receptor Notch is involved in many developmental processes, regulating cell fate and differentiation of progenitor cells (Artavanis-Tsakonas et al., 1999). Notch signaling is believed to maintain progenitors in an undifferentiated state, thereby preventing the depletion of progenitor pools due to premature differentiation. In mammals, Notch is activated by the transmembrane ligands Delta and Jagged by

Figure 1.4: Cell extrinsic components of the SVZ neurogenic niche. Both Notch1 and its ligand Jagged1 are expressed in the SVZ. Their exact location is not clear, but it seems that both are expressed in type B cells and may thus mediate lateral inhibition interactions between these cells. BMP4 is secreted by type B cells and can bind to BMP receptors in type B and A cells of the SVZ. The BMP antagonist Noggin is secreted by ependymal cells (E) and promotes neurogenesis by blocking the pro-gliogenic activity of BMPs. The neurotransmitter GABA is secreted by type A cells and activates $GABA_A$-R on type A and B cells, reducing their proliferation and A cell migration speed. Another neurotransmitter, Dopamine is released from axon terminals onto type C cells, which express the Dopamine receptor D2L, promoting their proliferation. The BDNF receptor TrkB is expressed in ependymal and type B cells, but only in its truncated, tyrosine-negative isoform (from data in this thesis). Many other receptors are expressed in SVZ cells, though the origin of their ligands (boxed text) is unknown. The role of these molecules in the SVZ niche is categorized under stem cell maintenance, neurogenic, gliogenic and proliferation actions. For some factors, such as Wnt/Frizzled signaling, the role is not yet clear, though it is inferred from the information presently available. Full arrows: origin of secreted molecules; dotted arrows: target/site of action of secreted molecules. Most receptors represented are of the tyrosine kinase type (double black bars), while Notch receptors (single black bar) are activated by cleavage of the intracellular domain (the Notch ligand Jagged is also a transmembrane protein), Smo and D2L (wavy black line) are 7-pass transmembrane receptors of the G protein-coupled receptor family and GABA receptors ($GABA_A$-R, short double black bars) are ligand-gated Cl^- ion channels.

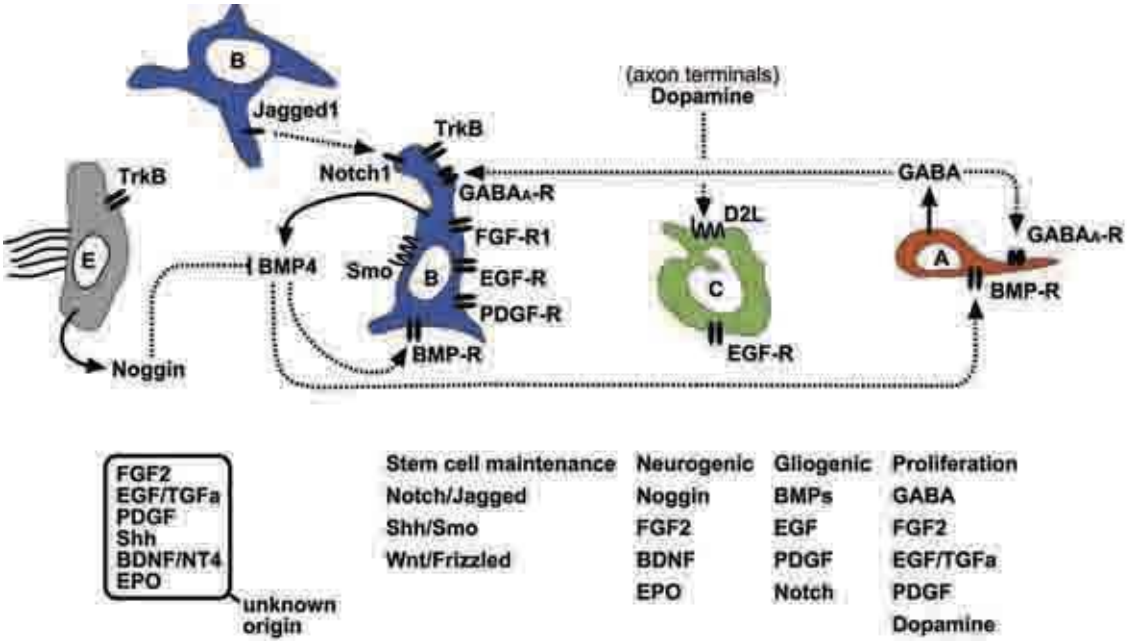
B
Jagged1
TrkB
Notch1
(axon terminals)
Dopamine
GABA
TrkB
GABAA-R
D2L
GABAA-R
E
BMP4
Smo
B
FGF-R1
EGF-R
A
BMP-R
PDGF-R
C
Noggin
BMP-R
EGF-R
FGF2
EGF/TGFa
PDGF
Shh
BDNF/NT4
EPO
unknown
origin
Stem cell maintenance
Notch/Jagged
Shh/Smo
Wnt/Frizzled
Neurogenic
Noggin
FGF2
BDNF
EPO
Gliogenic
BMPs
EGF
PDGF
Notch
Proliferation
GABA
FGF2
EGF/TGFa
PDGF
Dopamine

paracrine, cell contact interactions. Notch1 is expressed in the adult SVZ (Irvin et al., 2001; Stump et al., 2002; Givogri et al., 2006). The expression of the Notch downstream regulator Hes5 suggests active Notch signaling in this region (Stump et al., 2002) and the activated form of Notch1 has been detected in SVZ astrocytes (Tokunaga et al., 2004). The exact origin of this activation is not known but the Notch ligands Delta1 and Jagged1 are expressed in the SVZ (Stump et al., 2002; Givogri et al., 2006). Notch activation in the SVZ seems to affect proliferation and promote a radial glial or astrocytic state in detriment of neuronal production (Gaiano et al., 2000; Chambers et al., 2001; Nyfeler et al., 2005). Additionally, Jagged1 has been shown to promote self-renewal of SVZ-derived stem cells *in vitro* (Nyfeler et al., 2005). It is likely that Notch signaling has a pivotal role in maintaining stem cells in the SVZ throughout adulthood. Notch has also been associated with the differentiation of glial cells (Gaiano and Fishell, 2002). Considering the glial nature of stem cells in the lateral ventricle during development and adulthood (see above), these conclusions are by no means mutually exclusive.

Sonic hedgehog (Shh) and Wnt signaling pathways are also suspected to regulate stem cell self-renewal in the postnatal brain. Shh is a secreted molecule with important functions in neural development. The source of Shh for the adult neurogenic regions has not been determined, but Smoothened (Smo, mediator of Shh signaling) and Patched (Shh receptor) have been detected in both the SVZ and hippocampus (Traiffort et al., 1999; Lai et al., 2003). Furthermore, the transcription factor Gli1, commonly used as a readout of Shh signaling, is expressed in SVZ and SGZ (hippocampal germinal zone) by GFAP-positive cells with stem cell properties (Ahn and Joyner, 2005; Palma et al., 2005). Experiments manipulating Shh signaling in the adult brain have provided clues to its role in postnatal neurogenesis. Pharmacological inhibition of Shh signaling or conditional deletion of Smo lead to reduced proliferation and progenitor numbers in both the SVZ and SGZ. Conversely, stimulation of the Shh pathway resulted in increased proliferation *in vivo* and neurosphere production *in vitro* (Lai et al., 2003; Machold et al., 2003; Palma et al., 2005). Recent evidence indicates that primary cilia play a critical role in Shh signaling (Huangfu et al., 2003; Corbit et al., 2005; Huangfu and Anderson, 2005). It will

be interesting to determine whether type B cells, which exhibit primary cilia at the ventricle surface, are particularly responsive to Shh.

Wnt signaling promotes the self-renewal of stem cells of the hematopoietic lineage (Reya et al., 2003). Whether Wnts have a similar role in adult brain stem cell niches is not known. However, it is known that Wnt3 stimulates SGZ neurogenesis *in vivo* (Lie et al., 2005) and that Wnt3a and Wnt5a promote SVZ precursor proliferation and neuronal differentiation *in vitro* (Yu et al., 2006).

An important decision that progenitors in neurogenic niches must make is whether to produce neurons or glia. Although during development, neurogenesis and gliogenesis are temporally separated, in adult germinal zones, both occur concurrently. This is achieved by a balance of neuro and gliogenic signaling cues. As was mentioned above, Notch signaling may instruct stem cells to generate glial progeny. Other gliogenic cues include the secreted molecules of the BMP family, PDGF and EGF/TGFα. These are counteracted by factors promoting neurogenesis, such as Noggin, Erythropoietin (EPO), BDNF and FGF2. Several BMPs are expressed in the SVZ by type B cells and perhaps other cell types (Lim et al., 2000b). Noggin is a potent inhibitor of BMP signaling by binding to BMP molecules and preventing them from activating their receptors. In the SVZ, Noggin is secreted from ependymal cells, blocking the gliogenic effect of BMPs and thereby promoting neurogenesis (Lim et al., 2000b). BMPs and their inhibitors are also present in the hippocampal stem cell niche, where they appear to operate in similar ways (Fan et al., 2003; Ueki et al., 2003; Fan et al., 2004).

FGF2 and EGF are the most commonly used growth factors when culturing and expanding SVZ-derived stem cells *in vitro*. *In vivo*, both are potent stimulators of proliferation in the SVZ (Craig et al., 1996; Kuhn et al., 1997; Zheng et al., 2004). It is not clear whether EGF is expressed in the brain, but another ligand for the EGF receptor, TGFα, is produced in many brain structures, including the striatum adjacent to the SVZ (Wilcox and Derynck, 1988; Seroogy et al., 1993). TGFα also induces proliferation of SVZ cells (Fallon et al., 2000). Additionally, TGFα-null mice exhibit reduced proliferation and neuronal production in the SVZ (Tropepe et al., 1997), suggesting that TGFα may be the naturally available ligand for SVZ cells expressing EGF-R. In addition

to their role in proliferation, FGF2 and EGF/TGFα seem to influence cell fate decisions of SVZ progeny. FGF2 infusion increases the number of new neurons in the OB (Kuhn et al., 1997) and FGF2-null mice have smaller OBs (Zheng et al., 2004). EGF infusion has the opposite effect, inducing mainly the differentiation of glial cells and reducing the production of OB neurons (Craig et al., 1996; Kuhn et al., 1997; Doetsch et al., 2002). EGF has similar effects on hippocampal neurogenesis, while FGF2 has no influence on it (Kuhn et al., 1997). Both EGF and FGF receptors (EGF-R and FGF-R1) are expressed in cells of the SVZ (Morshead et al., 1994; Seroogy et al., 1995; Gritti et al., 1999; Zheng et al., 2004), but the identity of these cells is a highly debated issue. Type C cells express EGF-R and may be the main SVZ cell type responding to EGF *in vivo*, though some GFAP-positive cells also express EGF-R (Doetsch et al., 2002). In fact, several groups have proposed that the EGF-responsive cells are the stem cells (Morshead et al., 1994; Gritti et al., 1999). It is possible that EGF-R expression and EGF responsiveness in the stem cell population is a dynamic process, depending on the state of activation of individual stem cells (Doetsch et al., 2002). Stem cells are also thought to respond directly to FGF2 and to express its receptor FGF-R1 (Gritti et al., 1999; Zheng et al., 2004), though more research is needed to confirm these claims.

In addition to FGF2, other growth factors have been shown to increase the production of neurons by the SVZ. Intraventricular administration of BDNF increases production of OB interneurons and, unexpectedly, of striatal neurons normally not generated in the adult brain (Zigova et al., 1998; Benraiss et al., 2001; Pencea et al., 2001). Erythropoietin (EPO), a cytokine upregulated in response to hypoxia, can also increase the production of OB neurons from the SVZ and has been suggested to act directly on stem cells (Shingo et al., 2001). PDGF, on the other hand, shifts the differentiation of SVZ cells towards the production of oligodendrocytes (Jackson et al., 2006) The mode of action of these molecules remains to be identified.

An interesting regulatory mechanism recently uncovered in the SVZ involves paracrine signaling through GABA release. The neurotransmitter GABA is secreted by SVZ neuroblasts and $GABA_A$ receptors are present in both neuroblasts and type B astrocytes (Stewart et al., 2002; Nguyen et al., 2003; Wang et al., 2003; Liu et al., 2005).

GABA reduces the proliferation of both of these cell types (Nguyen et al., 2003; Liu et al., 2005) and may thus serve as a negative feedback system to control the production of neuronal progeny by SVZ stem cells. Consistent with that interpretation, after depleting the SVZ of neuroblasts by antimitotic drugs, type B astrocytes display increased proliferation as they repopulate the SVZ with the lost cell types (Doetsch et al., 1999a).

Environmental regulation

The *in vivo* source of most of the factors mentioned above is not clear and needs to be determined if we are to understand the regulation and function of adult neurogenesis. Another important question is what determines the levels of these signaling molecules. Hormones likely play an important role. The lactogenic hormone Prolactin (PRL) is upregulated at specific time points during pregnancy and after giving birth. PRL causes a significant increase in SVZ neurogenesis in pregnant female mice both at 7 days *post coitus* and immediately after parturition, resulting in increased addition of new neurons to the OB (Shingo et al., 2003). It is possible that such a mechanism exists to prepare the female for identifying and taking care of its pups by enhancing new odor recognition and memory. Another female hormone, Estrogen, can also influence adult neurogenesis, but seems to act only on the hippocampal SGZ, where it increases the number of dividing cells (Tanapat et al., 1999; Ormerod et al., 2003; Perez-Martin et al., 2003).

Physical activity and stress can also influence adult neurogenesis, mainly in the SGZ (van Praag et al., 1999; Dranovsky and Hen, 2006). These effects are likely mediated by hormones such as adrenal steroids, which are released in stress responses and are known to affect hippocampal neurogenesis (Lennington et al., 2003).

One way of connecting the outside world and the progenitors of the SVZ and SGZ may be through vasculature. Molecules produced distally, such as hormones, may travel through the bloodstream to reach neurogenic niches in the brain. In songbirds, new neurons are integrated in seasonal waves in one of the nuclei controlling song production, the high vocal center (HVC). Testosterone, which also fluctuates seasonally in male songbirds, is directly involved in the survival of the new HVC neurons (Rasika et al., 1994), an effect which is mediated by BDNF (Rasika et al., 1999). Interestingly, testosterone also seems to induce angiogenesis and it is the vascular endothelial cells that

produce the BDNF responsible for the increased survival of new HVC neurons (Louissaint et al., 2002). This is a good example of how hormones, blood vessels and growth factors can act in concert to regulate adult neurogenesis. Similar interactions may exist in the mammalian brain, as SGZ neurogenesis and angiogenesis are closely associated (Palmer et al., 2000) and endothelial cells can support SVZ neurogenesis in culture (Leventhal et al., 1999).

An intriguing possibility is that neuronal activity may directly regulate adult neurogenesis and it has been proposed that neurogenesis occurs in the SVZ and not elsewhere because of the convergence of dopaminergic and serotonergic axonal inputs on the SVZ (Hagg, 2005). In fact, SVZ type C cells express D2L dopamine receptors and receive direct synaptic inputs from dopaminergic neurons, apparently regulating their proliferation (Hoglinger et al., 2004).

Intrinsic cues

In addition to extracellular signaling molecules, it is becoming clear that progenitors in the SVZ must have unique cell-intrinsic properties without which neurogenesis is impossible, even in the most permissive environment. The nature of these properties is currently a mystery, but almost certainly involves specific combinations of transcription factors and chromatin remodeling enzymes. The homeobox transcription factor Vax1 is expressed in the SVZ and appears to be an important regulator of SVZ neurogenesis, because Vax1 mutants display excessive proliferation, aberrant differentiation of ependymal cells and type B astrocytes and a failure of neuroblasts to reach the OB (Soria et al., 2004). Another homeobox transcription factor, Sox2, is expressed in SVZ progenitors. Sox genes are important for multiple neural stem cell functions throughout development (Wegner and Stolt, 2005). Sox2 and the basic helix-loop-helix transcription factor Mash1 appear to play a role in adult SVZ neurogenesis by affecting the number of dividing precursors (Ferri et al., 2004; Parras et al., 2004). The homeobox factor Dlx2 is expressed in type C and type A cells but not type B astrocytes (Doetsch et al., 2002). Dlx transcription factors seem to be essential to the production of most GABAergic OB interneurons, as seen in Dlx1/2 mutants (Bulfone et al., 1998). Other transcription factors are expressed in more restricted SVZ subpopulations and regulate the production of

specific subtypes of cells: Pax6 is required for the production of superficial granular and dopaminergic periglomerular interneurons of the OB (Hack et al., 2005; Kohwi et al., 2005), whereas Sp8 affects the production of Calretinin$^+$ interneurons but not dopaminergic or Calbindin$^+$ OB interneurons (Waclaw et al., 2006). Additionally, Olig2 is expressed by a small subpopulation of type B and C cells, and may be involved in the production of oligodendrocytes from the SVZ. Other transcription factors, such as Er81, Pbx1 and Emx1, have been identified in the SVZ (Redmond et al., 1996; Stenman et al., 2003; Willaime-Morawek et al., 2006) and may also play important roles in neuro/gliogenesis.

All these transcription factors (and others that remain to be identified) are though to be under a global transcriptional regulation mediated by chromatin remodeling enzymes (histone acetylases, deacetylases, methylases, demethylases and SWI/SNF complexes) and members of the Polycomb and Trithorax protein complexes, acting in concert to either repress or activate multiple genomic loci (Doetsch, 2003; Buszczak and Spradling, 2006). Many of these molecules are expressed in the SVZ (Lim et al., 2006) and their roles in this stem cell niche remain to be explored.

A better understanding of stem cell niches will help answer some important biological questions, such as the role of adult neurogenesis in the normal and diseased brain, and will allow us to manipulate stem cell properties for therapeutic purposes.

1.5 Neurotrophins

The neurotrophin hypothesis

Neurotrophins were first discovered due to their strong growth and survival-promoting effects on neurons. Today, the known roles of this family of secreted factors have increased to include almost all aspects of neuronal development and function, such as cell migration, cell fate decisions, axon and dendrite growth, synapse formation and synaptic plasticity.

In 1952, the first neurotrophin, Nerve Growth Factor (NGF), was identified during a search for molecules responsible for the loss of motor and sensory neurons upon removal of their target organs (Levi-Montalcini, 1987). In 1982, a second neurotrophin, Brain-

Derived Neurotrophic Factor (BDNF), was discovered (Barde et al., 1982) which promoted the growth and survival of different types of neurons. Both molecules function as target-derived survival factors for specific populations of neurons. As was initially described in the neurotrophin hypothesis: targets of neuronal innervation secrete limiting amounts of survival factors, which function to balance the number of innervating neurons with the size of their target tissue.

Later, Neurotrophin-3 (NT3) and NT4/5 were discovered and added to the family of neurotrophins, as well as NT6 and NT7, which are only found in fish. Secreted factors such as Glial cell-Derived Neurotrophic Factor (GDNF) and Ciliary Neurotrophic Factor (CNTF) belong to different protein families but are sometimes called neurotrophins, as they have also been shown to regulate survival, development and function in the nervous system.

Neurotrophin receptors

Neurotrophins are small homodimeric secreted proteins. They exert their effects through one or more of 4 different transmembrane receptors: p75 (tumor necrosis factor receptor family) was the first to be discovered (Chao et al., 1986; Johnson et al., 1986), closely followed by TrkA, TrkB and TrkC (receptor tyrosine kinase family) (Klein et al., 1989; Cordon-Cardo et al., 1991; Kaplan et al., 1991b; Kaplan et al., 1991a; Klein et al., 1991; Lamballe et al., 1991; Middlemas et al., 1991). While all neurotrophins bind to p75 with similar affinity, their interactions with the Trk receptors are more specific (Fig. 1.5). NGF binds TrkA but not the other Trks, while BDNF and NT4 are specific for TrkB receptor. NT3 preferentially binds to TrkC, though it can also bind TrkA and TrkB with lower affinity.

Neurotrophin receptor isoforms

Interestingly, neurotrophin receptors can be alternatively spliced, which alters both their affinity for neurotrophin ligands as well as their signaling properties. A short juxtamembrane sequence on the extracellular side of TrkA can be alternatively spliced to produce a receptor that binds NGF but not NT3 (Clary and Reichardt, 1994). TrkB has been shown in chicks to have a similar alternatively spliced version, which leads to an

Figure 1.5: Neurotrophin ligands and receptor isoforms [adapted from Roux and Barker (2002)]. The three Trk receptor genes (TrkA, B and C) can be alternatively spliced to give rise to several isoforms. TrkA and TrkB receptors can have a short amino acid sequence inserted into their extracellular domain (black rectangle), giving them enhanced specificity for specific neurotrophin ligands (see arrows for interactions between neurotrophins and receptor isoforms). Additionally, TrkB and TrkC can be spliced to produce a truncated version of the receptor, which lacks the intracellular kinase domain, and TrkC has an alternatively spliced region within the kinase domain (black square). The pan-neurotrophin receptor p75 can also be expressed as a full-length protein or a truncated isoform lacking most of the extracellular domain due to alternative splicing. This isoform of p75 does not bind neurotrophins. Red: cysteine-rich regions. Yellow: Leucine-rich regions. Grey: kinase domain. TM: transmembrane domain; JM: juxtamembrane domain; DD: death domain; CRD1-4: cysteine-rich domains of p75 receptor.

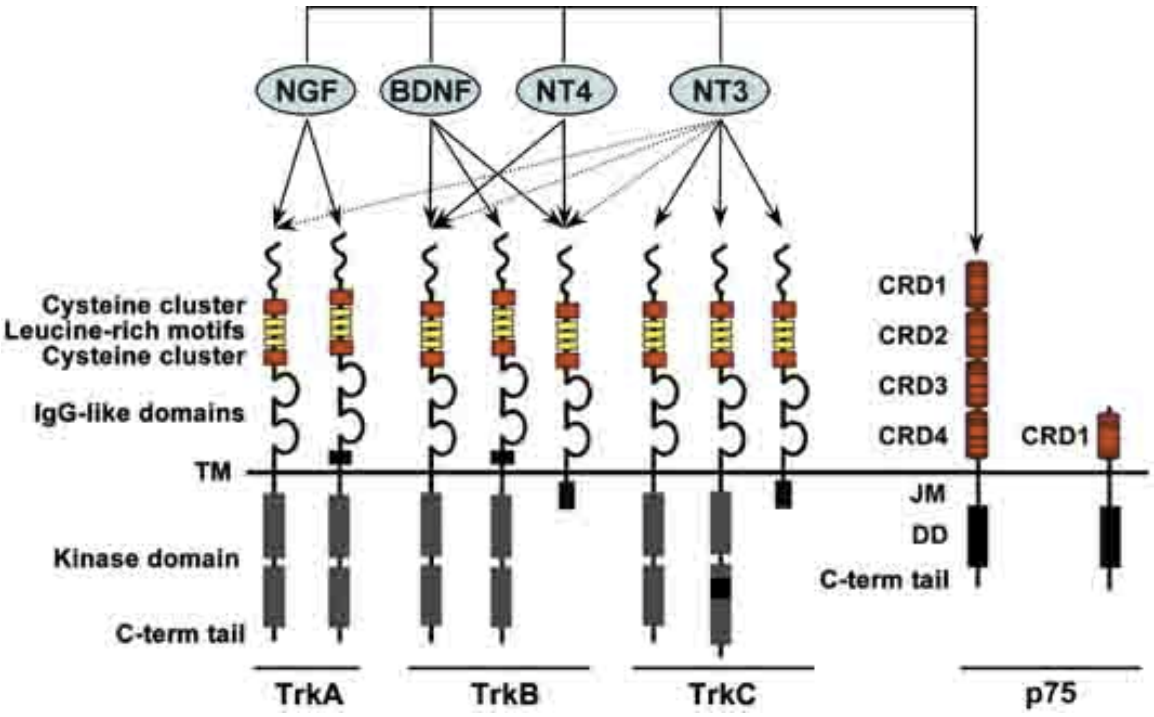
NGF
BDNF
NT4
NT3
Cysteine cluster
Leucine-rich motifs
Cysteine cluster
IgG-like domains
TM
Kinase domain
C-term tail
CRD1
CRD2
CRD3
CRD4
JM
DD
C-term tail
CRD1
TrkA
TrkB
TrkC
p75

isoform that can be activated by BDNF but not by NT4 or NT3 (Strohmaier et al., 1996). In the chick, separate populations of dorsal root ganglia (DRG) neurons express these isoforms (Boeshore et al., 1999), suggesting an important physiological role for this splice variant.

TrkB and TrkC also have splice variants that differ in the receptors' intracellular domain, including truncated isoforms which lack the kinase domain (Fig. 1.5) (Klein et al., 1989; Klein et al., 1990; Middlemas et al., 1991; Tsoulfas et al., 1993; Valenzuela et al., 1993). The function of these truncated receptors is still not well understood. Full length TrkB (TrkB-FL) is expressed in neurons while truncated TrkB (TrkB-TR) can be found in both neurons and glia. The expression level of TrkB-FL decreases in late embryonic and postnatal stages, whereas that of TrkB-TR increases. TrkB-TR is thought to act as a dominant-negative of TrkB-FL (Eide et al., 1996), preventing TrkB activation and inhibiting the pro-survival signaling of TrkB-FL in neurons (Dorsey et al., 2006). Different ratios of TrkB-FL to TrkB-TR can also influence dendritic growth patterns (Yacoubian and Lo, 2000). In glia, TrkB-TR has been proposed to allow these cells to form a barrier to diffusion of BDNF in the brain, thereby confining the actions of this trophic factor to specific regions (Biffo et al., 1995). Additionally, TrkB-TR has been shown *in vitro* to allow astrocytes to acquire BDNF from their surroundings through receptor endocytosis, which can later be released back into the medium (Alderson et al., 2000). Thus, TrkB-TR may allow astrocytes to regulate the spatial and temporal availability of TrkB ligands to TrkB-FL-expressing neurons. Other, more active roles for TrkB-TR are also possible. An emerging concept is that, despite lacking the kinase domain, TrkB-TR can activate intracellular signaling pathways of its own (Baxter et al., 1997; Rose et al., 2003). In astrocytes, TrkB-TR activation by BDNF triggers the release of intracellular Ca^{2+} through activation of an unknown G-protein and phospholipase C (Fig. 1.8H). The consequences of such signaling are not known, but it is clear that there is still much to be learned about this receptor.

As with Trk receptors, p75 exists in at least 2 different isoforms. Alternative splicing of exon 3 (extracellular region) leads to a p75 receptor that cannot bind neurotrophins, yet can interact normally with intracellular signaling molecules (Dechant and Barde, 1997) as well as with Trk receptors (von Schack et al., 2001). The role of this isoform is

at present not well understood, but it is expressed in neural tissues. Comparison of mice expressing only the truncated p75 isoform and mice lacking all p75 isoforms has shown that the latter have more severe defects in the nervous system as well as in large blood vessels, suggesting that truncated p75 might play a role in the development of these tissues (von Schack et al., 2001).

Trk receptor signaling

Full-length Trk receptors contain an intracellular tyrosine kinase domain which is essential for most known forms of signaling initiated by Trk receptor activation. Upon ligand binding, Trk receptors form homodimers and are activated by cross-phosphorylation of these intracellular domains. Several other kinases and adaptor molecules are then recruited and activated by Trk receptors.

The main signaling pathways downstream of Trk receptors are the PI3K/Akt pathway, the Ras/Raf/MAPK pathway, both initiated at the phosphorylated Y515 TrkB residue, and the PLCγ pathway, which is initiated at the phosphorylated Y816 TrkB residue (Fig. 1.6; equivalent residues exist in the other Trk receptors) (Huang and Reichardt, 2003; Reichardt, 2006). In many neurons, activation of PI3-kinase (PI3K) is the main pathway leading to survival-promoting signals. PI3K activates the kinase Akt, which, in turn, regulates several molecules involved in cell survival. Phosphorylation of BAD (a Bcl-2 protein family member) by Akt inhibits its pro-apoptotic effects by preventing its interaction with the anti-apoptotic protein Bcl-xL. Phosphorylation of FKHRL1 (a forkhead transcription factor) by Akt prevents it from activating transcription of a number of pro-apoptotic genes. Akt also phosphorylates IκB, which results in its degradation and release of NFκB, which can then activate transcription of several survival-promoting genes. In addition, PI3K can affect axon growth and neuronal differentiation.

Activation of MAP kinases (MAPK) by Trk receptors can occur through several pathways and is important for both neuronal survival and differentiation. Shc is an adaptor molecule that recruits Ras to the Y515 phospho-tyrosine residue of TrkB (or equivalent for TrkA, TrkC), thereby activating it. Ras then initiates a signaling cascade involving Raf, MEKs and MAPKs sequentially, ultimately activating transcription of a number of gene targets important for survival and differentiation. Another pathway starts

Figure 1.6: Trk and p75 neurotrophin receptor signaling pathways [adapted from Huang and Reichardt (2001)]. Binding of neurotrophin homodimers to the extracellular domains of Trk or p75 receptors leads to the recruitment of proteins that interact with specific sequences of the intracellular domain of these receptors. These interactions lead to the activation of signaling pathways such as the PI3K/Akt, the Ras/Raf/MAPK and the PLCγ pathways for Trk receptors, and the JNK, Ceramide, NFκB, Rho and other pathways for p75. Once active these signaling pathways can regulate survival, differentiation, neurite growth and synaptic plasticity, either directly or through regulation of gene expression. See text for additional details. Tyrosine residues (Y) on the intracellular domain of Trk are displayed as found on TrkB receptor, but equivalent residues are found in other Trk receptors. Green: adaptor proteins. Red: kinases. Blue: small G-proteins. Brown: transcription factors.

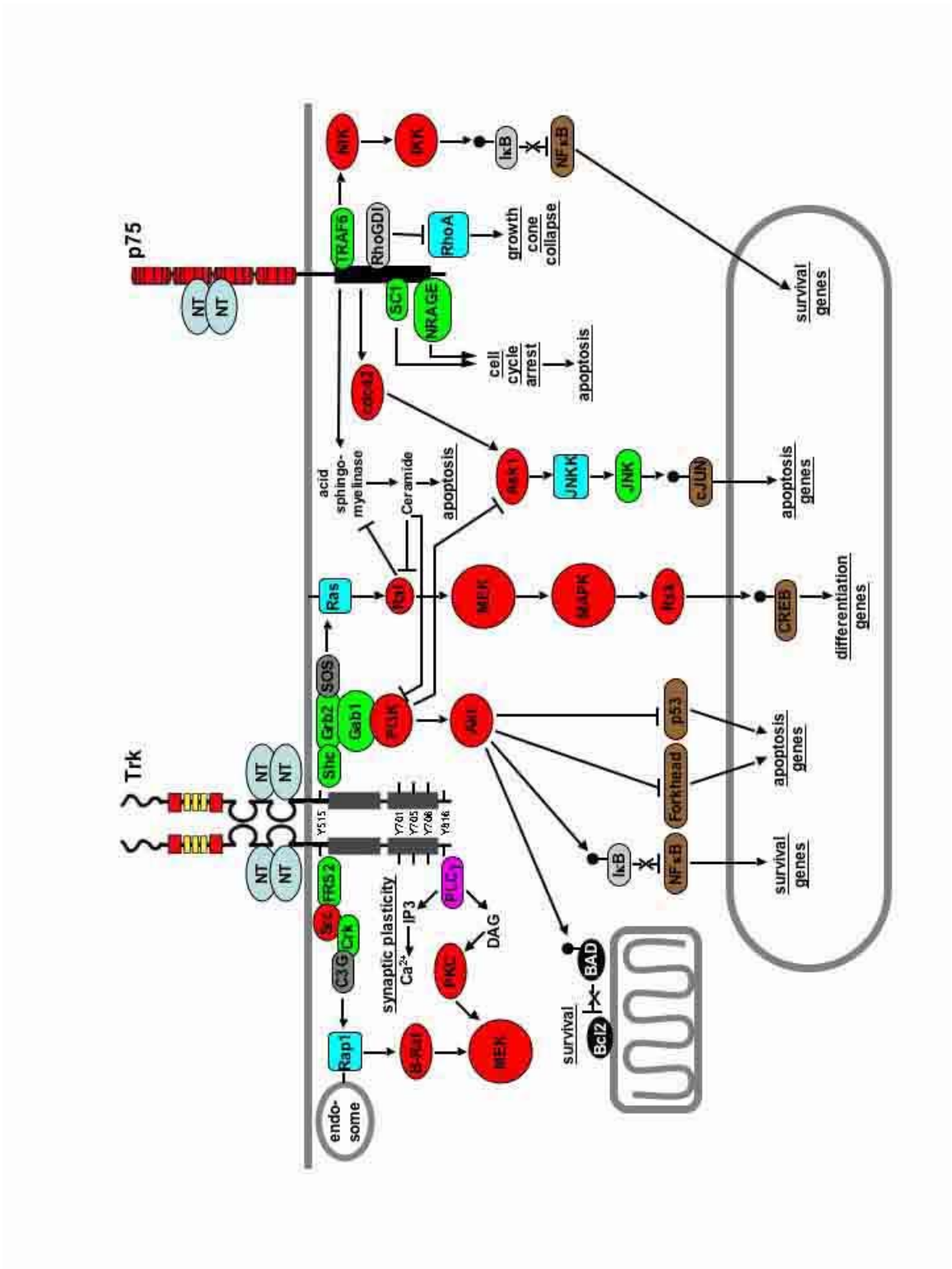
p75
NT
NT
TRAF6
RhoGDI
RhoA
growth cone collapse
NIK
IKK
IκB
NFκB
survival genes
SC1
NRAGE
cell cycle arrest
apoptosis
cdc42
acid sphingo-myelinase
Ceramide
apoptosis
MKK7
JNKK
JNK
cJUN
apoptosis genes
Ras
Raf
MEK
MAPK
Rsk
CREB
differentiation genes
Trk
NT
NT
NT
NT
SOS
Grb2
Gab1
PI3K
Akt
p53
Forkhead
apoptosis genes
Shc
Y515
Y701
Y705
Y706
Y816
IκB
NFκB
survival genes
FRS2
PLCγ
synaptic plasticity
IP3
Ca2+
DAG
Src
Crk
C3G
PKC
BAD
survival
Bcl2
Rap1
B-Raf
MEK
endo-some

with the adaptor protein FRS2, which recruits the kinase Src to the same Trk phospho-tyrosine residue Y515. Src causes the sequential activation of Rap1, Raf and the Erk signaling cascade (MEK/MAPK kinases). While the Shc/Ras pathway leads to transient activation of MAPKs, the FRS2/Src pathway leads to their prolonged activation. This can mean the difference between induction of proliferation in the case of transient signaling and differentiation in the case of prolonged signaling (Marshall, 1995; Grewal et al., 1999; Meakin et al., 1999). Thus, different cell types may respond differently to the same neurotrophin depending on their relative levels of Shc and FRS2, both of which compete for the same binding site on activated Trk receptors.

A different tyrosine residue, Y816 (TrkB), is required for the activation of PLCγ. Trk-activated PLCγ produces diacylglycerol (DAG) and inositol-P3 (IP3). These metabolites respectively induce activation of various protein kinase C (PKC) isoforms as well as the release of intracellular Ca^{2+}. This, in turn, will affect both neurite outgrowth and synaptic long-term potentiation (LTP).

An additional level of regulation involves the location of the activated receptors (Segal, 2003). Activated Trk receptors can move from the cell surface to the cytoplasm in endocytic vesicles. These vesicles are associated with several signaling molecules and can be retrogradely transported to the cell body, an event which is necessary for nuclear responses to Trk signaling. Interestingly, the pathways activated by Trk receptors vary in response to its subcellular localization: cell surface signaling is optimal for PI3K whereas endosomal signaling enhances MAPK cascades. Whether Trk receptors are activated at distal axons or near the cell body can also influence signaling outcome, and a recent study has shown this *in vivo* for TrkB signaling on retinal ganglion cells (Lom et al., 2002). Axonal stimulation of these cells in the tectum enhances dendritic growth in the retina, whereas dendritic activation of TrkB has the opposite effect.

Therefore, neurotrophins can elicit multiple different signaling pathways, leading to different cellular outcomes depending on variables such as the location of the receptor and which signaling molecules are expressed in a given cell type.

p75 receptor signaling

The role of p75, and even whether it leads to any significant signaling events, was at first difficult to determine. Though still less well understood than Trk receptors, p75 is now one of the most exciting molecules in neurotrophin research, with a surprising diversity of roles and interactions with several signaling pathways (Fig. 1.6).

Neurotrophin binding to p75 induces the Jun kinase (JNK) signaling cascade. This pathway is an important mediator of apoptosis in neurons by activating p53 as well as inducing the expression of the pro-apoptotic Fas ligand.

Another way by which p75 activation can induce apoptosis is by activating acid sphingomyelinase. This enzyme then generates ceramide, which is known to control many signaling pathways to promote apoptosis and inhibit growth (Ruvolo, 2003). Among other things, ceramide can induce membrane ruffling, activate the JNK pathway and inhibit the Ras/Raf/MAPK pathway as well as the PI3K/Akt pathway.

p75 signaling is also linked to cell cycle arrest, which could lead to apoptosis or terminal differentiation of the cells involved. A number of molecules have been identified which interact directly with the p75 intracellular domain and can regulate cell cycle progression: the transcription factor SC-1 (Chittka and Chao, 1999) and the adaptor protein NRAGE (Salehi et al., 2000) induce cell cycle arrest, whereas the adaptor protein Bex1 promotes cell proliferation (Vilar et al., 2006). Ceramide production can also induce cell cycle arrest.

p75 can also affect neurite outgrowth through its regulatory effect on the GTPase RhoA (Yamashita et al., 1999). Active RhoA (RhoA-GTP) induces cytoskeleton contraction and thus inhibits neurite growth as well as cell migration. Once the GTP molecule bound to RhoA is hydrolized to GDP, RhoA becomes inactive (RhoA-GDP) until a guanine exchange factor replaces the GDP with a new GTP. This exchange can be blocked by a Rho-specific dissociation inhibitor (Rho-GDI), which is constitutively bound to the intracellular domain of p75. Binding of neurotrophins to p75 releases Rho-GDI, which is then free to block RhoA activation, facilitating neurite outgrowth (Yamashita and Tohyama, 2003). Interestingly, non-neurotrophin ligands found in myelin can have the opposite effect and strengthen the Rho-GDI-p75 interaction (see below for details).

Adding to the complexity of this receptor's signaling properties is the fact that, in addition to its pro-apoptotic effects, it can also promote pro-survival pathways (Hamanoue et al., 1999; Middleton et al., 2000): binding of neurotrophins to p75 leads to the binding of Traf6 to the intracellular domain of p75. This interaction recruits a number of kinases, ultimately leading to the phosphorylation of IκB kinase-β (IKK-β). IKK-β then phosphorylates the IκB/NFκB complex on IκB, releasing the transcription factor NFκB, which can then travel into the nucleus and activate pro-survival genes.

Trk/p75 interactions

p75 signaling can modulate Trk receptor signaling and vice-versa, usually blocking each other's effects (Fig. 1.6): ceramide generated by p75 activation inhibits Ras/Raf and PI3K/Akt signaling. Ceramide can also silence Trk signaling by phosphorylating serine residues directly on these receptors. Conversely, Trk-induced Ras/Raf and PI3K/Akt signaling block p75 signaling via the JNK and ceramide pathways but do not affect the NFκB pathway. Consequently, p75 is much more effective at inducing apoptosis when activated by neurotrophins in the absence of Trk receptors, whereas in the presence of Trks, these receptors can act synergistically to promote neuronal survival (Yoon et al., 1998).

In addition to the cross-talk between signaling pathways downstream of p75 and Trk neurotrophin receptors, p75 can interact directly with Trks and modulate their activities in a number of ways. These interactions increase the affinity of Trk receptors for their ligands, which may be important *in vivo* to ensure neuronal survival under limiting amounts of neurotrophins. p75 can also sharpen specificity of Trk receptors for their preferred neurotrophins: binding of NT3 to TrkA and TrkB or of NT4 to TrkB is significantly attenuated in p75/Trk receptor complexes (Benedetti et al., 1993; Clary and Reichardt, 1994; Lee et al., 1994; Bibel et al., 1999). Finally, p75 bound to Trk receptors can recruit ubiquitinases to tag these receptors and facilitate their endocytosis, which is essential for certain types of Trk signaling (see above) (Geetha et al., 2005). p75 can interact with both full-length and truncated isoforms of Trk receptors (Bibel et al., 1999) and it has been suggested that p75/TrkB-TR complexes induce the formation of dendritic filopodia, which are often precursors of dendritic spines (Hartmann et al., 2004).

p75 interactions with other receptors

p75 also interacts with other cell surface receptors (Fig. 1.7) (Barker, 2004). p75 (but not Trks) binds pro-neurotrophins with an affinity 1000-fold higher than its affinity for neurotrophins. Pro-neurotrophins are partially processed forms of neurotrophins in which the pro-domain, an N-terminal sequence necessary for proper protein folding and secretion, has not been cleaved away. These pro-forms of neurotrophins are secreted into the extracellular medium and have a much stronger apoptotic effect on $p75^{+}$ cells than mature neurotrophins (Lee et al., 2001). However, these events require another transmembrane molecule, Sortilin, which interacts directly with p75 to form a receptor complex (Nykjaer et al., 2005).

Another receptor complex is known to contain p75. Nogo receptor (NogoR) binds to myelin proteins such as myelin-associated glycoprotein (MAG), oligodendrocyte myelin glycoprotein (OMgP) and Nogo66, leading to axonal growth cone collapse, which prevents axon regeneration after injury (McKerracher and Winton, 2002). Lingo1 is a recently-discovered transmembrane molecule that can interact with NogoR. These receptors alone are not sufficient to mediate the growth-inhibitory effects of NogoR ligands, consistent with their lack of known intracellular signaling sequences (Mi et al., 2004). For signaling to occur, NogoR and Lingo1 must interact directly with p75 to form a trimeric receptor complex. Binding of MAG, Nogo66 or OMgP to NogoR enhances the activation of RhoA by p75, leading to axonal growth cone collapse (Wang et al., 2002; Wong et al., 2002; Yamashita and Tohyama, 2003; Mi et al., 2004).

Roles of neurotrophins in the peripheral nervous system

Neurotrophins have a critical role in the survival of most neurons of the peripheral nervous system (PNS) (Huang and Reichardt, 2001). The sources of neurotrophins are either the final innervation target for these neurons (muscle, skin, viscera, etc.) or intermediate tissues, which provide trophic support while these neurons' axons are growing towards their target. In most cases, individual neuronal populations express a single Trk receptor and are lost in mutants of that receptor or of its ligand(s). DRG and trigeminal ganglia, which contain several types of sensory neurons in close proximity

Figure 1.7: p75 interactions with other receptors [adapted from Bandtlow and Dechant (2004)]. p75 receptor can activate intracellular signaling on its own or in a complex with other cell surface receptors. In complexes with Trk receptors, p75 acts as a modulatory receptor, increasing binding affinity of the complex for specific neurotrophin (NT) ligands, whereas the binding of other NT ligands is reduced. Signaling from this complex promotes outcomes such as cell survival and differentiation. The recently discovered p75/Sortilin complex triggers cell death when activated by binding of the unprocessed precursor form of NGF, and presumably of other unprocessed neurotrophin precursors (pro-NT). The formation of a complex between $p75^{NTR}$ and NogoR is stimulated by binding of one of three different myelin-derived inhibitory protein ligands, oligodendrocyte myelin glycoprotein (OmgP), Nogo66, or myelin-associated glycoprotein (MAG). For signal transduction, the p75/NogoR complex requires Lingo1, a novel transmembrane protein. This ternary complex might prevent regeneration of injured nerve fibers in the CNS through activation of RhoA. On oligodendrocytes, Rac is activated as a part of a $p75^{NTR}$-dependent proapoptotic pathway. Red: cysteine-rich domain. Yellow: leucine-rich domain. Loop: Immunoglobulin-like domain. Black: death domain. Gray: tyrosine kinase domain. Orange: Vps10p cysteine-rich domain. Blue: Fibronectin type III domain. Gray horizontal line: cell membrane.

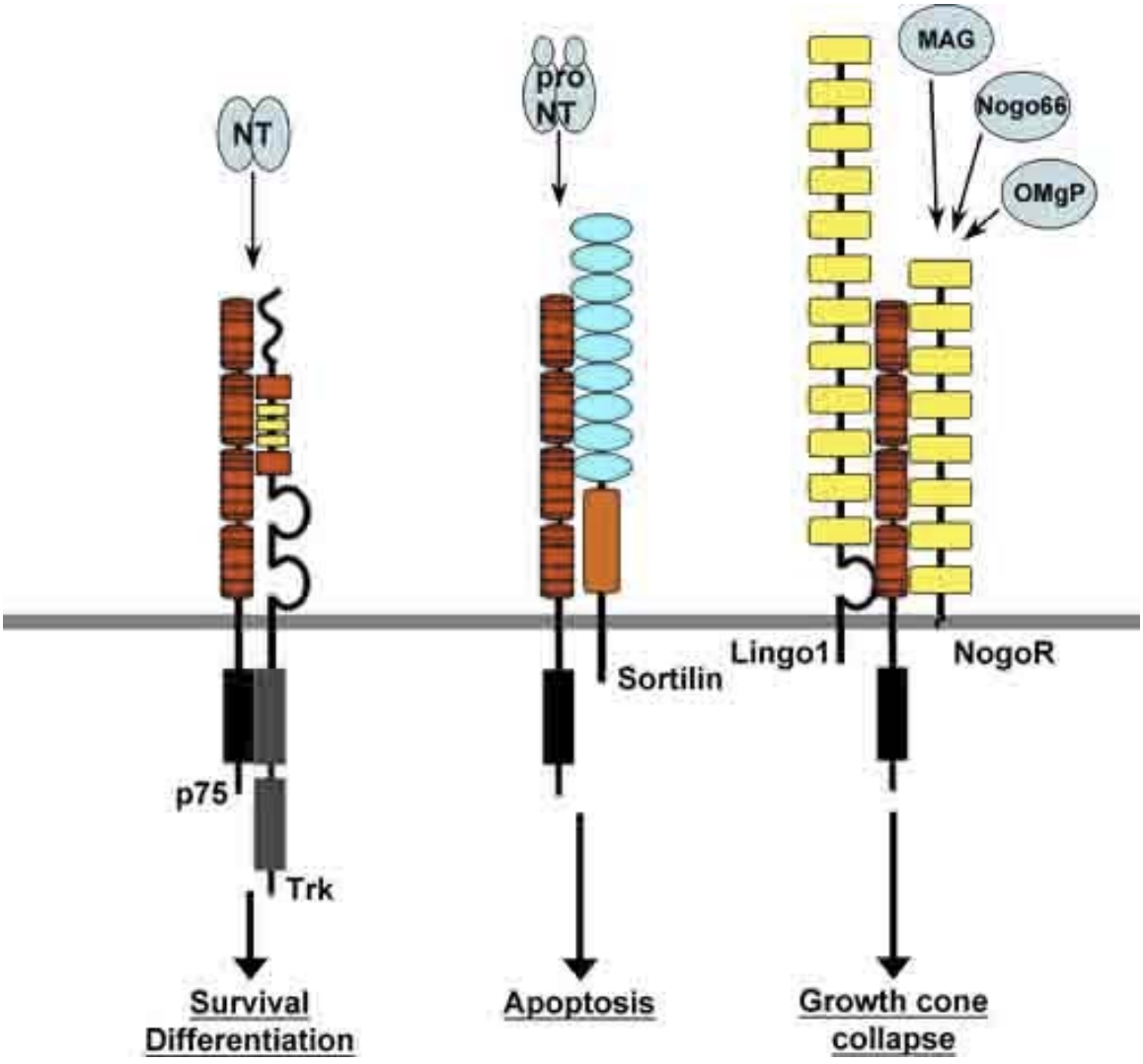
NT
pro
NT
MAG
Nogo66
OMgP
Sortilin
Lingo1
NogoR
p75
Trk
Survival
Differentiation
Apoptosis
Growth cone
collapse

with each other, are a good example of this dependence. Almost all nociceptive neurons express TrkA and are lost in TrkA or NGF mutants (Crowley et al., 1994; Smeyne et al., 1994), whereas proprioceptive neurons at spinal cord levels express TrkC and are completely lost in TrkC or NT3 mutants (Farinas et al., 1996). Sympathetic ganglia neurons are almost completely lost in TrkA or NGF mutants (Crowley et al., 1994; Smeyne et al., 1994), whereas enteric and parasympathetic neurons are much more dependent on GDNF and Neurturin (both of the same growth factor family), respectively, for survival and migration (Huang and Reichardt, 2001). All neurons of the nodose-petrosal (N-P) ganglion, which innervate visceral sensory organs, express TrkB and all are lost in TrkB mutants (Conover et al., 1995; Huang et al., 1999a). Depending on the neurotrophin expressed by their particular target organ, 50% of N-P neurons are lost in BDNF mutants and the other 50% are lost in NT4 mutants. Spinal cord motor neurons initially seemed to respond to a broad, redundant array of neurotrophic factors, including BDNF, NT3, NT4 and members of the GDNF and CNTF families of growth factors, because mutants of any one or even multiple of these factors display only moderate losses among this cell type. It is now apparent that rather than redundance in the roles of these growth factors, there is a great diversity of motor neuron subpopulations, each of which has very specific trophic requirements, but none of which accounts for a significant proportion of the total motor neuron pool (Kucera et al., 1995; Tanabe and Jessell, 1996; Garces et al., 2000; Oppenheim et al., 2000). In some instances, neurons may express more than one Trk receptor, in which case their survival can be sustained by several neurotrophins. This is the case of neurons in the cochlear ganglia, which innervate inner hair cells of the inner ear. These neurons express both TrkB and TrkC receptors and can be stimulated to survive by both BDNF and NT3 (Coppola et al., 2001; Farinas et al., 2001). However, because their target tissue expresses NT3 but not BDNF, single mutants of either NT3 or TrkC have a nearly complete loss of cochlear ganglia neurons, whereas deletion of TrkB or BDNF does not affect them. Therefore, either due to tightly regulated expression of single receptors in innervating neurons or to restricted expression of neurotrophins by the target organ, neurons of the PNS appear to be highly dependent on very specific neurotrophic signals for survival. Certain neurons of the DRG, trigeminal and vestibular ganglia express different neurotrophin receptors at different maturation

stages, causing them to switch neurotrophin dependence over the course of their development (Paul and Davies, 1995; Pinon et al., 1996; Molliver et al., 1997; Enokido et al., 1999; Hashino et al., 1999; Baudet et al., 2000; Doxakis et al., 2000; Acosta et al., 2001).

Roles of neurotrophins in the central nervous system

Neurotrophins are abundantly expressed in the CNS, yet their role there has been more difficult to discern. Contrary to what happens in the PNS, mutants for either neurotrophins or their receptors have apparently normal brains with no obvious cell loss. Both BDNF and TrkB are widely expressed in the developing and adult brain (Conner et al., 1997; Yan et al., 1997a; Yan et al., 1997b), most notably in the cortex, hippocampus and cerebellum. BDNF is expressed in excitatory pyramidal neurons but not in inhibitory interneurons, while TrkB is expressed in both. Survival defects have been reported in TrkB-KO and BDNF-KO mice, with several studies reporting increased apoptosis in several regions of the CNS, including cortex, striatum, hippocampal dentate gyrus, thalamus and cerebellum (Minichiello and Klein, 1996; Alcantara et al., 1997; Schwartz et al., 1997). Also, NGF and BDNF regulate the survival and maturation of basal forebrain cholinergic neurons (Chen et al., 1997; Ward and Hagg, 2000), which play an important part in learning and memory. However, these defects are less striking than in the PNS and take weeks rather than hours to develop, usually noticeable only in the 2nd and 3rd weeks after birth. This longer time scale of effects makes it technically difficult to study the requirements for neurotrophins in the CNS, as mice usually die soon after birth from the more serious PNS defects. Alternatively, this could imply that the roles these molecules play in the PNS and CNS are different. Xu et al. (Xu et al., 2000a) have used conditional TrkB knockout mice to circumvent the short survival of TrkB mutants. Targeting the deletion of TrkB to mature neurons in the cortex and hippocampus, these authors showed that TrkB is necessary for dendrite development of cortical pyramidal neurons. Higher levels of apoptosis were also detected in these neurons, but once again, only several weeks after the dendritic phenotype. It is possible that the death of these neurons is caused by the improper development of their dendrites, which would significantly reduce their electrical activity, rather than a direct consequence of the loss of

TrkB signaling. Observations by other authors are consistent with this interpretation: in conventional TrkB-KO mice, cerebellar Purkinje neurons also have defects in dendrite arborization but are unaffected in terms of cell survival (Minichiello and Klein, 1996). Interestingly, these defects were more pronounced in TrkB/TrkC double mutants and apoptosis was drastically increased among cerebellar and hippocampal granular neurons. It is possible that, contrary to the PNS, neurons in the CNS rely on more than one neurotrophin for survival.

However, deletion of BDNF or TrkB alone is sufficient to cause significant defects in synapse formation and plasticity in the CNS, a process mainly studied in excitatory synapses (Blum and Konnerth, 2005). BDNF is released at synapses in an activity-dependent manner, from both the pre and post-synaptic sides (Fig. 1.8A-C). Upon binding to TrkB locally, BDNF can modulate the activity of those synapses in many ways. At the pre-synaptic side, activation of TrkB can induce MAPK to phosphorylate Synapsin, leading to an increased release of synaptic vesicles/neurotransmitters (Fig. 1.8D). BDNF also increases membrane depolarization and neuron firing rates through post-synaptic mechanisms: activation of TrkB can lead to phosphorylation of NMDA receptors, facilitating the depolarizing influx of Na^+ and Ca^{2+} ions (Fig. 1.8E). Another Na^+/Ca^{2+} depolarizing channel that can be activated by TrkB is TrpC3, which is activated through the PLCγ-IP3-Ca^{2+} pathway (Fig. 1.8F). TrkB interacts directly with a Na^+ channel, $Na_v1.9$, allowing BDNF to act like a classic neurotransmitter, having an almost instant effect on membrane depolarization (Fig. 1.8G). All these mechanisms allow BDNF and TrkB to induce longer-lasting changes to synapses, in the form of long-term potentiation (LTP, a lasting strengthening of a synapse) and increasing the number of synapses. These effects on synaptic plasticity seem to depend heavily on TrkB signaling through the PLCγ-IP3-Ca^{2+} pathway (Minichiello et al., 2002). Interestingly, p75 can also regulate synaptic plasticity, though with opposite effects, weakening synapses (long-term depression, or LTD) and eliminating them. This occurs through the binding of pro-BDNF to p75, which seems to regulate the expression of AMPA receptor subunits as well as the NMDA receptor subunit NR2B (Schweigreiter, 2006).

Figure 1.8: BDNF and TrkB at synapses [adapted from Blum and Konnerth (2005)]. ***A***-***C***: neuronal release of BDNF at synapses. ***A***: postsynaptic release of BDNF requires postsynaptic Ca^{2+} influx through ionotropic glutamate receptors [*N*-methyl-D-aspartate receptor (NMDAR); α-amino-3-hydroxy-5-methyl-4-isoxazolepropionic acid receptor (AMPAR)] or voltage-operated Ca^{2+} channels (VOCC). ***B***: dual requirement of extracellular and intracellular Ca^{2+} for activity-dependent BDNF secretion. Ca^{2+} influx through N-type VOCC drives Ca^{2+}-dependent Ca^{2+} release from intracellular stores by ryanodine receptors (RyR). ***C***: Ca^{2+}-influx-independent neurotrophin release involves PLC activation and IP3-mediated Ca^{2+} release from intracellular stores. Glutamate-induced neurotrophin release is mediated by metabotropic glutamate receptor type I (mGluRI) and subsequent activation of PLC. VOSC, voltage-operated Na^{+} channel. ***D***, Regulation of synaptic transmission through BDNF. BDNF facilitates presynaptic release of glutamate or GABA through TrkB/MAPK-mediated phosphorylation of the synaptic vesicle protein Synapsin. ***E***-***G***, TrkB/BDNF mechanisms of rapid membrane depolarization at synapses. ***E***: TrkB-FL-dependent phosphorylation activates the nonreceptor protein tyrosine kinase Fyn that in turn increases the open probability of postsynaptic NMDA receptors. ***F***: TrkB/PLC-γ-mediated, IP3-dependent Ca^{2+} store depletion activates ion influx through transient receptor potential C3 (TrpC3) channels. ***G***: BDNF/TrkB activates the Na^{+} channel $Na_v1.9$. The resulting depolarization activates VOCC and thus produces Ca^{2+} influx. ***H***: truncated TrkB receptor (TrkB-TR) signaling in astrocytes. TrkB-TR mediates G protein-dependent PLC activation, IP3-dependent Ca^{2+} release from Ca^{2+} stores, and subsequent activation of store-operated ion channels (SOCC).

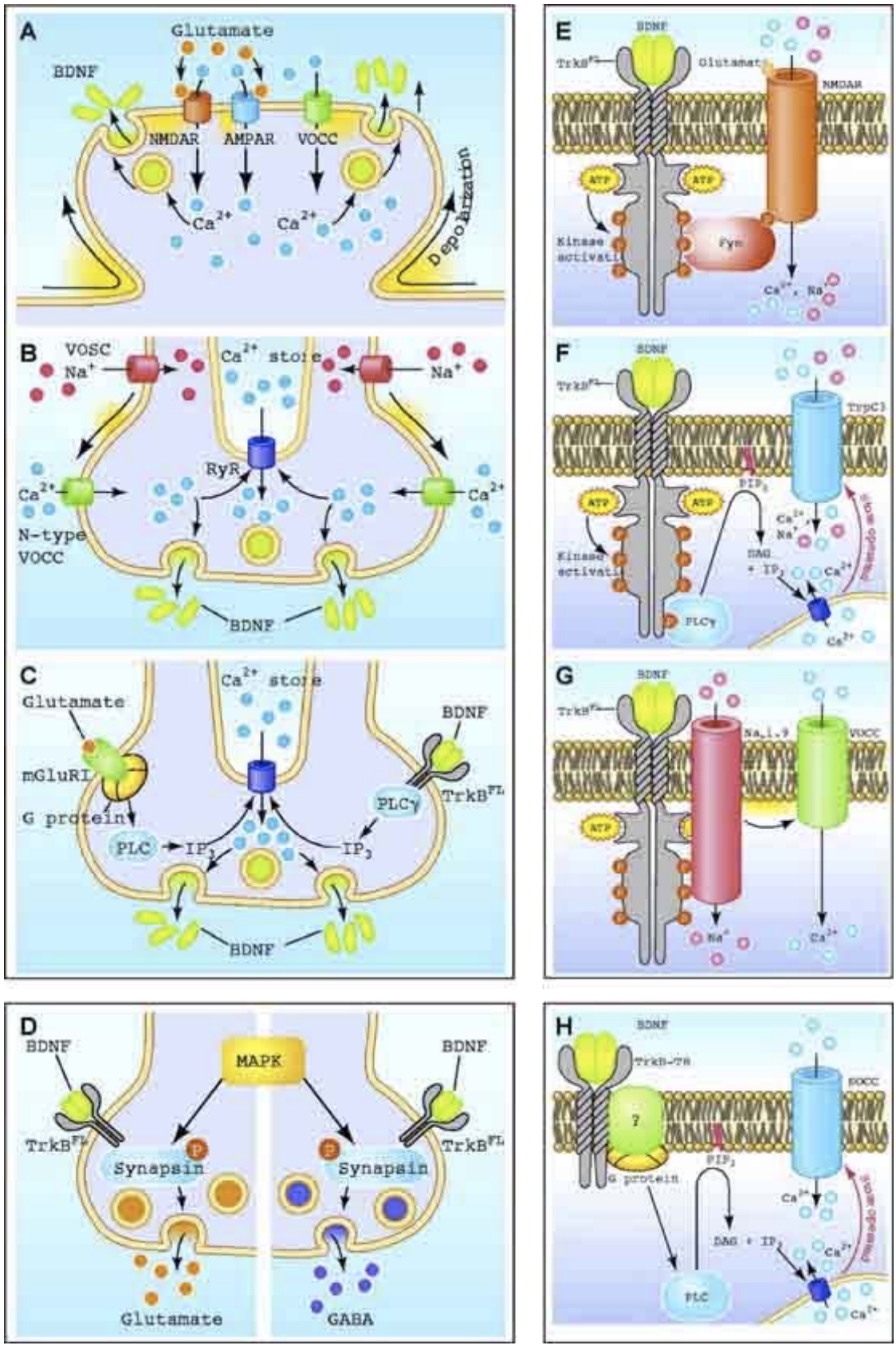
A
Glutamate
BDNF
NMDAR
AMPAR
VOCC
Depolarization
B
VOSC
Na+
Ca2+ store
RyR
N-type
VOCC
BDNF
C
Glutamate
Ca2+ store
BDNF
mGluRI
G protein
PLCγ
TrkBFL
PLC
IP3
BDNF
D
BDNF
MAPK
BDNF
TrkBFL
Synapsin
Synapsin
TrkBFL
Glutamate
GABA
E
BDNF
TrkBFL
Glutamate
NMDAR
ATP
ATP
Kinase
Fyn
F
BDNF
TrkBFL
TrpC3
ATP
ATP
PIP2
DAG
+ IP3
PLCγ
G
BDNF
TrkBFL
VOCC
ATP
H
BDNF
TrkB-TR
VOCC
?
PIP2
G protein
DAG + IP3
PLC

BDNF also affects synapses in inhibitory neurons. One example is the development/maturation of GABAergic interneurons (Woo and Lu, 2006). BDNF accelerates the maturation of inhibitory interneurons in multiple brain regions (cortex, hippocampus, cerebellum), increasing dendrite branching and elongation, promoting formation of inhibitory synapses and production of GABA, all of which is probably vital for the development of critical periods (defined window of time during which a given brain circuit is still plastic/modifiable). In fact, in transgenic mice overexpressing BDNF in the forebrain, the maturation of GABAergic interneurons, more specifically of the Parvalbumin^{+} subpopulation of interneurons, was significantly accelerated (Huang et al., 1999b; Aguado et al., 2003). These mice showed a precocious development of visual acuity and an earlier initiation and termination of the critical period for ocular dominance plasticity. Conversely, deletion of TrkB causes significant defects in synapse formation of cerebellar granule interneurons *in vivo* (Rico et al., 2002). Intriguingly, once inhibitory interneurons mature (during which GABAergic synapses shift from excitatory to inhibitory), BDNF has different effects on their synaptic activity, inhibiting them rather than promoting them. The effects of BDNF/TrkB signaling on inhibitory synaptic activity are, again, pre-synaptic, modulating the frequency of release of GABA neurotransmitter, as well as post-synaptic, regulating GABA receptor endocytosis.

As mentioned above for both excitatory (cortical pyramidal and cerebellar Purkinje neurons) and inhibitory neurons, neurotrophins have important roles in neurite morphology. It is particularly interesting that these roles appear to be instructive rather than merely permissive in establishing particular patterns of dendritic arborization. Studies in the visual cortex have shown that different neurotrophins promote dendritic growth of pyramidal neurons in a layer-specific manner (BDNF in layer 4, NT4 in layers 5/6, NT3 in layer 6 neurons; Fig. 1.9) and can even regulate each other's effects (BDNF inhibits NT3-mediated growth in layer 6 and NT3 inhibits BDNF-mediated growth in layer 4) (McAllister, 2001). Axonal growth is also regulated by neurotrophins, which promote both sprouting of axon terminals and seem to provide growth cone guidance cues *in vitro*. However, the relevance of such mechanisms *in vivo* is not clear, as neurotrophin mutants have no obvious axon guidance defects (McAllister, 2001).

Figure 1.9: Effect of neurotrophins on dendrites of visual cortex pyramidal neurons [adapted from McAllister et al. (1995)]. Total dendritic length, the number of primary dendrites, the number of dendritic branches and the number of protospines are all affected upon exposure to neurotrophins. The most dramatic and consistent modifications of dendritic arborization are caused by the TrkB ligands BDNF and NT4, though responses to these two factors are clearly distinct. NT3 treatment enhances dendrites of neurons mainly in layer 6, whereas NGF causes minimal dendritic changes in all cortical layers. L4-6: cortical layers 4-6, layer 6 being the deepest.

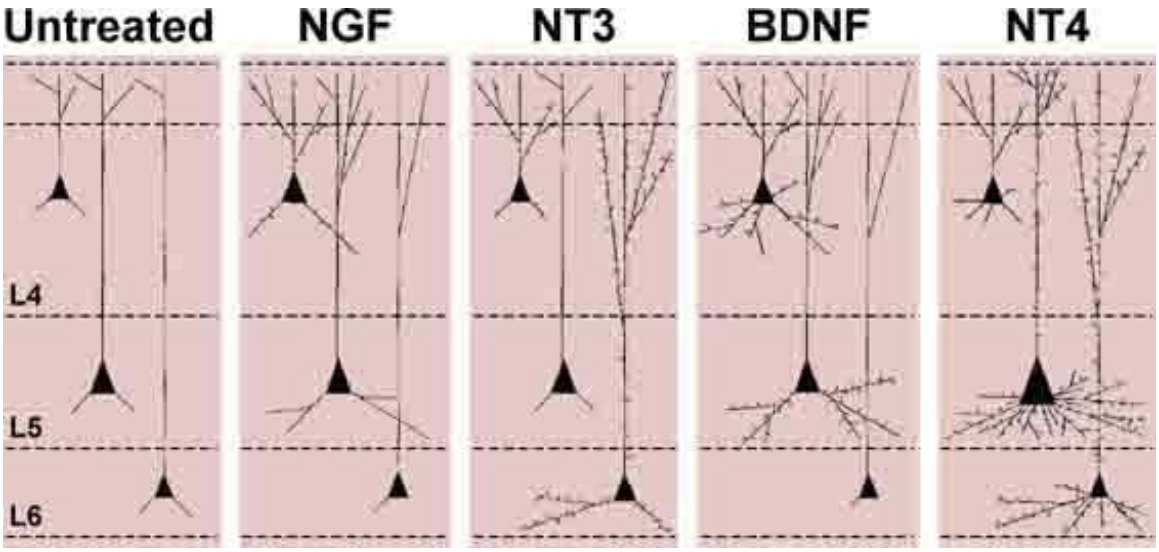
Untreated
NGF
NT3
BDNF
NT4
L4
L5
L6

Thus, neurotrophins in the CNS, and in particular BDNF and its receptor TrkB, play important roles in neurite outgrowth, synaptic formation and synaptic plasticity, while their survival-promoting role appears less relevant, perhaps even a secondary effect of their functional roles.

Neurotrophins in disease and therapy

The strong anti-apoptotic activity of neurotrophins in the PNS and their growth-promoting effects on axons and dendrites makes them good candidates to serve as therapeutic agents in neurologic trauma, preventing the death of neurons in the affected areas. Evidence for the effectiveness of neurotrophins in treating spinal cord injuries (acute trauma) is growing. Grafting BDNF-expressing cells at the site of a spinal cord lesion can protect damaged neurons from apoptosis and promote axonal re-growth (Murray et al., 2002). For similar reasons, neurotrophins have been investigated as possible treatments for chronic neurodegenerative diseases such as Alzheimer's, Parkinson's, Huntington's disease and amyotrophic lateral sclerosis (Connor and Dragunow, 1998), where they could act as neuroprotectants preventing the death of the affected neurons. In Alzheimer's disease in particular, BDNF may be one of the causes of the degeneration of basal forebrain cholinergic neurons (BFCNs), as its levels in Alzheimer's patients are significantly reduced in several cortical and hippocampal regions innervated by BFCNs (Fumagalli et al., 2006b). Furthermore, BDNF has been shown to promote survival and differentiation of BFCNs *in vivo* (Alderson et al., 1990; Nonomura and Hatanaka, 1992) and *in vivo* (Ward and Hagg, 2000) and BDNF can modulate cholinergic synapse function (Knipper et al., 1994). Therefore, restoring the levels of BDNF to the affected regions may help to stop the progression of this disease. Similarly, there may be a close relationship between BDNF and TrkB levels and the survival of dopaminergic neurons of the substantia nigra, which are lost in Parkinson's patients (Fumagalli et al., 2006a).

BDNF and TrkB also seem to be closely associated with mood disorders such as anxiety and depression (Kuipers and Bramham, 2006; Castren et al., 2007; Tanis et al., 2007). A human polymorphism of BDNF that impairs secretion has been linked to hippocampal defects and increased anxiety (Egan et al., 2003; Chen et al., 2006). Nearly

all types of antidepressant therapies have been shown to increase the levels of BDNF mRNA and protein in hippocampus and prefrontal cortex, which are atrophied in depressed individuals. Moreover, BDNF has been shown experimentally to be necessary and sufficient to elicit the antidepressant effects observed from these therapies. Antidepressants seem to also increase the levels of hippocampal neurogenesis, an effect which may participate in the treatment of depression (Drew and Hen, 2007). It is not yet known exactly how BDNF is involved in ameliorating the symptoms of depression. BDNF may enhance the survival of neurons in the hippocampus and prefrontal cortex, enhance synaptic plasticity to modify the output of certain brain circuits, enhance the production of new neurons to counteract the anti-neurogenic effects of stress, or a combination of these.

BDNF and TrkB are also important in the regulation of eating behavior by hypothalamic circuits (Pelleymounter et al., 1995; Kernie et al., 2000; Xu et al., 2003) and a human patient with a mutated TrkB receptor has been described with severe hyperphagic obesity (Yeo et al., 2004). Mutations in TrkA receptor are linked to another human disease, characterized by insensitivity to pain, mental retardation, fever and inability to sweat (Indo, 2001).

One major problem in using neurotrophins such as BDNF for therapy has been the ability to deliver it to the areas in need, because it will not cross the blood-brain barrier and systemic administrations have the risk of leading to unwanted side effects such as increased seizures (too much neuronal excitation) and hyperalgesia (due to axonal sprouting in the spinal cord). No therapies have been developed that successfully overcome these problems, but several methods are being tried, one of which is to implant in affected areas cells that were modified to secrete BDNF, a method that is showing promise in spinal cord injury models. Of particular interest, neural stem cells may be a good source of such cells, since they seem to secrete a number of trophic factors and may help create a microenvironment conducive to regeneration in several types of brain lesions. Nonetheless, the greatest hope for future uses of stem cells is the possibility of using them to generate new cells (either *in vitro* or endogenously) to replace those that are lost due to disease. In that field, neurotrophins can help by enhancing the survival of

the cells generated and/or promote their proper differentiation. Neurotrophins may also promote endogenous repair from adult neural stem cells (see below).

Neurotrophins in neurogenesis

Neurotrophins seem to act mainly on post-mitotic cells. However, some reports suggest that these molecules may act on proliferating progenitor pools as well, directly influencing neurogenesis.

Many breakthroughs in the field of adult neurogenesis have come from research using songbirds as models. In these animals, there is a continuous process of death and incorporation of interneurons and projection neurons in the High Vocal Center (HVC) (Nottebohm, 2002a), a brain nucleus involved in the control of song production. Seasonal fluctuations affect this process, as neurons born in the fall and spring are incorporated in much higher numbers than those born at other times of the year, correlating with peaks in testosterone levels (Rasika et al., 1994) and increased singing (Li et al., 2000). Interestingly, both testosterone and singing seem to increase the number of new HVC neurons by increasing the expression of BDNF in this nucleus (Rasika et al., 1999; Li et al., 2000). The requirement for BDNF seems to be limited to a short time window between 14 and 20 days after the new neurons are born (Alvarez-Borda et al., 2004). Testosterone drives angiogenesis in the HVC and endothelial cells are the main source of BDNF in this region (Louissaint et al., 2002). BDNF in the HVC seems to exert its effect by promoting the survival of post-mitotic neurons rather than through a direct action on progenitor cells.

The role of neurotrophins in mammalian adult neurogenesis is less clear. Nitric oxide (NO), which is produced in the brain by neurons, endothelial cells and microglia, is a known regulator of cell proliferation, promoting neuronal differentiation at the expense of proliferation. NO may affect adult mammalian neurogenesis, as blocking endogenous NO increases proliferation in the SVZ and dentate gyrus (Cheng et al., 2003; Packer et al., 2003). BDNF appears to play a role in this regulation, promoting the expression of neuronal NO synthase (nNOS) and the production of NO in differentiating neurons (Xiong et al., 1999; Cheng et al., 2003). The interactions between NO and BDNF are not clear, but it is possible that both are part of a feedback loop used to control neural

progenitor proliferation/differentiation. Another neurotrophin, CNTF, has been suggested to increase adult neurogenesis in hypothalamic nuclei involved in regulating appetite and eating behaviors (Kokoeva et al., 2005). This neurogenic effect seems to be at the source of the weight loss effect of this neurotrophin, which has raised interest as a therapy for obesity. CNTF has also been reported to increase proliferation in neurogenic areas of the adult brain: the SVZ and hippocampus (Emsley and Hagg, 2003). Interestingly, BDNF also elicits marked weight loss (Pelleymounter et al., 1995; Kernie et al., 2000; Xu et al., 2003), though no effect of BDNF on hypothalamic neurogenesis has been reported. Its effect on hippocampal and SVZ neurogenesis, however, have been tested directly. BDNF-KO mice exhibit increased apoptosis in SVZ and hippocampal dentate gyrus (Linnarsson et al., 2000). In the hippocampus, BDNF infusion seems to cause an increase in the number of new neurons in both the dentate gyrus, where neurogenesis normally occurs, and in the hilus, where it does not (Scharfman et al., 2005). Administration of exogenous BDNF to the lateral ventricle walls has similar effects on SVZ neurogenesis. BDNF has been reported to increase by 2 to 3-fold the production of new olfactory bulb interneurons as well as to promote the production of striatal medium spiny projection neurons, a cell type normally not produced in the adult brain (Zigova et al., 1998; Benraiss et al., 2001; Pencea et al., 2001; Chmielnicki et al., 2004). It is not clear whether these new ectopic neurons arise from the SVZ and migrate into the striatum or if they are produced locally, perhaps from a dormant precursor stimulated by BDNF. Unexpectely, the receptor through which BDNF acts on SVZ cells may be p75 and not TrkB, as one report has shown *in vitro* that BDNF promotes neurogenesis in $p75^+$ but not in $p75^-$ SVZ cells and that TrkB and p75 are expressed in different pools of cells (Young et al., 2007). Other studies indicate that TrkB-TR may be involved, but this is not clear, as some claim that TrkB-TR enhances neurogenesis while others report increased gliogenesis instead (Tervonen et al., 2006; Cheng et al., 2007).

These results raise hope for the use of BDNF in regenerative therapies. BDNF could be useful in the treatment of stroke lesions, which often lead to a loss of striatal medium spiny neurons. If BDNF can influence the neurogenic potential of progenitors from the SVZ niche, other applications are possible. Dopaminergic interneurons are one of the cell

types naturally produced by the adult SVZ. Enhancing the production of these neurons could be useful in developing therapies for Parkinson's disease, the symptoms of which are caused mainly by the loss of dopaminergic innervations to the striatum. Additionally, the SVZ seems to respond to several types of injuries to the CNS with increased proliferation and perhaps even a rerouting of some of its progenitors to the damaged areas. Such responses raise the possibility of using the SVZ for endogenous repair, rather than having to resort to cell grafts or *in vitro* manipulations. However, the SVZ's response is limited and would likely need to be enhanced before it can significantly repair injuries. Knowing which growth factors can enhance neuronal production (or even simply proliferation) in the SVZ would thus be very useful for therapeutic applications, whether the goal is to manipulate progenitors *in vitro* to produce the desired cell types or *in vivo* to enhance endogenous repair. In the following chapter, I present work I performed with the aim of better understanding the actions of BDNF in the SVZ. My results point to some surprising conclusions, such as that BDNF does not appear to be the strong neurogenic stimulator it has been described to be in previous studies and that, based on expression analysis, the p75 receptor appears more likely to mediate the actions of BDNF on SVZ cells than TrkB. The exact role of BDNF in adult SVZ neurogenesis is not clear but it could act as an inhibitor rather than a stimulator of neuron production. Such information will be critical in future therapeutic applications of this neurotrophin and also has the potential to uncover interesting physiological mechanisms of regulation of adult neurogenesis.

Chapter Two: Brain-Derived Neurotrophic Factor Signaling in Adult Mice and Rats Does Not Stimulate Subventricular Zone Neurogenesis

2.1 Introduction

As reviewed in section 1 of this thesis, neurogenesis continues throughout adulthood in vertebrates, due to endogenous progenitor cells which could be useful for brain repair (Lie et al., 2004). In rodents, there are two known adult neurogenic regions: the subventricular zone (SVZ) and the hippocampal dentate gyrus. The SVZ contains $GFAP^+$, astrocytic stem cells (type B cells), which generate highly proliferative intermediate cells (type C cells) that differentiate into neuroblasts (type A cells) (Alvarez-Buylla and Garcia-Verdugo, 2002). These neuroblasts migrate in chains through the SVZ (Doetsch and Alvarez-Buylla, 1996) and rostral migratory stream (RMS) towards the olfactory bulb (OB) (Luskin, 1993; Lois and Alvarez-Buylla, 1994), where cells migrate radially into the granular (GCL) and glomerular (GL) layers and differentiate into inhibitory interneurons (Carleton et al., 2003). We still know very little about the molecules that regulate the generation of thousands of neuroblasts daily from the SVZ.

Growth factors are important components of stem cell niches (Horner and Palmer, 2003). Cells in the SVZ respond to multiple extracellular factors, including EGF, FGF2, PDGF, BMPs, Noggin, Prolactin and Erythropoietin, which influence SVZ proliferation and neurogenesis (Craig et al., 1996; Kuhn et al., 1997; Lim et al., 2000a; Shingo et al., 2001; Shingo et al., 2003; Zheng et al., 2004; Jackson et al., 2006). Recent findings indicate that neurotrophins may also play a fundamental role in adult neurogenesis. Neurotrophins are well known for promoting neuronal survival and for modulating synaptic plasticity (Schinder and Poo, 2000; Huang and Reichardt, 2001; Chao, 2003). Two laboratories have now reported that exposing the SVZ to the neurotrophin Brain-Derived Neurotrophic Factor (BDNF) increases production of OB interneurons and, unexpectedly, of striatal neurons normally not generated in adult brains (Zigova et al., 1998; Benraiss et al., 2001; Pencea et al., 2001; Chmielnicki et al., 2004). Another

neurotrophin, CNTF, has been suggested to stimulate adult neurogenesis in the hypothalamus (Kokoeva et al., 2005). While these findings are of significant interest for regenerative therapies, we still do not understand the biological mechanisms underlying these neurotrophins' effects on adult stem cell niches. Most importantly, we do not know which cells directly respond to these neurotrophins nor the nature of their response.

I addressed these questions in the SVZ, focusing on the postulated neurogenic effects of BDNF and its receptors TrkB and p75. TrkB exists in two isoforms: a full-length receptor, activated by intracellular domain cross-phosphorylation, and a truncated receptor, lacking most of the intracellular region (Klein et al., 1989; Klein et al., 1990; Middlemas et al., 1991). p75 binds several neurotrophins and its activation can affect cell survival, proliferation, migration, axonal elongation and synaptic plasticity (Dechant and Barde, 2002; Barker, 2004). p75 seems to affect neurogenesis from SVZ progenitors (Young et al., 2007). I found that truncated TrkB is expressed in type B and ependymal cells, but not in neuroblasts, whereas p75 is expressed in type C cells and neuroblasts. My data show that SVZ neurogenesis can continue in the absence of TrkB and that, with the exception of dopaminergic cells, TrkB-KO and WT OB interneurons display similar survival, molecular and morphological properties. Importantly, BDNF did not increase SVZ neurogenesis in mice and even decreased neurogenesis in rats.

2.2 Results

RT-PCR Characterization of neurotrophins and their receptors in the SVZ

I used semi-quantitative RT-PCR to characterize the expression of multiple neurotrophins (CNTF, GDNF, NGF, NT3, NT4, BDNF) and their receptors (CNTFR, gp130, GFRα1, Ret, p75, TrkA, TrkB, TrkC; see Fig. 2.1 legend for details) (Neet and Campenot, 2001) in the adult mouse SVZ (Fig. 2.1A, B). Because it is not possible to obtain RNA from the SVZ without some contamination from the adjacent striatum, I included in my analysis RNA collected from striatum close to the SVZ and compared expression levels between the two tissues. I found that TrkB is the most abundant neurotrophin receptor in SVZ samples (Fig. 2.1A). TrkB is also the only receptor whose expression is significantly enriched in SVZ when compared to striatum. This enrichment seems to be due to high levels of expression of TrkB-TR isoform, since TrkB-FL was

Figure 2.1: RT-PCR analysis of neurotrophin receptors and ligands. I used semi-quantitative RT-PCR to determine the relative expression levels of multiple neurotrophins and their receptors in the adult mouse brain (CNTFR, gp130: receptors for CNTF; GFRα1, Ret: receptors for GDNF; p75: low affinity receptor for NGF, NT3, NT4, BDNF; TrkA: high affinity receptor for NGF; TrkB: high affinity receptor for NT4, BDNF; TrkC: high affinity receptor for NT3). ***A***, neurotrophin receptor expression levels in SVZ and striatum. ***B***, neurotrophin expression levels in SVZ and striatum. ***C***, neurotrophin expression levels in choroid plexus. All values are normalized to GAPDH expression and represent average ± SEM. Data in ***A***, ***B***, represent average from two experiments, pooling RNA from 8 adult mice/experiment; data in **C**, represents RNA of 16 adult mice pooled in one experiment. See technical details in sections 5.3, A7.

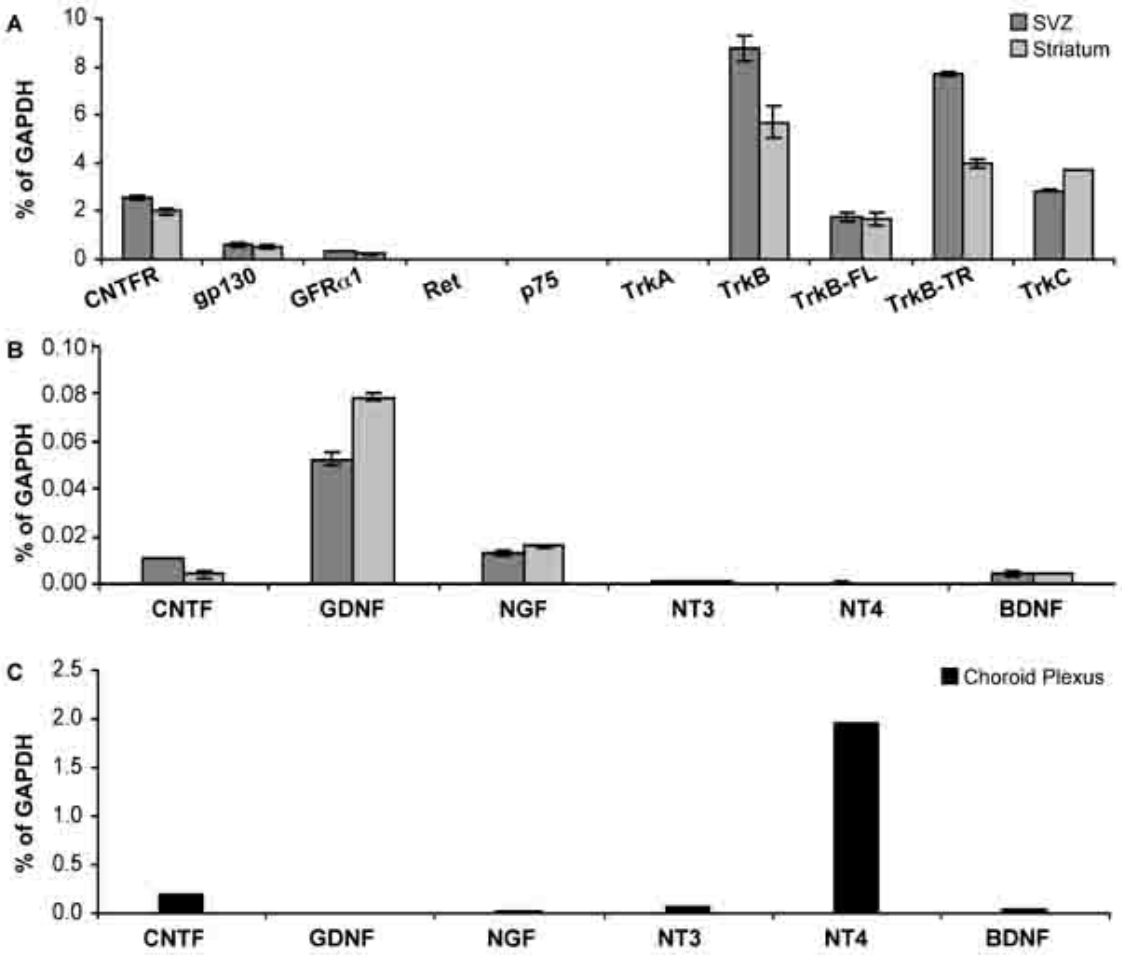
A
% of GAPDH
10
8
6
4
2
0
SVZ
Striatum
CNTFR
gp130
GFRα1
Ret
p75
TrkA
TrkB
TrkB-FL
TrkB-TR
TrkC
B
% of GAPDH
0.10
0.08
0.06
0.04
0.02
0.00
CNTF
GDNF
NGF
NT3
NT4
BDNF
C
% of GAPDH
2.5
2.0
1.5
1.0
0.5
0.0
Choroid Plexus
CNTF
GDNF
NGF
NT3
NT4
BDNF

detected at lower levels and showed no enrichment in the SVZ. Other neurotrophin receptors, such as CNTFR and TrkC, were also detected in SVZ samples, but their expression level was very similar in striatal samples, which might have contributed to some of the SVZ signal. However, based on this analysis, I cannot discard possible roles for TrkC and CNTFR in the SVZ.

Neurotrophin expression levels in the SVZ were in general extremely low and none seemed to be enriched in the SVZ when compared to striatum (Fig. 2.1B). I looked at the expression of neurotrophins from the choroid plexus, which secretes many of the cerebral spinal fluid (CSF) components and is thus a possible distant source of neurotrophins for SVZ cells. As in the SVZ, most neurotrophins were detected at low levels, with the exception of the TrkB ligand NT4 (Fig. 2.1C).

Based on these results as well as those of previous publications (Zigova et al., 1998; Benraiss et al., 2001), the neurotrophin signaling molecules most likely to play a role in adult SVZ neurogenesis are the receptor TrkB and its ligands. Therefore, I decided to further characterize these molecules in the context of SVZ neurogenesis.

BDNF expression in SVZ

Consistent with the results presented in Fig. 2.1, *in situ* hybridization revealed very low levels of BDNF mRNA in the adult mouse SVZ (Fig. 2.2A, B). Nonetheless, low levels of BDNF protein were detected in the SVZ, suggesting that cells in this neurogenic niche are exposed to endogenous BDNF (Fig. 2.2C).

Although BDNF expression was almost undetectable at the mRNA level, it is possible that this gene is temporally regulated, increasing its expression at specific times. I therefore tested the neurotransmitter Dopamine (Dopa), the adrenal hormone Epinephrine (Epi) and the lactogenic hormone Prolactin (PRL), molecules whose expression can vary temporally and/or in response to external stimuli (Kiyatkin, 2002; Torner and Neumann, 2002; Carrasco and Van de Kar, 2003; Sharp, 2005; Monti and Monti, 2007), for their ability to induce BDNF gene expression from cultured SVZ astrocytes. As a positive control, I included the phorbol ester phorbol 12-myristate 13-acetate (TPA). TPA is a protein kinase C (PKC) activator, previously shown to increase BDNF expression in both neurons and astrocytes (Zafra et al., 1992; Miklic et al., 2004). Non-neurogenic

Figure 2.2: Regulation of BDNF gene expression. ***A***, ***B***, *in situ* hybridization detects very low levels of BDNF mRNA at all levels of the adult SVZ (***A***, anterior SVZ; ***B***, medial/posterior SVZ). ***C***, immunostaining detection of BDNF protein in the adult SVZ. ***D***, experimental design. SVZ and cortex (boxed areas) were dissected from P3 mouse brains, dissociated and cultured to confluence. Cells were then changed to a serum/antibiotics-free medium for 2 days, exposed to the experimental molecules (see below) for 4 or 24 hours and processed to collect RNA. ***E***, semi-quantitative real-time RT-PCR for BDNF expression in cultured SVZ and cortex astrocytes after 4 or 24 hour exposure to phorbol 12-myristate 13-acetate (TPA, 100 nM, positive control), Dopamine (Dopa, 0.15 mM), Epinephrine (Epi, 0.15 mM), Prolactin (PRL, 1 μg/ml) or no treatment (Control). All values are represented as a percentage of the expression level of the housekeeping control gene Gus, averaging 2 wells/condition from one single experiment. PCR and data collection were performed using Applied Biosystems fluorescent TaqMan technology. ***F***, ***G***, BDNF *in situ* hybridization in SVZ sections of adult female mice at 7 days *post coitus* (7 d.p.c., ***F***) and 19 d.p.c. (***G***), showing upregulation at 7 d.p.c.. Scale bars: 100 μm (***A***-***C***), 200 μm (***F***, ***G***). See technical details in sections 5.5, 5.9, 5.12, A2.

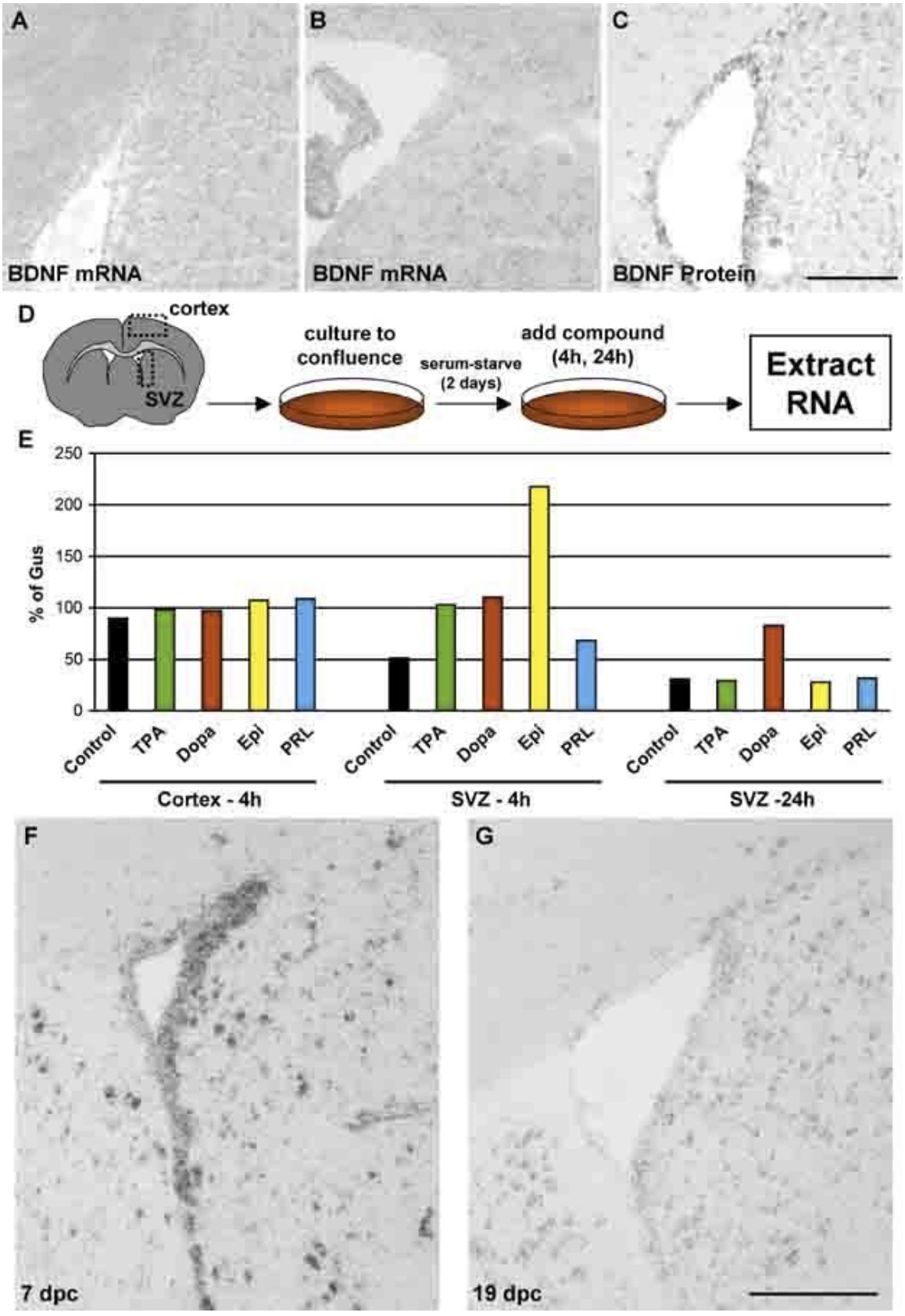
A
BDNF mRNA
B
BDNF mRNA
C
BDNF Protein
D
cortex
SVZ
culture to confluence
serum-starve (2 days)
add compound (4h, 24h)
Extract RNA
E
% of Gus
250
200
150
100
50
0
Control
TPA
Dopa
Epi
PRL
Cortex - 4h
SVZ - 4h
SVZ -24h
F
7 dpc
G
19 dpc

astrocytes from cortex were also tested for comparison. For both types of astrocytes, tissue was collected from 3 day old WT CD1 mice and cultured to confluence. Astrocytes were then changed to a defined, serum-free medium for 2 days, after which the experimental molecules were added to the culture medium for 4 hours (SVZ, cortex) or 24 hours (SVZ only) (Fig. 2.2D). I used semi-quantitative RT-PCR and TaqMan technology to compare the relative levels of BDNF transcripts between the various treatments (Fig. 2.2E).

SVZ astrocytes responded to all molecules tested after just 4 hours of treatment, most noticeably to Dopa and Epi, which elicited a 2.2-fold and 4.3-fold increase in BDNF expression, respectively (compared to untreated cells) (Fig. 2.2E). PRL induced a smaller, 34% increase in BDNF expression. As expected, TPA also increased BDNF expression in SVZ astrocytes (2-fold increase). However, TPA did not seem to affect cortical astrocytes (10% increase in BDNF levels). Cortical astrocytes were noticeably less responsive to all compounds, hardly changing their levels of BDNF after 4 hours of treatment (8%, 20% and 22% increase for Dopa, Epi and PRL, respectively). Interestingly, after 24 hours of treatment, only Dopa continued to induce BDNF gene transcription from SVZ astrocytes (2.7-fold increase), whereas Epi and PRL-treated cells expressed BDNF at levels similar to untreated controls. Therefore, the expression of BDNF from SVZ astrocytes can be modulated by Dopa, Epi, and perhaps to a lesser degree by PRL, though Epi and PRL seem to have only a transient effect. These results were derived from only 1-2 separate experiments and thus more replicates will be needed to assess the statistical significance of the observed effects.

Interestingly, I observed by *in situ* hybridization increased levels of BDNF mRNA in the SVZ of female CD1 mice 7 days *post coitus* (d.p.c.) (Figure 2.2F, G). This result suggests that BDNF expression in the SVZ may indeed be temporally regulated, responding to specific environmental cues such as pregnancy. PRL is also upregulated at 7 d.p.c. in female mice and is known to enhance SVZ neurogenesis (Shingo et al., 2003). Whether PRL and BDNF influence each other's expression *in vivo* and whether BDNF participates in the PRL-induced SVZ neurogenesis are important questions that remain to be investigated.

TrkB expression in SVZ

I then analyzed the expression of TrkB in the SVZ by immunohistochemistry and confocal microscopy, using a TrkB-specific antibody (Fig. 2.3A-C) as well as a TrkB:Tau-LacZ reporter mouse line (Fig. 2.4; see Materials and Methods for details). Both methods confirmed abundant expression of TrkB in the adult SVZ. TrkB is strongly expressed in ependymal cells (Fig. 2.3A, 2.4B). Using cell type-specific markers, I could also detect TrkB in many $GFAP^+$ astrocytic type B cells in the SVZ (Fig. 2.3A, Fig. 2.4B). It is widely believed that SVZ stem cells divide slowly (Morshead et al., 1994; Chiasson et al., 1999; Doetsch et al., 1999b). To label slowly dividing cells in the SVZ, I administered BrdU to adult mice for 1 week, followed by a 3 week chase period before sacrificing the mice. Cells dividing frequently will lose the BrdU staining by dilution; furthermore, in the SVZ, such cells become neuroblasts which migrate away within 2-6 days, leaving the stem cells behind. Many of the BrdU-retaining cells in the SVZ (putative stem cells) expressed the reporter product β-Gal (Fig. 2.4A). Though not all $BrdU^+$ cells are necessarily stem cell, this observation suggests that SVZ stem cells themselves may express TrkB. I found that TrkB does not colocalize with PSA-NCAM, a marker for migrating neuroblasts produced in the SVZ (Fig. 2.3B, Fig. 2.4D). The same expression pattern (colocalization with GFAP and not with PSA-NCAM) was observed in the adult mouse RMS (Fig. 2.4C, E). This result was unexpected because previous publications suggest that neuroblasts in the SVZ and RMS express TrkB (Kirschenbaum and Goldman, 1995; Gascon et al., 2005; Chiaramello et al., 2007; Bath et al., 2008). To confirm my finding, I immunolabeled acutely dissociated SVZ cells from early postnatal pups with an antibody specific for the extracellular domain of TrkB. The SVZ cells were fixed and stained no later than 1 hour after dissociating the tissue, so that the staining would more accurately reflect the *in vivo* expression of TrkB. As a control for possible non-specific labeling by the antibody used, I processed cells isolated from TrkB knockout (TrkB-KO) and wild-type (WT) littermates in parallel. Nearly all $TrkB^+$ cells were negative for the neuroblast markers Tuj1 (Fig. 2.3C, 68 of 70 cells) and Dcx (data not shown, 36 of 38 cells). I also used two additional anti-TrkB antibodies to characterize TrkB expression in SVZ sections, both of which gave results consistent with the data mentioned above (Fig. 2.5A-E). Furthermore, tissue from adult TrkB:Tau-LacZ reporter

Figure 2.3: Expression analysis of TrkB in the mouse SVZ. ***A***, ***B***, confocal images of TrkB immunostaining in adult mouse SVZ. ***A***, TrkB protein (green) colocalizes with the astrocyte marker GFAP (red); arrows: multi-ciliated ependymal cells lining the ventricular wall. ***B***, TrkB protein (green) does not colocalize with the neuroblast marker PSA-NCAM (red). ***C***, immunostaining for TrkB receptor (green) on acutely dissociated neonatal SVZ cells confirms that SVZ neuroblasts (detected with Tuj1 antibody, red) do not express TrkB (arrowheads: two $TrkB^+$ cells isolated from SVZ are negative for Tuj1). Scale bars: 50 μm (***A***, ***B***), 30 μm (***C***). cc: corpus callosum; LV: lateral ventricle; St: striatum. See technical details in sections 5.9, A13.

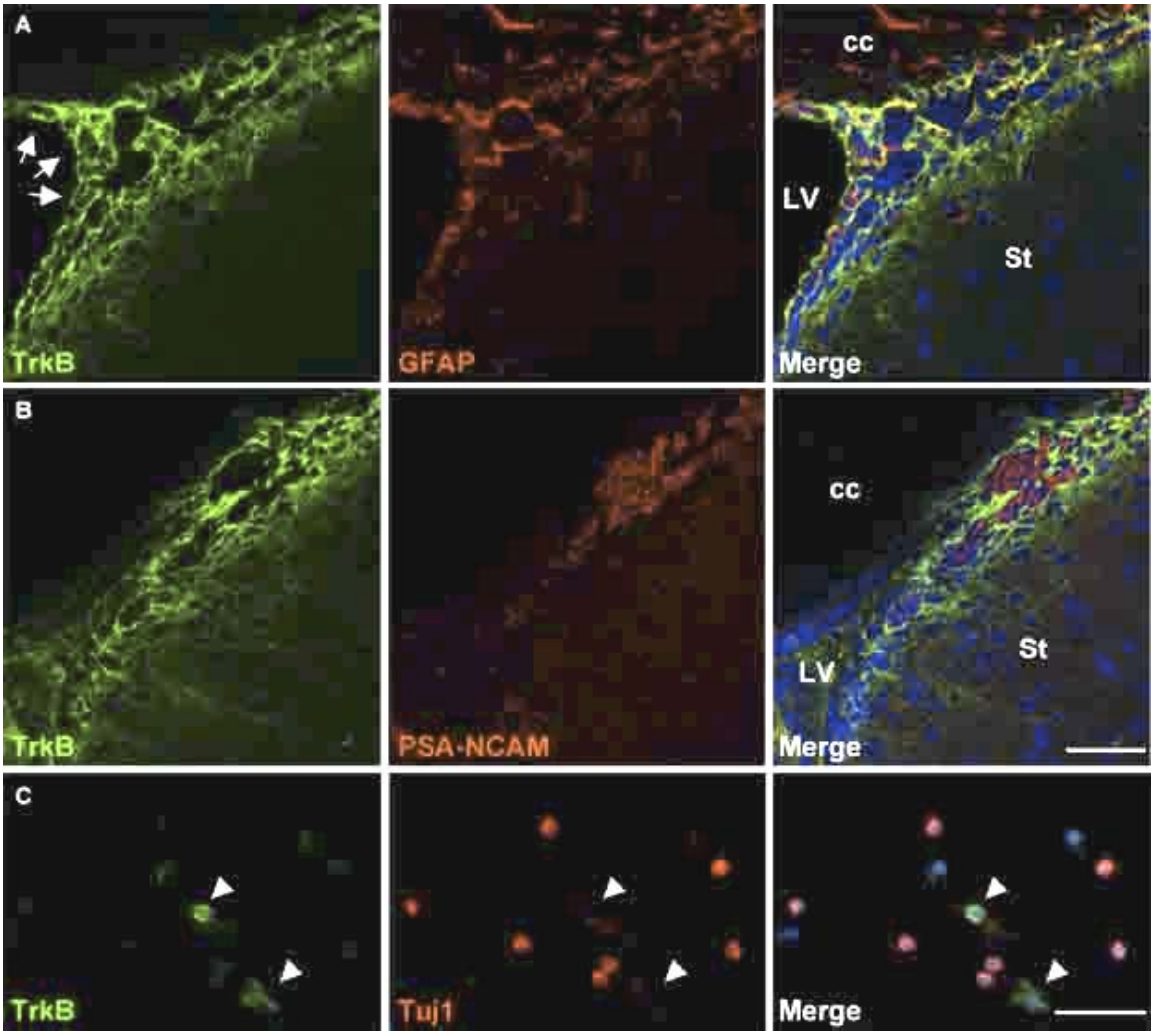
A
TrkB
GFAP
cc
LV
St
Merge
B
TrkB
PSA-NCAM
cc
St
LV
Merge
C
TrkB
Tuj1
Merge

Figure 2.4: TrkB:Tau-LacZ reporter mouse expression analysis. ***A***, BrdU was administered for 1 week, followed by a 3 week chase period to label BrdU-retaining cells in the SVZ (red), many of which express the reporter β-Gal (green, arrows). ***B***, ***C***, β-Gal expression (green) colocalizes with the astrocyte marker GFAP (red) in the SVZ (***B***; arrowheads: multi-ciliated ependymal cells on the ventricular wall) and RMS (***C***). ***D***, ***E***, β-Gal (green) does not colocalize with the neuroblast marker PSA-NCAM (red) in the SVZ (***D***) or RMS (***E***). Scale bar: 30 μm. cc: corpus callosum; LV: lateral ventricle; St: striatum. See technical details in sections 5.4, 5.9, A1, A13.

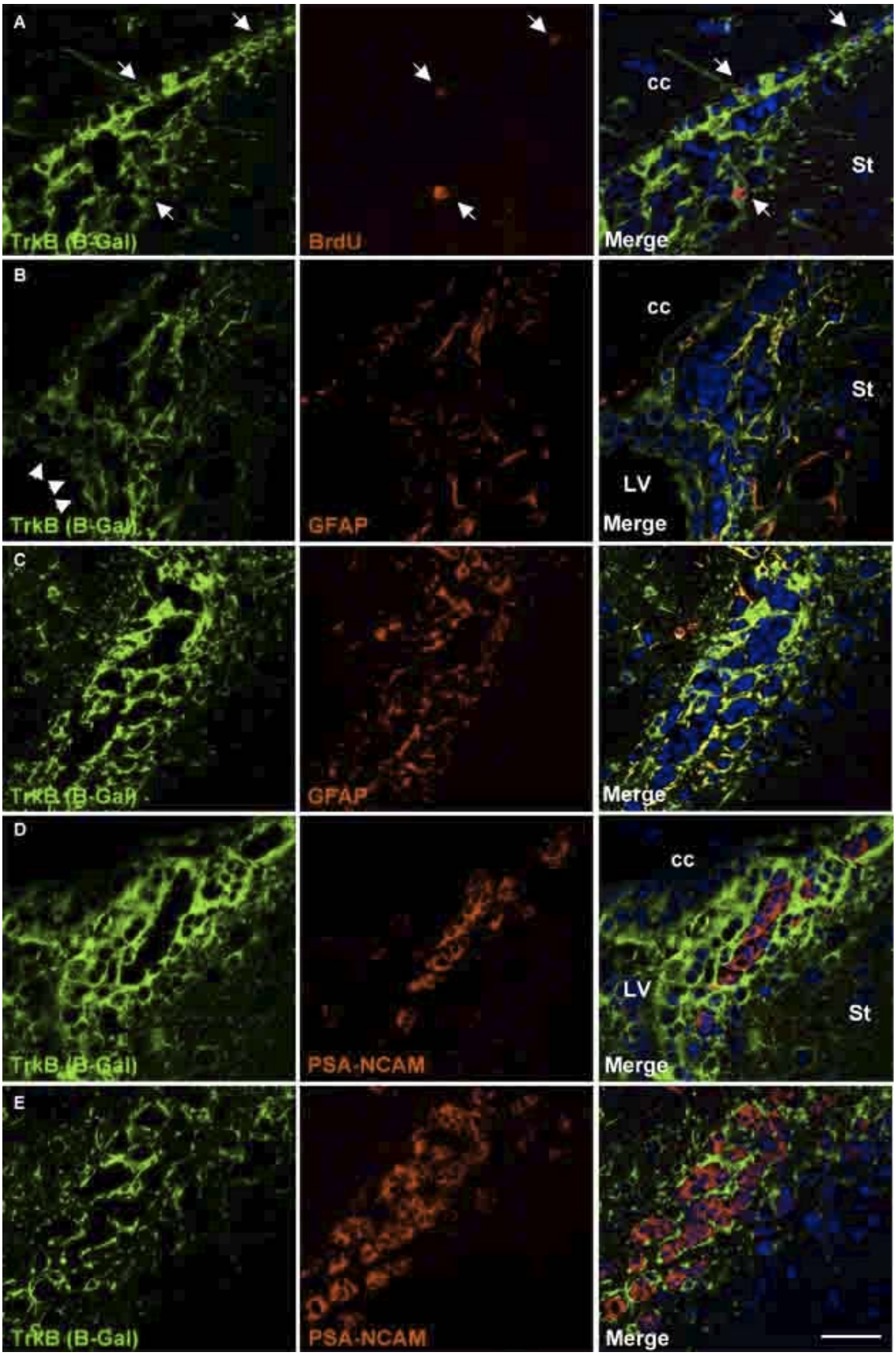
A
TrkB (B-Gal)
BrdU
cc
St
Merge
B
TrkB (B-Gal)
GFAP
cc
St
LV
Merge
C
TrkB (B-Gal)
GFAP
Merge
D
TrkB (B-Gal)
PSA-NCAM
cc
LV
St
Merge
E
TrkB (B-Gal)
PSA-NCAM
Merge

Figure 2.5: TrkB expression in the SVZ. (***A***-***H***) TrkB protein detected using an antibody specific for the truncated isoform of TrkB (green, Santa Cruz cat.# sc-119) (***A***-***C***), or two different antibodies that recognize all isoforms of TrkB (green, Chemicon cat.# AB9872, ***D***, ***E***, and cat.#AB5372, ***F***-***H***). Sections were counterstained for GFAP (***A***, ***D***, ***F***) or PSA-NCAM (***B***, ***E***, ***G***) (red) as well as the nuclear dye DAPI (blue, all panels). Western blots confirming the specificity of the TrkB antibodies are shown to the left of the respective immunostainings. All Western blots were performed on whole brain protein extracts from newborn TrkB-KO and WT mice and β-Actin was used as a loading control. See technical details in sections 5.7, 5.9, A3, A13.

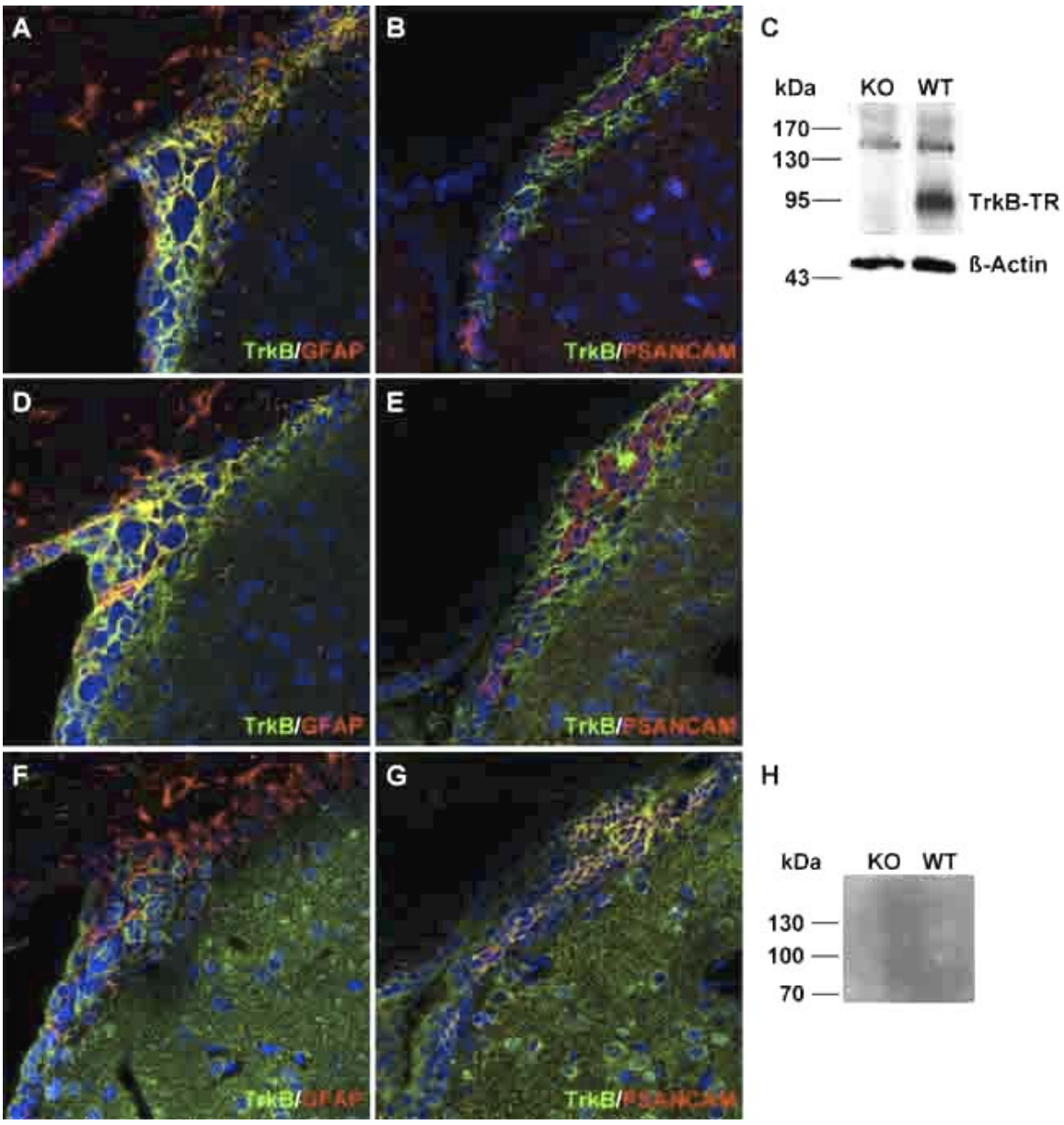
A
TrkB/GFAP
B
TrkB/PSANCAM
C
kDa
KO
WT
170
130
95
43
TrkB-TR
ß-Actin
D
TrkB/GFAP
E
TrkB/PSANCAM
F
TrkB/GFAP
G
TrkB/PSANCAM
H
kDa
KO
WT
130
100
70

Figure 2.6: Electron microscopy analysis of TrkB expression in adult mouse SVZ. ***A***, ***B***, electron microscopy of TrkB:Tau-LacZ reporter mice. Notice dark X-Gal precipitates (black arrows: examples of X-Gal precipitates) around the periphery of the nucleus of ependymal cells (E) and type B cells (B), but not type A neuroblasts (A); X-Gal precipitates are also visible in ependymal cell cilia (***B***, arrowheads). White arrows on brain section diagrams to the right show approximate origin of pictures. Scale bars: 2 μm. See technical details in sections 5.6, A8, A9.

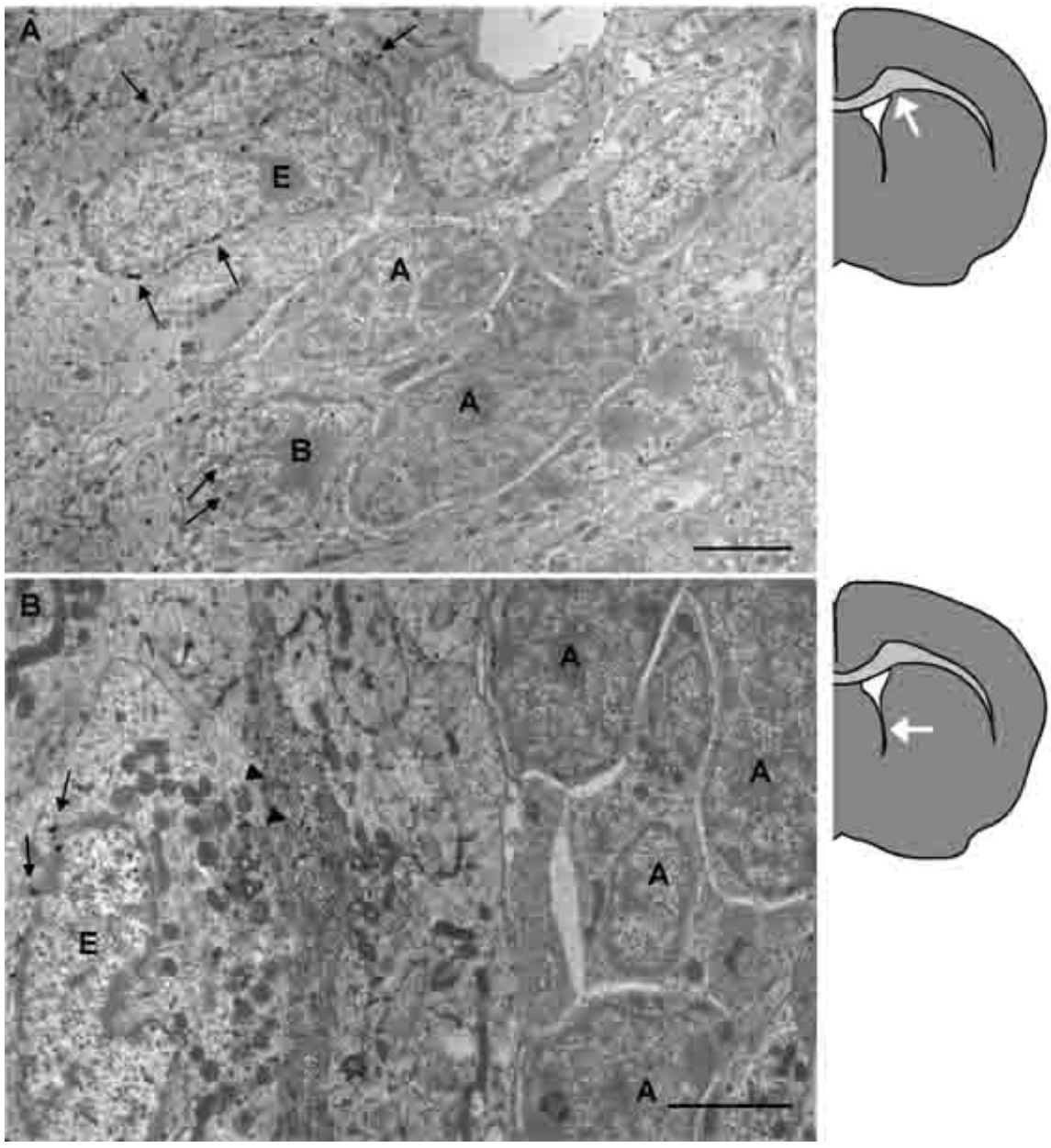
A
E
A
A
B
B
A
A
A
A
E
A

mice was stained by β-Gal enzymatic reaction and analyzed at the electron microscope. Again, ependymal cells and type B cells were heavily labeled with β-Gal precipitates, whereas neuroblasts were not (Fig. 2.6).

Cells in SVZ and RMS express the truncated isoform of TrkB

The TrkB receptor exists in two different isoforms, full-length (TrkB-FL) and truncated (TrkB-TR), generated by alternative splicing (Klein et al., 1989; Klein et al., 1990; Middlemas et al., 1991). TrkB-FL is responsible for most known effects of TrkB activation, while TrkB-TR functions are poorly understood. These isoforms differ greatly in their intracellular signaling ability due to the absence of the intracellular kinase domains in TrkB-TR. Because I could not discriminate between these two isoforms by immunohistochemistry alone, I performed *in situ* hybridization with a probe specific for TrkB-FL as well as with one that recognizes all TrkB isoforms (TrkB-all). Consistent with all the data described above, TrkB mRNA in the adult mouse SVZ was abundant in some cells but undetectable in others. Typically, TrkB-all$^+$ cells were distributed in ring-like patterns surrounding unlabeled cells (Fig. 2.7A). Such staining likely reflects the known distribution of SVZ type B cells surrounding chains of migrating neuroblasts (Jankovski and Sotelo, 1996; Lois et al., 1996; Peretto et al., 1997). TrkB was also strongly expressed in the adult mouse RMS, exhibiting a pattern very similar to that of the SVZ (Fig. 2.7B). Strikingly, the expression of TrkB-FL was radically different, as I did not detect any TrkB-FL in either the SVZ or RMS (Fig. 2.7D, E). I found at best 1-2 TrkB-FL$^+$ cells/SVZ section, contrasting with an abundance of TrkB$^+$ cells when using the TrkB-all probe. Conversely, in other regions, such as the striatum (Fig. 2.7A, D) and hippocampus (Fig. 2.7C, F), I noticed no major difference between the expression patterns detected by TrkB-all and TrkB-FL probes, confirming that the difference found in the SVZ and RMS is not due to an inability of the TrkB-FL probe to detect mRNA transcripts.

To corroborate this finding at the protein level, I characterized TrkB expression by Western blot in SVZ and striatal samples from adult CD1 mice, which allowed me to distinguish TrkB-FL and TrkB-TR isoforms by molecular weight (145 kDa and 95 kDa respectively). As predicted by the *in situ* hybridization data, the great majority of TrkB

Figure 2.7: Expression of TrkB isoforms in the adult mouse SVZ. ***A-C***, *in situ* hybridization to detect all isoforms of TrkB (TrkB-all) shows strong staining in the SVZ (***A***), RMS (***B***) and hippocampal dentate gyrus (***C***). ***D-F***, *in situ* hybridization to specifically detect the full-length isoform of TrkB (TrkB-FL) shows that SVZ (***D***) and RMS (***E***) cells do not express this isoform, though hippocampal cells (***F***) do. ***G***, Western blot for TrkB shows that the predominant isoform in the SVZ is TrkB-TR at the protein level as well. Striatum protein was run for comparison and samples from TrkB-KO and WT whole brain (collected at P1) were used as controls; all samples were probed for β-Actin as loading control. Scale bar: 100 μm. Dashed line: outline of RMS. See technical details in sections 5.5, 5.7, A2, A3.

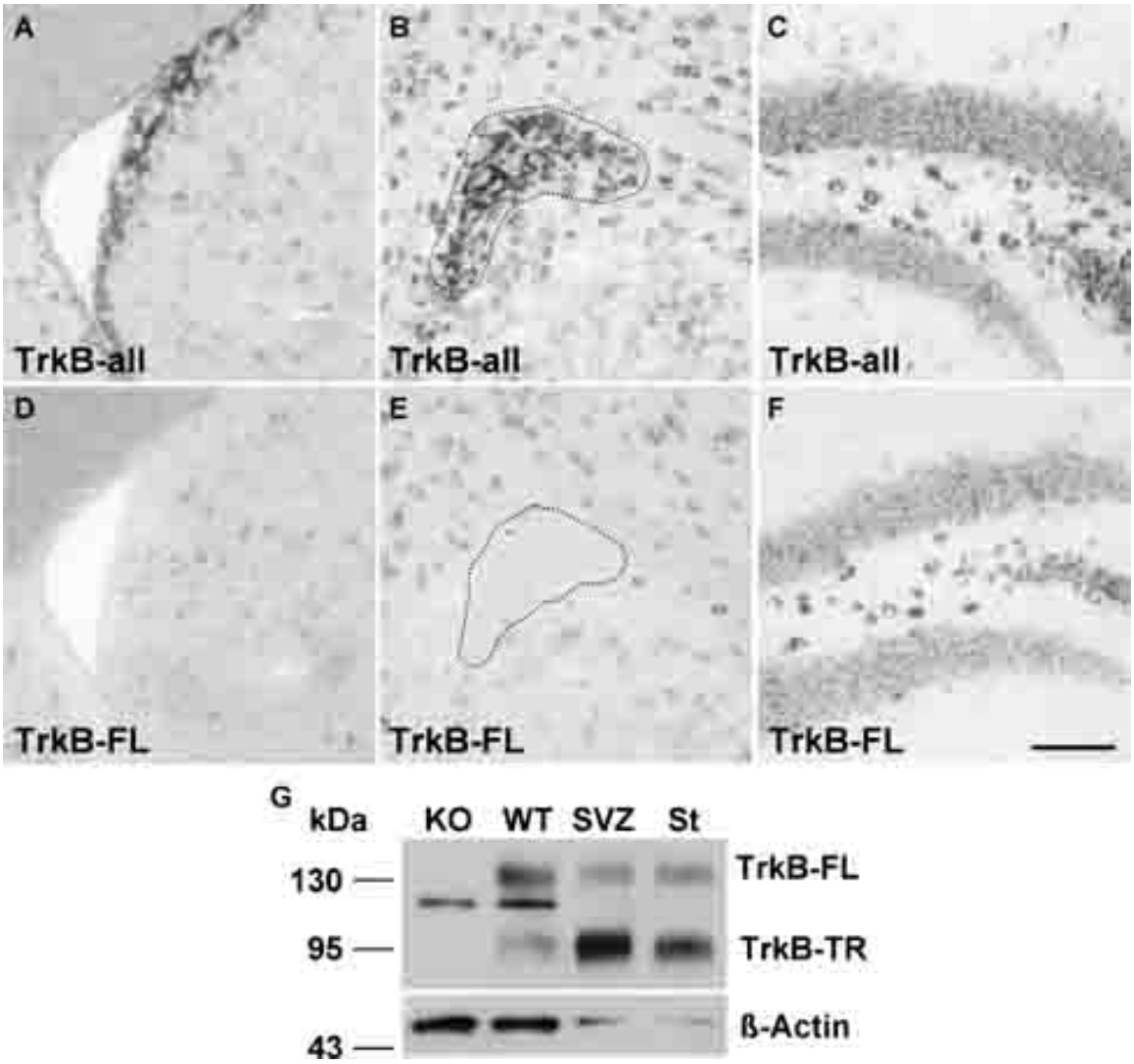
A
B
C
TrkB-all
TrkB-all
TrkB-all
D
E
F
TrkB-FL
TrkB-FL
TrkB-FL
G
kDa
KO
WT
SVZ
St
130
95
43
TrkB-FL
TrkB-TR
ß-Actin

protein detected in SVZ samples was of the truncated isoform (Fig. 2.7G). A light band of TrkB-FL protein was detected in SVZ samples. This band may come from very low level expression in the SVZ or more likely from inevitable contamination of SVZ samples with striatal tissue, where TrkB-FL was detected by *in situ* hybridization as well as by Western blot. Based on both mRNA localization and protein analysis, I conclude that the bulk of the TrkB found in the SVZ and RMS consists of the truncated isoform of the receptor. Consistently, I detected numerous TrkB-TR$^+$ cells in adult SVZ sections using an antibody specific to this receptor isoform (Fig. 2.5A, B).

It was possible that the low levels of TrkB-FL in the SVZ were due to a low level of stem cell proliferation under normal conditions. I therefore decided to characterize the expression of TrkB-TR and TrkB-FL in the SVZ after infusing the brain with the antimitotic drug cytosine-β-D-arabinofuranoside (AraC). This treatment eliminates rapidly proliferating cell types from the SVZ (type C cells and neuroblasts), whereas many type B cells survive and ependymal cells are largely unaffected. After termination of AraC treatment, SVZ B cells become activated and regenerate the neurogenic niche (Doetsch et al., 1999a). Using a microosmotic pump, I infused AraC unilaterally onto the surface of the brain of adult mice for 6 days and sacrificed the mice immediately thereafter. I found that TrkB receptor was still detected at high levels in the SVZ with the TrkB-all *in situ* probe but not with the TrkB-FL probe (Fig. 2.8C, E). Therefore, eliminating the majority of type C cells and neuroblasts from the SVZ does not affect the expression of TrkB isoforms in this region. This result confirms that type B and ependymal cells are the main source of TrkB in the adult mouse SVZ and suggests that, even when challenged to repopulate the SVZ, these cells express only the truncated isoform of TrkB.

TrkB-KO stem cells can generate new neurons

Regardless of the isoform, there are clearly high levels of TrkB receptor in SVZ and RMS (Fig 2.1A, 2.2D-F, 2.4, 2.7A, B) and previous reports have suggested that the TrkB ligand BDNF can enhance SVZ neurogenesis. Therefore, I decided to use TrkB-KO mice to determine whether this signaling pathway is required for SVZ neurogenesis. Because these mice do not survive beyond 1-3 days after birth, I performed my analysis on

Figure 2.8: Depleting SVZ of type C cells and type A neuroblasts does not qualitatively alter expression of TrkB isoforms. ***A***, experimental strategy: AraC was pumped onto the surface of the brain for 6 days, thus depleting the SVZ of rapidly proliferating cells. ***B-E***, *in situ* hybridization for TrkB-all (***B, C***) and TrkB-FL (***D, E***) after vehicle (***B, D***) or AraC (***C, E***) treatment. Dashed line: outline of SVZ. Scale bar: 100 μm. See technical details in sections 5.5, 5.10, A2, A12.

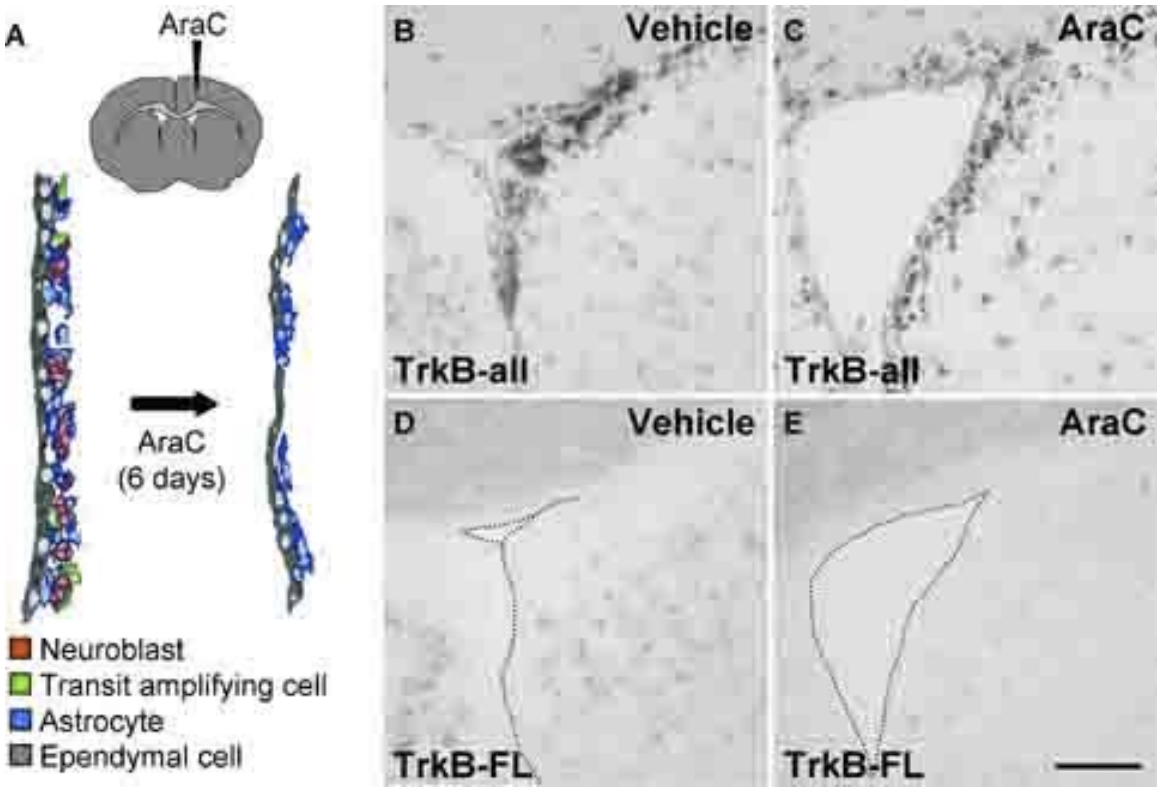
A
AraC
AraC
(6 days)
Neuroblast
Transit amplifying cell
Astrocyte
Ependymal cell
B
Vehicle
TrkB-all
C
AraC
TrkB-all
D
Vehicle
TrkB-FL
E
AraC
TrkB-FL

newborn, postnatal day 0 (P0) brains. I found that proliferation, as measured by phosphorylated histone H3 (pH3) labeling, is reduced by 28% in the SVZ of TrkB-KO mice (Fig. 2.9G). Apoptosis, as measured by TUNEL labeling, is 77% higher in the SVZ and 80% higher in the OB of TrkB-KO mice (Fig. 2.9H). To determine whether these defects in proliferation and survival result in fewer neurons added to the OB in TrkB heterozygotes, I labeled a cohort of cells by injecting BrdU at P21 and killing the mice 15 days later. Consistent with the results described above, I detected a small decrease in $BrdU^+$ cells in the OB of TrkB heterozygotes compared to WT littermates (14.2% decrease, p=0.098, n=3 WT and 4 heterozygous mice). However, both homozygous and heterozygous TrkB mutant mice have various other defects unrelated with the SVZ, leading to death (TrkB-KO) or obesity ($TrkB^{+/-}$) (see also section 1.5). It is thus difficult to determine whether the results in the SVZ are directly caused by loss of TrkB or by these secondary defects. Moreover, due to early lethality, I could not determine the effect of complete deletion of TrkB on SVZ neuronal production postnatally using these mice.

To better determine the importance of TrkB receptors in the adult brain, I used $TrkB^{lox/lox}$ mice (Xu et al., 2000b) to conditionally eliminate TrkB from a subset of stem cells in the dorsal anterior SVZ. Briefly, I injected a replication-deficient adenovirus expressing Cre recombinase (Ad:Cre) into the dorsolateral striatum of newborn mice (Fig. 2.10A). At this age, radial glia located on the lateral wall of the lateral ventricle still extend their processes through the striatum. Thus, Ad:Cre is taken up by these processes and retrogradely transported to the ventricular wall, where it eliminates TrkB specifically from radial glia. These cells then give rise to the adult astrocytic stem cells (Merkle et al., 2004), which will themselves be TrkB-KO, as will all of their progeny. Using this method on $TrkB^{lox/lox}$ mice crossed to Z/AP mice, which express the reporter gene alkaline phosphatase (AP) upon Cre recombination, I followed the fate of TrkB-KO cells from their genesis in the SVZ to their final destination in the OB. Under these conditions, all non-targeted cells in SVZ, RMS and OB are WT. Mice were sacrificed 15 days after the initial adenoviral targeting to allow new neurons to arrive and integrate in the OB.

I found AP^+ cells with a migrating morphology in the RMS and OB core of both $TrkB^{+/+}$ and $TrkB^{lox/lox}$ mice (Fig. 2.10B, C), suggesting that TrkB-KO stem cells continue to produce neuroblasts. In the OB of both $TrkB^{+/+}$ and $TrkB^{lox/lox}$ mice, AP^+

Figure 2.9: *In vivo* consequences of TrkB-KO. P0 mice were stained for phosphorylated histone H3 (pH3) and TUNEL to detect proliferating and apoptotic cells, respectively, in the SVZ and OB. ***A***, ***D***, pH3 immunostaining (red) in SVZ of TrkB-WT (***A***) and TrkB-KO (***D***) mice. ***B***, ***E***, TUNEL labeling (red) in SVZ of TrkB-WT (***B***) and TrkB-KO (***E***) mice. ***C***, ***F***, TUNEL labeling (red) in OB of TrkB-WT (***C***) and TrkB-KO (***F***) mice. ***G***, quantification of pH3 staining in SVZ shows a decrease in proliferation in TrkB-KO mice. ***H***, quantification of TUNEL staining shows an increase in apoptosis in SVZ and OB of TrkB-KO mice. Blue: DAPI (all panels). All values represent average ± SEM; **$p<0.01$ by t-Student test; n=6 mice (TrkB-WT), n=4 mice (TrkB-KO). Scale bar: 100 μm (***A***, ***D***), (***B***, ***E***), 1mm (***C***, ***F***). See technical details in sections 5.8, 5.9, A4, A13.

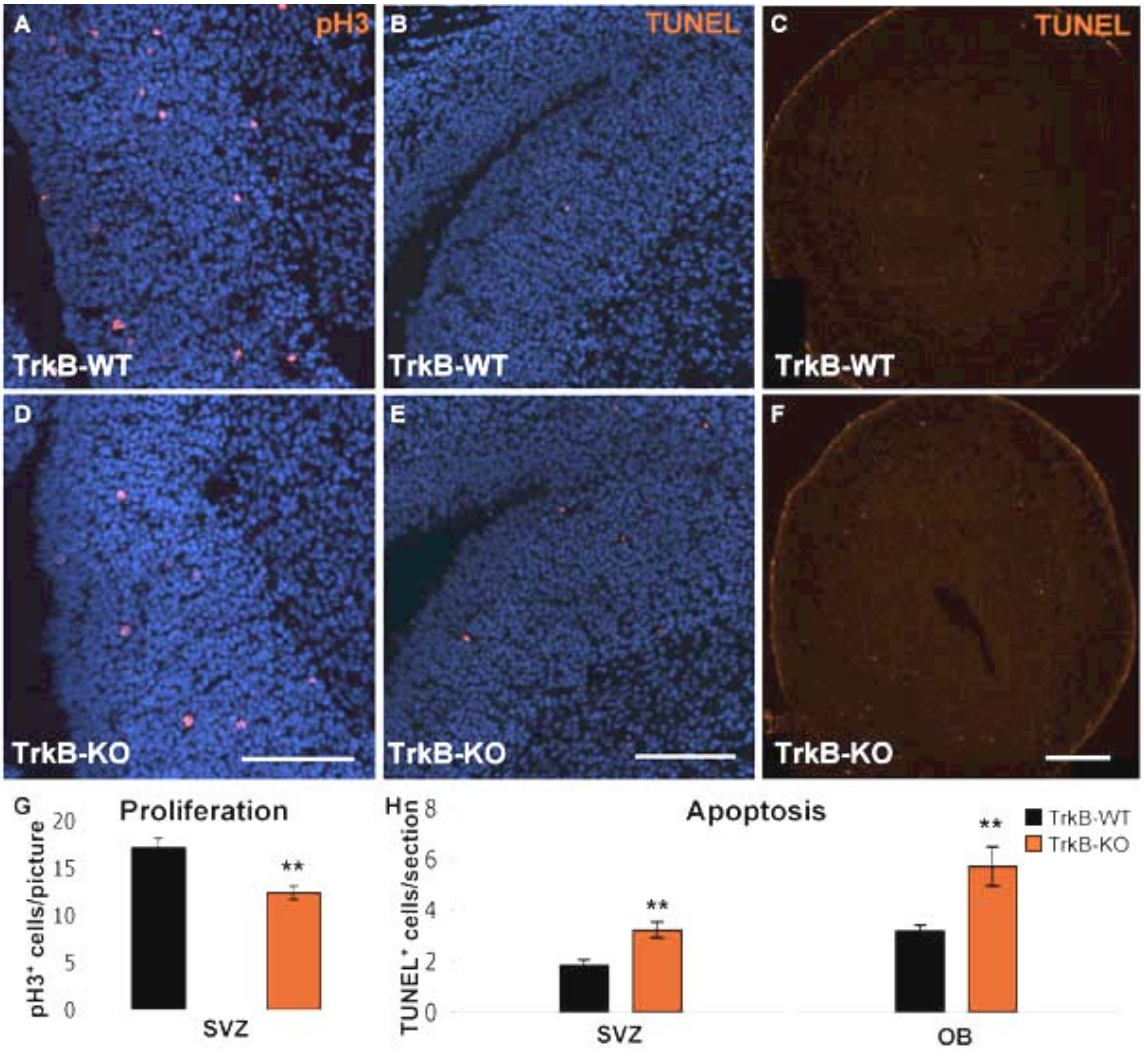
A
pH3
TrkB-WT
B
TUNEL
TrkB-WT
C
TUNEL
TrkB-WT
D
TrkB-KO
E
TrkB-KO
F
TrkB-KO
G
Proliferation
pH3+ cells/picture
20
15
10
5
0
**
SVZ
H
Apoptosis
TUNEL+ cells/section
8
6
4
2
0
**
**
SVZ
OB
TrkB-WT
TrkB-KO

Figure 2.10: Conditional TrkB-KO in SVZ can produce new OB neurons. ***A***, experimental design: radial glia in P0 mice were targeted for Cre-mediated recombination as previously described (Merkle et al., 2004) (Ad:Cre, arrow); this resulted in excision of TrkB and/or LacZ genomic locus, leading to Alkaline Phosphatase (AP) expression. ***B***, ***C***, AP staining on coronal section of OB, ipsilateral to adenovirus injection, 15 days after surgery in TrkB-WT (***B***) or $TrkB^{lox/lox}$ (***C***) mouse. Insets: SVZ area targeted by distal injection. ***D***, quantification of AP^{+} cells in OB, showing a reduced number of neurons in OB of $TrkB^{lox/lox}$ mice, mostly due to deficiencies in areas outside the OB core; *$p<0.05$ (t-Student test, statistically significant); n=8 mice (TrkB-WT), n=7 mice ($TrkB^{lox/lox}$). All values represent average ± SEM. Scale bars: 1 mm. See technical details in sections 5.10, A11.

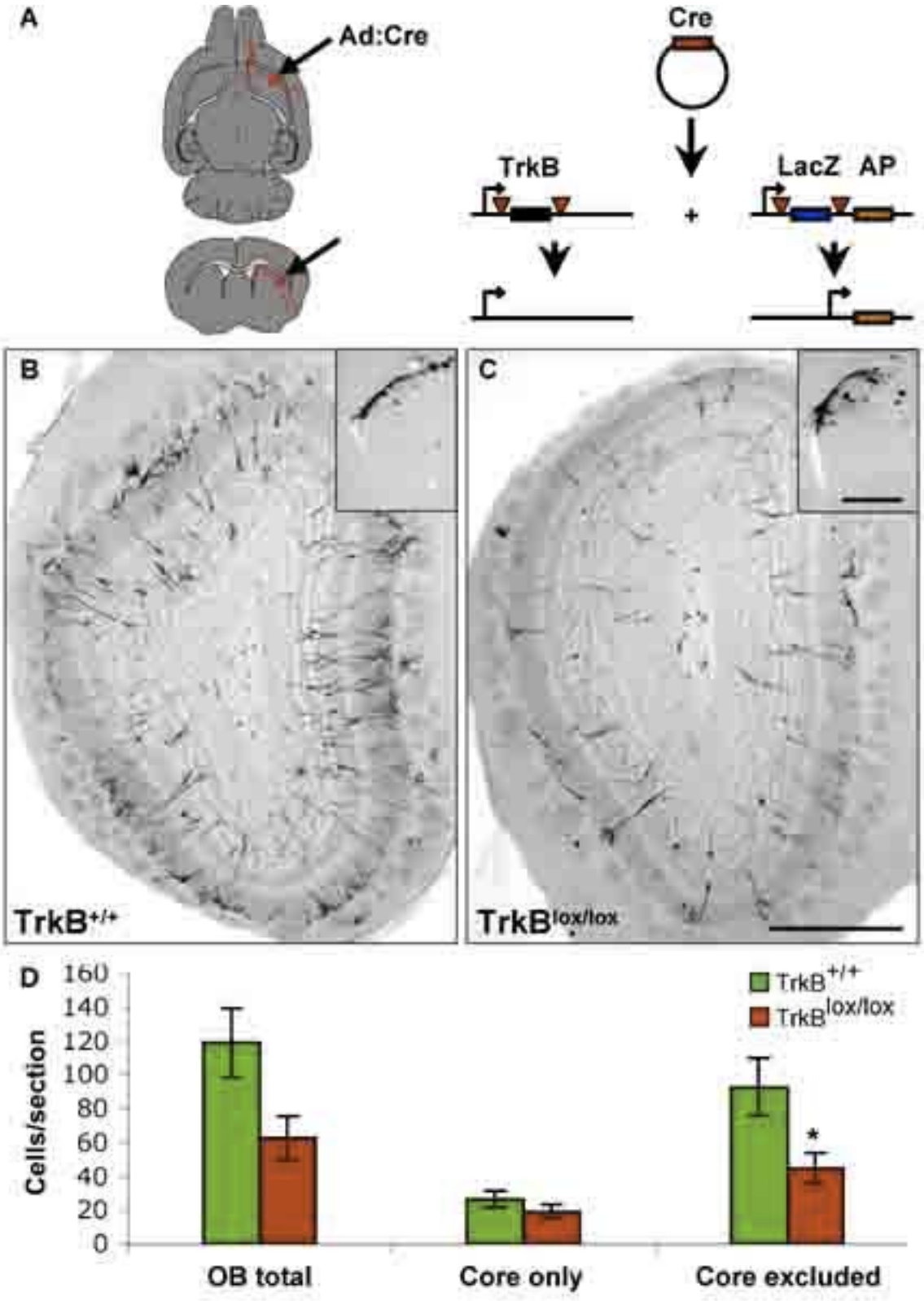
A
Ad:Cre
Cre
TrkB
LacZ AP
+
B
C
TrkB+/+
TrkBlox/lox
D
Cells/section
160
140
120
100
80
60
40
20
0
TrkB+/+
TrkBlox/lox
*
OB total
Core only
Core excluded

neurons were found in all layers, indicating that both granular and periglomerular interneurons were produced. Many cells exhibited fully differentiated morphologies with extensive dendrite branching (Fig. 2.10B, C). However, there was a general trend towards a lower number of AP^+ cells in Cre-injected $TrkB^{lox/lox}$ mice. This deficit was significantly more pronounced outside the core of the OB (rostral extension of the RMS) than within it (Fig. 2.10D; 48% and 28% reduction, respectively), suggesting that TrkB may become increasingly important for SVZ-derived neuroblasts as they mature in their final destination. Importantly, many new neurons were produced in the absence of TrkB, suggesting this receptor is not essential for postnatal neurogenesis.

The conditional TrkB mouse line I used has several important caveats. $TrkB^{lox/lox}$ mice were constructed by inserting the cDNA of TrkB-FL into the endogenous TrkB locus (Fig. 2.11A) (Xu et al., 2000b). Therefore, these mice cannot express TrkB-TR, the main isoform of TrkB in the SVZ, but express TrkB-FL instead (Fig. 2.11E), which is undetectable in the SVZ of TrkB-WT mice. Furthermore, $TrkB^{lox/lox}$ mice are hypomorphic (Fig. 2.11C), expressing only 33% and 24% of the WT TrkB mRNA and protein levels, respectively (Xu et al., 2000b), and are smaller than WT mice [$TrkB^{lox/lox}$: 5g (n=2); $TrkB^{WT}$: 18g (n=4), average weight at P28] and extremely ataxic (data not shown). Because of these problems, the apparent reduction in production of OB neurons in $TrkB^{lox/lox}$ mice is difficult to interpret.

TrkB-KO neurons survive, mature and integrate in the OB

To circumvent the problems inherent with conventional and conditional TrkB mutants, I homotopically grafted SVZ cells from TrkB-KO and WT mice into the SVZ of WT adult mice. This allowed me to test the behavior of SVZ progenitors lacking TrkB in a normal postnatal brain. Donor cells were labeled by a β-Actin:GFP transgene and were collected from P1 pups, before TrkB deficiency becomes lethal. I then waited 15, 45 or 180 days and assessed the survival and maturation of the grafted cells (Fig. 2.12L). The total number of GFP^+ cells in the granular cell layer (GCL) of recipient mice increased significantly between 15 and 180 days in both TrkB-WT and TrkB-KO grafts (Fig. 2.12B) and I found numerous GFP^+ cells in all layers of the OB. To determine the survival rate of a defined cohort of cells, grafted mice were given BrdU in the drinking

Figure 2.11: Conditional TrkB mutant mice misexpress TrkB in the SVZ. ***A***, schematic representation of the knock-in strategy. The cDNA sequence for the full-length isoform of TrkB flanked by loxP sequences and followed by a tau-lacZ reporter gene was inserted into a targeting vector. The first coding exon of TrkB (exon S) was targeted by flanking the trkB-tau-lacZ construct with the genomic sequences surrounding exon S (thick lines). After homologous recombination, the inserted construct is under the control of the endogenous TrkB promoter. After Cre recombination, TrkB cDNA is excised from the genome and the tau-lacZ reporter gene is activated [diagram adapted from Xu et al. (2000b)]. ***B***-***E***, *in situ* hybridization for TrkB-all (***B***, ***C***) and TrkB-FL (***D***, ***E***) in the SVZ of adult $TrkB^{WT}$ (***B***, ***D***) and homozygous conditional $TrkB^{lox/lox}$ (***C***, ***E***) mice. TrkB expression is considerably attenuated in $TrkB^{lox/lox}$ mice (***C***) and many cells expressing TrkB-FL are present in the SVZ of $TrkB^{lox/lox}$ mice (***E***), whereas none can be found in $TrkB^{WT}$ mice (***D***). Scale bar: 100 µm. See technical details in sections 5.5, A2.

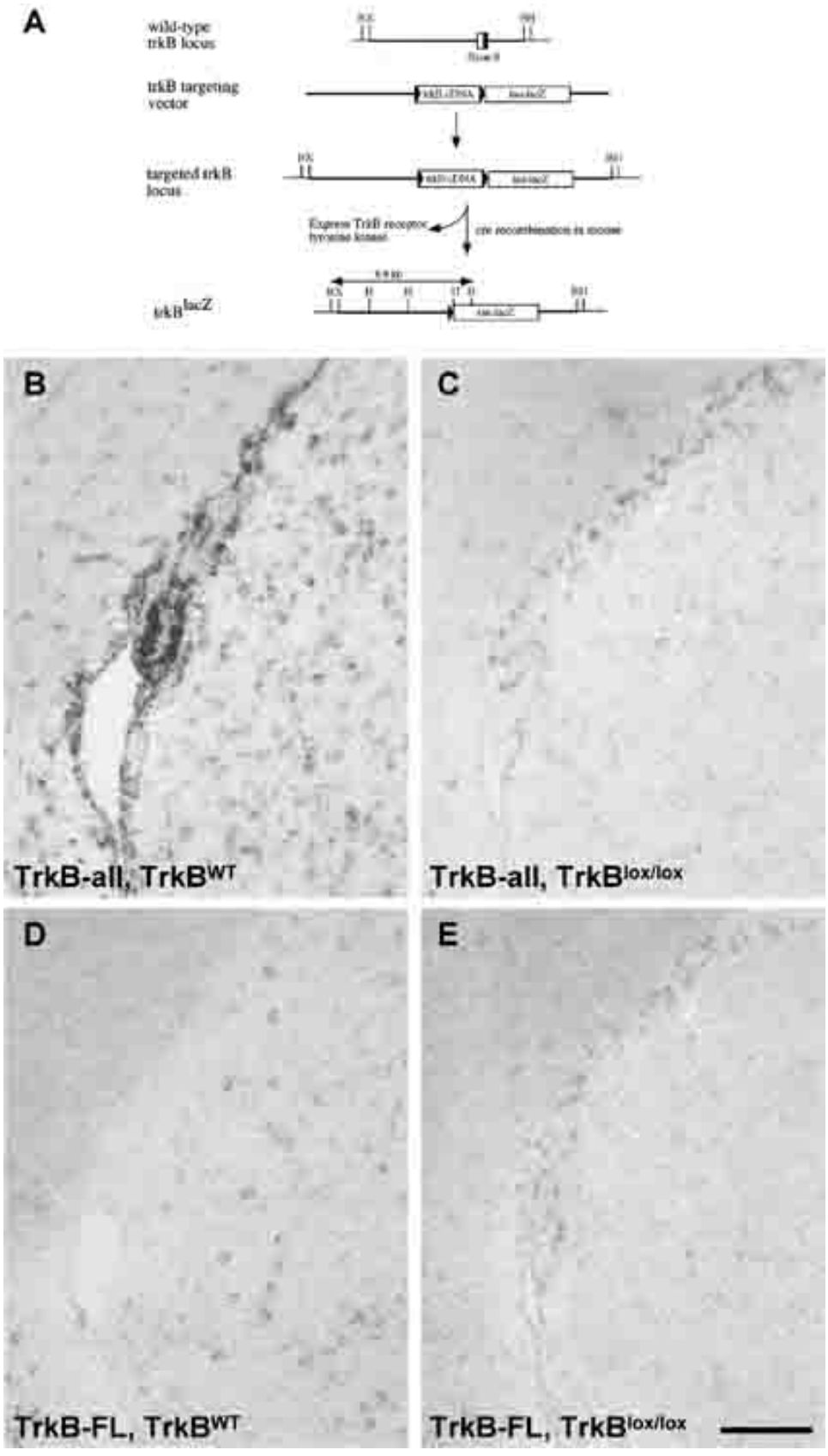
A
wild-type trkB locus
trkB targeting vector
targeted trkB locus
trkB^lacZ
B
TrkB-all, TrkB^WT
C
TrkB-all, TrkB^lox/lox
D
TrkB-FL, TrkB^WT
E
TrkB-FL, TrkB^lox/lox

Figure 2.12: Grafted TrkB-KO cells can survive and mature in OB. β-actin:GFP^+ cells from SVZ of TrkB-WT or TrkB-KO P1 mice were grafted into the SVZ of WT, P90 mice; GFP^+ cells were then analyzed in the OB 15, 45 and 180 days after surgery; BrdU was administered during the first 3 days after surgery. ***A***, ***C***, GFP/BrdU (green/red) staining in the granular cell layer (GCL) of the OB of mice grafted with TrkB-WT (***A***) or TrkB-KO (***C***) cells. ***B***, quantification of all GFP^+ cells/picture in GCL of OB, showing increase in both TrkB-WT and TrkB-KO cells throughout entire experiment; n=3 (15 day graft), n=2 (45 day graft), n=2 (180 day graft). ***D***, quantification of the proportion of grafted cells labeled with BrdU in GCL of OB, showing identical dynamics for TrkB-WT and TrkB-KO cells; n=3 (15 day graft), n=4 (45 day graft), n=2 (180 day graft). ***E***, ***G***, GFP/TH (green/red) staining in the glomerular layer (GL) of the OB of mice grafted with TrkB-WT (***E***) or TrkB-KO (***G***) cells. ***F***, proportion of grafted cells expressing TH protein in GL of OB: there is a sharper drop in TH^+ cells among TrkB-KO cells than among TrkB-WT cells between 45 and 180 days after surgery; n=4 (all time points except 45 day TrkB-WT, for which n=3, and 180 day TrkB-KO, for which n=5). ***H***, diagram of a coronal section of OB (dorsal to the left), showing general location from which data was collected (box 1: origin of data in ***A***-***D***; box 2: origin of data in ***E***-***K***). ***I***, ***K***, GFP/CalB (green/red) staining in the GL of mice grafted with TrkB-WT (***I***) or TrkB-KO (***K***) cells. ***J***, proportion of grafted cells expressing CalB protein in GL of the OB: both TrkB-WT and TrkB-KO grafted cells increase between 45 and 180 days after surgery; n=4 (all time points except 45 day TrkB-KO, for which n=3). ***L***, experimental design. All values represent average ± SEM. All images shown were taken at 45-day graft survival. Scale bars: 100 μm (***A***, ***C***), 50 μm (***E***, ***G***, ***I***, ***K***). See technical details in sections 5.4, 5.9, A1, A13, A14.

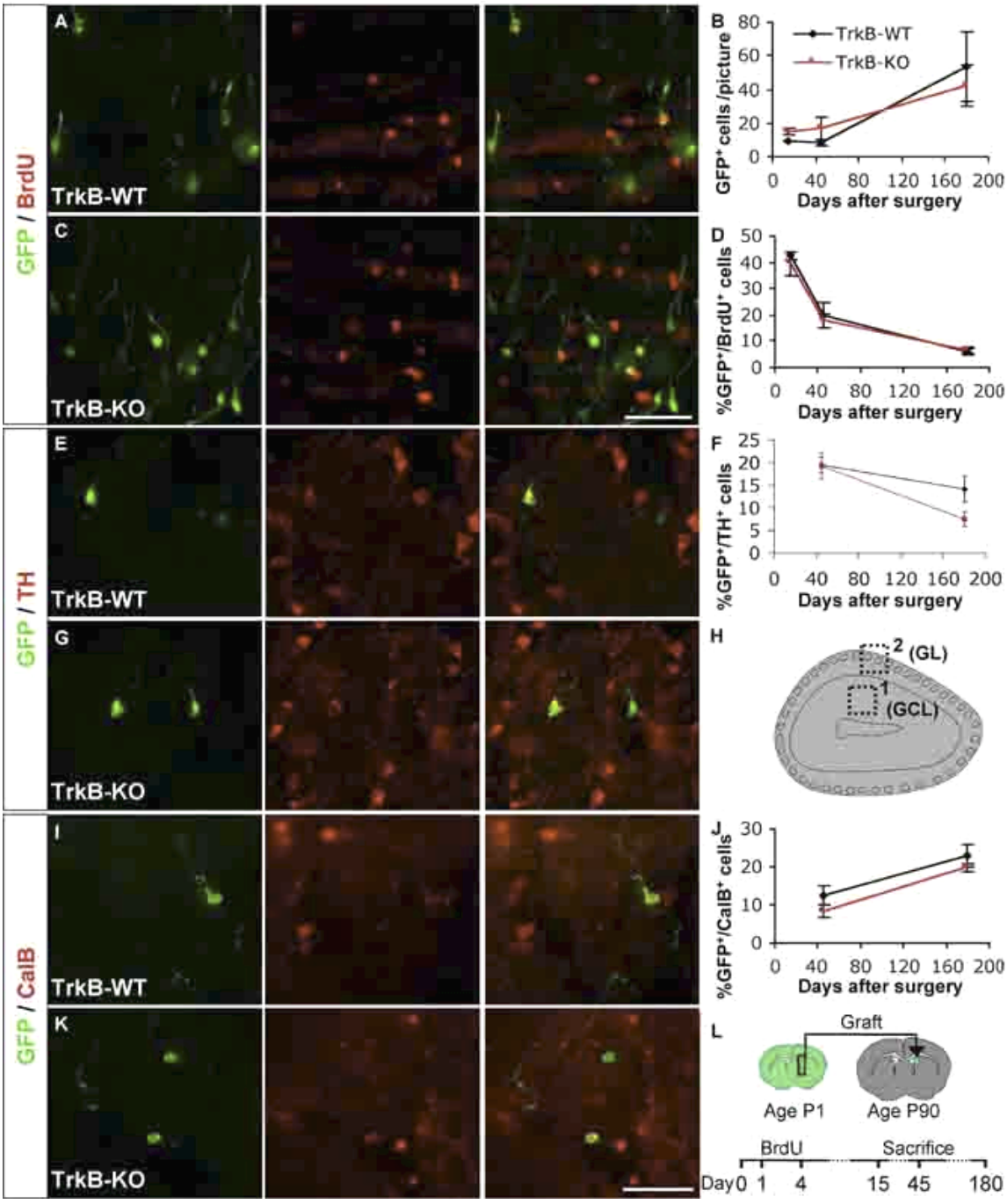
A
TrkB-WT
C
TrkB-KO
GFP / BrdU
B
TrkB-WT
TrkB-KO
GFP+ cells /picture
Days after surgery
D
%GFP+/BrdU+ cells
Days after surgery
E
TrkB-WT
G
TrkB-KO
GFP / TH
F
%GFP+/TH+ cells
Days after surgery
H
2 (GL)
1 (GCL)
I
TrkB-WT
K
TrkB-KO
GFP / CalB
J
%GFP+/CalB+ cells
Days after surgery
L
Graft
Age P1
Age P90
BrdU
Sacrifice
Day 0 1 4 15 45 180

water for the first 3 days after surgery. I then counted the proportion of $BrdU^+$ cells among all GFP^+ cells in the GCL. Grafted TrkB-WT and TrkB-KO cells had indistinguishable proportions of $BrdU^+$ cells at all time points analyzed, both undergoing a ~50% decline between 15 and 45 days, followed by a more gradual loss after 45 days (Fig. 2.12D). This behavior is identical to the population dynamics described by Petreanu and Alvarez-Buylla (2002) for new neurons in the adult WT GCL. These results show that TrkB-WT and TrkB-KO interneurons face similar survival challenges in the OB. The accumulation of GFP^+ neurons in the OB (Fig. 2.12B), together with the presence of GFP^+ cells in the RMS even 180 days after the graft (Fig. 2.13A, B), also show that both TrkB-WT and TrkB-KO stem cells can continuously give rise to new neurons.

TrkB may be involved in the maturation of OB interneurons rather than their survival. To address this possibility, I counted the proportion of grafted cells that express tyrosine hydroxylase (TH) or Calbindin (CalB). TH is the rate-limiting enzyme in the synthesis of the neurotransmitter dopamine and CalB is a neuron-specific Ca^{2+}-binding protein. These molecules are expressed in distinct subpopulations of mature OB periglomerular neurons (Rogers, 1992; Kosaka et al., 1995). Fourty five days after the graft, ~19% of GFP^+ periglomerular cells were TH^+, irrespectively of their genotype (Fig. 2.12F). CalB expression was slightly lower at 45 days (8.5% of TrkB-KO cells were $CalB^+$, compared to 12.7% among TrkB-WT cells; Fig. 2.12J). However, this difference was not statistically significant ($p=0.27$ by t-Student test). At 180 days, TH expression dropped slightly to 14.1% in TrkB-WT cells and more drastically to 7.5% in TrkB-KO cells (Fig. 2.12F, $p=0.07$ by t-Student test). On the other hand, CalB expression increased to 22.9% and 19.9% among TrkB-WT and TrkB-KO grafted cells, respectively (Fig. 2.12J). The observation that the proportion of TH expression among grafted cells drops between 45 and 180 days whereas that of CalB continues to rise is consistent with others' observations (Kohwi et al., 2007) and probably reflects differences in the maturation time and/or turnover rate for these different cell types.

TH and CalB expression are dependent on synaptic activity (Baker et al., 1983; Philpot et al., 1997). The detection of TH and CalB, as well as of dendritic spines in TrkB-KO neurons (Fig. 2.13C, D) suggests that at least some of these cells are capable of functionally integrating into the OB circuitry. Overall, the results of my grafting

Figure 2.13: TrkB-KO and WT cells grafted from P1 to P90 mice generate new neurons and exhibit mature properties after 6 months. ***A***, ***B***, GFP^+ (green) migratory neuroblasts in coronal sections of RMS, indicating that TrkB-KO stem cells can continue to generate new neurons long after being grafted into a WT background. ***C***, ***D***, dendrites of TrkB-WT and KO grafted cells show multiple dendritic spines in the external plexiform layer of the OB, suggesting full maturation (green, GFP). Insets: magnified view of dendritic spines in boxed areas. Scale bars: 50 μm (***A***, ***B***), 30 μm (***C***, ***D***). See technical details in sections 5.9, A13, A14.

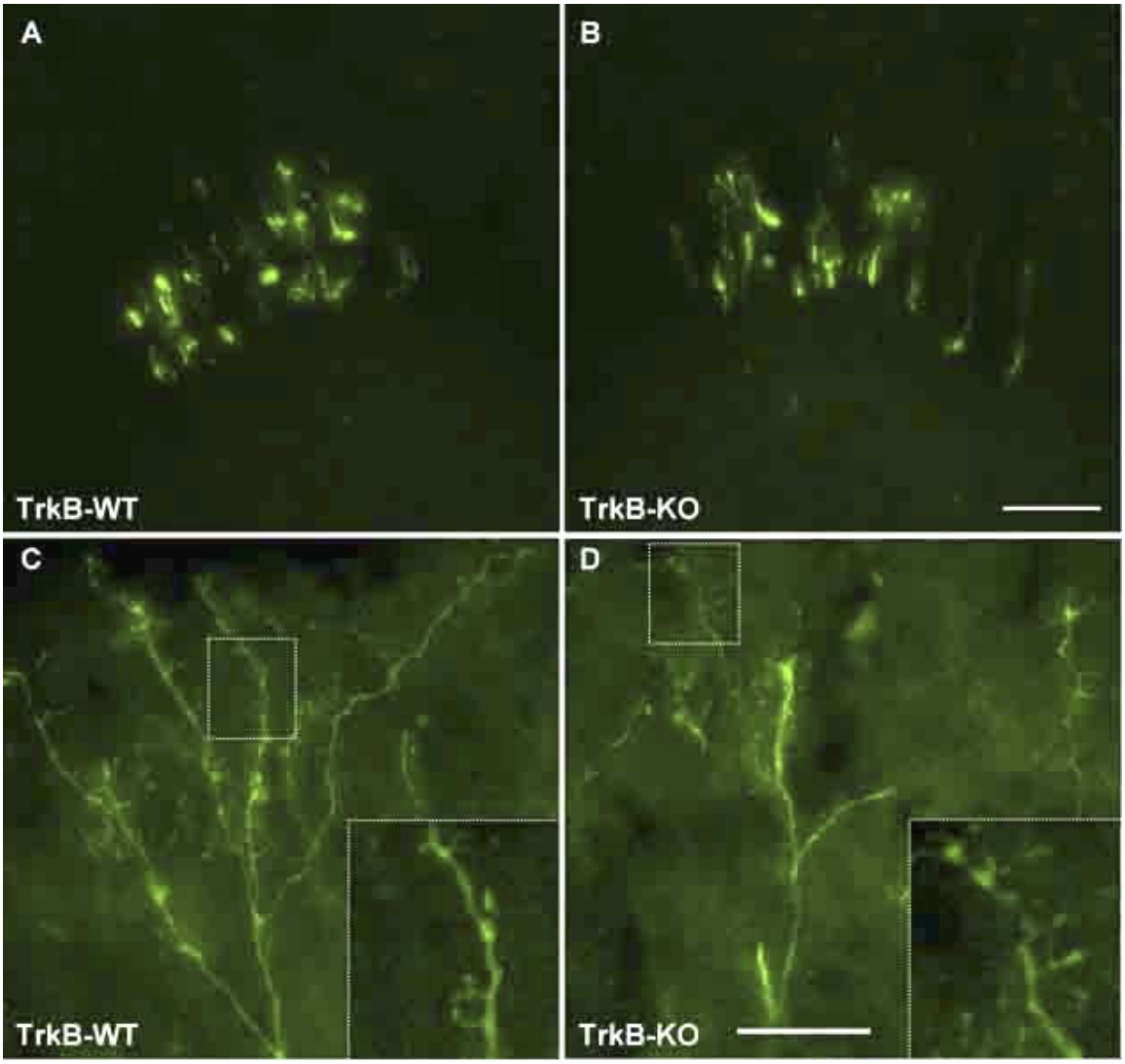
A
TrkB-WT
B
TrkB-KO
C
TrkB-WT
D
TrkB-KO

experiment indicate that TrkB is not essential for the production, migration and long-term survival of most new OB neurons, though some cell types may be more affected than others.

TrkB, TrkB-FL and BDNF expression in the OB

To better understand the potential role of BDNF/TrkB signaling in maturing SVZ-derived interneurons, I characterized the expression of these molecules in the OB. I performed *in situ* hybridization on OB section from adult mice, using probes specific for BDNF, all TrkB receptor isoforms (TrkB-all) and the full-length-specific isoform of the receptor (TrkB-FL). TrkB mRNA was strongest in the core of the OB, where the new neurons are arriving via the RMS (Fig. 2.14A, C). Outside of the core, TrkB was prominently detected in the mitral cell layer (MCL) as well as in cells of the external plexiform (EPL) and glomerular (GL) layers (Fig. 2.14A, C, E). Expression of TrkB in the granular cell layer seemed limited to just a few cells (Fig. 2.14A, C). The expression pattern of TrkB-FL in the OB is very similar to that of TrkB-all, with the exception of the OB core. Though absent from cells in the core, TrkB-FL is also clearly expressed in the MCL and in several cells of the EPL and GL (Fig. 2.14B, D, F). A few rare cells in the GCL were clearly labeled by the TrkB-FL probe (Fig. 2.14B, D). Thus, while cells in the core of the OB express only the truncated isoform of TrkB (likely astrocytes as described in more posterior sections of the RMS of TrkB:Tau-LacZ reporter mice), mitral, tufted and at least some periglomerular and granular cells express the full-length isoform of TrkB (and perhaps also truncated TrkB). I currently do not know the identity of these cells, though they are likely neurons because glia do not normally express the TrkB-FL isoform.

Transcripts of the TrkB ligand BDNF are also found in the OB, either by RT-PCR (data not shown), *in situ* hybridization or BDNF:LacZ reporter gene expression. By *in situ* hybridization, BDNF is strongest on the MCL, EPL and GL, though it is also detectable in cells of the GCL (Fig. 2.15A, C, D). This pattern of expression is largely consistent with what I observed in BDNF:LacZ reporter mice.

Therefore, both BDNF and its receptor TrkB are expressed in the OB. As suggested by the cell grafting experiment, TrkB signaling may thus play a role in the maturation and

Figure 2.14: TrkB receptor expression in olfactory bulb. *In situ* hybridization staining for all isoforms of TrkB (TrkB-all: ***A***, ***C***, ***E***) as well as specifically for the full length isoform of TrkB (TrkB-FL: ***B***, ***D***, ***F***) in coronal sections of mouse OB. ***A***, ***B***, overall staining pattern of TrkB-all (***A***) and TrkB-FL (***B***) in the core, granular and mitral cell layers (from center to periphery), showing strong expression of TrkB-all in core and mitral layer as well as in a small number of cells in the granular layer. The expression of TrkB-FL is very similar to that of TrkB-all in all layers, except in the core of the OB, where TrkB-FL is not expressed. ***C***, ***D***, magnified view of boxed area in ***A***, ***B***, showing TrkB-all (***C***) and TrkB-FL (***D***) expression levels in OB core, granular and mitral cell layers (left to right). ***E***, ***F***, magnified view of OB layers outside of the area depicted in ***A***, ***B***, showing TrkB-all (***E***) and TrkB-FL (***F***) expression levels in mitral, external plexiform and glomerular layers (left to right). Both RNA probes detect TrkB in these outer layers of the OB. For all panels, TrkB-all and TrkB-FL staining was performed on adjacent brain sections to ensure comparison of identical regions of the OB. RMS: rostral migratory stream. GCL: granular cell layer. MCL: mitral cell layer. EPL: external plexiform layer. GL: glomerular layer. Scale bars: 200 μm (***A***, ***B***), 100 μm (***C***-***F***). See technical details in sections 5.5, A2.

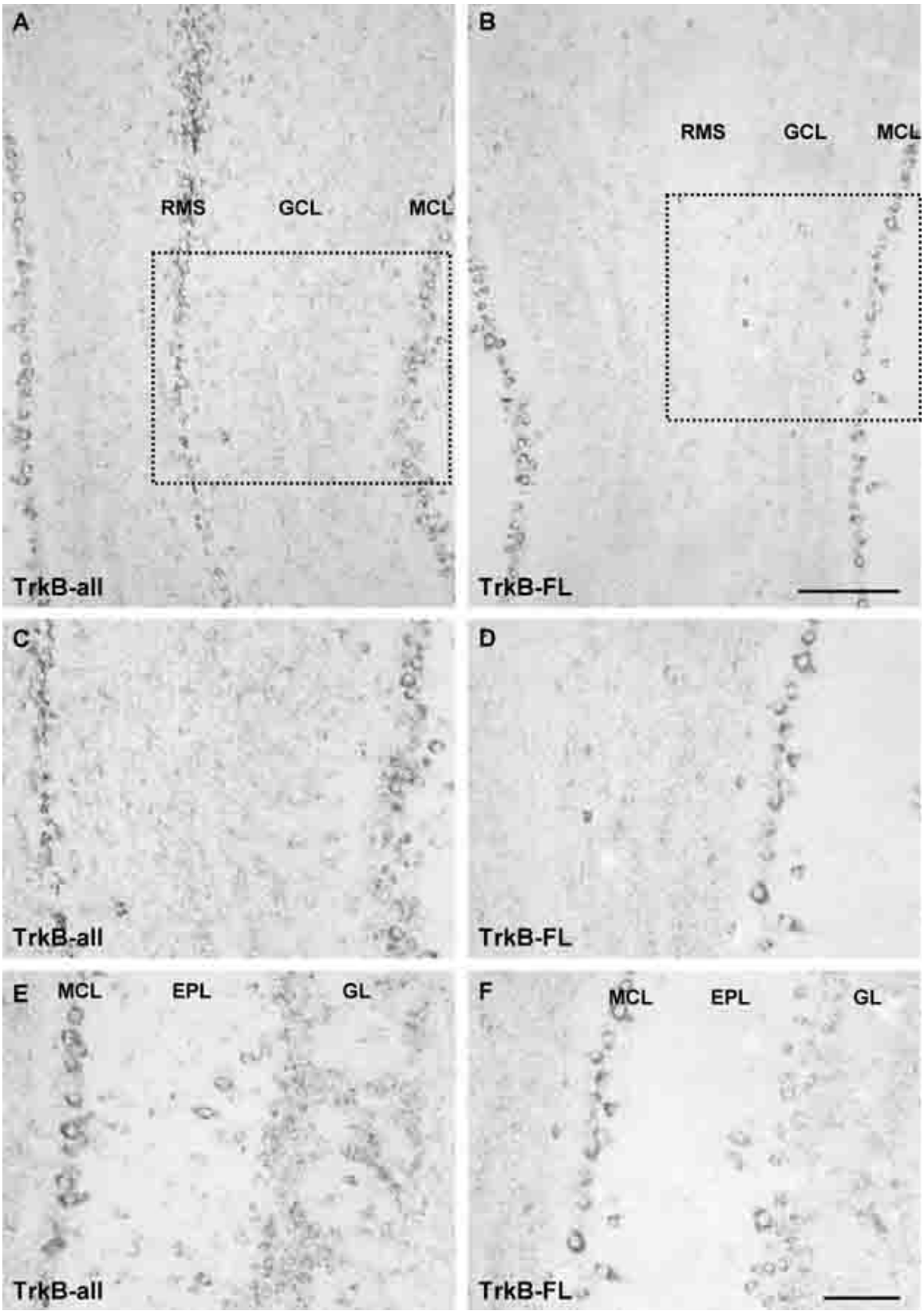
A
RMS
GCL
MCL
TrkB-all
B
RMS
GCL
MCL
TrkB-FL
C
TrkB-all
D
TrkB-FL
E
MCL
EPL
GL
TrkB-all
F
MCL
EPL
GL
TrkB-FL

Figure 2.15: BDNF expression in olfactory bulb. ***A***, BDNF mRNA labeling by *in situ* hybridization in a horizontal section of the OB from an adult mouse. Labeled cells are detected in all layers of the OB but are strongest in the mitral and glomerular layers. Boxed areas represent regions of the OB similar to those shown in ***C*** and ***D***. ***B***, β-Gal enzymatic staining in the OB of an adult BDNF:LacZ reporter mouse, showing BDNF-expressing cells in similar layers to what is detected by *in situ* hybridization. C, D, BDNF mRNA labeling by *in situ* hybridization, showing labeled cells in the granular and mitral layers (***C***), as well as in the external plexiform and glomerular layers (***D***). AOB: accessory olfactory bulb. GCL: granular cell layer. MCL: mitral cell layer. EPL: external plexiform layer. GL: glomerular layer. Scale bars: 500 μm (***A***), 200 μm (***B***), 100 μm (***C***, ***D***). See technical details in sections 5.5, A2, A8.

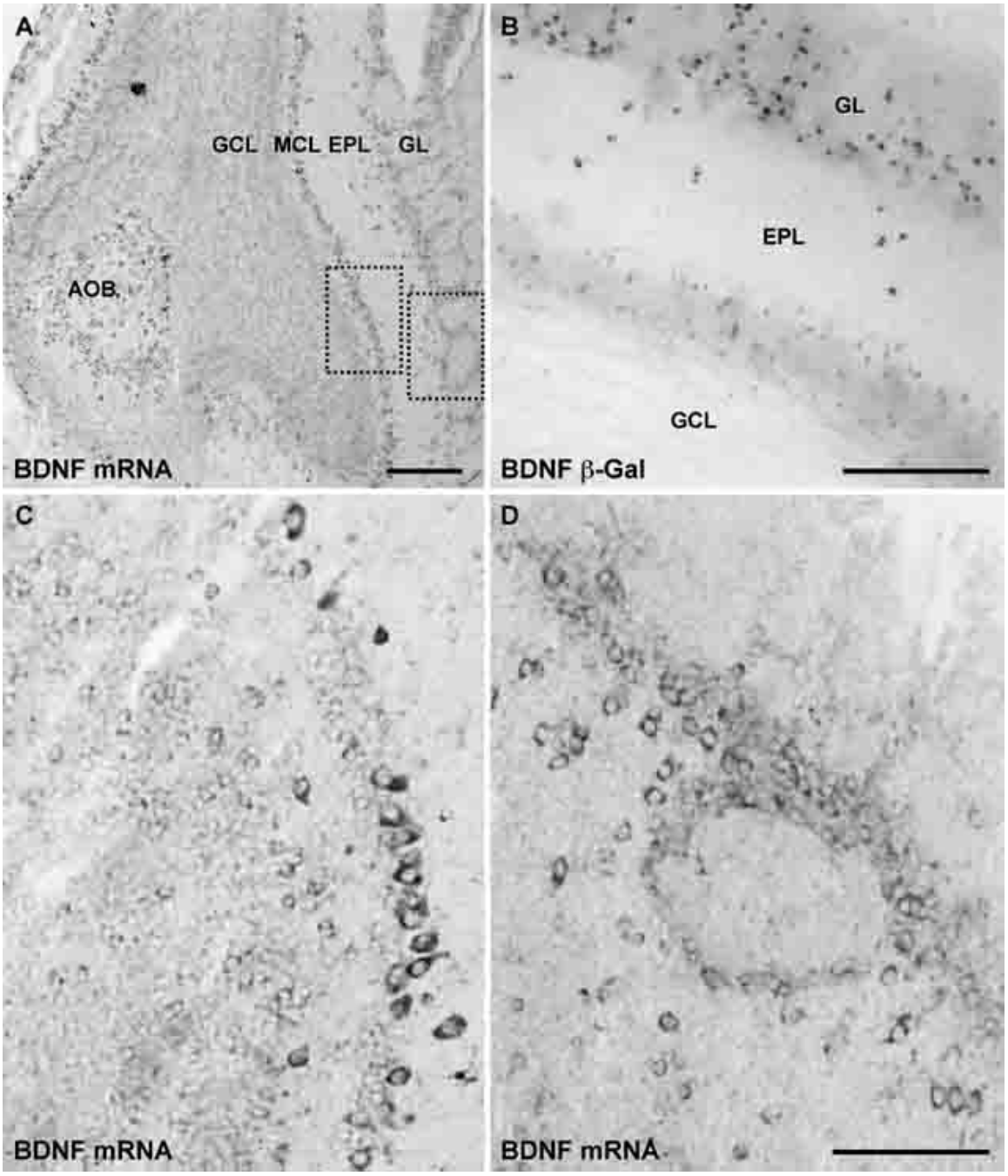
A
GCL MCL EPL GL
AOB
BDNF mRNA
B
GL
EPL
GCL
BDNF β-Gal
C
BDNF mRNA
D
BDNF mRNA

function of a subpopulation of OB cells.

BDNF does not affect mouse neurogenesis

The above results suggest that TrkB-FL is not present in SVZ progenitors suggesting that this receptor is not mediating possible effects of BDNF in adult SVZ neurogenesis. However, it was possible that BDNF could act through a different receptor to regulate SVZ neuron production. To test this hypothesis, I used microosmotic pumps to infuse a concentrated solution of BDNF (1 mg/ml) into the lateral ventricle of WT adult mice for 14 days. BDNF delivered intraventricularly has been shown to penetrate the brain tissue deep enough to reach cells in the SVZ (Yan et al., 1994; Anderson et al., 1995).

To determine the proliferation rate in the SVZ, I immunostained for pH3 and counted the number of $pH3^+$ cells. I found that BDNF-infused mice had lower numbers of $pH3^+$ cells in the SVZ ipsilateral to the pump implant when compared to vehicle-infused mice (Fig. 2.16G, 22.5% reduction, p=0.048 by t-Student test).

Intracerebroventricular BDNF administration has previously been shown to significantly increase the number of new cells added to the OB (Zigova et al., 1998; Benraiss et al., 2001). I therefore analyzed the OB of the mice I had infused with BDNF and vehicle for 14 days. To label newly-generated cells, mice were injected with BrdU every 4 days, starting on the 4^{th} day after pump implantation and ending 2 days before the mice were sacrificed (Fig. 2.16A). Consistent with previous reports (Zigova et al., 1998; Benraiss et al., 2001), the vast majority of $BrdU^+$ cells in the OB were neuronal (90.3% in vehicle-infused and 86.5% in BDNF-infused mice, as determined by HuC/D staining). Small numbers of $BrdU^+$ cells were identified as $Olig2^+$ oligodendroglia (4.3% in vehicle-infused and 4.2% in BDNF-infused mice) and $Iba1^+$ microglia (0.9% in vehicle-infused and 1.1% in BDNF-infused mice). Surprisingly, though, I did not detect any difference in the total number of $BrdU^+$ cells in the OB after 14 days of BDNF infusion (Fig. 2.16H, 352 and 348 $BrdU^+$ cells/OB section in vehicle and BDNF-infused mice respectively, n=5 mice/group). This result differs from previous findings, which reported 2 to 3-fold increases in $BrdU^+$ cells in the OB of BDNF-treated mice (Zigova et al., 1998; Benraiss et al., 2001). However, I did observe other known effects of BDNF: the weight of BDNF-infused mice dropped continuously, averaging 31.4% less than that of control

Figure 2.16: *In vivo* effect of BDNF infusion in adult mice. ***A***, experimental design: microosmotic pumps were implanted on P90 mice to infuse BDNF for 14 days; BrdU was administered every 4 days by intraperitoneal injection; on day 14, mice were sacrificed for analysis. ***B***, effect of BDNF infusion on mouse weight. ***C***, ***E***, phosphorylated histone H3 (pH3, green) staining ipsilateral to pump implant, in SVZ of vehicle (***C***) and BDNF (***E***) infused mice. ***D***, ***F***, BrdU (green) staining of OB ipsilateral to pump implant in vehicle (***D***) and BDNF (***F***) infused mice. ***G***, quantification of pH3 staining in SVZ ipsilateral to pump; *$p<0.05$ (t-Student test, statistically significant); n=5 mice/group. ***H***, quantification of BrdU staining in OB ipsilateral to pump; n=5 mice/group. All values represent average ± SEM. SVZ inset (***C***, ***E***): pH3/Hu (green/red); OB inset (***D***, ***F***): BrdU/Hu (green/red). Blue: DAPI (all panels). Scale bar: 100 μm (OB, SVZ). See technical details in sections 5.4, 5.9, 5.10, A1, A12, A13.

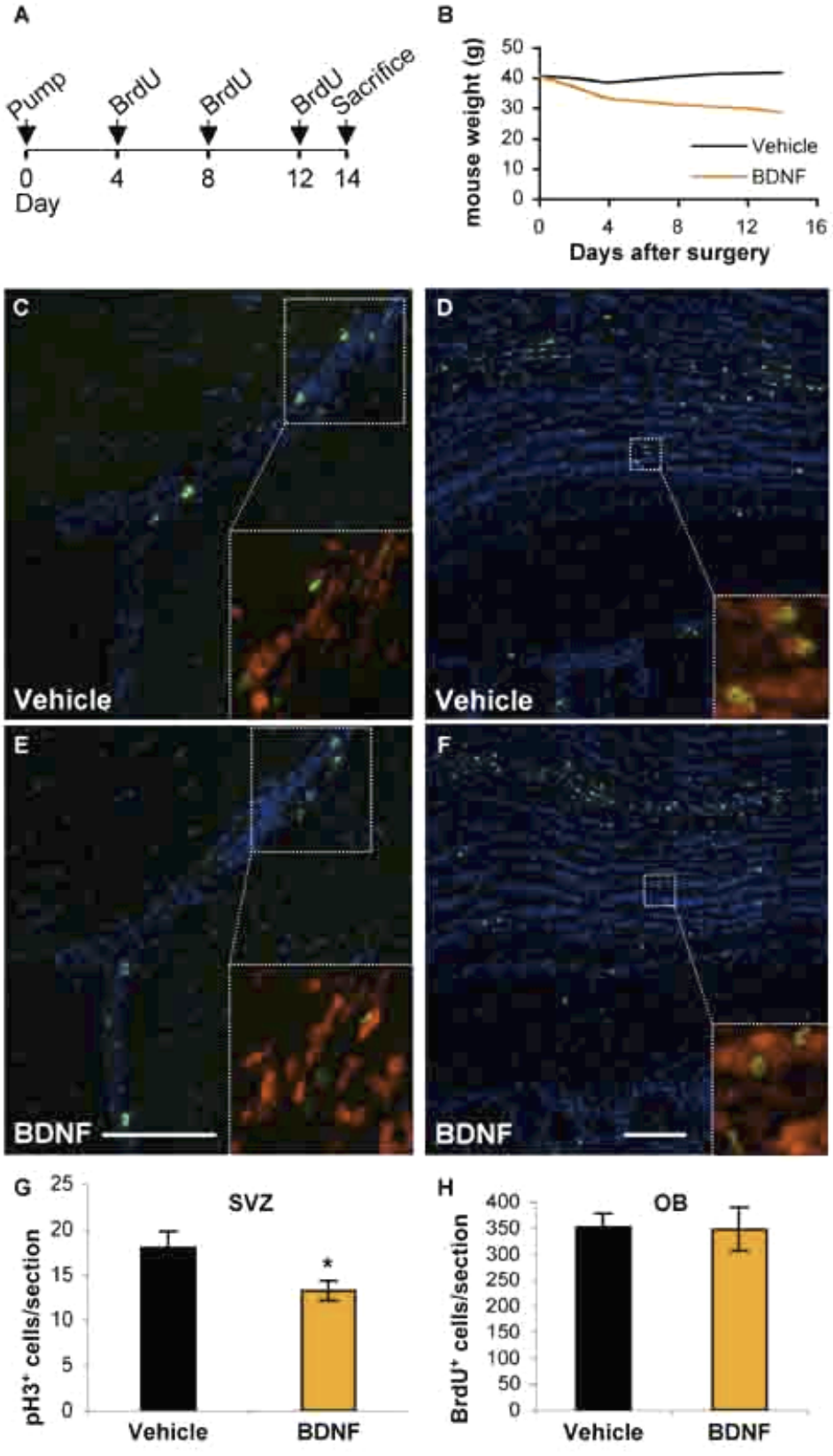
A
Pump
BrdU
BrdU
BrdU
Sacrifice
0
Day
4
8
12
14
B
mouse weight (g)
50
40
30
20
10
0
Vehicle
BDNF
0
4
8
12
16
Days after surgery
C
Vehicle
D
Vehicle
E
BDNF
F
BDNF
G
SVZ
pH3+ cells/section
25
20
15
10
5
0
*
Vehicle
BDNF
H
OB
BrdU+ cells/section
400
350
300
250
200
150
100
50
0
Vehicle
BDNF

mice by the 14th day of treatment (Fig. 2.16B). Benraiss et al. (2001) reported a similar weight loss during their experiment. As BDNF is a known appetite suppressant, (Pelleymounter et al., 1995; Kernie et al., 2000; Xu et al., 2003), this observation confirms that BDNF was being delivered and was biologically active throughout the experiment. As further corroboration of the quality of the BDNF solution, I observed that dorsal root ganglia (DRG) neurons responded to as little as 10 ng/ml BDNF *in vitro* with extensive neurite outgrowth and an increased number of surviving neurons (Fig. 2.17) (Lindsay et al., 1985; Davies et al., 1986). Additionally, I visually confirmed on brain sections that the pump cannula penetrated into the lateral ventricle lumen in all mice analyzed (Fig. 2.18A, B) and I immunolabeled SVZ sections of pump-implanted mice with a BDNF antibody to confirm the protein was being delivered (Fig. 2.19). Because labeling for BDNF and BrdU require different tissue processing methods (see Materials and Methods), these stainings were performed on different mice.

These findings are consistent with my *in vitro* observations. Adult SVZ astrocytes were cultured in subconfluent conditions with or without BDNF for 7 days, then labeled for 1 hour with BrdU. Alternatively, SVZ astrocytes from P3 pups were grown to confluence and then allowed to generate neuroblasts in the presence or absence of BDNF for 6 days. I then added BrdU for 12 hours before fixing the cultures. BDNF did not increase proliferation of either SVZ astrocytes or neuroblasts (Fig. 2.20G, H). I also cultured TrkB-KO and WT SVZ neuroblasts purified from GFP^+ P3 pups on a feeder layer of GFP^-, non-neurogenic cortical astrocytes. Neither exposure to the BDNF ligand nor deletion of the TrkB receptor affected the total number of neuroblasts after 5 days (Fig. 2.20I; see Materials and Methods for details).

Overall, my results suggest that BDNF delivered to the ventricle does not significantly enhance adult neurogenesis, contrary to what other laboratories have reported (Zigova et al., 1998; Benraiss et al., 2001), nor does it seem to affect proliferation or survival of SVZ astrocytes and neuroblasts in short-term cultures.

BDNF inhibits rat neurogenesis

One possible cause for the contradiction between the results reported above and those published by other groups is that I used mice as model organisms for my BDNF infusion

Figure 2.17: BDNF elicits strong response in dorsal root ganglia (DRG) cultures. ***A***-***D***, immunostaining for neuronal marker β-III tubulin (red, β-III tubulin; blue, DAPI) in DRG explants cultured in various concentrations of BDNF. ***A***, I found very few neurons and short processes when DRG explants from E12.5 embryos were cultured in medium without neurotrophins. ***B***-***D***, In contrast, DRG explants cultured with BDNF exhibited extensive axonal growth and increased number of neuronal cell bodies. Scale bar: 100 μm. See technical details in sections 5.13.

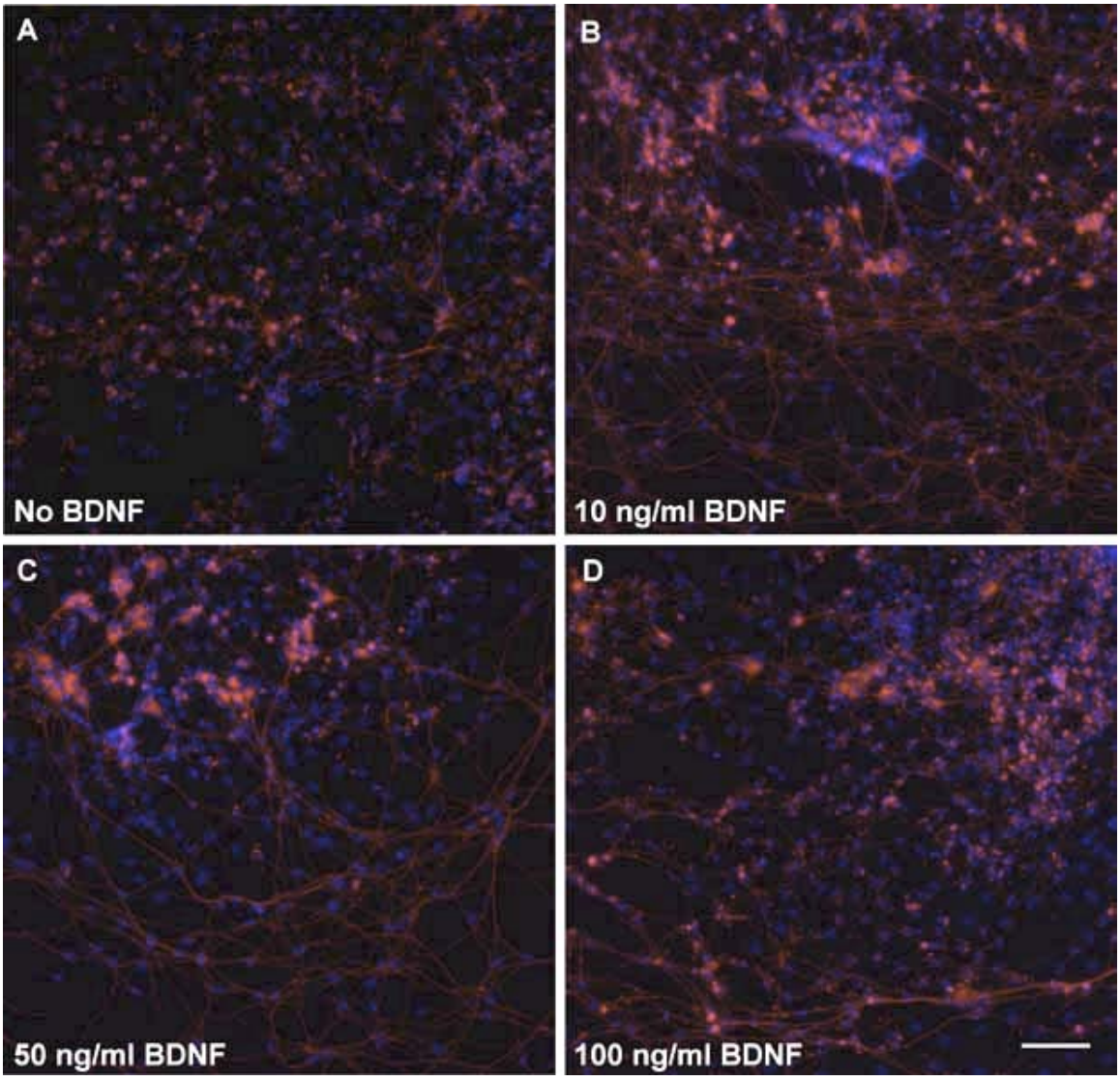
A
No BDNF
B
10 ng/ml BDNF
C
50 ng/ml BDNF
D
100 ng/ml BDNF

Figure 2.18: Pump cannulas penetrated the ventricular lumen in all animals analyzed. ***A***, ***B***, DAPI staining of coronal sections from adult mice implanted with vehicle (***A***) and BDNF (***B***) pumps show that the cannula penetrated the lateral ventricle lumen. ***C***, ***D***, DAPI staining of coronal sections from adult rats implanted with vehicle (***C***) and BDNF (***D***) pumps show that the cannula penetrated the lateral ventricle lumen. In all images, the choroid plexus is occupying part of the cavity left by the cannula. Scale bars 500 μm (***A***, ***B***), (***C***, ***D***). See technical details in sections 5.10, A12.

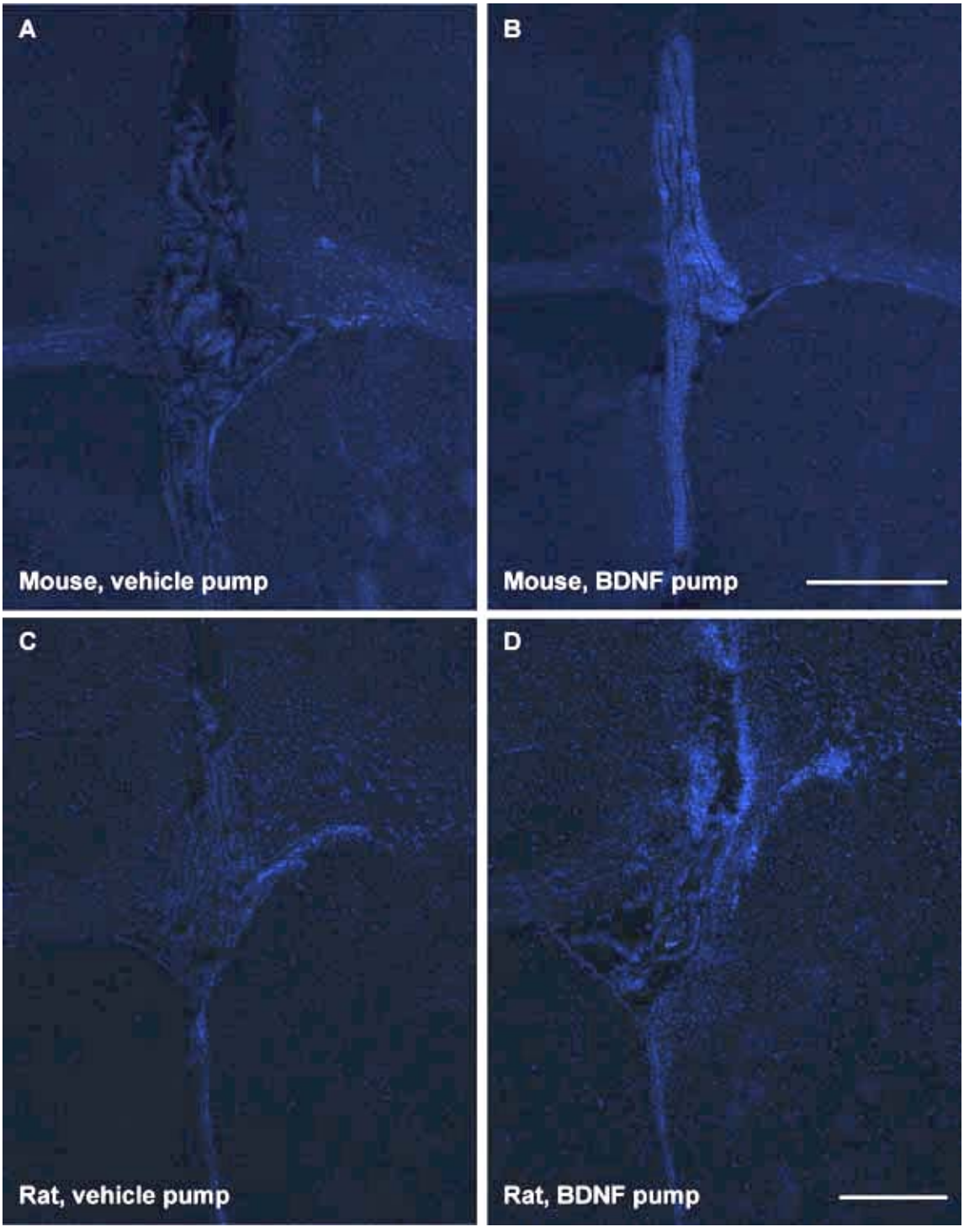
A
Mouse, vehicle pump
B
Mouse, BDNF pump
C
Rat, vehicle pump
D
Rat, BDNF pump

Figure 2.19: BDNF protein is delivered *in vivo* by pumps. ***A***, ***B***, immunohistochemical detection of BDNF protein at the lateral ventricle anterior and ipsilateral to pump entry site in adult mice infused for 4 days with 1 mg/ml BDNF (***A***) or vehicle (***B***). These images were taken at equivalent distances from the pump entry site and show a higher level of BDNF in BDNF-infused mice. ***C***, ***D***, adjacent sections of BDNF-infused (***C***, 40 μm posterior to ***A***) and vehicle-infused (***D***, 10 μm posterior to ***B***) mice were stained with BDNF antibody pre-incubated with blocking peptide as a negative control to demonstrate staining specificity. Scale bar: 100 μm. See technical details in sections 5.9.

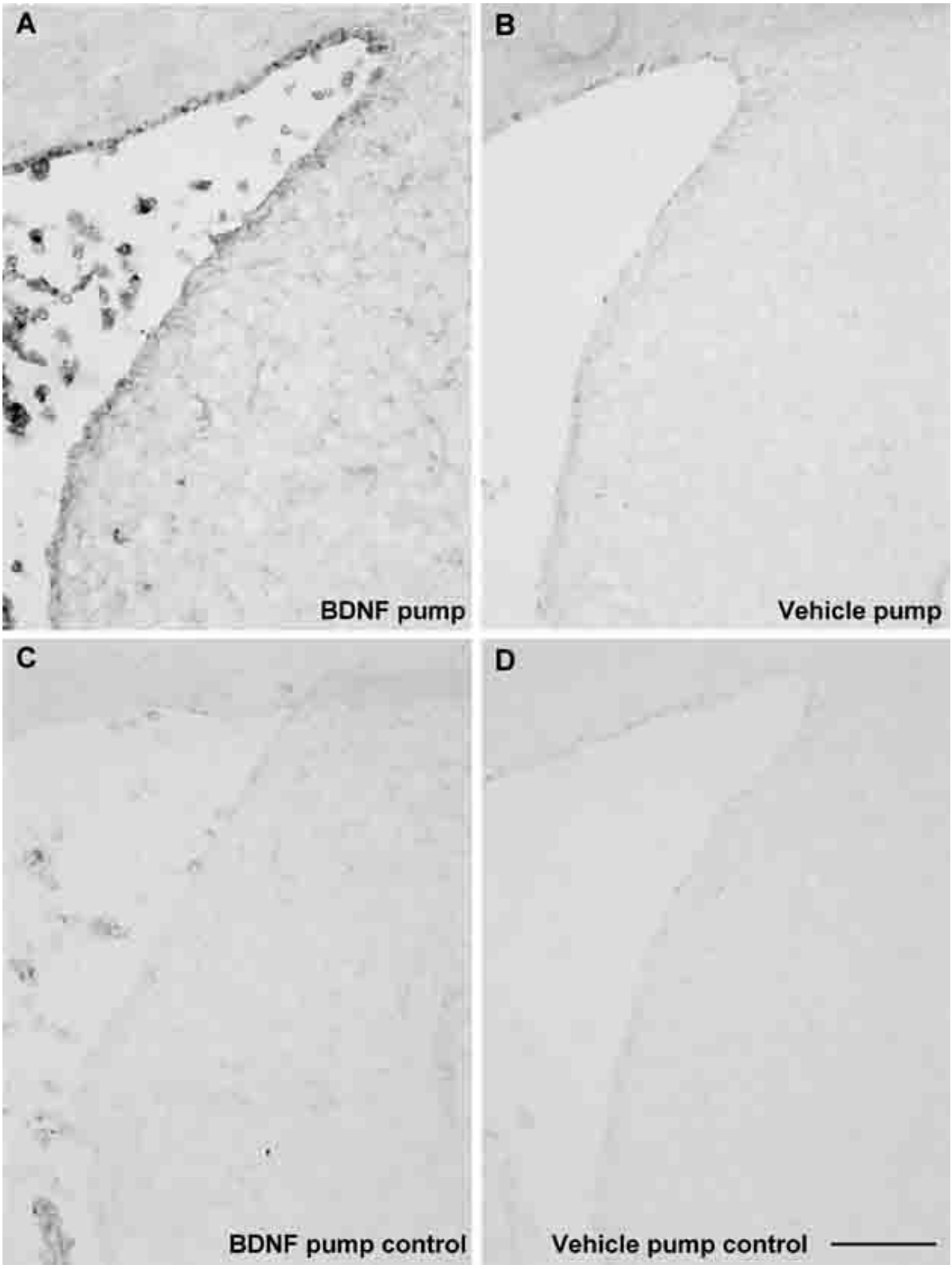
A
BDNF pump
B
Vehicle pump
C
BDNF pump control
D
Vehicle pump control

Figure 2.20: Effects of BDNF on cultured SVZ cells. ***A***, ***D***, WT SVZ astrocytes were isolated from adult mice and cultured in sub-confluent conditions for 7 days with no added BDNF (***A***) or in the presence of 100 ng/ml BDNF (***D***) (green: BrdU, red: GFAP). ***B***, ***E***, confluent monolayers of early post-natal WT SVZ cells cultured for 6 days give rise to $Tuj1^+$ neuroblasts (red) *in vitro* with no added BDNF (***B***) or in the presence of 100 ng/ml BDNF (***E***) (green: BrdU). ***C***, ***F***, GFP^+ (green) SVZ neuroblasts isolated from early post-natal mice and cultured on a monolayer of WT cortical astrocytes. Both TrkB-WT (***C***) and TrkB-KO (***F***) neuroblasts seem to develop normally after 5 days in culture (red: Tuj1; images shown are from cultures that were not supplemented with exogenous BDNF). ***G***, quantification of proliferation in subconfluent adult SVZ astrocyte cultures; n=3 experiments. ***H***, quantification of neuroblast proliferation in early postnatal SVZ monolayer cultures with increasing concentrations of BDNF; n=4 experiments. ***I***, quantification of TrkB-WT and TrkB-KO neuroblasts isolated from early post-natal SVZ and cultured on WT cortical astrocyte monolayers with and without BDNF; n=2 experiments. All values represent average ± SEM. Blue: DAPI (all panels). pic: picture. Scale bar: 50 μm. See technical details in sections 5.4, 5.9, 5.11, A1, A13.

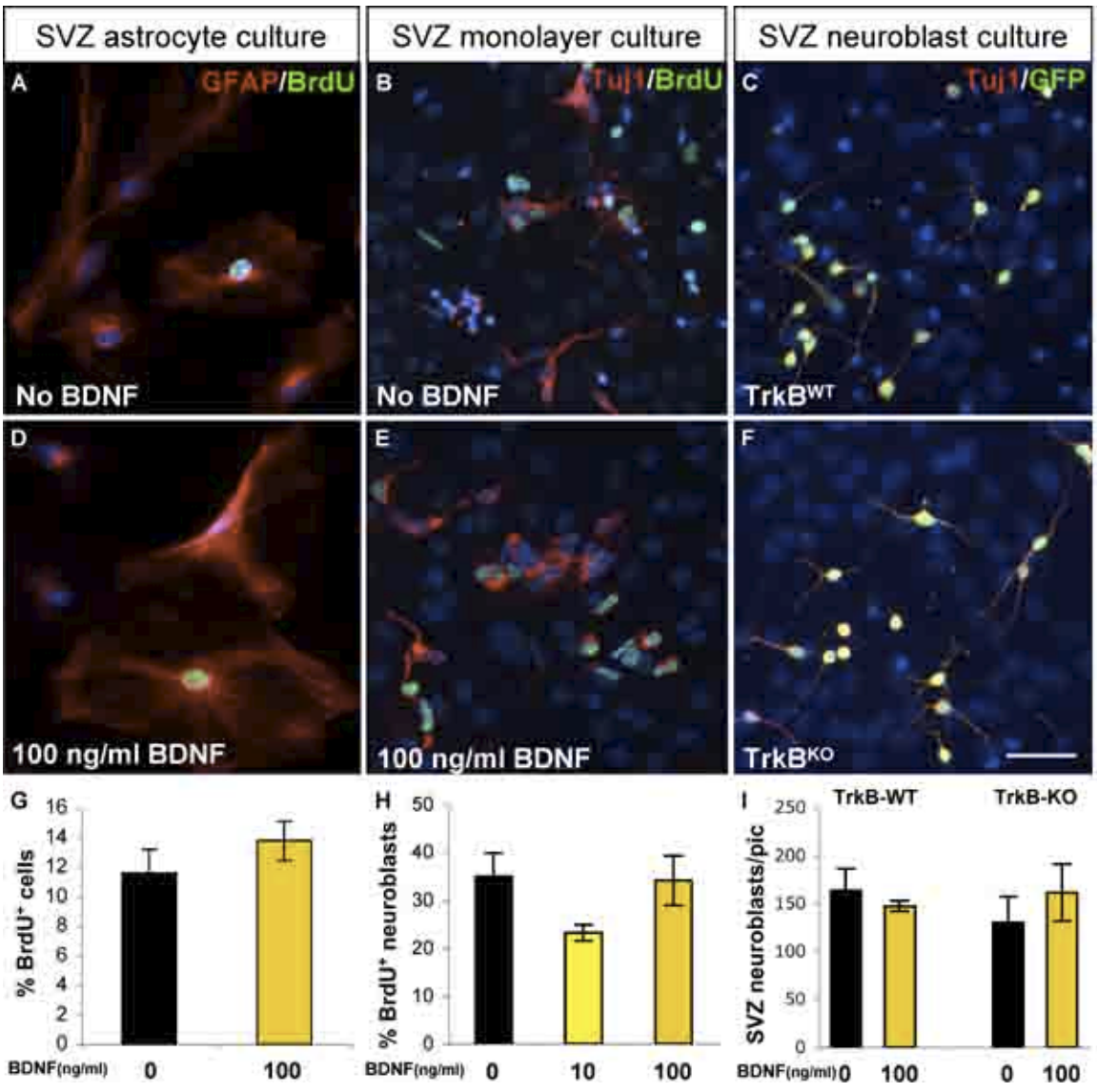
SVZ astrocyte culture
SVZ monolayer culture
SVZ neuroblast culture
A
GFAP/BrdU
No BDNF
B
Tuj1/BrdU
No BDNF
C
Tuj1/GFP
TrkB^WT
D
100 ng/ml BDNF
E
100 ng/ml BDNF
F
TrkB^KO
G
% BrdU+ cells
BDNF(ng/ml) 0 100
H
% BrdU+ neuroblasts
BDNF(ng/ml) 0 10 100
I
TrkB-WT
TrkB-KO
SVZ neuroblasts/pic
BDNF(ng/ml) 0 100 0 100

experiments, whereas others used rats. Therefore, I tested whether mice and rats might differ in their ability to respond to BDNF, perhaps due to species-specific differences in expression of BDNF receptors. By *in situ* hybridization, I found considerable levels of TrkB mRNA in the adult rat SVZ, with the ependymal layer prominently labeled as well as patches of cells within the SVZ (Fig. 2.21A). However, as in mice, virtually no TrkB-FL was detected in the rat SVZ (Fig. 2.21D). This result shows that expression of TrkB isoforms is very similar in adult mice and rats.

I also characterized the SVZ expression of the low affinity neurotrophin receptor p75, to which BDNF also binds. Based on the staining pattern obtained with 2 different anti-p75 antibodies (detecting the receptor's intracellular or extracellular domains; see Materials and Methods), $p75^+$ cells were extremely rare in the adult mouse SVZ and RMS (Fig. 2.21C, F and data not shown). This result is consistent with the undetectable levels of p75 mRNA in the SVZ by RT-PCR (Fig. 2.1A). In adult rats, however, p75 was abundantly expressed in the SVZ (Fig. 2.21B, E). I found large numbers of $p75^+$ cells from the subcallosal area to the ventral tip of the lateral ventricle at all rostrocaudal levels of the SVZ, as well as on the medial wall of the lateral ventricle in more rostral sections. This expression pattern was confirmed using 5 different anti-p75 antibodies (detecting the receptor's intracellular or extracellular domains; see Materials and Methods). I also detected numerous $p75^+$ cells in the adult rat RMS, though their numbers gradually decreased at increasingly rostral levels (data not shown). I detected many $p75^+$ cells in the medial septum of both rats and mice (Fig. 2.21B, C), indicating that the antibodies used can function on tissue from both species. In both rats and mice, $p75^+$ cells were often $Mash1^+$ (Fig. 2.21E, F), a transcription factor strongly expressed by type C cells (Parras et al., 2004). This observation is consistent with previous findings suggesting that, in the SVZ, p75 is expressed mainly by type C cells (Giuliani et al., 2004; Young et al., 2007). I also detected p75 protein on a subpopulation of PSA-$NCAM^+$ cells in rat SVZ, indicating that type A neuroblasts also express this receptor (Fig. 2.21G). p75 did not colocalize with GFAP (Fig. 2.21H).

In light of the striking difference in p75 expression in mouse and rat SVZ, I then tested whether rats would respond differently from mice to intraventricular BDNF infusions. I implanted microosmotic pumps in adult rats, delivering BDNF (1 mg/ml) or vehicle

Figure 2.21: p75 but not TrkB receptor expression is different in adult rat and mouse SVZ. ***A***, ***D***, *in situ* hybridization to detect all isoforms of TrkB (TrkB-all, ***A***) shows strong staining in the ependymal layer and in some cells of the adult rat SVZ, whereas the full-length isoform of TrkB (TrkB-FL, ***D***), though present in striatal cells, is undetectable in the rat SVZ. ***B***, p75 was detected by immunohistochemistry in many cells at all levels of the adult rat SVZ as well as in the medial septum. ***C***, in contrast, virtually no p75 staining was detected in the adult mouse SVZ, though the medial septum contained many $p75^+$ cells. ***E***, ***F***, $p75^+$ cells often co-expressed the transcription factor Mash1 (red) in both rat (***E***) and mouse (***F***) SVZ. ***G***, ***H***, confocal microscopy (single image) of adult rat SVZ reveals significant coexpression of p75 (green) with the neuroblast marker PSA-NCAM (***G***, red) but not with the astrocyte marker GFAP (***H***, red). Insets show individual markers from boxed areas; arrows indicate several double-labeled cells (blue: DAPI). Scale bar: 100 μm (***A***, ***D***), (***E***, ***F***), 500 μm (***B***, ***C***), 50 μm (***G***, ***H***). See technical details in sections 5.5, 5.9, A2, A13.

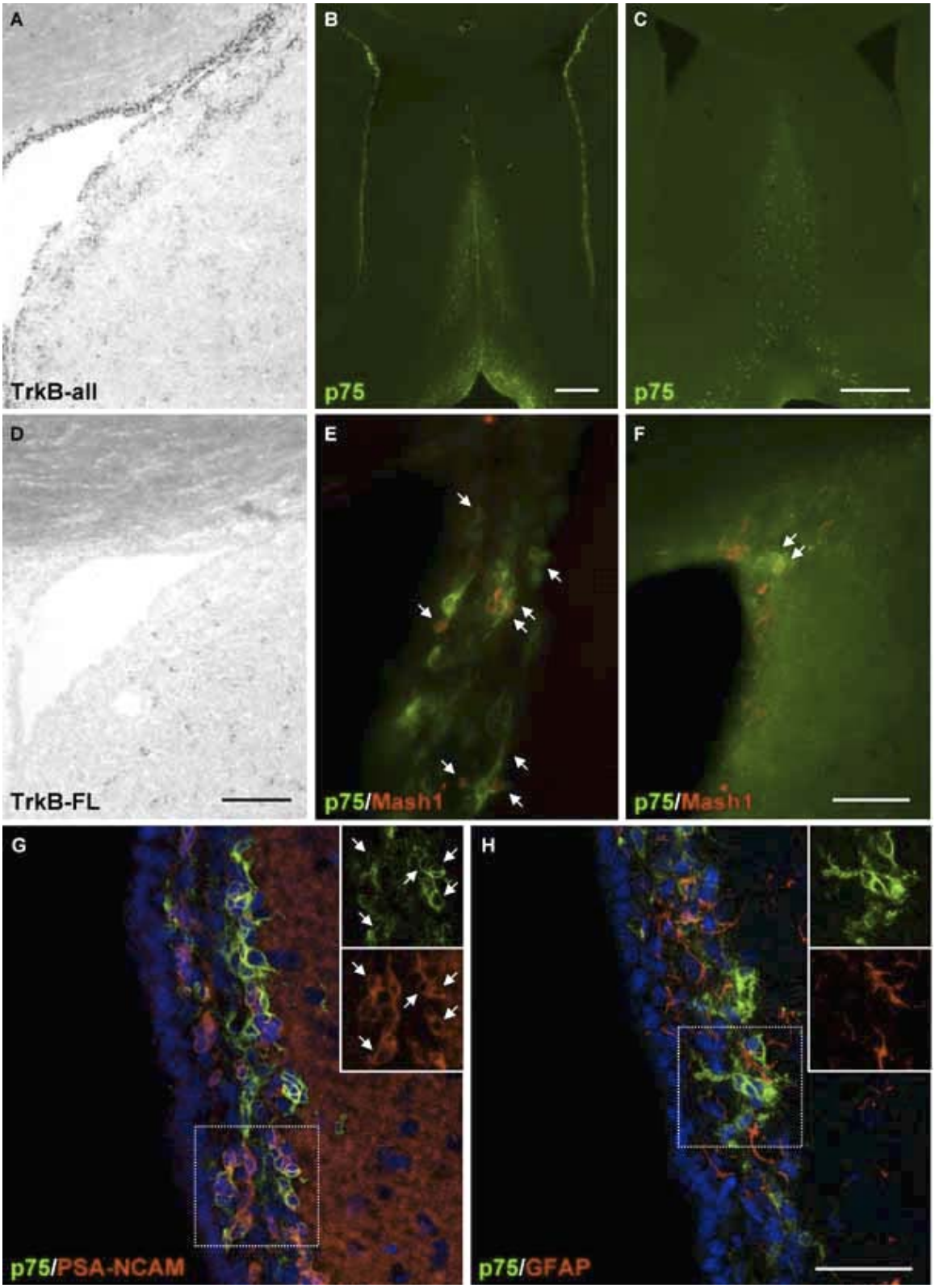
A
TrkB-all
B
p75
C
p75
D
TrkB-FL
E
p75/Mash1
F
p75/Mash1
G
p75/PSA-NCAM
H
p75/GFAP

(0.9% NaCl with 0.1% bovine serum albumin) into the lateral ventricle for 14 days. As with mice, BrdU was injected intraperitoneally (IP) at day 4, 8 and 12 after pump implantation and rats were killed at day 14 (Fig. 2.22A). As observed with mice, the weight of BDNF-infused rats decreased, whereas that of vehicle-infused animals increased (Fig. 2.22B). At day 14, BDNF-treated rats weighed 44% less than control rats, having lost on average 13.7% of their original weight, indicating that BDNF was active and was delivered into the ventricle. As further confirmation, I visually checked on brain sections that the pump cannula penetrated into the lateral ventricle lumen in all rats used in this study (Fig. 2.18C, D). At the end of the infusion experiment, I collected the BDNF remaining in the pump of each rat separately and tested its activity using DRG cultures. DRG neurons responded strongly to the presence of BDNF in all cases (data not shown), as described above. Therefore, BDNF was delivered into the lateral ventricle and was biologically active throughout the entire experiment in every rat analyzed.

I stained OB sections of equivalent regions from 5 vehicle-treated and 6 BDNF-treated rats to count $BrdU^+$ cells, using the position of the accessory olfactory bulb (AOB) and number of sections cut as references. I found that BDNF-treated rats had significantly fewer $BrdU^+$ cells in all layers of the OB (Fig. 2.22C; decrease values: 31.6% overall, p=0.02; 37.3% in OB core, p=0.02; 23.5% in granular cell layer, p=0.07; 28.7% in external plexiform layer, p=0.03; 34.1% in glomerular layer, p=0.0004; p values determined by t-Student test). As in mice, most $BrdU^+$ cells were neuronal (83.4% and 77.7% in vehicle and BDNF-infused rats, respectively, based on HuC/D labeling), while some were labeled with the oligodendrocyte marker Olig2 (6.7% and 8.4% in vehicle and BDNF-infused rats, respectively) or with the microglial marker Iba1 (1.9% and 2.4% in vehicle and BDNF-infused rats, respectively).

I then analyzed the SVZ of the same rats to determine the cause of the apparent decrease in neuron production among BDNF-treated animals. I measured apoptosis in the SVZ ipsilateral to infusion by TUNEL labeling, which revealed a trend towards a higher number of apoptotic cells among BDNF-infused rats, though not statistically significant (Fig. 2.22D; 17.1 % increase, P=0.34 by t-Student test). Using the mitosis marker pH3, I also detected a significant decrease in proliferation in the SVZ of rats infused with BDNF (Fig. 2.22E; 20.1% reduction compared to controls, p=0.04 by t-Student test). Consistent

Figure 2.22: *In vivo* effect of BDNF infusion in adult rats. ***A***, experimental design: microosmotic pumps were implanted on ~250g rats to infuse BDNF for 14 days; BrdU was administered every 4 days by intraperitoneal injection; on day 14, rats were sacrificed for analysis. ***B***, effect of BDNF infusion on rat weight. ***C***, quantification of BrdU staining in rat OB ipsilateral to pump; results are presented for all OB layers together (Total) as well as for each individual layer (Core; GCL, granular cell layer; EPL, external plexiform layer; GL, glomerular layer; AOB, accessory olfactory bulb). ***D-F***, quantification of TUNEL (***D***), pH3 (***E***) and Mash1 (***F***) staining in rat SVZ ipsilateral to pump. ***G***, summary of quantifications for mouse (Ms) and rat BDNF infusion experiments; p values represent statistical significance by t-Student test; *p<0.05, ***p<0.001. n=5 animals/group for all mouse quantifications; n=6 animals/group for all rat quantifications, except BrdU (n=5 Vehicle rats, 6 BDNF rats) and TUNEL (n=6 Vehicle rats, 5 BDNF rats) quantifications. All values represent average ± SEM. See technical details in sections 5.4, 5.9, 5.10, A1, A12, A13.

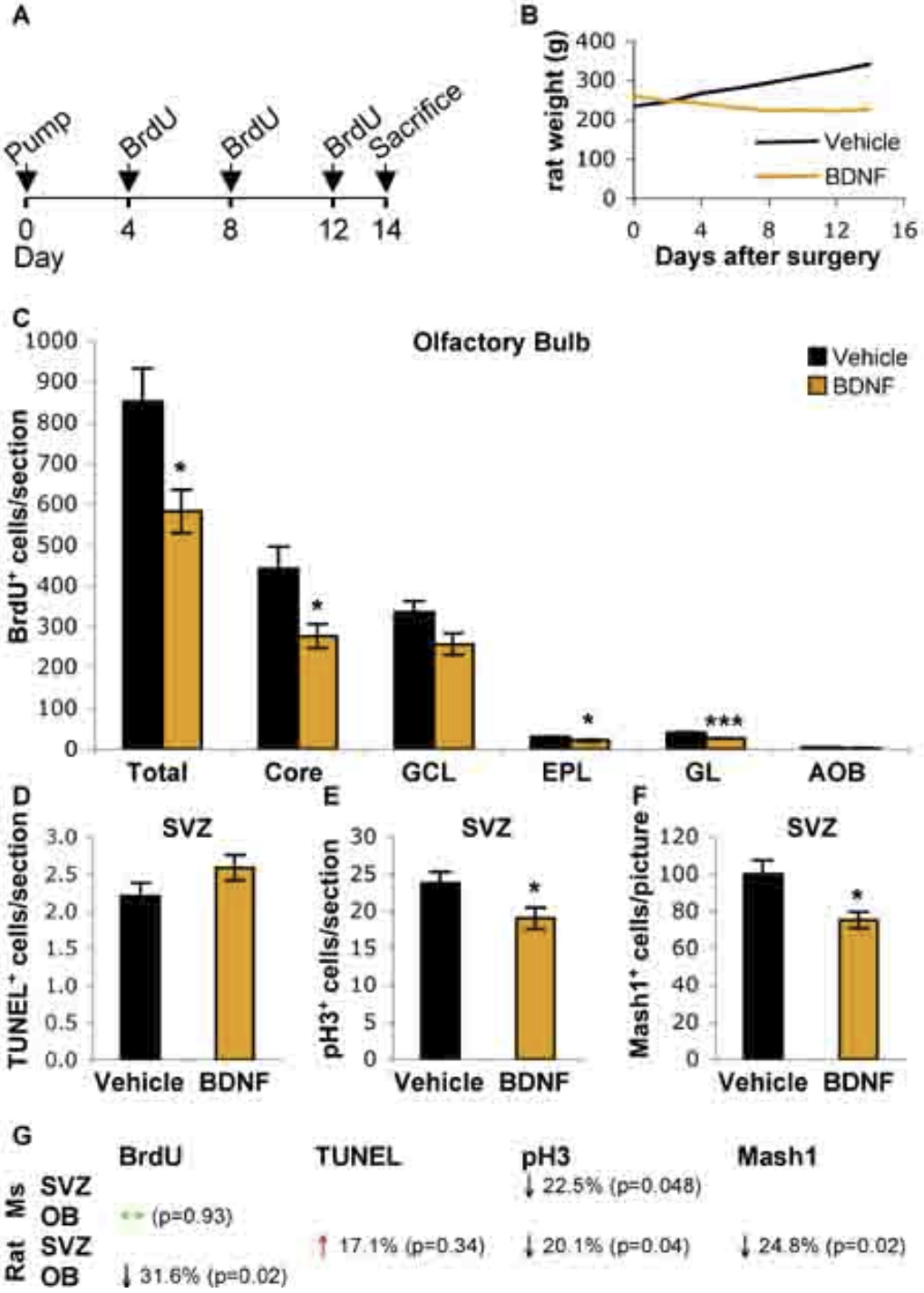
A
Pump
BrdU
BrdU
BrdU
Sacrifice
0
4
8
12
14
Day
B
rat weight (g)
400
300
200
100
0
Vehicle
BDNF
0
4
8
12
16
Days after surgery
C
Olfactory Bulb
Vehicle
BDNF
BrdU+ cells/section
1000
900
800
700
600
500
400
300
200
100
0
*
*
*
***
Total
Core
GCL
EPL
GL
AOB
D
SVZ
TUNEL+ cells/section
3.0
2.5
2.0
1.5
1.0
0.5
0.0
Vehicle
BDNF
E
SVZ
pH3+ cells/section
30
25
20
15
10
5
0
*
Vehicle
BDNF
F
SVZ
Mash1+ cells/picture
120
100
80
60
40
20
0
*
Vehicle
BDNF
G
BrdU
TUNEL
pH3
Mash1
Ms
SVZ
↓ 22.5% (p=0.048)
OB
↔ (p=0.93)
Rat
SVZ
↑ 17.1% (p=0.34)
↓ 20.1% (p=0.04)
↓ 24.8% (p=0.02)
OB
↓ 31.6% (p=0.02)

with the decrease in proliferation, I found that the number of SVZ cells labeled by Mash1, a transcription factor expressed mainly by the highly proliferative type C cells (Parras et al., 2004), was also significantly reduced in BDNF-treated rats (Fig. 2.22F; 24.8% lower than control, p=0.02 by t-Student test).

Therefore, although BDNF triggers no changes in neurogenesis levels in adult mice, it does affect neurogenesis in adult rats, decreasing the number of new OB neurons generated. This effect may be due to increased apoptosis, decreased proliferation, or both, among SVZ cells. This result is again in contrast with previous reports, which had stated that BDNF increases adult SVZ-derived neurogenesis in rats (Zigova et al., 1998; Benraiss et al., 2001).

2.3 Discussion

I report here that TrkB-TR, but not TrkB-FL, is strongly expressed in adult ependymal and SVZ type B cells and that TrkB-KO progenitors grafted into a WT brain continue to generate neurons *in vivo* for up to 6 months. Consistently, BDNF did not increase SVZ-to-OB neurogenesis *in vivo* and even decreased it in rats.

Neurotrophin expression in SVZ

Interestingly, although none of the neurotrophins I analyzed is expressed strongly in the adult SVZ, I detected BDNF protein in the SVZ. This BDNF could have originated distally. BDNF could be acquired from anterograde axonal transport by neurons projecting close or into the SVZ, from CSF by ependymal cells and ventricle-contacting B cells of the SVZ or from neighboring blood vessels by astrocyte processes. In songbirds, where BDNF promotes the survival of newly formed neurons in the adult high vocal center (Rasika et al., 1999), vascular endothelial cells seem to be the source of this neurotrophin (Louissaint et al., 2002). An intriguing possibility is that BDNF levels could be temporally regulated, increasing in response to specific stimuli, such as stress (Fiore et al., 2003; Fiore et al., 2005) or pregnancy (Shingo et al., 2003). Such mechanisms would be consistent with my observations that BDNF expression in SVZ cells can be influenced by neurotransmitters and hormones and seems to be upregulated during pregnancy.

It is not clear from my results what role endogenous BDNF may have in adult neurogenesis. Though exposing the SVZ to exogenous BDNF has either no effect or decreases neurogenesis, it is possible that a more controlled endogenous delivery, both temporally and in terms of effective concentration, might yield more noticeable results, perhaps accelerating differentiation or inducing apoptosis of SVZ progenitors (see also sections below and Chapter 4).

TrkB is not expressed in SVZ neuroblasts

Though it has long been known that TrkB is expressed in the SVZ (Yan et al., 1994; Yan et al., 1997a), the cell types in which this expression occurs have only recently been analyzed *in vivo*. Two publications have reported TrkB expression *in vivo* on SVZ neuroblasts and not on astrocytes (Chiaramello et al., 2007; Bath et al., 2008). My stainings with three different TrkB-specific antibodies as well as a TrkB:Tau-LacZ reporter mouse indicate that TrkB is expressed in ependymal and type B cells but not in neuroblasts. This result was corroborated by the fact that depleting the SVZ of neuroblasts and type C cells with AraC does not affect TrkB expression in this region. It is possible that the antibodies used in previous studies are not specific for TrkB in SVZ sections. Indeed, Western blot analysis of the antibody used in Bath et al. (2008) reveals that it strongly binds to one or more proteins of approximately 80 kDa in an adult mouse SVZ extract, a weight that does not correspond to known TrkB isoforms (95 or 145 kDa, Fig. 2.23M). I also tested this antibody on TrkB-KO material. I could not detect a clear staining using TrkB-KO and WT newborn sections or protein extracts (Fig. 2.23J-L). However, using sections from adult mice grafted with GFP^+ cells for 6 months, I detected numerous GFP^+/TrkB-KO cells labeled by the pTrkB antibody used in Bath et al. (2008), strongly suggesting it is detecting something other than TrkB (Fig. 2.24). Similarly, I believe the TrkB antibody used in Chiaramello et al. (2007) is not specific for TrkB because its staining pattern is opposite to that of three other TrkB antibodies (Fig. 2.2D-F, 2.5), two of which were confirmed by Western blot (Fig. 2.7G, 2.5C).

Some reports have detected TrkB in neurons isolated from the SVZ (Kirschenbaum and Goldman, 1995; Gascon et al., 2005). Importantly, in Kirschenbaum and Goldman (1995), neurons were stained for TrkB after 21 days in culture and Gascon et al. (2005)

Figure 2.23: Characterization of pTrkB staining in the SVZ. ***A***-***C***, pTrkB (green) labels nearly all PSA-NCAM$^+$ cells (red) in the adult mouse SVZ. ***D***-***F***, pTrkB (green) does not colocalize with the astrocyte marker GFAP (red) in the adult mouse SVZ. DAPI nuclear stain (blue) is shown in merge panels ***C*** and ***D***. ***G***-***I***, pTrkB$^+$ cells (green) rarely express the transcription factor Mash1 (red) in the adult mouse SVZ. ***J***, ***K***, SVZ sections of neonatal brain from WT (***J***) and TrkB-KO (***K***) mice were stained with pTrkB antibody (green); no clear difference in staining is visible (close-up views of the boxed areas are shown to the right of each panel). ***L***, ***M***, Western blot characterization of pTrkB antibody. ***L***, anti-TrkB antibody, detecting all isoforms of TrkB, and pTrkB antibody were tested in whole brain protein extracts of neonatal WT and TrkB-KO mice. Anti-TrkB antibody detected both the full-length and truncated isoforms of TrkB (145 kDa and 95 kDa, respectively) in WT but not TrkB-KO samples, whereas anti-pTrkB antibody detected only a series of weak, non-specific bands in both WT and TrkB-KO brain samples. ***M***, In adult SVZ samples, the anti-TrkB antibody detected again both TrkB isoforms, whereas the pTrkB antibody labeled a strong double band at ~80 kDa. As a loading control, all samples were also probed for β-Actin (shown below the TrkB bands). Scale bars: 50 μm (***A***-***I***, close-ups of ***J***, ***K***), 200 μm (***J***, ***K***). See technical details in sections 5.7, 5.9, 5.10, A3, A13.

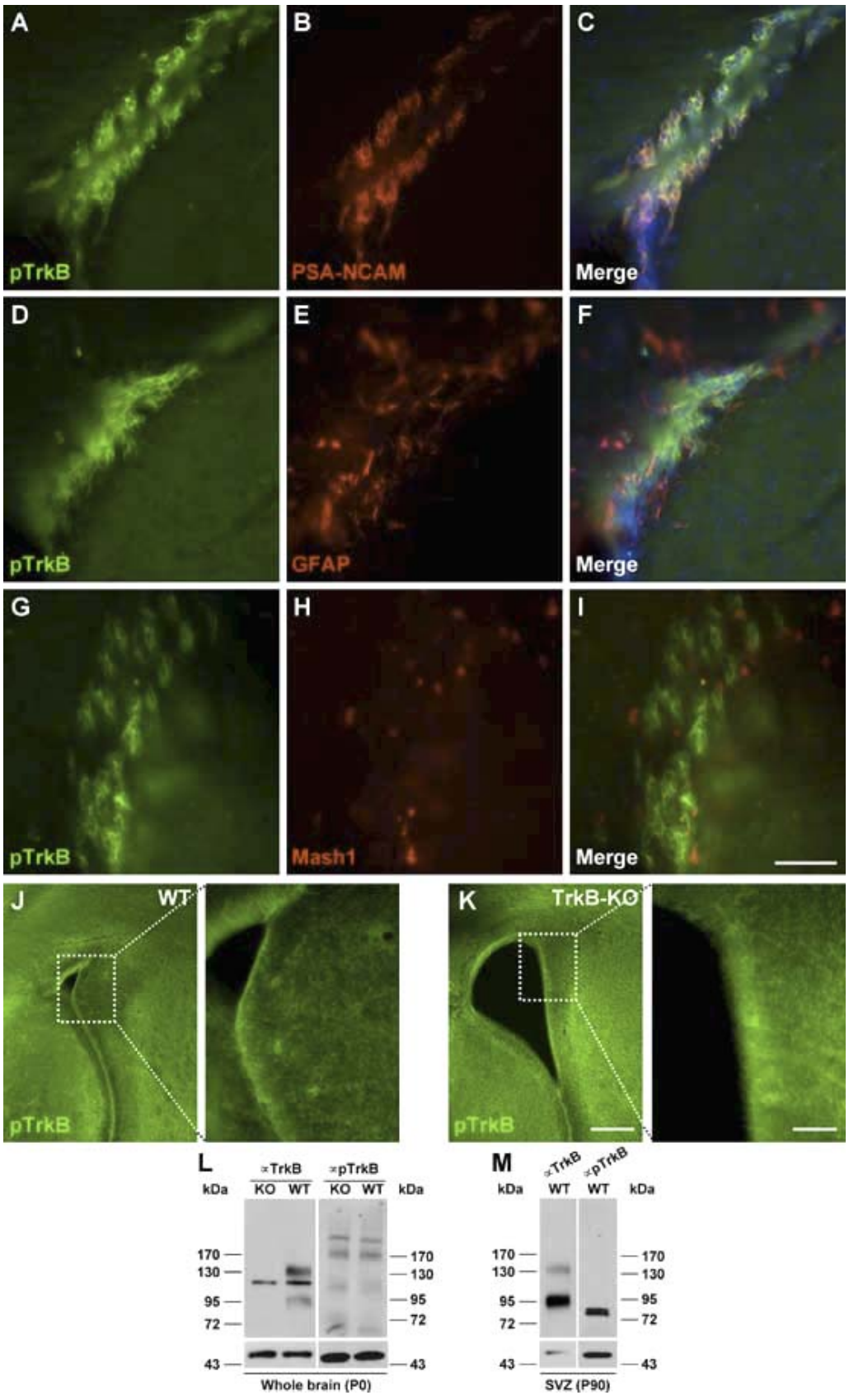
A
pTrkB
B
PSA-NCAM
C
Merge
D
pTrkB
E
GFAP
F
Merge
G
pTrkB
H
Mash1
I
Merge
J
WT
pTrkB
K
TrkB-KO
pTrkB
L
αTrkB
αpTrkB
kDa
KO WT KO WT
kDa
170
130
95
72
43
Whole brain (P0)
M
αTrkB
αpTrkB
kDa
WT WT
kDa
170
130
95
72
43
SVZ (P90)

Figure 2.24: pTrkB antibody labels TrkB-KO cells. Adult WT CD1 mice grafted with GFP^+ WT or TrkB-KO cells for 6 months were used to test the specificity of the pTrkB antibody. ***A***-***C***, GFP staining at the level of the RMS of mice grafted with WT (***A***) or TrkB-KO (***B***, ***C***) cells. ***D***-***F***, pTrkB staining at the level of the RMS of mice grafted with WT (***D***) or TrkB-KO (***E***, ***F***) cells. ***G***-***I***, PSA-NCAM staining at the level of the RMS of mice grafted with WT (***G***) or TrkB-KO (***H***, ***I***) cells. ***J***-***L***, Merged view of all stainings, including DAPI nuclear staining (blue), at the level of the RMS of mice grafted with WT (***J***) or TrkB-KO (***K***, ***L***) cells. Arrows: examples of GFP^+ grafted cells that are labeled with both pTrkB and the neuroblast marker PSA-NCAM. Boxed areas are shown at higher magnification as insets. Scale bar: 50 μm. See technical details in sections 5.9, 5.10, A12, A13.

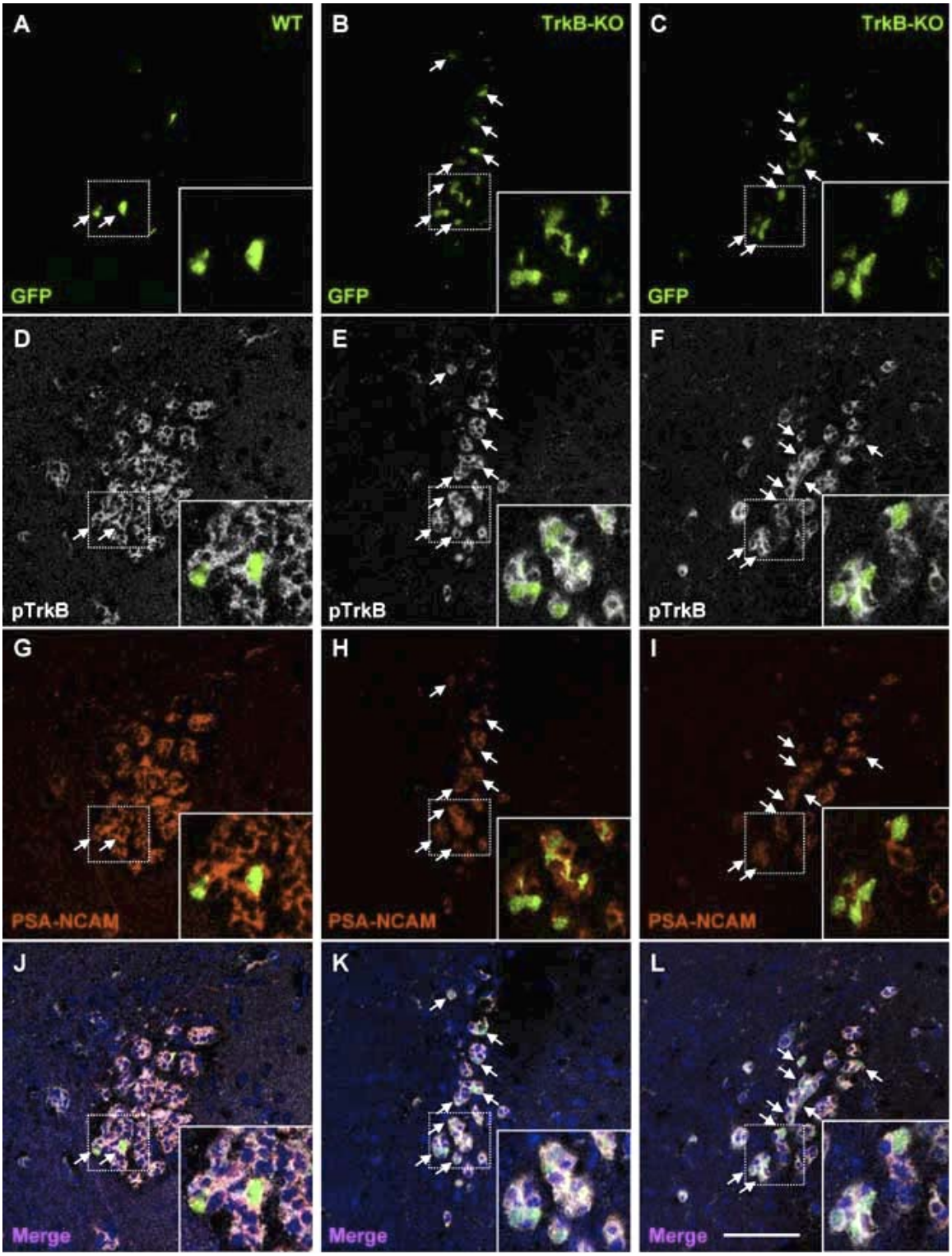
A
WT
GFP
B
TrkB-KO
GFP
C
TrkB-KO
GFP
D
pTrkB
E
pTrkB
F
pTrkB
G
PSA-NCAM
H
PSA-NCAM
I
PSA-NCAM
J
Merge
K
Merge
L
Merge

report that TrkB levels in SVZ neuroblasts increase significantly over the course of 6 days *in vitro*. Immature, migratory SVZ neuroblasts *in vivo* may be negative for TrkB and may depend on factors other than BDNF for trophic support. Once they reach their final destination in the OB, neuroblasts begin differentiating and establishing connections with other neurons, events which could trigger the expression of TrkB. In fact, I detected $TrkB^+$ cells in both the granular and glomerular OB layers by *in situ* hybridization using TrkB-all and TrkB-FL probes (Fig. 2.14). This scenario would be consistent with both the expression data presented here and that of Kirschenbaum and Goldman (1995) and Gascon et al. (2005).

Why TrkB-TR?

Although I cannot rule out that low levels of TrkB-FL may be present, nearly all TrkB in the SVZ seems to be of the truncated isoform. In neurons, TrkB-TR can act as a dominant-negative of the $kinase^+$ TrkB-FL and can modulate dendritic growth patterns (Yacoubian and Lo, 2000). In glia, TrkB-TR has been proposed to allow these cells to form a barrier to diffusion of BDNF in the brain, thereby confining the actions of this trophic factor to specific regions (Biffo et al., 1995). Additionally, TrkB-TR has been shown *in vitro* to allow astrocytes to acquire BDNF from their surroundings, which can later be released back into the medium (Alderson et al., 2000). The high levels of TrkB-TR in ependymal and type B cells could serve to regulate the levels of BDNF available to other SVZ cells, at least some of which express the neurotrophin receptor p75 (Calzá et al., 1998; Giuliani et al., 2004; Petratos et al., 2004; Young et al., 2007) (Fig. 2.21). An emerging concept is that TrkB-TR can activate intracellular signaling pathways of its own (Baxter et al., 1997; Rose et al., 2003). In astrocytes, TrkB-TR activation by BDNF triggers the release of intracellular Ca^{2+} through activation of an unknown G-protein and phospholipase C. It is therefore possible that SVZ glial cells actively respond to BDNF in ways that are not yet understood.

p75 receptor expression in the SVZ

Interestingly, mice and rats differ in their expression of p75, which has been previously described in the rat SVZ and has been proposed to occur mainly in proliferating type C-

like cells (Calzá et al., 1998; Giuliani et al., 2004; Young et al., 2007). I detected many $p75^+$ cells in the rat SVZ, often colocalizing with Mash1, a transcription factor expressed mainly by type C cells (Parras et al., 2004). Surprisingly, the mouse SVZ is almost entirely devoid of $p75^+$ cells, though there too, they are often $Mash1^+$. Petratos et al. (2004) and Gascon et al. (2007) have also reported few $p75^+$ cells in the mouse SVZ. This difference might imply that mice and rats use different signaling pathways to regulate C cell behavior. I also detected p75 in a significant subpopulation of PSA-$NCAM^+$ cells in the rat SVZ, suggesting a greater role for p75 in SVZ neuroblasts than previously thought. p75 activation by BDNF can induce apoptosis, particularly if not coexpressed with Trk receptors (Nykjaer et al., 2005). p75 activation can also induce cell cycle exit (Chittka and Chao, 1999; Salehi et al., 2000; Chittka et al., 2004; Wen et al., 2004; Vilar et al., 2006) and/or promote neuronal differentiation (Yamashita et al., 1999; Gascon et al., 2005). Hypothetically, TrkB-TR expressed in ependyma and SVZ astrocytes might non-cell-autonomously control survival and/or differentiation of $p75^+$ type C cells and neuroblasts by limiting these cells' access to BDNF.

Does TrkB play a role in postnatal neurogenesis?

My grafting experiment clearly shows that TrkB is not essential cell-autonomously for neurogenesis at the level of the SVZ or OB. However, this does not necessarily mean that this receptor plays no role in the production, migration, survival or maturation of new neurons destined for the OB. In fact, TrkB-KO mice exhibited fewer proliferating cells in the SVZ and more apoptotic cells in the SVZ and OB at birth, and 1 month-old TrkB heterozygotes had fewer new OB cells than WT controls. I cannot rule out that these may be indirect effects due to the constitutive nature of these mutants. Indeed, newborn TrkB-KO mice appeared to have increased apoptosis throughout the brain, which I confirmed by quantifying $TUNEL^+$ cells in the cortex and corpus callosum (Fig. 2.25), and others have reported increased apoptosis in various brain regions of TrkB-KO mice (Minichiello and Klein, 1996; Alcantara et al., 1997; Xu et al., 2000a). However, my grafting experiment also shows that TrkB-KO cells in a WT brain accumulate more slowly and lose TH^+ cells in the OB more rapidly than their WT counterparts, though these results did not reach statistical significance. These deficiencies may be due to

Figure 2.25: Quantification of apoptosis in cortex and corpus callosum of neonatal TrkB-KO mice. Newborn (P0) TrkB-KO and WT mice were labeled by TUNEL to detect apoptosis. The number of $TUNEL^{+}$ cells was then counted in the cortex and corpus callosum above the lateral ventricles. All values represent average ± SEM; n=6 mice (TrkB-WT), n=4 mice (TrkB-KO). See technical details in sections 5.8, A4.

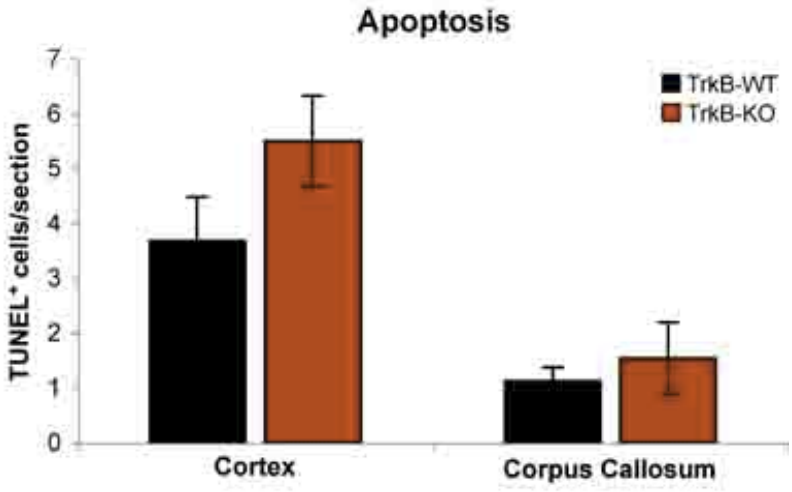
Apoptosis
TrkB-WT
TrkB-KO
TUNEL+ cells/section
0
1
2
3
4
5
6
7
Cortex
Corpus Callosum

insufficient trophic support in TrkB-KO cells or to a greater difficulty for these cells in establishing or maintaining connectivities in the OB circuit. The latter case would lead activity-dependent genes such as TH to be turned down (Baker et al., 1983) and would be consistent with the known role of TrkB in the development of dendritic branches, synaptic formation and plasticity (McAllister et al., 1999; Cohen-Cory, 2002).

My data suggest that TrkB is not essential for survival of most new neurons in the OB, perhaps indicating the presence of survival factors other than BDNF or NT4 in the OB. However, TrkB may have a selective role in the regulation of maturation/survival of specific subtypes of OB interneurons, rather than a generalized effect on SVZ neurogenesis. In fact, my results show that the maturation and/or survival of dopaminergic (TH^+) periglomerular interneurons are affected by TrkB loss, dropping to half of the WT levels 6 months after SVZ transplantation. TrkB may be important for other OB interneuron subtypes which were not examined in this work. It was recently reported that loss of BDNF selectively decreases the number and dendritic complexity of Parvalbumin$^+$ (PV^+) neurons in the OB external plexiform layer (Berghuis et al., 2006). Because few to no PV^+ cells were made from my grafts after 6 months (data not shown), I was unable to determine the effect of TrkB-KO on this neuronal subpopulation. For similar reasons, I also could not study the Calretinin$^+$ subpopulation of OB interneurons.

BDNF does not increase neuroblast production *in vivo*

My results suggest that exogenous BDNF delivered into the lateral ventricles does not enhance SVZ neurogenesis. In fact, depending on the species, BDNF infusion leads to either a 23% decrease in SVZ proliferation (mice) or to a 32% decrease in the number of new OB neurons as well as a 20% decrease in SVZ proliferation (rats). My findings contrast sharply with two previous studies in rats, in which BDNF delivered to the lateral ventricle induced a 2-3-fold increase in the number of new OB cells (Zigova et al., 1998; Benraiss et al., 2001). Recently, another laboratory overexpressed BDNF in the rat SVZ and also could not detect an increase in new OB neurons, though they did observe more $BrdU^+$ cells in the RMS (Henry et al., 2007). It is possible that BDNF effects on SVZ change over the period of infusion. If BDNF increases the production of new neurons by accelerating progenitor differentiation and/or favoring a neuronal rather than glial lineage

(Ahmed et al., 1995; Cheng et al., 2003; Young et al., 2007), this increase could be unsustainable, leading in the long run to a reduction in SVZ neuron production due to a depletion of the progenitor pool. A recent report indicating that BDNF increases neuronal production in neurosphere cultures (Young et al., 2007) could be reconciled with my data based on this interpretation and/or on the fact that these are *in vitro* experiments whereas mine are *in vivo*. The same report provides evidence that BDNF is acting through p75, which, as discussed above, can affect cell proliferation and differentiation. Indeed, I detected a reduction in SVZ proliferation after 14 days of BDNF infusion in both mice and rats as well as fewer $Mash1^+$ cells in BDNF-infused rats. However, only in rats was this reduced proliferation accompanied by a decrease in OB neuronal recruitment. It could be that rats respond more quickly than mice to BDNF, perhaps due to the higher levels of p75 in rats. The reduction in mouse SVZ proliferation may just come too late to result in lower neuron numbers in the OB at the time of my analysis. This interpretation matches the observation that, at 14 days, rats have fewer $BrdU^+$ cells in all layers of the OB, whereas mice have slightly fewer $BrdU^+$ cells only in the OB core, where the most recently generated cells are arriving (data not shown).

A depletion of progenitor pools alone cannot explain the different results of previous studies versus mine, as all exposed the SVZ to BDNF for at least 12 days. However, these studies differ in the BDNF delivery method and the BrdU administration regimen. Zigova et al. (1998) and myself infused BDNF protein with microosmotic pumps, whereas Benraiss et al. (2001) injected an adenovirus into the lateral ventricles to induce BDNF overexpression. Though the comparison is difficult, the viral method likely exposes SVZ cells to lower BDNF levels. Based on a rat CSF volume of 250 μl and a turnover rate of 2 hours (Bass and Lundborg, 1973), I calculate that the CSF should contain approximately 4 μg/ml exogenous BDNF in pump experiments, whereas Benraiss et al. (2001) report 2 ng/ml BDNF in the CSF. However, I used the same BDNF doses as Zigova et al. (1998) and several other laboratories have reported biological effects when infusing BDNF into the brain at similar doses (Siuciak et al., 1996; Scharfman et al., 2005; Givalois et al., 2006).

To quantify neurogenesis, I used a total of 3 BrdU injections (50 mg/kg each) over 14 days. The other studies used significantly higher levels of BrdU, often administered more

frequently. Such BrdU doses could be toxic for proliferating cells of the SVZ/RMS. If so, BDNF may be more important as a neuroprotectant in those studies than in mine, perhaps explaining our opposite results in rats.

Conclusion

My results indicate that TrkB, though abundant in the SVZ, is not required for the birth and migration of new neurons in the adult mouse SVZ. Nevertheless, TrkB does appear to play some role in the adult, either in survival of progenitor cells, maturation/synaptic connectivity of new interneurons or both. However, neither survival nor synaptic activity of most new OB neurons depend exclusively on TrkB signaling, as I have shown that many new neurons are generated, migrate along the RMS and become established in the OB without this receptor. Furthermore, my data does not support the current views that BDNF may be used to enhance endogenous SVZ neurogenesis. On the contrary, BDNF may decrease it. I did not analyze the effect of BDNF infusions on brain regions other than the SVZ/OB, so it is possible that it enhances neurogenesis elsewhere in the brain (Benraiss et al., 2001; Pencea et al., 2001; Chmielnicki et al., 2004; Scharfman et al., 2005). Nonetheless, more research is clearly needed to understand the role of this neurotrophin in endogenous neurogenesis before it can be deemed promising for human therapy.

Chapter Three: Single cell RT-PCR characterization of SVZ

3.1 Introduction

The cellular composition of the SVZ was described by electron microscopy in 1997 and three main cell types were defined: type B, C and A cells (Doetsch et al., 1997). Type B cells have many properties of astrocytes, including the expression of the intermediate filament GFAP, and have been identified as the SVZ neural stem cells (Doetsch et al., 1999b; Doetsch et al., 1999a). Type C cells are produced by type B astrocytes and are undifferentiated, highly proliferative intermediate progenitors. These cells no longer express GFAP and turn on the transcription factor Dlx2. Type A cells are derived from type C cells. These are migratory neuroblasts and they express several markers of immature neurons, such as Doublecortin (Dcx) and PSA-NCAM, while maintaining expression of Dlx2 (see table 3.1 below). In the past 10 years, little progress has been made in further characterizing these cells. It is thought that several subtypes of type B astrocytes exist in the SVZ, some acting as stem cells while others have structural/supportive roles. There are currently no molecular markers to distinguish these subtypes, making it difficult to study their differences. For similar reasons, type A and C cells have thus far been poorly characterized and they are usually thought of as homogeneous populations. Recent work indicates that type A neuroblasts are molecularly diverse, since transcription factors such as Pax6 and Sp8 are expressed in subpopulations of type A neuroblasts (Kohwi et al., 2005; Waclaw et al., 2006). Additionally, neuroblasts generated by type B cells from different regions of the embryonic and postnatal SVZ become different OB interneurons (Kelsch et al., 2007; Kohwi et al., 2007; Merkle et al., 2007), indicating that type A cells are quite heterogeneous from very early on, though it is not clear when they commit to a specific fate. These differences are likely to extend to type C and B cells, the precursors of type A cells.

In this section I developed several techniques based on mRNA reverse transcription (RT) and amplification by polymerase chain reaction (PCR) to study SVZ heterogeneity at the single cell level. Single cell RT-PCR (SC-RT-PCR) methods provide the cellular resolution of other techniques such as immunocytochemistry or *in vivo* hybridization, while at the same time allowing for a significantly larger number of genes to be studied in each cell. These properties will allow us to use SC-RT-PCR to reveal more subclasses within type B, C and A cells and to characterize the differences separating progenitor and non-progenitor SVZ astrocytes, as well as those defining progenitors of different SVZ regions, at a molecular level. In order to optimize these protocols, I focused mainly on genes whose expression had been previously detected and characterized in the SVZ (table 3.1). Below, I report on results showing that it is possible to detect multiple gene products from single SVZ cells.

Gene	Description	Method
GAPDH	Enzyme, housekeeping gene (positive control)	1
Gus	Enzyme, housekeeping gene (positive control)	2, 3
GFAP	Intermediate filament, astrocyte marker	1, 2, 3
Dcx	Microtubule stabilizing protein, expressed in all type A cells	2, 3
NCAM	Neural cell adhesion molecule, polysialylated form is expressed in all type A cells	1
Dlx2	Homeobox transcription factor, expressed in all type C and A cells	1, 2, 3
Pax6	Homeobox transcription factor, expressed in some type B, C and A cells	1, 2, 3
Sox2	Homeobox transcription factor, expressed in most SVZ cells	1, 2, 3
Er81	ETS transcritpion factor, expressed in type A cells	1
Mash1	Proneural transcription factor, expressed in type C and some type B and A cells	2, 3
BDNF	Neurotrophin, secreted growth factor	1, 2, 3
TrkB	Specific, high affinity BDNF/NT4 receptor	1
p75	Non-specific, low affinity neurotrophin receptor	1, 2, 3
Notch1	Receptor, can lead to proneural gene downregulation when activated	1, 2, 3
LeX	Carbohydrate expressed in B and C cells; primers for Fut4, LeX-producing enzyme	1

Table 3.1: Genes used in single cell RT-PCR optimization experiments. GAPDH: Glyceraldehyde 3-phosphate dehydrogenase; Gus: Beta-glucuronidase; GFAP: Glial-Fibrillary Acidic Protein; Dcx: Doublecortin; NCAM: Neural Cell Adhesion Molecule; Dlx2: Distal-less homeobox gene 2; Pax6: Paired box gene 6; Sox2: SRY box containing gene 2; Mash1: Mouse achaete-scute homologue 1; BDNF: Brain-Derived Neurotrophic Factor; TrkB: Tyrosine kinase B receptor; LeX: Fucosyltransferase 4. Methods: 1, multiplex nested RT-PCR; 2, real time RT-PCR; 3, antisense RNA amplification RT-PCR.

3.2 Results

Real-Time RT-PCR

Real-time PCR was developed in the early 1990s (Holland et al., 1991; Higuchi et al., 1992; Higuchi et al., 1993). In this method, information about the level of amplification

of a PCR product is constantly measured and recorded throughout the PCR reaction. Real-time PCR primers consist of conventional forward and reverse primers to which a third, short oligonucleotide is added, called a probe. The probe is also specific for the gene in question, annealing to the sequence between the 2 primers, and it is coupled to 2 molecules: a fluorescent dye and a fluorescence quenching dye. While these dyes are close to each other, no fluorescence is detectable. When the DNA Polymerase used in the PCR reaction passes through the area bound by the probe, its 5'-3' exonuclease activity degrades the probe to single nucleotides, releasing the fluorescent dye from its quencher (Fig. 3.1A). The real-time PCR machine repeatedly excites samples with a laser and measures the level of fluorescence in each tube, which is proportional to the number of copies of the amplified sequence. This method gives rise to reliable, highly reproducible results and can be performed on small volumes (5-20 μl reactions). Because all samples are compared based on a pre-determined detection threshold, reached during the exponential phase of the PCR amplification, quantitative (if a calibration curve is done using know amounts of specific RNA sequences) or semi-quantitative (if calibrated to an internal control gene) information can easily be determined from real-time PCR data. Such analyses are also possible with conventional PCR methods, but are much more labor-intensive and thus more prone to error. Furthermore, due to the different design of the primer/probe sets used for real-time PCR, amplification products can be detected with greater sensitivity and specificity.

Cells were collected by fluorescence-activated cell sorting (FACS), using forward/side scatter (cell size/granularity) and the cell viability marker propidium iodide (PI) to ensure selection of healthy, single cells (rather than cell clusters, dead cells or debris). I chose this method over manual collection due to its high-throughput, automated nature. Cells were placed directly into cell lysis buffer (no DNAse necessary) to which RT reagents and enzymes were then added and cDNA synthesized (20 μl reaction). Each cDNA sample was used for a maximum of 4 separate PCR reactions, run for 40-50 cycles using real-time PCR primer/probe sets designed and sold by Applied Biosystems. Results were recorded and analyzed using Applied Biosystems software. For the RT reaction, I tested oligo-d(T) primers (bind to mRNA 3' polyA tails) and random decamers (no bias to any

Figure 3.1: Methods used in single cell RT-PCR experiments. ***A***, real-time RT-PCR principle. (i) DNA (long black lines) is denatured allowing the primers (blue) and the probe (short black line) to anneal to their specific targets. The probe is bound to a fluorescent dye (pink ball) and its quencher molecule (gray ball). (ii) as the DNA is replicated (black arrows), the probe is displaced from the DNA template. (iii) The exonuclease activity of the DNA Polymerase degrades the probe into single nucleotides, releasing the fluorescent dye from its quencher. Fluorescence is now detectable from the dye (red ball). (iv) At the end of each cycle, the target DNA is fully replicated and the bound probes are completely degraded. ***B***, antisense RNA amplification principle. mRNA is converted to cDNA in a first RT reaction using a oligo-d(T) primer modified to contain the sequence of the T7 RNA polymerase promoter (green). At the end of the extension phase, the RT enzyme adds several dC nucleotides to the 3' end of the cDNA, to which another primer (SMART III primer, Clontech, red) will bind. The RT enzyme now switches templates and adds the sequence complementary to the SMART III primer to the cDNA. All cDNAs now have the same sequences at the 3' and 5' ends. Adding primers specific to these sequences, I performed a PCR reaction (20 cycles) to produce the 2^{nd} cDNA strand as well as to amplify the cDNA sample. The product of this PCR reaction was then used in an *in vitro* transcription (using T7 RNA Polymerase) to produce multiple RNA copies of each DNA fragment. The RNA from this reaction is then purified and converted back to single strands of cDNA in a second RT reaction (using random hexamer primers). All reactions in this amplification method are non-specific and so all mRNAs are amplified. The cDNA has now been amplified several-fold and is ready for detection by real-time PCR. ***C***, multiplex nested RT-PCR. Cell samples were collected into a small volume in a PCR tube without RNA purification steps and the RT reaction was performed to produce cDNA. In the same tube, I performed a PCR reaction using a cocktail of 12 primer pairs, each specific for a different gene (multiplex PCR, 40 cycles). The sample was then separated into 12 different reactions, each specific for a different gene, using a second pair of primers designed to anneal within the area amplified by the first primer pair (nested PCR). All reactions were then run on an agarose gel to detect the gene products. See technical details in sections 5.3, 5.15-17, A5, A6.

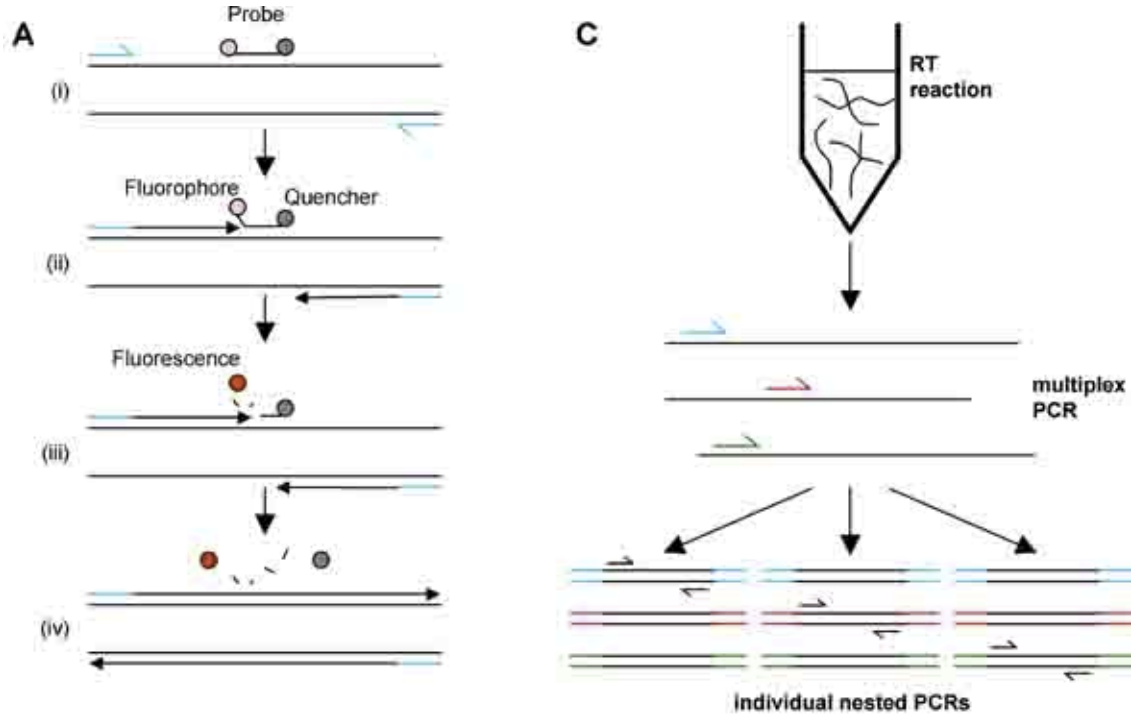
A
Probe
(i)
Fluorophore
Quencher
(ii)
Fluorescence
(iii)
(iv)
C
RT
reaction
multiplex
PCR
individual nested PCRs

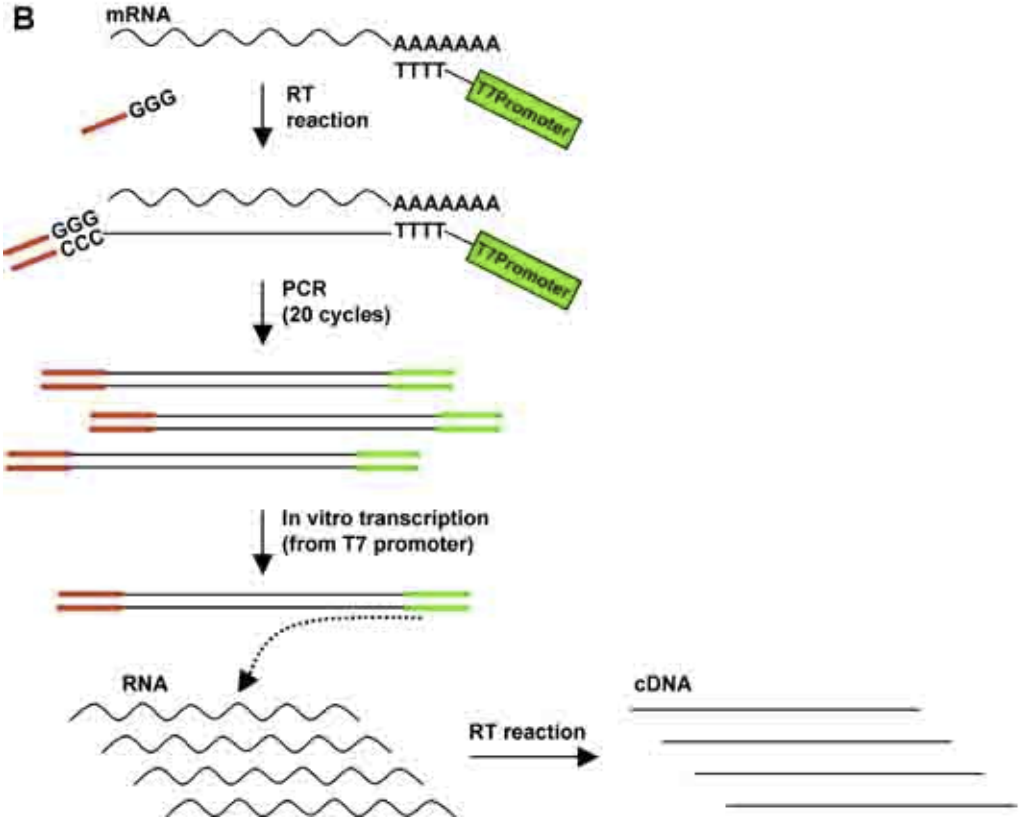
B
mRNA
AAAAAAA
TTTT
T7Promoter
GGG
RT
reaction
AAAAAAA
GGG
CCC
TTTT
T7Promoter
PCR
(20 cycles)
In vitro transcription
(from T7 promoter)
RNA
RT reaction
cDNA

region of transcripts, bind all types of RNA). Random decamers were consistently better, yielding lower C_T values (number of PCR cycles required for fluorescence levels to cross the detection threshold; the lower the C_T value, the greater the initial amount of RNA) for all tested genes and were thus used in all experiments.

1000, 100, 10, 1 and 0 cells/PCR tube were collected from 3 different sources: cultured early post-natal (P3) mouse SVZ, freshly-dissected P5 and adult mouse SVZ. Ideally, one should be able to analyze uncultured, adult SVZ cells. However, SVZ cultures from young mice provide a simple, astrocyte-enriched source of cells for optimization of this single cell analysis technique. Detection of gene transcripts was increasingly difficult from cultured neonatal, to fresh neonatal, to fresh adult cells (Fig. 3.2A), probably due to the observed smaller cell size (and likely lower RNA content) of the latter relative to the former cell types. This was apparent from the progressively higher C_T values and the increasing frequency of unamplified replicates (samples in which 1 or more of 4 replicates did not amplify) and of replicate variability (samples in which the standard deviation among replicates was > 0.5), even in 1000-cell samples (Fig. 3.2A). Results for single cell samples reflected these trends. Samples from early postnatal (P3) cultured SVZ were successfully analyzed for Gus (positive control), GFAP and Pax6 expression (Fig. 3.2B). Seven of 10 cells were GFAP-positive, most of which also expressed Pax6. Two GFAP-positive cells were Pax6-negative and 1 Pax6-positive cell was GFAP-negative. Gus was only detected in 4 of 10 cells, but a higher detection frequency might have been achieved had this PCR been run for more than 40 cycles. Only 2 samples failed to amplify any of the tested genes and no cases of unamplified replicates or high replicate variability was observed. Single cell analysis from freshly-dissected P5 mouse SVZ was less efficient: 7 out of 20 samples failed to amplify any of the tested genes (GFAP, Pax6, Dlx2, Dcx; failure to detect GFAP is likely due to the low number of GFAP-positive cells in the early postnatal SVZ) and more than half of the times a gene was detected, its replicate sample failed to amplify (Fig. 3.2C). As expected, single cells isolated from fresh adult tissue performed the worst: 18 out of 20 samples not amplifying at all and the remaining 2 amplifying only 1 of 2 replicates (GFAP, Pax6 and Sox2 tested; data not shown).

Figure 3.2: Real-time single cell RT-PCR. ***A***, ***B***, ***C***, summary tables of real-time RT-PCR data. 1000, 100, 10, 1 or 0 cells were FACS-sorted directly into cell lysis buffer in individual PCR tubes. Each sample was then reverse-transcribed and divided into 4 replicates. Three different cell sources were used: SVZ astrocytes of neonatal (P3) mice cultured for several days before cell collection, fresh neonatal (P5) SVZ dissected on the day of cell collection, and fresh adult SVZ dissected on the day of cell collection. Values represent the number of PCR cycles at which fluorescence levels passed a pre-determined threshold: the more cycles required, the weaker the expression of a given gene (all reactions were run for 40-45 PCR cycles). Parentheses: number of PCR replicates done for the same tube and primers. ##: no amplification. Red: one or more of the replicates did not amplify. Blue: standard deviation among sample replicates > 0.5. Yellow highlight: negative control that failed (amplified in absence of sample). ***A***, summary table of sensitivity titration tests for real-time PCR primers using 1000, 100, 10 or 0 cells/sample. Each sample was used to test only one primer/probe set, except for the 0 cell samples, which were used to test 2 primer/probe sets (2 replicates each). ***B***, ***C***, summary table of real-time RT-PCR done on single cells obtained from P3 SVZ cultures (***B***) or freshly-dissected SVZ of P5 mice (***C***). ***D***, ***E***, FACS plots of cells sorted from P3 SVZ cultures for real-time RT-PCR. Cells were collected from the gated area (red ellipse). SSC: side scatter (cell granularity). FSC: forward scatter (cell size). PI: propidium iodide (cell viability). ***F***, real-time PCR fluorescence measurements from the Gus sensitivity titration (green box in ***A***), using 1000, 100, 10 and 0 cultured SVZ cells/sample. ΔRn: changes in fluorescence levels compared to baseline. Cycles: number of PCR cycles elapsed. Green bar: fluorescence detection threshold for determining C_T value (set at 0.2 fluorescence units). ***G***, real-time PCR fluorescence measurements from a single cultured SVZ cell (purple box in ***B***). This cell was considered positive for Gus, GFAP and Pax6 (detection threshold set at 0.07; notice that the threshold is lower than in F, facilitating detection of lower abundance transcripts). See technical details in section 5.16.

A

	Cells	Gus	GFAP	Pax6	Dlx2	Dcx	BDNF	Notch1	Sox2	p75	Mash1
Cultured P3 cells	1000	33.12 (4)	24.30 (4)	28.66 (4)							
	100	35.51 (4)	25.85 (4)	30.25 (4)							
	10	38.08 (4)	27.99 (4)	33.80 (4)							
	0	## (4)	## (2)	## (2)							
Fresh P5 cells	1000	35.61 (4)	35.30 (4)	33.50 (4)	35.79 (4)	32.14 (4)					
	100	38.34 (4)	35.25 (4)	34.17 (4)	36.67 (4)	33.66 (4)					
	10	38.92 (4)	34.91 (4)	36.32 (4)	39.32 (4)	39.97 (4)					
	0	## (2)	## (2)	## (2)	## (2)	## (2)					
Fresh adult cells	1000	40.36 (4)	41.74 (4)	36.30 (4)	39.85 (4)	36.74 (4)	44.17 (4)	41.43 (4)	34.64 (4)	## (4)	32.42 (4)
	100	40.90 (4)	41.80 (4)	38.50 (4)	38.37 (4)	38.52 (4)	## (4)	## (4)	37.75 (4)	## (4)	33.21 (4)
	0	## (2)	## (2)	## (2)	## (2)	## (2)	## (2)	## (2)	## (2)	## (2)	44.35 (2)

B

	Cells	Gus	GFAP	Pax6	Dlx2	Dcx
Cultured P3 SVZ cells	1	## (1)	31.13 (1)	35.26 (2)		
	1	## (1)	30.31 (1)	33.62 (2)		
	1	38.80 (1)	30.09 (1)	35.88 (2)		
	1	## (1)	## (1)	## (2)		
	1	## (1)	37.71 (1)	35.11 (2)		
	1	38.42 (1)	31.81 (1)	## (2)		
	1	38.70 (1)	27.84 (1)	35.43 (2)		
	1	## (1)	## (1)	## (2)		
	1	39.51 (1)	## (1)	38.93 (2)		
	1	## (1)	37.43 (1)	## (2)		
	0	## (4)				
	0		## (2)	## (2)		

C

	Cells	Gus	GFAP	Pax6	Dlx2	Dcx
Freshly dissected P5 SVZ cells	1		## (2)	## (2)		
	1		## (2)	## (2)		
	1		## (2)	## (2)		
	1		## (2)	39.35 (2)		
	1		39.10 (2)	36.86 (2)		
	1		## (2)			37.79 (2)
	1		## (2)			39.40 (2)
	1		## (2)			## (2)
	1		## (2)			40.74 (2)
	1		## (2)			41.23 (2)
	1			37.50 (2)	39.08 (2)	
	1			## (2)	## (2)	
	1			## (2)	37.97 (2)	
	1			## (2)	39.06 (2)	
	1			37.51 (2)	38.98 (2)	
	1			37.44 (2)	## (2)	
	1			## (2)	39.30 (2)	
	1			37.55 (2)	## (2)	
	1			## (2)	## (2)	
	1			## (2)	## (2)	
	0		## (2)			
	0			## (2)		## (2)
	0				## (2)	## (2)

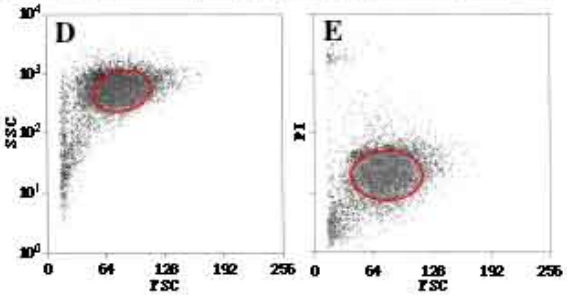

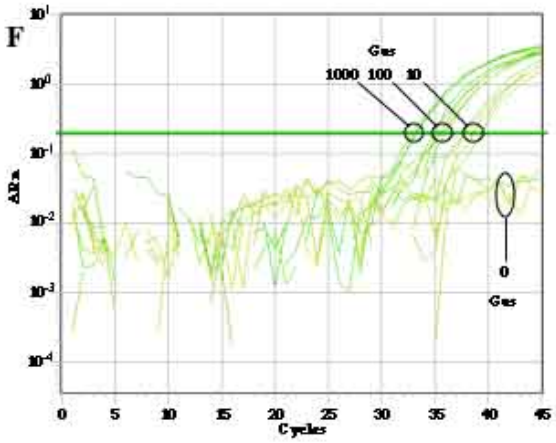

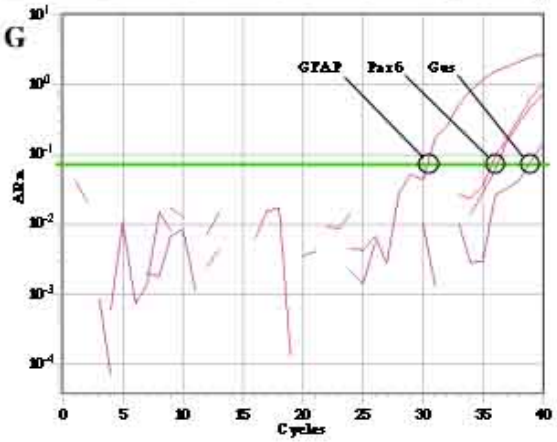

Antisense RNA amplification RT-PCR

To improve the performance of the previous protocol when using freshly-dissected SVZ cells and to increase the number of gene products that can be analyzed for each cell (limited to 3-4 with the first method), I decided to include an amplification step that should increase the amount of RNA available for analysis. This method is essentially identical to the real-time RT-PCR protocol in what concerns the cell collection and the final PCR detection reaction. Between these two steps, I added a series of cDNA production and RNA transcription steps (Van Gelder et al., 1990; Eberwine et al., 1992). The main advantage of this method over PCR amplification is that it linearly increases the amounts of all transcripts, thus better preserving the quantitative information that can be drawn from the processed samples.

Briefly, mRNA was first converted to single-stranded cDNA by RT reaction using a modified oligo-d(T) primer that also contains the T7 promoter sequence (Fig. 3.1B). By taking advantage of the reverse transcriptase's terminal transferase activity, which adds several deoxycytosine (dC) nucleotides to the 3' end of all cDNA strands, a know sequence can be added to the 3' end of all cDNAs. This was done by including in the initial RT reaction a SMART primer (Clontech), containing a known sequence and a sequence complementary to the dC stretch. The reverse transcriptase then switches templates and adds the sequence complementary to the SMART primer to the 3' end of the cDNA. At this point, all cDNAs have the same known sequences at each end. In a second step, I ran a 20-cycle PCR reaction using primers against those known sequences, thus obtaining multiple copies of double stranded cDNA of each initial template. Templates can be further amplified by using this cDNA, which contains a T7 promoter at one end, in an *in vitro* transcription reaction, yielding multiple RNA copies of each template. A final RT reaction converts these RNAs back into cDNA, which can be used for real-time PCR amplification and detection.

I applied this method to 100-cell and 0-cell samples of adult, freshly-dissected SVZ, either performing the entire amplification procedure (Long Amplification), a shorter version ending after the 20 cycle PCR reaction (Short Amplification) or no amplification as a control (Fig. 3.3). I chose to analyze Pax6 and Dcx because these were the most

Figure 3.3: Antisense RNA amplification. 100 or 0 freshly-dissected adult SVZ cells were collected by FACS sorting into PCR tubes and processed for amplification of antisense RNA. Amplified RNA was then converted to cDNA and PCR-amplified for detection of individual transcripts by real-time RT-PCR (Pax6 and Dcx; 45 cycles). Values represent the number of PCR cycles at which fluorescence levels passed a pre-determined threshold (the more cycles required, the weaker the expression of a given gene). Parentheses: number of PCR replicates done for the same tube and primers. ##: no amplification. Red: one or more of the replicates did not amplify. Blue: standard deviation among sample replicates > 0.5. Yellow highlight: negative control that failed (amplified in absence of sample). See technical details in sections 5.17, A6.

	Amplif.	Cells	Pax6	Dcx
Fresh adult SVZ cells	None	100	37.48 (4)	35.39 (4)
		0	## (2)	## (2)
	Short	100	35.51 (4)	44.38 (4)
		0	38.73 (2)	## (2)
	Long	100	34.71 (4)	39.11 (4)
		0	33.09 (2)	## (2)

reliably detected transcripts in previous experiments using adult cells (Fig. 3.2A). Results from these amplification methods were unreliable. Pax6 transcripts were detected at progressively lower cycle numbers (from 37.5 cycles without amplification to 34.7 cycles with the long amplification, Fig. 3.3), suggesting both amplification procedures improved the sensitivity of this assay. However, Pax6 transcripts were also detected in the no cell controls, raising doubts on the significance of the rest of the Pax6 data. Conversely, Dcx no cell controls were all negative, but transcript detection was not improved by the short or long antisense RNA amplification treatments, rather, it seemed to worsen (Fig. 3.3).

Multiplex nested RT-PCR

The antisense RNA amplification described above is a long, labor-intensive process (see also Appendix A6), which is most useful when quantitative information needs to be preserved, such as in microarray analysis. Since that method seemed unreliable, I decided to use a different amplification protocol, based on two successive PCR reactions. This procedure, though not as quantitative, should provide sufficient amplification in fewer steps, making it more practical and less prone to errors.

As in the real-time RT-PCR method, single cells from either freshly-dissected adult SVZ or early post-natal (P5) SVZ astrocyte cultures were collected by FACS sorting directly into a cell lysis buffer. Because I could not design all primers to span introns, I included DNAase in this buffer to degrade genomic DNA. The RNA of the sorted cells was converted to cDNA by reverse transcription. At this point, gene transcripts from a single cell can be amplified by PCR until they are detectable. Using a two-step nested PCR, a higher degree of amplification and specificity can be obtained compared to conventional PCR methods. This is achieved by running a first PCR reaction with a given set of primers, then taking aliquots from the first reaction as template for a second round of PCR amplification using a different set of primers, designed to anneal within the fragment amplified by the first set of primers. To analyze the expression of multiple genes, the first PCR reaction can be run with a cocktail of primer pairs, each specific for a different gene product (multiplex PCR). In the second PCR reaction, nested primers specific for each gene are used in separate reactions (Fig. 3.1C). Finally, PCR products are run on an agarose gel for detection of amplification (Fig. 3.4B-D).

Figure 3.4: Multiplex nested RT-PCR of single SVZ cells. ***A***, summary table of all single cells collected and processed by multiplex nested RT-PCR method. Each cell was tested for expression of 12 different genes. Two different types of cells are represented: some were obtained from SVZ astrocytes of early postnatal (P5) mice cultured for 4 days before cell collection, others were obtained from fresh adult SVZ dissected and dissociated on the day of cell collection. Some genes were never detected in single cells and some cells could not be amplified for any gene (indicating either failed cell collection events or low sensitivity of detection method). ~~DNAse~~: no DNAse treatment during cell collection; black diamond: DNA band was detected after running final PCR product on agarose gel. ***B***, RNA titration test for primers used in RT-PCR. Total RNA was collected from dissected SVZ tissue and serially diluted to test primer sensitivity. Sox2 and Dlx2 (both highly expressed in the SVZ) could be detected at 1 ng RNA/reaction, while GAPDH, GFAP and Notch1 were only detected at 100 ng RNA/reaction. Other genes were only detected when DNAse treatment was omitted, perhaps indicating that DNAse treatment is degrading part of the RNA. Because some primer pairs do not span introns, signal detected in DNAase-untreated samples may be due to genomic DNA amplification. ***C***, ***D***, examples of RT-PCR results from single cells of cultured neonatal SVZ (***C***) or fresh adult SVZ (***D***). Although the serial RNA dilution test showed 1 ng RNA/reaction as the limiting threshold for detection, several transcripts were detectable from single cells. DNA ladder: 100-1000 bp length in increments of ~100 bp. See technical details in sections 5.15, A5.

A

	Cell	GAPDH	GFAP	Pax6	Sox2	Dlx2	Er81	TrkBFL	TrkBTR	BDNF	LeX	Notch1	NCAM
Culture P5 SVZ	A	◆	◆		◆								
	B	◆	◆		◆	◆							
	C	◆			◆								
	D	◆			◆								
	E	◆			◆					◆			
	F	◆		◆	◆	◆				◆			
	~~DNAse~~	◆			◆								
	No cell												
Adult, freshly dissected SVZ	G	◆			◆								
	H	◆		◆	◆								
	I												
	J	◆			◆								
	K				◆								
	L	◆											
	M				◆								
	N	◆			◆								
	O	◆			◆								
	P	◆			◆					◆	◆		
	Q												
	R												
	S												
	T												
	U												
	V				◆								
	W				◆								
	X												
	Y	◆			◆								
	Z	◆			◆								
	AA			◆	◆								
	AB				◆								
	AC	◆			◆					◆			

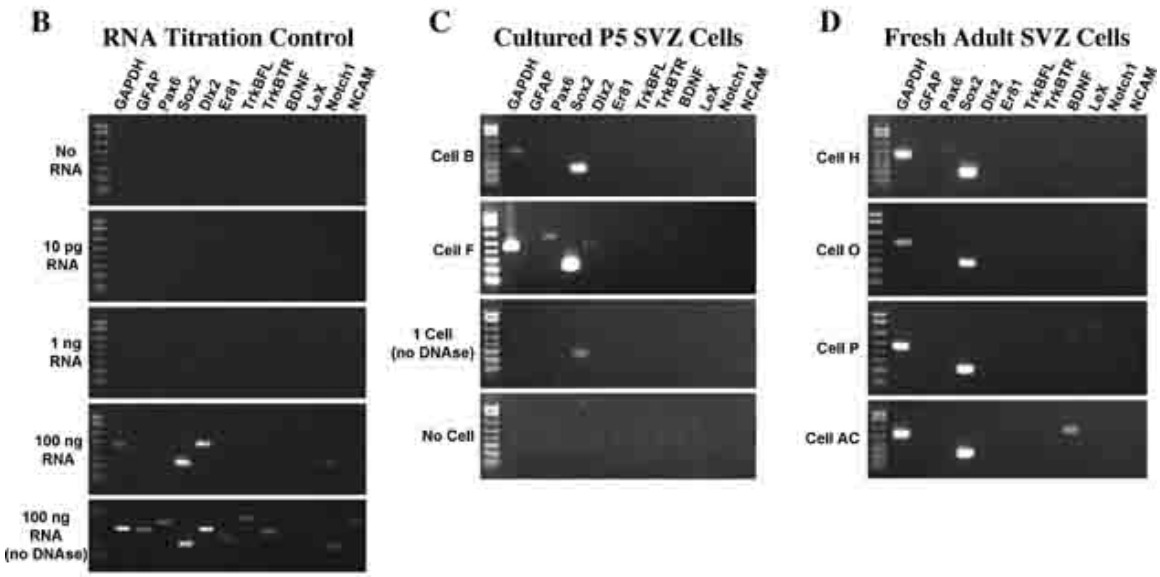

Using this multiplex nested RT-PCR protocol, I successfully detected several gene transcripts from single cells of both cultured P5 SVZ and freshly-dissected adult SVZ (Fig. 3.4). Expression of the housekeeping gene GAPDH (used as a positive control) was detected in 17 out of a total of 30 single cell samples. The most commonly detected genes were Sox2 (22 samples), BDNF (4 samples) and Pax6 (3 samples). Other gene products detected include GFAP (2 samples), Dlx2 (2 samples) and fucosyltransferase-4 (henceforth referred to as LeX, its carbohydrate product) (1 sample), while Er81, TrkB (TrkB-FL or TR), Notch1 and NCAM were never detected. Seven of the single cell samples did not amplify any of the 12 gene products tested. This may indicate that no cell was sorted into these tubes or it may reflect lack of sensitivity of my protocol/primers to consistently amplify from low amounts of starting material. An additional 6 samples expressed Sox2 (one of which also expressed Pax6) without detection of the control gene GAPDH. This is unlikely to be due to contamination of the reagents because in the adult cell L , which did amplify GAPDH, Sox2 was undetectable (Fig. 3.4). Further, the no cell control in the cultured sample experiment and a number of samples in the adult sample experiment were also negative for Sox2. This result may have been caused by different efficiencies of the different primer pairs in amplifying specific cDNAs from very few copies, though at least when starting from 100 ng RNA and omitting the DNAse treatment, all primers were capable of generating a visible band (Fig. 3.4B). Some of the most interesting single cell results are shown in Fig. 3.4C, D. These include a cultured cell that was positive for GFAP, Sox2 and Dlx2 (cell B). The coexpression of GFAP and Dlx2 may be an artefact of cell culture or this could be a type B astrocyte that is in transition to become a type C or type A cell. Another cultured cell was positive for Pax6, Sox2, Dlx2 and BDNF, but negative for GFAP (cell F). This cell also could represent a type C or type A precursor. Among the freshly dissected adult SVZ samples, I detected a cell positive for Sox2, BDNF and LeX (cell P), which may be a type C cell. Unfortunately, most sorted cells were negative for GFAP. In the case of fresh adult samples, this lack of success in identifying astrocytes may reflect the need to use additional parameters in the cell sorting procedure to ensure an enriched collection of the desired cell type. However, I expected greater success among the cultured samples, as

~90% of these cells are GFAP-positive by immunocytochemistry (data not shown). Once again, it may be that this protocol and/or primers are insufficiently sensitive.

3.3 Discussion

The multiplex nested RT-PCR protocol provided encouraging results on the ability to detect multiple gene transcripts from single SVZ cells. In several cases, 4-5 out of 12 different gene products tested were identified in the same cell. Interestingly, data obtained with this approach suggest that some SVZ cells might express BDNF. I detected BDNF transcripts in two out of ten $GAPDH^+$ single cells isolated from adult SVZ. Both of these cells were also $Sox2^+$ and one was LeX^+. Sox2 is expressed in most SVZ cells as well as in ependymal cells (Ferri et al., 2004), whereas LeX is not expressed by ependymal cells and is closely associated with neurosphere-generating cells (Capela and Temple, 2002), which include type B astrocytes as well as type C cells (Doetsch et al., 1999b; Doetsch et al., 2002). Therefore, BDNF-expressing cells in the adult SVZ are likely rare in numbers, as suggested by results presented in Chapter 2 (Fig. 2.1B, 2.2A, B), but may include neural stem cells. No GFAP or Dlx2 expression was detected in these $BDNF^+$ cells. This is probably due to insufficient detection sensitivity rather than a real negative result, since all SVZ cells are either $GFAP^+$ (type B cells) or $Dlx2^+$ (type C and A cells) and none of the adult SVZ single cells analyzed was positive for either (Fig. 3.4A). This interpretation is consistent with the results of the RNA titration control (Fig. 3.4B), in which several primers fail to amplify even at the higher RNA quantities. Suboptimal primer design might underlie these sensitivity problems. Another weakness of the multiplex nested RT-PCR method is the need to undergo 70 PCR cycles before detection (40 in the first PCR round and 30 in the second round). Such high numbers of a non-linear amplification method could lead to false positives as well as to the loss of rare transcripts, outcompeted by more common ones in the multiplex PCR amplification step.

Despite the poor performance with some samples, the sensitivity/reliability of real-time RT-PCR seems to be greater than that of the multiplex nested RT-PCR. When analyzing astrocytes collected from neonatal SVZ cultures, only 29% (2/7) of the single cells were positive for GFAP using a multiplex nested RT-PCR approach (Fig. 3.2A).

Using real-time RT-PCR, 70% (7/10), perhaps even 88% (if we exclude the 2 samples negative for all genes) of the neonatal cultured SVZ single cells tested were positive for GFAP (Fig. 3.2B). Furthermore, GFAP was detected at an average of 32 PCR cycles, versus 70 cycles with the previous method. Nonetheless, real-time RT-PCR alone does not seem to be sufficiently sensitive to reliably detect transcripts from uncultured single SVZ cells and is limited to a maximum of 3-4 genes that can be analyzed for each cell.

Based on my real-time RT-PCR data, most cultured SVZ astrocytes expressed the homeobox transcription factor Pax6 (Fig. 3.2B). This is in contrast to what occurs *in vivo*, where Pax6 expression seems to be mainly associated with type C cells (Kohwi et al., 2005). It is possible that the distinctions between type B astrocytes and type C cells becomes less well demarcated *in vitro*, as type B cells are induced to proliferate more rapidly. This interpretation is consistent with the detection of a $GFAP^+/Dlx2^+$ cell in SVZ astrocyte cultures analyzed by the multiplex nested RT-PCR method (cell B, Fig. 3.4A, C).

In conclusion, the multiplex nested RT-PCR method provided the greatest amplification and allowed for a greater number of genes to be analyzed for each cell, while the real-time RT-PCR method was the most reliable and provided semi-quantitative information. The antisense RNA amplification protocol is potentially useful but will require more extensive optimization. The ideal approach should combine several of these methods into one reproducible and sensitive protocol, perhaps using in a 1^{st} phase a multiplex PCR amplification and in a 2^{nd} phase real-time TaqMan PCR primers "nested" within the 1^{st} set of non-TaqMan primers. This optimal protocol might then be used to answer pressing questions regarding SVZ biology, such as the nature of type B, C and A cell heterogeneity.

Chapter Four: Conclusion and Future Perspectives

Summary and implications for the field of neurogenesis

In my thesis, I have studied the role of the neurotrophin BDNF and of its receptor TrkB in adult neurogenesis. I have also developed new techniques that will allow to characterize the SVZ at the single cell level rather than merely at the population level.

My characterization of the expression of the neurotrophin receptors TrkB and p75 in the SVZ and RMS has provided important new data and corrected several inaccurate reports. Future studies of the effects of BDNF on the SVZ should be performed with this information in mind. I have identified for the first time the cell types expressing TrkB in these regions as ependymal and type B cells (Fig. 2.3, 2.4, 2.5, 2.6). Further analysis showed that TrkB-TR is the main isoform of TrkB in the SVZ and RMS (Fig. 2.7, 2.8). These findings provide clues for the possible role of TrkB in adult neurogenesis and suggest that other receptors might be involved in responses to BDNF. The pan-neurotrophin receptor p75 has recently been suggested as such an alternative receptor in the SVZ (Young et al., 2007). This idea is reinforced by my own findings describing the effect of BDNF infused into the lateral ventricle and the expression of p75 in the SVZ and RMS.

Importantly, my studies have uncovered errors in the field of adult SVZ neurogenesis, claiming that exposing the SVZ to BDNF increases neuroblast production (Zigova et al., 1998; Benraiss et al., 2001; Henry et al., 2007) and that the neuroblasts themselves express TrkB receptor *in vivo* (Chiaramello et al., 2007; Bath et al., 2008). Contrary to current views, my data indicates that SVZ neuroblasts *in vivo* do not express TrkB (Fig. 2.3, 2.4, 2.5, 2.6), that TrkB is not essential for neuroblast production (Fig. 2.9, 2.10, 2.12) and that BDNF does not increase neuroblast numbers (Fig. 2.16, 2.20, 2.22). The exact cause of the discrepancy in results regarding the effects of BDNF infusion on neurogenesis is not clear at present. However, recent reports claiming that TrkB and even phosphorylated TrkB is expressed in neuroblasts of the SVZ and RMS (Chiaramello et al., 2007; Bath et al., 2008) were performed with antibodies that are not specific to TrkB

receptor, as I have clearly shown here (Fig. 2.5, 2.23, 2.24). If left unchallenged, these inaccuracies would likely mislead future efforts by other laboratories studying neurotrophin regulation of neurogenesis. Another surprising finding was the striking difference in p75 receptor expression between mice and rats (Fig. 2.21). Perhaps due to this difference, these closely related species have somewhat different responses to BDNF infusion, which seems to have no effect on the total neuronal output of the SVZ in mice while decreasing it in rats (Fig. 2.16, 2.22). More work will be necessary to determine the therapeutic potential of BDNF as well as its possible physiological roles in adult mammalian neurogenesis.

Origin and regulation of BDNF in SVZ

Though the physiological role, if any, of BDNF on adult SVZ neurogenesis is at present unknown, my work clearly shows that it does not increase neuron production when administered into the lateral ventricles. However, BDNF does have several effects on SVZ cells, increasing apoptosis as well as decreasing proliferation, the number of $Mash1^+$ cells and neuron production (Fig. 2.16, 2.22). Therefore, it is likely that if the SVZ is exposed to BDNF endogenously, this could affect its neurogenic output. Importantly, I detected BDNF protein in the adult SVZ (Fig. 2.2C), though mRNA levels were nearly undetectable (Fig. 2.1B, 2.2A, B). BDNF is a secreted protein and so it might be produced in other brain regions and subsequently transported to the SVZ. Indeed, BDNF is known to be anterogradely transported along axons and can be released in an activity-dependent manner (Altar and DiStefano, 1998). Alternatively, BDNF expression in the SVZ may be temporally regulated, perhaps responding to external stimuli.

Environmental factors might influence SVZ neurogenesis through hormones. The adrenergic hormones Epinephrine (Epi) and Norepinephrine (Norepi) are involved in stress, "fight-or-flight" responses. Both molecules exert their effects through adrenergic receptors, which are known to be expressed in astrocytes (Hertz et al., 2004). BDNF and TrkB are upregulated in the SVZ in mice exposed to behavioral paradigms of stress and aggression (Fiore et al., 2003; Fiore et al., 2005). In this thesis, I have shown that SVZ astrocytes exposed to Epi in culture upregulate BDNF expression by over four-fold (Fig. 2.3B). Therefore, environmental factors that stimulate adrenergic and noradrenergic

circuits, such as stress, could also modulate BDNF availability and perhaps neurogenesis in the SVZ. In fact, stress is well known to inhibit proliferation and perhaps neuronal output of the adult hippocampal dentate gyrus (Mirescu and Gould, 2006), outcomes which are similar to what I observed in the SVZ after intraventricular BDNF infusions.

I also tested the effects of the lactogenic hormone prolactin (PRL) and of the neurotransmitter dopamine (Dopa) on BDNF expression by SVZ astrocytes in culture. Contrary to stress, these molecules have been reported to increase SVZ proliferation and neuron production (Shingo et al., 2003; Hoglinger et al., 2004), effects which are opposite to what I observed after BDNF infusions (Fig. 2.16, 2.22). However, I found that PRL can increase expression of BDNF in cultured SVZ astrocytes by 34% and Dopa by more than two-fold (Fig. 2.3B). If the same regulation occurs *in vivo*, PRL and Dopa could affect SVZ neurogenesis through BDNF. In fact, the SVZ receives dopaminergic synaptic contacts directly onto type C cells from axon terminals presumably originating in the *substancia nigra* (Hoglinger et al., 2004). Additionally, the PRL receptor is expressed in the SVZ (Shingo et al., 2003; Mak et al., 2007) and I observed increased levels of BDNF mRNA in the SVZ of 7 d.p.c. pregnant mice (Fig. 2.3C, D), a time at which PRL levels are also elevated compared to later in pregnancy (Barkley et al., 1978; Freeman et al., 2000).

The possibility that physiological stimuli such as neuronal activity, pregnancy or stress can regulate adult neurogenesis by modulating BDNF levels in the SVZ is an exciting one. However, while the *in vivo* effects of stress on adult neurogenesis are similar to those of BDNF, those of Dopa and PRL are opposite (Shingo et al., 2003; Hoglinger et al., 2004). It is therefore intriguing that BDNF levels should be elevated in the SVZ of 7 d.p.c. pregnant mice or that Dopa or PRL should increase BDNF expression in SVZ cultures. The relevance of these findings for the physiological regulation of adult SVZ neurogenesis is unclear at the moment and will require further testing.

Hypothesis for BDNF regulation of SVZ neurogenesis

Based on the results presented in this thesis, BDNF may have a dual role in the production of new neurons from the adult SVZ. For cells in the SVZ and RMS, BDNF may induce apoptosis or cell cycle arrest/differentiation of progenitor cells through the

p75 receptor. Once in the OB, neuroblasts may start expressing the TrkB receptor, which would alter these cells' response to BDNF. This hypothesis differs significantly from previous interpretations in that the effect of BDNF at the SVZ level is detrimental to neurogenesis rather than stimulatory (Zigova et al., 1998; Benraiss et al., 2001; Pencea et al., 2001; Henry et al., 2007; Young et al., 2007). Nonetheless, this interpretation is consistent with the majority of my data and it is based on a more thorough analysis than what had previously been published.

My results as well as those of others indicate that p75 is expressed in SVZ type C cells and some neuroblasts, whereas most astrocytes do not express this receptor. Conversely, I have shown that TrkB-TR is abundant in SVZ astrocytes and ependymal cells but is undetectable in neuroblasts (Fig. 2.3, 2.4, 2.5, 2.6, 2.7, 2.8). TrkB is likely not expressed in type C cells, because it has been reported that $p75^+$ and $TrkB^+$ cells are distinct SVZ populations (Young et al., 2007) and depleting the SVZ of type C cells and neuroblasts with AraC does not decrease the intensity of TrkB staining by *in situ* hybridization (Fig. 2.8B, C). I observed that intraventricular BDNF infusions increase apoptosis and decrease the number of proliferating and $Mash1^+$ cells in the SVZ. Additionally, the number of young neurons is decreased in the OB of BDNF-infused rats, which have high levels of p75 in the SVZ and RMS. The high levels of TrkB-TR in ependymal cells and SVZ/RMS astrocytes, which ensheath migrating neuroblasts, might act as a barrier, limiting neuroblasts' access to BDNF from the surrounding parenchyma and ventricular lumen (Fig. 4.1). This would protect these cells from p75-induced premature cell cycle exit and/or apoptosis while still in the SVZ and RMS. Once neuroblasts reach the OB and migrate radially away from the RMS, they might downregulate p75, which is not detectable in OB interneurons by immunohistochemistry (data not shown), and upregulate TrkB expression, including the full-length isoform, which is found in several cells of the granular and glomerular layers (Fig. 2.14). This would change the response of these cells to BDNF, perhaps promoting neuronal differentiation and integration into the OB circuit, regulating dendrite morphology, synapse formation and plasticity, all of which can occur through TrkB receptor activation. Consistent with this interpretation, another study has shown that SVZ neuroblasts in culture initially respond to several neurotrophins through p75, but gradually increase TrkB expression, ultimately

responding only to BDNF (Gascon et al., 2005), which promotes dendrite development. Additionally, I observed that conditional deletion of TrkB from the SVZ neurogenic lineage has greater consequences on the number of new neurons in the differentiated layers of the OB than in the core of the OB, where immature neurons are located (Fig. 2.10D). This result suggests that TrkB is more important to neuroblasts as they mature than while they are being produced in the SVZ or migrating to the OB. TrkB upregulation *in vivo* might occur only in specific subpopulations of OB interneurons because few of these cells are $TrkB^+$ by *in situ* hybridization (Fig. 2.14) and only TH^+ interneurons seemed to be affected by the loss of TrkB in my grafting experiment (Fig. 2.12F). Other OB cells that might upregulate TrkB expression while maturing are the $Parvalbumin^+$ interneurons of the external plexiform layer, which are partially lost and develop stunted dendrites in BDNF-KO mice (Berghuis et al., 2006). Alternatively, new OB interneurons may all go through a short period of TrkB expression while they are maturing, later turning this gene down or off in all but TH^+ and $Parvalbumin^+$ cells.

What then could be the role of p75 expression in the SVZ? Perhaps this receptor is necessary to eliminate neuroblasts produced in excess and/or that stray away from the normal migratory routes. p75 might also be involved in the production of other cell types from the SVZ such as oligodendrocytes, the cells responsible for myelination in the CNS. The adult SVZ produces low numbers of oligodendrocytes, which can migrate to nearby white matter tracts such as the corpus callosum, striatum and fimbria (Levison et al., 1993; Levison and Goldman, 1993; Luskin and McDermott, 1994; Menn et al., 2006). p75 is know to be important for the migration and maturation of Schwann cells in the PNS (Bentley and Lee, 2000; Cosgaya et al., 2002) and might play similar roles for oligodendrocyte precursors in the CNS, at least some of which express this receptor (Cohen et al., 1996; Althaus et al., 1997; Du et al., 2003). The adult SVZ can participate in repair of demyelinated lesions (Nait-Oumesmar et al., 1999; Picard-Riera et al., 2002; Menn et al., 2006). Interestingly, several reports indicate that p75 expression in the SVZ is upregulated in animal models of multiple sclerosis, a chronic demyelinating disease (Calzá et al., 1998; Petratos et al., 2004), raising the possibility that p75 is important for the reaction of the SVZ to these conditions, perhaps by increasing its production of oligodendrocyte precursors and/or promoting their migration towards the damaged areas.

Figure 4.1: A model for the role of BDNF and its receptors in SVZ neurogenesis. Ependymal cells (E) and type B astrocytes (B) express high levels of the truncated TrkB receptor (TrkB-TR). This isoform lacks the intracellular kinase domain responsible for activating most known signaling pathways associated with neurotrophins. Type C intermediate precursors (C) and type A neuroblasts (A), on the other hand, express another neurotrophin receptor, p75. These cell types are typically surrounded by type B astrocyte processes and therefore have little/no direct contact with the surrounding brain parenchyma (brown) or ventricle lumen (light blue). Additionally, BDNF protein, a ligand for both TrkB-TR and p75, is present in the SVZ. Given these facts, TrkB-TR expression by ependymal and type B cells might be important to form a shield around type A and type C cells, regulating their access to BDNF, which, through p75, could induce premature cell cycle exit, differentiation or apoptosis of SVZ precursors.

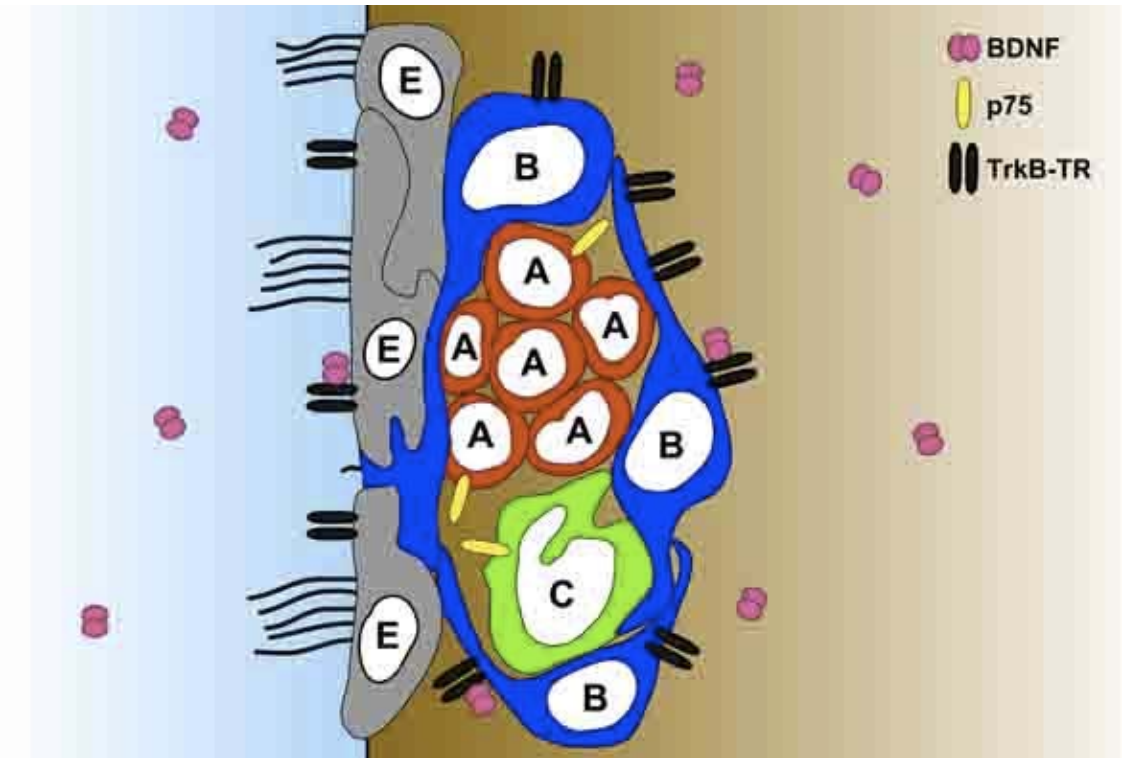
BDNF
p75
TrkB-TR
E
B
A
A
A
E
A
A
A
A
B
C
E
B

Trophic support for SVZ-derived neurons

My work has shown that neuroblasts in the mouse SVZ and RMS do not express TrkB receptor and that large numbers of TrkB-KO neuroblasts migrate from the SVZ to the OB when grafted into a WT recipient mouse (Fig. 2.12B, 2.13A, B). Furthermore, very few SVZ cells express the p75 receptor (though rats have more significant numbers of $p75^{+}$ neuroblasts; Fig. 2.21). These results suggest that BDNF does not provide survival signals for neuroblasts in the SVZ or RMS. Other candidate factors for this role remain to be identified.

Equally little information is available on what keeps new neurons alive once in the OB. However, it is known that these cells are subjected to a strong selection process shortly after they leave the RMS and begin maturing in the differentiated layers of the OB. Approximately 50% of all new neurons that arrive in the OB are eliminated between 15 and 45 days after they are born in the SVZ (Petreanu and Alvarez-Buylla, 2002). The selection mechanism is not clear, but seems to depend at least in part on neuronal activity: mice in which the incoming activity from olfactory receptor neurons (ORN) is eliminated have significantly higher levels of apoptosis among young OB neurons (Najbauer and Leon, 1995; Petreanu and Alvarez-Buylla, 2002). Consistent with a role of activity, this effect is only detectable after neurons have developed dendritic spines, at around 15 days after cell birth (Petreanu and Alvarez-Buylla, 2002). This process of activity-based selection is not yet understood at the molecular level, but neurotrophins such as BDNF are ideal candidates to mediate these effects. BDNF is detected in the granular, mitral, external plexiform and glomerular layers of the OB (Fig. 2.15) (Yan et al., 1997b). Furthermore, BDNF levels in the OB are reduced by olfactory deprivation (McLean et al., 2001), suggesting that its expression is regulated by activity. Axonal arborizations of ORNs in glomeruli are also subject to an activity-dependent competition. ORNs with inactive synapses are at a competitive disadvantage towards those with active synapses, leading to axonal arbor pruning and fewer connections (Cao et al., 2007). This competitive process appears to be mediated by activity-dependent release of BDNF from the synaptic targets of ORNs (M/T and periglomerular neurons), whereas ORNs do not express BDNF themselves. One possible interpretation is that ORN stimulation of their

target neurons through neurotransmitter release promotes the local secretion of BDNF from the target cells, thus stabilizing the active ORN's axonal branches and strengthening its synapses. The more active the ORN, the more it can outcompete other ORNs, whose axonal branches will instead be weakened and pruned away. A similar mechanism might be at play for maturing OB interneurons as they establish their synapses with mitral and tufted neurons, culminating with apoptosis for cells that are outcompeted.

As mentioned above, BDNF may be important only for specific subpopulations of OB interneurons. Other neurons might depend on different trophic factors, such as Glial-Derived Neurotrophic Factor (GDNF), which provides strong survival signals to midbrain dopaminergic neurons and spinal cord motor neurons (Lin et al., 1993; Oppenheim et al., 1995; Tomac et al., 1995). GDNF is strongly expressed in the OB, including in mitral and tufted projection neurons, and granular and periglomerular interneurons express GDNF receptors Ret and GFRα2 (Buckland and Cunningham, 1998; Burazin and Gundlach, 1999; Matsuo et al., 2000; Maroldt et al., 2005). Understanding what regulates the survival and integration of new neurons in a mature circuit in the adult brain will be crucial to the success of future therapeutic approaches trying to replace neurons lost due to injury or neurodegenerative diseases. The adult rodent OB is an ideal model to study these processes.

What drives neuronal replacement in the OB?

As mentioned in section 1.3, some clues about the role of adult OB neurogenesis have been uncovered. However, this area of research is still largely unexplored. Does cell replacement really confer a higher level of plasticity to the OB circuit than would be possible by synaptic plasticity alone? Why would the OB require such high levels of plasticity? How are new neurons selected for circuit integration? And what drives established neurons in the OB to die? Is the death of old neurons necessary for the incorporation of new neurons or do the new neurons induce old ones to die?

BDNF and TrkB might be part of the answer for several of these questions, based on the classical paradigm defined in the neurotrophin hypothesis (competition for a limited supply of neurotrophins provided by target organs determines the survival of appropriate numbers of innervating neurons) (Levi-Montalcini, 1987) and on the known involvement

of neurotrophins in synaptic formation and plasticity. As mentioned above, BDNF could be involved in the selection process undergone by new OB neurons between 15 and 45 days after their genesis. Despite the continuous arrival of new neurons, the size and cell density of the adult OB are constant, indicating that elimination of mature neurons and incorporation of new ones are somehow coordinated. Competition for limited amounts of trophic support might be a part of this coordination. Studies in songbirds have shown that inducing the death of mature HVC neurons increases the level of incorporation of new neurons in this nucleus (Scharff et al., 2000), suggesting that neuronal death promotes the recruitment of replaceable neurons. The number of "vacancies" in this circuit may be a critical variable for neuronal replacement: one neuron may need to be eliminated before a new one can be added in its place.

The role of neurotrophins and cell competition in neuronal replacement within the adult mammalian OB has not yet been tested. This could be achieved by either modulating the number of new neurons arriving into the OB, the levels of particular neurotrophins or a combination of both. The number of new OB neurons could be increased with intraventricular infusions of FGF2 or Erythropoietin (EPO) (Kuhn et al., 1997; Shingo et al., 2001). Alternatively, SVZ-derived neuroblasts can be purified and grafted in specific numbers directly into the OB. These approaches would allow to test whether there is a limited number of "vacancies" in the OB circuit for new neurons. In addition, by monitoring the levels of apoptosis among mature OB neurons, one could also test if new neurons promote the elimination of old ones. It is also possible to decrease the number of new OB interneurons by infusing AraC, which would reversibly deplete the proliferating type C and type A cells from the SVZ (Doetsch et al., 1999a). Alternatively, EGF has been shown to skew SVZ progenitors towards a glial rather than neuronal lineage, which also leads to fewer new neurons migrating into the OB (Craig et al., 1996; Kuhn et al., 1997; Doetsch et al., 2002). GFAP:TK mice could also be used to eliminate neuroblast production in the adult brain upon Ganciclovir administration (Garcia et al., 2004). Other transgenic mouse lines could be used to kill mature OB interneurons in a spatio-temporally-controlled way. Rosa26R-DTA mice express diphtheria toxin in any cell subjected to Cre-mediated DNA recombination, thus inducing that cell's death (Brockschnieder et al., 2006). Injecting a Cre-expressing virus into a selected region of

the OB of these mice would eliminate neurons from that region. If new neurons are incorporated faster in the interneuron-depleted regions of these mice's OB than in the surrounding regions, it would suggest that cell elimination does promote the integration of new neurons in the OB.

Experimentally regulating the levels of BDNF in the OB would provide important insight into the involvement of this neurotrophin in neuronal replacement. Mice overexpressing BDNF in the forebrain are available (Huang et al., 1999b), as are mice with reduced levels of secreted BDNF in the OB (Bath et al., 2008), both of which could be used to address this question. In fact, in the latter study, the authors found reduced numbers of new OB neurons, suggesting that BDNF may indeed be controlling survival of these cells, though by which means is not clear at present. By combining manipulations of OB neuron numbers and BDNF levels, the mechanisms regulating neuronal replacement in the OB could be further dissected. For example, if increasing the number of new neurons arriving in the OB also increases the number of new neurons that become incorporated in the OB circuit, one could test if this can still occur in a mouse model with reduced levels of BDNF in the OB. Conversely, if the number of stably-integrated new neurons is the same regardless of how many arrive in the OB, one could test whether more new neurons can survive in a mouse model with increased levels of BDNF. The knowledge gained from such experiments would complement the work I present in this thesis, so that not only would we better understand the effects of BDNF on neurogenic niches, but also its effects on differentiating cells that are integrating into a mature brain circuit. If BDNF can promote the survival or maturation of such cells, this neurotrophin may become very useful for therapies where damaged neurons need to be replaced with new ones.

Single cell RT-PCR analysis

Single cell PCR methods aimed at amplifying genomic DNA are currently being used for pre-implantation genetic diagnosis, whereby 1-2 cells from embryos generated *in vitro* can be removed for screening of a variety of genetic disorders (Fragouli, 2007), and are also useful in studies of cells with high genomic variability such as B and T lymphocytes. However, for most cells, what makes them unique is the combination of

genes they express. Methods such as immunohistochemistry and *in situ* hybridization are limited in the number of gene products they can detect simultaneously and standard Western blot or RT-PCR methods are useful for population analyses but lack single cell resolution. Single cell RT-PCR (SC-RT-PCR) methods combine detection sensitivity and ability to detect multiple gene products with single cell resolution. Furthermore, SC-RT-PCR allows the study of gene expression among cell populations that are heterogeneous but hard to distinguish from each other, either morphologically, molecularly or by location. One such case is that of SVZ type B astrocytes, which include neural stem cells but probably also non-neurogenic, "structural" astrocytes. Without a stem cell marker, one cannot distinguish these cells. Additionally, stem cell properties are likely conferred onto a cell by the expression/repression of multiple genes rather than by 1-2 key genes. Single cell analysis of gene expression will be very useful to determine the heterogeneity of SVZ type B astrocytes and begin identifying the combination of gene products that distinguish neurogenic from "structural" astrocytes in the SVZ. This analysis could be extended to astrocytes of other regions, where dormant adult neurogenic potential might be waiting to be discovered. While it will not be immediately apparent from SC-RT-PCR alone which subgroup of type B astrocytes are neurogenic and which are not, one can focus on the different subgroups and perform tests that will allow to correlate a specific gene expression pattern with cells exhibiting stem cell properties such as self-renewal and multipotentiality. Depending on the outcome of such gene expression profiling studies, this could be achieved by designing mouse strains with specific combinations of reporter genes, select cells that express the appropriate reporter genes and perform neurosphere cultures or grafting experiments to test specific cell types' neuro/gliogenic capabilities. The homeobox transcription factor Pax6 could be one candidate gene for this type of analysis: my results using real time SC-RT-PCR suggest that most but not all SVZ astrocytes in culture express Pax6 (Fig. 3.2B). Pax6 is also expressed in SVZ astrocytes *in vivo*, though at a much lower frequency (Minoree Kohwi, unpublished observations). If culturing SVZ astrocytes activates their neurogenic potential, the higher numbers of $Pax6^{+}$ cells *in vitro* could be a reflection of more activated stem cells. Therefore, Pax6 might be useful to distinguish two different populations of astrocytes and could be indicative of an activated progenitor.

Another interesting observation was made with the multiplex nested SC-RT-PCR, in which two out of 15 freshly-dissected adult SVZ cells expressed the neurotrophin BDNF (Fig. 3.4). One of these cells was also LeX^+, an extracellular matrix factor that has been closely associated with SVZ stem cells (Capela and Temple, 2002). Therefore, BDNF might define yet another subpopulation among SVZ progenitors. Based on the data presented in section 2.2, which suggests that BDNF might in some cases decrease SVZ neurogenesis, it is intriguing that stem cells themselves could express BDNF. One possible interpretation is that BDNF, which promotes neuronal differentiation, is involved in the transition from type B to type C cells, or from type C to type A cells. If so, a short, localized exposure of SVZ cells to BDNF could be beneficial to the production of neuroblasts. However, a permanent exposure to uncontrolled levels from parenchymal and/or ventricular BDNF sources could cause a depletion of SVZ progenitors by promoting too many of them to become more committed precursors. This interpretation is consistent with the model described above for the roles of TrkB-TR, p75 and BDNF in adult SVZ neurogenesis.

SC-RT-PCR could also be used to study type A neuroblasts, which are beginning to be seen not as a homogeneous population, but rather as a diverse group of cells expressing different genes (Kohwi et al., 2005; Waclaw et al., 2006; Long et al., 2007). Furthermore, since neuroblasts produced in different regions of the SVZ give rise to different neurons in the OB (Kelsch et al., 2007; Merkle et al., 2007), there must be specific gene expression profiles embedded into these cells from the time of their birth, but which cannot be determined with histological stainings or general tissue dissection and neuroblast purification. It would be very interesting to know if $p75^+$ SVZ neuroblasts (Fig. 2.21G) have a gene expression pattern distinct from $p75^-$ neuroblasts and if this corresponds to the production of a particular interneuron subtype in the OB.

Type C cells are at present completely unexplored. Are all type C cells identical or do they have different properties and potentials? A subpopulation of type C cells is $Olig2^+$, (Menn et al., 2006), a transcription factor essential for the production of oligodendrocytes (Rowitch et al., 2002; Rowitch, 2004). This finding could imply that certain type C cells are destined to become oligodendrocytes, while different ones give rise to type A

neuroblasts. SC-RT-PCR techniques can help answer these questions, thus better characterizing this SVZ cell type.

One potential problem of studying SVZ cellular heterogeneity by SC-RT-PCR is that one cannot eliminate the possibility that differences in gene expression patterns are not merely derived from cells oscillating between different states of gene expression over time. Cells that are caught at different phases of such oscillations, but are otherwise identical, would appear to be different from each other. Another problem of SC-RT-PCR analyses is that the detection of mRNA for a given gene does not necessarily imply that the protein is also present. Developments in the field of proteomics allowing to detect, quantify and identify protein from extremely small sample sizes may soon allow to overcome that limitation (Ekstrom et al., 2001; Zhang et al., 2001).

As shown in section 3.2, dissecting the SVZ and collecting single cells for analysis without enriching for any particular cell type makes for a less efficient procedure. Ideally, one should be able to select and focus the analysis on a particular cell type. Ependymal cells can be easily identified by flow cytometry due to their larger size and granularity. Selecting SVZ cell types is more difficult. SVZ astrocytes and neuroblasts can be enriched by culturing dissociated SVZ cells on a glass or plastic substrate. Loosely attached cells are mainly neuroblasts and the more strongly attached cells are enriched for astrocytes. However, these methods involve *in vitro* steps, which could alter the gene expression profiles of the cells being studied. Alternatively, to select for type B astrocytes, one could transfect SVZ cells with an adenovirus expressing GFP under the astrocyte-specific GFAP promoter and, after a short survival period, collect the tissue and FACS-sort for GFP^+ cells. Endogenous markers could also be used for immunostaining/FACS purification, such as the extracellular matrix carbohydrate LeX, which is expressed by at least some SVZ stem cells (Capela and Temple, 2002), or the cell-surface receptor PDGFRα, which is expressed in most SVZ astrocytes (Jackson et al., 2006). These approaches have the caveat that such labelings might be pre-selecting for specific subpopulations of type B astrocytes.

After the FACS-based cell collection, single cell gene expression is analyzed by RT-PCR. Based on the findings in my thesis, the best approach might be to combine a 1st

phase using a multiplex PCR approach and a 2nd phase using real-time TaqMan PCR primers "nested" within the 1st set of non-TaqMan primers. This would combine the much simpler amplification by PCR with the more sensitive detection method of TaqMan. To further expand the number of genes analyzable per cell, the 2nd PCR reaction can also be multiplexed by combining TaqMan primer/probe sets labeled with different fluorophores. Due to the non-linear nature of the 1st PCR amplification step, quantitative data would be somewhat lost, but one would gain in the ability to detect more rare transcripts and more genes/cell than by just using real-time PCR. Whenever quantitative or semi-quantitative information is required, such as for microarray analysis, linear amplification methods such as the antisense RNA amplification pioneered by James Eberwine (Van Gelder et al., 1990; Eberwine et al., 1992) can be used.

The field of single cell analysis continues to evolve. Whole genome microarray analysis on single cells is now a reality and techniques such as *in situ* cDNA synthesis and laser capture can be used to collect and analyze single cells from fixed, slide-mounted tissue. Other new techniques are being developed, such as following gene expression in single cells from genomic locus to RNA to protein in real time, using time lapse video imaging and reporter genes tagged with fluorescent proteins of multiple colors (Tsukamoto et al., 2000; Janicki et al., 2004). If such techniques are ever expanded to study gene expression from multiple loci, they would permit to integrate mRNA and protein information as well as fluctuations in gene expression over time in a single cell, likely shedding light onto complex genomic interactions that are at present not understood. As billionaire Howard Hughes would have said, single cell analysis is "the way of the future" (The Aviator, 2004).

Chapter Five: Materials and Methods

5.1 Animals

Mice and rats were maintained in standard conditions with food and water *ad libitum*. All experimental procedures were approved by the UCSF Committee on Animal Health and Care. All rat experiments were performed on adult male Sprague Dawley animals (~250 g) purchased from Charles River Laboratories (Wilmington, MA). For gene expression analysis and graft recipients, adult CD-1 mice were purchased from Charles River Laboratories. BDNF:LacZ and conditional $TrkB^{lox/lox}$ mutant mice were a kind gift of Louis Reichardt (Bennett et al., 1999) (Xu et al., 2000b). In these mice, exon 1 of the trkB gene was disrupted by the insertion of a construct containing the complete cDNA sequence of full-length TrkB flanked by loxP sites, followed by a tau-lacZ reporter gene which is activated only after Cre-mediated excision of trkB. Because this reporter gene is under the control of the endogenous trkB promoter, I crossed $TrkB^{lox/lox}$ mice to the conditional reporter mouse line Z/AP (purchased from Jackson Laboratories, Bar Harbor, ME), in which the reporter gene alkaline phosphatase (AP) is under a ubiquitous promoter and is activated by Cre-mediated recombination. Mice derived from this cross allowed me to follow TrkB-KO cells in a wild-type background after targeted conditional deletion of TrkB. Conditional $TrkB^{lox/lox}$ mice were also crossed to β-actin:cre mice (Lewandoski et al., 1997) to generate a constitutive TrkB reporter line (TrkB:Tau-LacZ), in which cDNA encoding the fusion protein Tau-LacZ is under the control of the endogenous TrkB gene promoter. These mice were used to study the expression of TrkB gene in the SVZ and RMS. TrkB:Tau-LacZ mice were also used as a constitutive TrkB mutant line. For grafting experiments, I crossed TrkB:Tau-LacZ mice to β-actin:GFP mice (Hadjantonakis et al., 1998), thus generating TrkB constitutive mutant mice whose cells can be traced by GFP expression. Genotyping for Z/AP and GFP transgenes was performed by detection of β-Galactosidase activity or fluorescence, respectively, in mouse tail samples. Genotyping for all other genes was performed by PCR (see Appendix A10 for details), using the following primer sequences: N2 (ATG TCG CCC TGG CTG AAG TG) and C8 (ACT GAC ATC CGT AAG CCA GT) for wild-type TrkB allele, N2

and C7 (GAT GAT TTC TAG CCT TTT CTG G) for floxed TrkB allele, Tau1 (CAG GCT CTG AAA CCT CTG ATG C) and Tau2 (GTC ATC GGG TCC AGT CCC ATC) for deleted TrkB allele.

5.2 Histology

For cryostat sectioning, animals were deeply anesthetized with Avertin (Tribromoethanol, mice) or Ketamine/Xylazine (rats) and transcardially perfused with a 0.9% saline solution. For immunohistochemical detection of BDNF, mice were perfused with Acetate-Buffered Saline (ABS; 5% acetic acid in 0.9% saline, pH 3.0) instead of saline (Zhou et al., 1994). Brains were then removed and immediately frozen in methyl butane at -40^{o}C and 10 μm-thick sections (12 μm for rat brains) were cut on a cryostat. Cryosectioning of early postnatal animals was performed on brains embedded in O.C.T. (Sakura, Torrance, CA): mice were transcardially perfused with 0.9% saline followed by 4% PFA in 0.1M phosphate buffer. Brains were then removed and post-fixed overnight at 4^{o}C in 4% PFA. After washing off the PFA with phosphate-buffered saline (PBS), brains were immersed in O.C.T. for 30 minutes at 4^{o}C and subsequently transferred to a plastic mold filled with O.C.T. and frozen in dry ice-chilled ethanol. Before use, all cryostat sections were thawed/dried at room temperature for 10 minutes and fixed 10 minutes in 4% paraformaldehyde (PFA), except sections for BDNF immunohistochemistry, which were fixed 10 minutes in 100% methanol pre-chilled at -20^{o}C. BDNF sections were then incubated with 3% H_2O_2 (diluted in PBS) 30 minutes at room temperature to inactivate endogenous peroxidase activity. For vibratome sectioning, animals were deeply anesthetized with Avertin (mice) or Ketamine/Xylazine (rats) and transcardially perfused with 0.9% saline followed by 4% PFA in 0.1M phosphate buffer. Brains were then removed and post-fixed overnight at 4^{o}C in 4% PFA. After washing off the PFA with phosphate-buffered saline (PBS), 50 μm-thick sections were cut on a vibratome.

5.3 Semi-quantitative RT-PCR

Total RNA was isolated from freshly-dissected mouse tissue using Trizol reagent (Gibco, Carlsbad, CA, Cat. #15596-026; see Appendix A7 for details), then DNAase-digested to eliminate genomic DNA contaminants. cDNA was generated using random

decamers and the Cells-to-Signal kit (Ambion, Foster City, CA, Cat. #AM1723). PCR primers were designed using Primer Express software (Applied Biosystems, Foster City, CA). To prevent non-specific amplifications, I designed primers to span at least 1 exon/intron boundary (except BDNF, NT4, TrkB-TR) and selected primer sequences with no significant homology to undesired sequences (as determined by BLAST software). Primer efficiency was further tested by serial dilution of control cDNA samples and melting curve analysis. PCR reactions were performed on Applied Biosystems 7900HT light cycler, using AmpliTaq Gold DNA polymerase (Applied Biosystems, Cat. #4311806) and SYBR Green dye (Molecular Probes, Eugene, OR), which fluoresces when bound to double-stranded DNA and excited by a light source.

Gene	Forward primer	Reverse primer
CNTFR	ATC ACC TTT GAC GAA TTC ACC A	ATG TAT TCC TTC CCT GCG TAG G
gp130	CTC ACA CGG AGT ACA CGC TGT C	CTC TTG GAA GGA TCA GGA ACA TTA G
GFRα1	GGA CAA TAC GTG TCT CAA AAA TGC	ATT ATC AGA AAG ACA GAG ATG TGT ACT GC
Ret	GGC TGT CCC GAG ATG TTT ATG	GTA CAT TTC CTC GCT GCA GTT GT
p75	GAC CGG CTG CGC CTG	GGT AGT AGC CAT AGG AGC ATC GG
TrkA	GGC CCG TTG CTC ATG GT	CCA GAC AGT TGC GTG TGG C
TrkB	GAA TAA CGG AGA CTA CAC CCT GAT G	ACC ACA GAT GCA ATC ACC ACC
TrkB-FL	TGG CGT CCC AAC ACT TTG T	CTT GCC GTA GGT GAA GAT CTC C
TrkB-TR	GGA CTG CTG TTG CCT ATC CC	CAG CTC GCT TTT CAT TAG AGA GG
TrkC	GAC TAT GTG GGC TCC GTG CT	GCT TCT GGA GTC CCG TGT AGA G
CNTF	TGG CTT TCG CAG AGC AAT C	GGA GGT TCT CTT GGA GTC GCT
GDNF	CGC CCG CTG AAG ACC AC	AAA CGC ACC CCC GAT TTT
NGF	GCC AAG GAC GCA GCT TTC TAT A	CGG GTC TGC CCT GTC ACT
NT3	CGG ATG CCA TGG TTA CTT CTG	TGC CTC TGC TTT GGG CAG
NT4	GGC TGC TCT ACC GTG CCT TAT	CCA GGG TCC TCT GAT GTT AAA ATG
BDNF	GGT CAC AGC GGC AGA TAA AAA G	TGA ATC GCC AGC CAA TTC TC

5.4 Bromodeoxyuridine administration

For label retention and grafting experiments, the DNA synthesis marker bromodeoxyuridine (BrdU) was administered to mice in drinking water (1 mg/ml) for 1 week or 3 days, respectively. For quantification of neurogenesis in TrkB heterozygous and WT mice, BrdU was injected once intraperitoneally at 50 mg/kg at postnatal day 21 (P21) and mice were killed and analyzed 15 days later. For BDNF infusion experiment in mice and rats, BrdU was injected intraperitoneally at 50 mg/kg every 4 days after surgery. BrdU was added to culture medium at a final dose of 10 μM 1 hour (SVZ astrocyte subconfluent cultures, Fig. 2.20A, D, G) or 12 hours (SVZ neurogenic cultures, Fig. 2.20B, E, H) before fixing cells. See Appendix A1 for more details.

5.5 *In situ* hybridization

In situ hybridization was performed as described previously (Fior and Henrique, 2005), with modifications. Briefly, cryostat sections were fixed 10 minutes in 4% PFA, acetylated and incubated overnight in highly stringent conditions (50% formamide, 3X SSC, 60^{o}C) with DIG-labeled RNA probes. Unbound probes were removed with 50% formamide/1X SSC and MABT washes. Tissue was blocked in 2% blocking reagent (Roche, Indianapolis, IN, #1096176) and 20% goat serum, then incubated overnight at 4^{o}C with anti-DIG/AP antibody (1:2000, Roche, #11093274910). Sections were then washed with MABT and incubated in AP staining buffer with NBT/BCIP substrate (Roche, #11681451001). Staining was performed at 37^{o}C for 2-5 hours. A probe specific for the full-length isoform of TrkB (TrkB-FL) was generated as follows: a 1000 base pair sequence unique to TrkB-FL was amplified by PCR from total mouse brain cDNA using the primers TTGGCATCACCAACAGTCAGC and GTCAGCGGCAGTCAAGAGGTT (see sequence #NM_001025074 for TrkB-FL). This fragment was then purified and cloned using a T/A cloning kit (Invitrogen, Carlsbad, CA). The cloned fragment was sequenced to confirm that the correct DNA sequence had been cloned. See Appendix A2 for more details.

5.6 Electron microscopy

Adult TrkB:Tau-LacZ reporter mice were transcardially perfused with 2.5% Glutaraldehyde and 2% Paraformaldehyde (PFA). The brains were post-fixed overnight in 2.5% Glutaraldehyde at 4^{o}C, then cut on a vibratome (100 μm sections). Sections were stained for β-Gal enzymatic activity (see Appendix A8 for details) for 24 hours at 37^{o}C. Sections were then incubated 1.5 hours in OsO_4, then 3.5 hours in uranyl acetate. After being dehydrated in ethanol, sections were embedded in araldite. Further processing and imaging was performed as previously described (Doetsch et al., 1997) (see Appendix A9 for details).

5.7 Western blot

SVZ, striatum or whole brain were dissected and triturated in RIPA buffer (1% Triton X100, 0.1% SDS, 5 mM EDTA, 1% deoxycholic acid in PBS, protease inhibitors added

before use) with a 27-gauge needle. Total protein amount was quantified by the Bradford method and run on a denaturing gel loading 10-20 μg protein/well. Protein was electrotransferred to a PVDF membrane, which was then blocked overnight (5% skimmed milk). Primary antibodies were incubated overnight at 4 ^{o}C: rabbit anti-TrkB (1:750, Upstate, Lake Placid, NY, #07-225), rabbit anti-TrkB-TR (1:200, Santa Cruz Biotechnology, Santa Cruz, CA, #sc-119), rabbit anti-TrkB (1:750, Chemicon, Temecula, CA, #AB5372) rabbit anti-β-Actin (1:1000, AbCam, Cambridge, MA, #ab8227). Secondary antibody was incubated in blocking solution 1 hour at room temperature: goat anti-rabbit-HRP (1:5000, AbCam, #ab6721). Membrane was developed using ECL Plus reagent (GE Healthcare, Piscataway, NJ, #RPN2132). See Appendix A3 for more details.

5.8 TUNEL labeling

TUNEL labeling was performed on cryostat sections, using the Cell Death Detection kit (Roche, Cat. #12156792910). Tissue sections were dried at room temperature for 10 minutes, then fixed in 4% PFA for 20 minutes. Tissue was then washed in PBS and pre-treated by microwaving 1 minute (High setting) in Citrate buffer, after which I followed the manufacturer's instructions for staining. See Appendix A4 for more details.

5.9 Immunohistochemistry

The following primary antibodies were used: mouse anti-β-Galactosidase (1:500, Promega, Madison, WI, #Z3781), mouse anti-GFAP (1:500, Chemicon, #MAB3402), rat anti-BrdU (1:100, AbCam, #ab6326), mouse anti-PSA-NCAM (1:500, AbCys, Paris, France, # AbC0019), rabbit anti-BDNF (1:100, Santa Cruz Biotechnology, #sc-546), rabbit anti-TrkB (1:200, Upstate, #07-225), rabbit anti-TrkB-TR (1:200, Santa Cruz Biotechnology, #sc-119), rabbit anti-TrkB (1:200, Chemicon, #AB9872), rabbit anti-TrkB (1:200, Chemicon, #AB5372), rabbit anti-pTrkB (1:200, or 0.9 μg/ml, a gift from Moses Chao, elution fraction 18664#6), mouse anti-βIII Tubulin (Tuj1) (1:500, Covance, Berkeley, CA, #MMS-435P), chicken anti-GFP (1:500, Aves Labs, Tigard, OR, #GFP-1020), rabbit anti-tyrosine hydroxylase (1:500, PelFreez, Rogers, AR, #P40101), mouse anti-Calbindin (1:1000, Swant, Bellinzona, Switzerland, #300), rabbit anti-phosphorylated histone H3 (1:200, Upstate, #06-570), mouse anti-HuC/D (1:10,

Molecular Probes, #MAB16A11), rabbit anti-p75 (1:2000, a gift from Louis Reichardt, raised against p75 extracellular domain) (Weskamp and Reichardt, 1991) and mouse anti-Mash1 (1:150, BD Pharmingen, San Jose, CA, #556604). Additional anti-p75 antibodies were used to confirm p75 expression pattern in mice and rats: rabbit anti-p75 (1:1000, Promega, #G3231, used on mouse and rat tissue, raised against p75 intracellular domain), mouse anti-p75 (1:100, Chemicon, #MAB365, used on rat tissue, raised against p75 extracellular domain), rabbit anti-p75 (1:500, a gift from Moses Chao, antibody 9651, used on rat tissue, raised against p75 extracellular domain) (Huber and Chao, 1995) and rabbit anti-p75 (1:500, a gift from Moses Chao, antibody 9992, used on rat tissue, raised against p75 intracellular domain). The following Alexa-conjugated secondary antibodies (Molecular Probes) were used for fluorescence detection: donkey anti-rabbit 488, donkey anti-rabbit 594, donkey anti-mouse 488, donkey anti-mouse 594, goat anti-chicken 488, goat anti-mouse IgG1 594, goat anti-mouse IgM 594 (all diluted 1:500) (see Appendix A13 for details on fluorescence immunohistochemistry). β-Galactosidase and BrdU stainings were amplified using a biotinylated goat anti-mouse IgG2a (1:500, Southern Biotech, Birmingham, AL) or a biotinylated donkey anti-rat (1:500, Jackson Immunoresearch, West Grove, PA) secondary antibody, respectively, followed by 1 hour incubation with Streptavidin-Cy2 (1:500, Jackson Immunoresearch) or Streptavidin-488 (1:500, Molecular Probes), respectively. For BrdU detection, 10 μm cryostat sections were pre-treated with 2N HCl 30 minutes at 37^{o}C, then washed with Boric acid buffer (0.1 M boric acid, 0.02 M sodium tetraborate (Borax), pH 8.4) and PBS. Whenever BrdU and another antigen were detected in the same sample, staining was done sequentially, first for the other antigen and post-fixing 10 minutes with 4% PFA before performing the HCl treatment. All samples were blocked 1 hour with 3% bovine serum albumin (BSA), 10% serum (goat or donkey) and 0.1% Triton X-100, except BDNF detection, which was done without Triton X-100 (see also Histology section for details on tissue collection and fixation specific to BDNF detection protocol). BDNF detection was performed with biotinylated donkey anti-rabbit secondary antibody (Jackson Immunoresearch) and Vector Labs' (Burlingame, CA) ABC kit and DAB substrate. Most primary antibodies were incubated overnight at 4^{o}C and all secondary antibodies 1 hour at room temperature. Anti-BDNF antibody was incubated 4 overnights at 4^{o}C. For anti-pTrkB

immunohistochemistry, vibratome sections were blocked 1 hour at room temperature with 8% normal goat serum and 0.1% Triton X100 in TBS, then washed once with TBS and incubated with pTrkB antibody overnight at room temperature, then 48 hours at 4^{o}C (1:200 diluted in 2% normal goat serum and 0.01% Triton X100 in TBS). For the direct detection of TrkB protein on dissociated SVZ cells using Upstate anti-TrkB antibody, SVZ was dissected and triturated in PBS. A 3:1 ratio of cells:Matrigel was then applied to a glass coverslip, allowed to solidify 1 hour in a humidified incubator, then fixed 10 minutes with 4% PFA. The cell sample was then used for immunocytochemical detection as described above.

5.10 Surgical procedures

For all surgical procedures (see also Appendix A12, A14 for details), mice were anesthetized with Avertin (adults) or on ice (newborns) and rats with Ketamine/Xylazine, and their heads were immobilized on a stereotaxic apparatus. For adult mice and rats, buprenorphine was injected to minimize post-surgery pain. AraC infusions were performed on CD-1 adult mice as previously described (Doetsch et al., 1999b). Ara-C (2%, Sigma) in vehicle (0.9% saline) or vehicle alone was infused onto the surface of the brain of adult CD-1 male mice (2–3 months) with a mini-osmotic pump (Alzet, Cupertino, CA, model 1007D; flow rate 0.5 μl/hour, 7 day pump). Cannulas were implanted onto the surface of the brain at anterior 0 mm, lateral 1.1 mm relative to Bregma. This treatment produced no lesion on the ventricular cavities or in the SVZ. After 6 days of infusion, mice were killed immediately and processed for analysis.

For BDNF infusions, osmotic pumps (0.5 μl/hour, 14 day pumps, Alzet) were filled with 1 mg/ml BDNF in vehicle solution (0.9% saline with 0.1% BSA) or vehicle alone. BDNF was a gift of Regeneron Pharmaceuticals (Tarrytown, NY). Pumps were then implanted onto the skull of CD-1 adult male mice (P90, ~40 g weight) at -0.2 mm anteroposterior and 0.95 mm lateral relative to Bregma; pump cannula was cut at 2.7 mm length so that it would penetrate the lateral ventricle.

Identical pumps were also implanted onto the skull of adult male Sprague Dawley rats (~250 g weight) at 0 mm anteroposterior and 1.6 mm lateral relative to Bregma; pump cannula was cut at 4.5 mm length so that it would penetrate the lateral ventricle. Accurate

pump placement was visually confirmed for all animals after cryostat sectioning of the brains.

TrkB conditional deletions were performed injecting a Cre-expressing adenovirus into neonatal (P0) $TrkB^{lox/lox}$/Z/AP mice as previously described (Merkle et al., 2004). Briefly, animals were anesthetized on ice for 1-2 minutes, then taped down on a head mold to stabilize the head in a horizontal position. A thin glass needle filled with Ad:Cre adenovirus (titer ~10^{11}) was used to pierce through the skin and skull at a 45^{o} angle at the upper/posterior corner of an imaginary square around the eye, penetrating 1.4 mm into the head. 30 nl of virus were then slowly injected and after 2 minutes the needle was removed and the animal was returned to its cage.

For grafting experiments, I dissected and triturated the SVZ of post-natal day 1 (P1) TrkB:Tau-LacZ/GFP and wild-type/GFP mice, then grafted the cell suspensions into CD-1 adult mice using a stereotaxic apparatus (bilateral injections into the SVZ at 2 different coordinates: anterior 0.5 mm, lateral 1.1 mm, depth 1.7 mm; anterior 1 mm, lateral 1 mm, depth 2.3 mm relative to Bregma and brain surface; 4 injections total) as previously described (Kohwi et al., 2005).

All brains were processed and cut on vibratome for analysis, except AraC-infused brains, which were flash-frozen and cut on cryostat (see section 5.2 for details).

5.11 Cell culture

All cultures were performed with tissue obtained from 1-3 day-old mice, except SVZ astrocyte cultures (Fig. 2.20A, D, G), which were derived from adult mice. Dissected tissue was digested in 0.25% trypsin/0.02% versene (adult tissue only) and triturated by repeatedly pipetting through a 1 ml Rainin pipette tip. All cultures were grown on laminin-coated plastic or poly-D-lysine/laminin-coated glass. SVZ and cortical astrocytes were cultured in Dulbecco modified Eagle medium (DMEM) supplemented with 10% fetal bovine serum (FBS), L-Glutamine and antibiotics/antimicotics. To allow neurogenesis to occur from SVZ astrocytes, cells were grown to confluence, then changed to a serum-free medium of Neurobasal-A/B27-A for 6 days. SVZ neuroblasts were purified by differential adhesion (Lim and Alvarez-Buylla, 1999): freshly-dissociated SVZ cells were plated on laminin-coated plastic flasks in DMEM/10% FBS

and incubated overnight at 37°C, allowing astrocytes to attach to the bottom, while neuroblasts are still unattached. By collecting the culture medium after the overnight incubation, I can obtain a cell suspension enriched for SVZ neuroblasts and depleted of astrocytes. Neuroblasts purified in this manner were then plated at 50000 cells/cm^2 on a cortical astrocyte monolayer in Neurobasal-A/B27-A medium and cultured for 5 days (Fig. 2.20C, F, I). All cultures were fixed by aspirating culture medium and directly adding 4% PFA for 10 minutes at room temperature. See "BrdU administration" section for details on BrdU labeling *in vitro*.

5.12 BDNF expression level regulation

SVZ and cortical astrocytes were obtained from 3 days old CD1 mice and cultured in 6-well plates in DMEM supplemented with 10% fetal bovine serum, L-Glutamine and antibiotics/antimicotics. At confluence, wells were washed twice with PBS, then cultured for 2 additional days in serum/antibiotics-free medium (DMEM/L-Glutamine only). This step was added to prevent possible confounding results due to the presence of serum and to prevent Dopamine degradation by Pennicillin-like compounds. I allowed 2 days for the cells to adapt to the medium change. SVZ and cortical astrocytes were then exposed to Dopamine (Dopa, 0.15 mM final concentration), phorbol 12-myristate 13-acetate (TPA, 4 mM stock prepared in DMSO, 100 nM final concentration), Epinephrine (Epi, 0.15 mM final concentration), Prolactin (PRL, 1 μg/ml final concentration) or no additives (control) for 4 hours or 24 hours in DMEM/L-Glutamine medium supplemented with 200 μM ascorbic acid (anti-oxidant to further protect Dopamine from degradation) and DMSO (0.1 μl/4 ml medium, except TPA wells, which already contain DMSO). Prior to adding the experimental media, astrocyte monolayers were depleted of contaminating neuroblasts by streaming PBS several times across the surface (Lim and Alvarez-Buylla, 1999). Total RNA was then collected from each well separately, adding 1 ml/well Trizol reagent (Gibco). RNA purification and cDNA production was performed as described in "Semi-quantitative RT-PCR" section, omitting the DNAase treatment (unnecessary due to the intron-spanning nature of the PCR primers used, see below). Relative levels of BDNF mRNA were compared between samples by semi-quantitative RT-PCR using a

TaqMan primer/probe pair specific for BDNF (Applied Biosystems, #Mm00432069_m1).

5.13 Dorsal root ganglia cultures

Whole dorsal root ganglia (DRG) were dissected from E12.5 wild-type embryos and cultured as explants on glass slides coated with poly D-lysine and laminin. Culture medium consisted of F14 medium with insulin (10 mg/ml), transferrin (5 μg/ml), bovine serum albumin (0.35% w/v), progesterone (60 ng/ml), putrescine (16 μg/ml), sodium selenite (38 ng/ml), L-thyroxine (400 ng/ml) and tri-iodo thyronine (314 ng/ml). Medium was supplemented with BDNF (0, 10, 50 or 100 ng/ml). Two days later, medium was replaced and cytosine arabinoside (10 μM) and aphydicolin (10 μg/ml) were added to block cell proliferation. After being cultured for a total of 3 days, cells were fixed 10 minutes in 4% PFA and processed for immunocytochemistry.

5.14 Quantifications

To measure proliferation rates in the SVZ of neonatal TrkB-KO and WT mice (Fig. 2.9G), I randomly selected 4 sections of anterior SVZ in each mouse to photograph the dorsal SVZ using a 20X objective. All $pH3^+$ cells within each picture were counted. A total of 412 cells (TrkB-WT) or 198 (TrkB-KO) cells were counted; n=6 WT and 4 KO mice.

To measure apoptosis in the SVZ and OB of neonatal TrkB-KO and WT mice (Fig. 2.9H), 5 sections of anterior SVZ or OB were selected at 30 μm intervals and all $TUNEL^+$ cells in both SVZs or both OBs of each section were counted under a fluorescence microscope. In 6 WT mice, a total of 108 (SVZ) and 173 (OB) cells were counted. In 4 KO mice, a total of 123 (SVZ) and 228 (OB) cells were counted; n=6 WT and 4 KO mice.

To compare overall neurogenic levels in TrkB heterozygous and WT mice, I counted $BrdU^+$ cells in the OB of mice injected with BrdU at P21 and killed 15 days later at P36. For each mouse, 50 μm vibratome sections were selected for counting, both anterior and posterior to the anterior-most region of the accessory OB (5 OB sections/mouse total). Pictures covering all layers of the OB (but only a small part of the section) were taken of

each section in all mice. I then counted all $BrdU^+$ cells in focus in each picture. Among 3 WT mice, I counted a total of 1190 cells. Among 4 heterozygous mice, I counted a total of 1486 cells. n=3 WT and 4 heterozygous mice.

To compare the survival of TrkB-KO and WT neurons in the OB (Fig. 2.12A-D), $GFP^+/BrdU^+$ grafted cells were counted. For each timepoint, 18 to 33 pictures/mouse were taken randomly from multiple OB sections (50 μm vibratome sections) with a 40X objective, choosing similar regions in all mice (based on DAPI staining). A total of 693 (among all WT mice, 15 days time point), 1099 (among all KOs, 15 days time point), 434 (among all WTs, 45 days time point), 966 (among all KOs, 45 days time point), 2555 (among all WTs, 180 days time point) or 2080 (among all KOs, 180 days time point) GFP^+ cells were counted; n=2 to 4 mice/time point (see Fig. 2.12 legend for details).

To compare the proportions of TH^+ and $CalB^+$ cells among grafted periglomerular cells in the OB (Fig. 2.12E-K), GFP^+ cells in the whole glomerular layer of 7-15 sections/mouse (50 μm vibratome sections at 300 μm intervals) were counted directly under a fluorescence microscope. GFP/TH or GFP/CalB double-labeled cells were identified by total overlap and identical contour of cellular labeling. A total of 667 (among all WTs, 45 days time point), 1071 (among all KOs, 45 days time point), 1306 (among all WTs, 180 days time point) or 828 (among all KOs, 180 days time point) [for TH analysis] and 1080 (among all WTs, 45 days time point), 696 (among all KOs, 45 days time point), 1532 (among all WTs, 180 days time point) or 786 (among all KOs, 180 days time point) [for CalB analysis] GFP^+ cells were counted; n=3 to 5 mice/time point (see Fig. 2.12 legend for details).

To determine the proliferation rate of SVZ astrocytes cultured for 7 days in the presence or absence of BDNF (Fig. 2.20A, D, G), $BrdU^+$ cells were counted from non-overlapping pictures taken with a 20X objective at fixed intervals across the middle of the culture wells. The number of pictures counted totaled 36/condition for one experiment (2 conditions: No BDNF and 100 ng/ml BDNF; 12 pictures/well, 3 replicates/experiment) and 24 for each of 2 additional experiments (12 pictures/well, 2 replicates/experiment). A total of 4038 or 2843 cells were counted (No BDNF and BDNF, respectively), n=3 experiments/group.

To determine the proliferation rate of neuroblasts generated in culture by a monolayer of SVZ astrocytes in the presence of varying amounts of BDNF (Fig. 2.20B, E, H), $Tuj1^+$ and $Tuj1^+/BrdU^+$ cells were counted from non-overlapping pictures taken with a 10X objective at fixed intervals across the middle of the culture wells. The number of pictures counted totaled 16/condition and 14/condition for two experiments (3 conditions: No BDNF, 10 and 100 ng/ml BDNF; 8 pictures/well and 2 replicates/condition in the first experiment and 7 pictures/well and 2 replicates/condition in the second experiment) and 8 pictures/condition for each of 2 additional experiments (4 pictures/well, 2 replicate wells/experiment). A total of 5582, 6269 or 7446 cells were counted (No BDNF, 10 and 100 ng/ml BDNF respectively).

To determine the survival/proliferation of SVZ neuroblasts in the presence or absence of BDNF and with or without TrkB (Fig. 2.20C, F, I), $GFP^+/Tuj1^+$ cells were counted from pictures of cells cultured in each of these conditions. Non-overlapping pictures were taken with a 10X objective at fixed intervals across the middle of the culture wells, but only the top half of each picture was counted due to the high numbers of cells (numbers presented are an extrapolation of cells/picture from those countings). The number of pictures counted totaled 18/condition (6 pictures/well, 3 replicates/experiment). A total of 2946 cells (TrkB-WT, No BDNF), 2179 cells (TrkB-KO, No BDNF), 2648 cells (TrkB-WT, 100 ng/ml BDNF) or 2614 cells (TrkB-KO, 100 ng/ml BDNF) were counted, n=2 experiments/group.

To determine the proliferation rates in the SVZ of BDNF and vehicle-infused mice (Fig. 2.16C, E, G), $pH3^+$ cells were counted in 28 10 μm cryostat sections taken at 50 μm intervals (spanning a total of 1350 μm) in each mouse, ipsilateral to the pump side. Counted sections were taken from the anterior-most region of the lateral ventricle (1.2 mm rostral to Bregma) to the site of entry of the pump cannula into the ventricle (0.2 mm caudal to Bregma). The number of $pH3^+$ cells in the entire SVZ of each section was counted under a fluorescence microscope. A total of 2414 or 1872 $pH3^+$ cells were counted (among all vehicle or BDNF-infused mice, respectively), n=5 mice/group.

To determine the apoptosis rates in the SVZ of BDNF and vehicle-infused rats (Fig. 2.22D), $TUNEL^+$ cells were counted in 24 to 36 12 μm cryostat sections in each rat, ipsilateral to pump side, at 60 μm intervals (spanning a total of 1380 to 2100 μm).

Counted sections were taken from the anterior-most region of the lateral ventricle (1.4 to 2.1 mm rostral to Bregma) to the site of entry of the pump cannula into the ventricle (Bregma level) and the entire SVZ in each picture was counted under a fluorescence microscope, excluding sections where the SVZ was significantly damaged by the cannula. A total of 424 or 319 $TUNEL^+$ cells were counted (among all vehicle or BDNF-infused mice, respectively), n=6 rats for vehicle and 5 rats for BDNF group.

To determine the proliferation rates in the SVZ of BDNF and vehicle-infused rats (Fig. 2.22E), $pH3^+$ cells were counted in 24 12 μm cryostat sections in each rat, ipsilateral to pump side, at 60 μm intervals (spanning a total of 1380 μm). Counted sections were taken from the anterior-most region of the lateral ventricle (1.4 mm rostral to Bregma) to the site of entry of the pump cannula into the ventricle (Bregma level) and the entire SVZ in each picture was counted under a fluorescence microscope, excluding sections where the SVZ was significantly damaged by the cannula. A total of 3276 or 2498 $pH3^+$ cells were counted (among all vehicle or BDNF-infused mice, respectively), n=6 rats/group.

To determine the number of $Mash1^+$ cells in the SVZ of BDNF and vehicle-infused rats (Fig. 2.22F), I used a 20X objective to take 4 pictures of the dorsal SVZ of each rat analyzed, ipsilateral to the pump side. Pictures were taken at ~360 μm intervals, spanning the same region of the rostro-caudal axis analyzed for pH3 quantifications and all $Mash1^+$ cells therein were counted. A total of 2397 or 1803 $Mash1^+$ cells were counted (among all vehicle or BDNF-infused mice, respectively), n=6 rats/group.

To determine the number of new neurons added to the OB during the course of BDNF or vehicle infusions in mice (Fig. 2.16D, F, H) and rats (Fig. 2.22C), $BrdU^+$ cells were counted from pictures of OB sections. Three OB sections at 500 μm (mice) or 1200 μm (rats) intervals from each other were selected from the OB ipsilateral to the pump of each animal. Sections were considered of equivalent regions between animals using the location of the accessory OB (AOB) as a landmark, making sure the 3rd section selected for each animal was immediately before (mice) or at (rats) the appearance of the AOB. For mice, a total of 6 non-overlapping pictures were taken with a 10X objective for each OB section selected, covering 90-100% of the section (depending on section size). For rats, a total of 8 non-overlapping pictures were taken with a 10X objective for each OB

section selected, covering 80-90% of the section. All the $BrdU^+$ cells in these pictures were counted. A total of 5278 or 5212 $BrdU^+$ cells (vehicle or BDNF-infused mice, respectively) were counted, n=5 mice/group. A total of 12773 or 10491 $BrdU^+$ cells (vehicle or BDNF-infused rats, respectively) were counted, n=5 rats for vehicle group and 6 rats for BDNF group. Co-labeling and counting of BrdU and the lineage markers HuC/D, Iba1 and Olig2 was performed separately on each of the 3 OB sections/animal used for the total BrdU quantifications (n=5 mice/group or n=2 vehicle rats and 3 BDNF rats; in each case, the first section was used for BrdU/HuC/D labeling, the second for BrdU/Iba1 and the third for BrdU/Olig2).

5.15 Multiplex nested RT-PCR

Single cells from several sources (see section 3.2 for details) were collected by FACS sorting directly into 9 µl of DNAase I solution. Samples were immediatley frozen. After heat-inactivating the DNAase I, reagents to perform an RT-PCR reaction were added to each sample tube (OneStep Superscript II / Platinum Taq mix, Invitrogen, # 10928034), using a cocktail of PCR primers for all desired genes. A second PCR reaction was then performed using primers of individual genes for each reaction and using amplified cDNA from the first PCR reaction as template. See Appendix A5 for more details.

Gene	Forward primer (1^{st} PCR/2^{nd} PCR)	Reverse primer (1^{st} PCR/2^{nd} PCR)
GAPDH	CCC ACT AAC ATC AAA TGG GG	ATG TAG GCC ATG AGG TCC AC
	ATG TTT GTG ATG GGT GTG AAC CAC	CTG GTC CTC AGT GTA GCC CAA GAT
GFAP	ATG CCA CGT TTC TCC TTG TC	GCC TCG TAT TGA GTG CGA AT
	GCC ACG TTT CTC CTT GTC TCG A	GCT TCA TGT GCC TCC TGT CTA T
NCAM	ACC TCA AGG TCT TTG CAA AG	CTT CTT TGG CAT CAT ACC AC
	ATG GAA CTA GAG GAG CAA GTC	CTC TGG CTC ATC AAA CTG C
Dlx2	ACG ATT TTC TAA CCT CGA GTG	GTT GGG AGA GCT GGA ATT C
	TGA GAC ACC GTG TTC TTC AG	TAG GTG ATA GGG TGG AGT AGG
Pax6	CAA TAA ACA GAG TTC TTC GCA	GAA CTG ACA CTC CAG GTA AA
	GCA GAC GGC ATG TAT GAT AA	CAA AGC ACT GTA CGT GTT GG
Sox2	GGT GAT GCC GAC TAG AAA AC	GGG TAG GAT TGA ACA AAA GC
	GAG TTC GCA AAA GTC TTT ACC	CTT CCT TGT TTG TAA CGG TC
Er81	GGT TGA TAG AAG TCC AGA TCC	CTT CTG ATC ATA GGC ACT GAC
	AAA CTG TAC CGA GAA ACC AAC	GAC ATT GTA CAG GCA CTT TTC
BDNF	AAA GAA GTA AAC GTC CAC GG	GCT ATC CAT AGT AAG GGC CC
	GTA AAC GTC CAC GGA CAAG	TAG TAA GGG CCC GAA CAT AC
TrkB-FL	AGT CGA CTA CGA GAC AAA CC	CGT GCT TCA TGT ACT CAA AG
	GAC AAA CCC AAA TTA CCC TG	CCA CAC AGA CAC CGT AGA AC
TrkB-TR	AGT CGA CTA CGA GAC AAA CC	TCC AAT GAG ATT TCA CTT CG
	GAC AAA CCC AAA TTA CCC TG	GGA GAT TAC CCA TTT CCA CC
p75	CTG CCT GGA CAG TGT TAC G	GTC ACC ATT GAG CAG CTT C
	ACA GTG TTA CGT TCT CTG ACG	CAT TGA GCA GCT TCT CGA C

Notch1	GGA AAC AAG TCA GAT GAT GTG	TCA GTT GGA TTT GGA TGA TG
	GTG TGG ACT TGA AGA AGT GTC	GCA GTG TTT TCT CTA GGA GG
LeX	TAG TAA GGG CCC GAA CAT AC	TCA GAC GGT TTG AGG AAT C
(Fut4)	CCT TTG AGA ACT CAC GGC ACG	GGT TTG AGG AAT CCA ACC AC

5.16 Real-time RT-PCR

One to one thousand cells were collected by FACS sorting from several sources (see section 3.2 for details) directly into 4 μl of cell lysis buffer (Cells-to-Signal kit, Ambion, #AM1723) in PCR tubes at room temperature. Samples were then gently agitated for 2 minutes at room temperature to lyse the cells. Immediately after cell lysis, cDNA was generated using random decamers and the Cells-to-Signal kit. cDNA samples were then amplified by 40-50 PCR cycles, using Applied Biosystems TaqMan primer/probe sets (see list below) and AmpliTaq Gold DNA polymerase (Applied Biosystems, Cat. #4311806) in an Applied Biosystems 7900HT light cycler. No DNAase treatment is necessary for these experiments, since TaqMan primer/probes are designed to span introns.

Gene	Assays on Demand	Gene	Assays on Demand
Gus	Mm00446953_m1	BDNF	Mm00432069_m1
GFAP	Mm00546086_m1	Notch1	Mm00435245_m1
Pax6	Mm00443072_m1	Sox2	Mm00488369_s1
Dlx2	Mm00438427_m1	p75	Mm00446294_m1
Dcx	Mm00438401_m1	Mash1	Mm01228155_q1

5.17 Antisense RNA amplification

Briefly, mRNA was first converted to single-stranded cDNA by RT reaction using a modified oligo-d(T) primer that contains the T7 promoter sequence. and a SMART primer (Clontech). All cDNAs generated in this manner have the same known sequences at each end. In a second step, a 20-cycle PCR reaction was run using primers against the 3' and 5' known sequences, thus obtaining multiple copies of double stranded cDNA of each initial template. Templates were then further amplified in an *in vitro* transcription reaction, yielding multiple RNA copies of each template. A final RT reaction converts these RNAs back into cDNA, which can be used for real-time PCR amplification and detection. See section 3.2 and Appendix A6 for details.

Chapter Six: References

Acosta CG, Fabrega AR, Masco DH, Lopez HS (2001) A sensory neuron subpopulation with unique sequential survival dependence on nerve growth factor and basic fibroblast growth factor during development. J Neurosci 21:8873-8885.

Aguado F, Carmona MA, Pozas E, Aguilo A, Martinez-Guijarro FJ, Alcantara S, Borrell V, Yuste R, Ibanez CF, Soriano E (2003) BDNF regulates spontaneous correlated activity at early developmental stages by increasing synaptogenesis and expression of the K+/Cl- co-transporter KCC2. Development 130:1267-1280.

Ahmed S, Reynolds BA, Weiss S (1995) BDNF enhances the differentiation but not the survival of CNS stem cell-derived neuronal precursors. JNeurosci 15:5765-5778.

Ahn S, Joyner AL (2005) In vivo analysis of quiescent adult neural stem cells responding to Sonic hedgehog. Nature 437:894-897.

Alcantara S, Frisen J, del Rio JA, Soriano E, Barbacid M, Silos-Santiago I (1997) TrkB signaling is required for postnatal survival of CNS neurons and protects hippocampal and motor neurons from axotomy-induced cell death. J Neurosci 17:3623-3633.

Alderson RF, Alterman AL, Barde Y-A, Lindsay RM (1990) Brain-derived neurotrophic factor increases survival and differentiated functions of rat septal cholinergic neurons in culture. Neuron 5:297-306.

Alderson RF, Curtis R, Alterman AL, Lindsay RM, DiStefano PS (2000) Truncated TrkB mediates the endocytosis and release of BDNF and neurotrophin-4/5 by rat astrocytes and schwann cells in vitro. Brain Res 871:210-222.

Allen E (1912) The cessation of mitosis in the central nervous system of the albino rat. JCompNeurol 22:547-568.

Alonso M, Viollet C, Gabellec MM, Meas-Yedid V, Olivo-Marin JC, Lledo PM (2006) Olfactory discrimination learning increases the survival of adult-born neurons in the olfactory bulb. J Neurosci 26:10508-10513.

Altar CA, DiStefano PS (1998) Neurotrophin trafficking by anterograde transport. Trends Neurosci 21:433-437.

Althaus HH, Hempel R, Kloppner S, Engel J, Schmidt-Schultz T, Kruska L, Heumann R (1997) Nerve growth factor signal transduction in mature pig oligodendrocytes. J Neurosci Res 50:729-742.

Altman J (1969a) Autoradiographic and Histological Studies of Postnatal Neurogenesis. II. A Longitudinal Investigation of the Kinetics, Migration and Transformation of Cells Incorporating Tritiated Thymidine in Infant Rats, With Special Reference to Postnatal Neurogenesis in Some Brain Regions. JCompNeurol 128:431-474.

Altman J (1969b) Autoradiographic and Histological Studies of Postnatal Neurogenesis. IV. Cell Proliferation and Migration in The Anterior Forebrain, With Special Reference to Persisting Neurogenesis in The Olfactory Bulb. JCompNeurol 137:433-458.

Altman J, Das GD (1965) Autoradiographic and histological evidence of postnatal hippocampal neurogenesis in rats. JCompNeurol 124:319-336.

Alvarez-Borda B, Haripal B, Nottebohm F (2004) Timing of brain-derived neurotrophic factor exposure affects life expectancy of new neurons. Proc Natl Acad Sci U S A 101:3957-3961.

Alvarez-Buylla A, Nottebohm F (1988) Migration of young neurons in adult avian brain. Nature 335:353-354.

Alvarez-Buylla A, Garcia-Verdugo JM (2002) Neurogenesis in adult subventricular zone. J Neurosci 22:629-634.

Alvarez-Buylla A, Theelen M, Nottebohm F (1990) Proliferation "hot spots" in adult avian ventricular zone reveal radial cell division. Neuron 5:101-109.

Anderson KD, Alderson RF, Altar CA, DiStefano PS, Corcoran TL, Lindsay RM, Wiegand SJ (1995) Differential distribution of exogenous BDNF, NGF, and NT-3 in the brain corresponds to the relative abundance and distribution of high-affinity and low-affinity neurotrophin receptors. JCompNeurol 357:296-317.

Anthony TE, Klein C, Fishell G, Heintz N (2004) Radial glia serve as neuronal progenitors in all regions of the central nervous system. Neuron 41:881-890.

Artavanis-Tsakonas S, Rand MD, Lake RJ (1999) Notch signaling: cell fate control and signal integration in development. Science 284:770-776.

Astic L, Pellier-Monnin V, Saucier D, Charrier C, Mehlen P (2002) Expression of netrin-1 and netrin-1 receptor, DCC, in the rat olfactory nerve pathway during development and axonal regeneration. Neuroscience 109:643-656.

Baker H, Kawano T, Margolis FL, Joh TH (1983) Transneuronal regulation of tyrosine hydroxylase expression in olfactory bulb of mouse and rat. J Neurosci 3:69-78.

Bandtlow C, Dechant G (2004) From cell death to neuronal regeneration, effects of the p75 neurotrophin receptor depend on interactions with partner subunits. Sci STKE 2004:pe24.

Barde Y-A, Edgar D, Thoenen H (1982) Purification of a new neurotrophic factor from mammalian brain. The EMBO Journal 1, No. 5:549-553.

Barker PA (2004) p75NTR is positively promiscuous: novel partners and new insights. Neuron 42:529-533.

Barkley MS, Bradford GE, Geschwind, II (1978) The pattern of plasma prolactin concentration during the first half of mouse gestation. Biol Reprod 19:291-296.

Bass NH, Lundborg P (1973) Postnatal development of bulk flow in the cerebrospinal fluid system of the albino rat: clearance of carboxyl-(14 C)inulin after intrathecal infusion. Brain Res 52:323-332.

Bath KG, Mandairon N, Jing D, Rajagopal R, Kapoor R, Chen ZY, Khan T, Proenca CC, Kraemer R, Cleland TA, Hempstead BL, Chao MV, Lee FS (2008) Variant brain-derived neurotrophic factor (Val66Met) alters adult olfactory bulb neurogenesis and spontaneous olfactory discrimination. J Neurosci 28:2383-2393.

Baudet C, Mikaels A, Westphal H, Johansen J, Johansen TE, Ernfors P (2000) Positive and negative interactions of GDNF, NTN and ART in developing sensory neuron subpopulations, and their collaboration with neurotrophins. Development 127:4335-4344.

Baxter GT, Radeke MJ, Kuo RC, Makrides V, Hinkle B, Hoang R, Medina-Selby A, Coit D, Valenzuela P, Feinstein SC (1997) Signal transduction mediated by the truncated trkB receptor isoforms, trkB.T1 and trkB.T2. J Neurosci 17:2683-2690.

Beech RD, Cleary MA, Treloar HB, Eisch AJ, Harrist AV, Zhong W, Greer CA, Duman RS, Picciotto MR (2004) Nestin promoter/enhancer directs transgene expression to precursors of adult generated periglomerular neurons. J Comp Neurol 475:128-141.

Belluzzi O, Benedusi M, Ackman J, LoTurco JJ (2003) Electrophysiological differentiation of new neurons in the olfactory bulb. J Neurosci 23:10411-10418.

Benedetti M, Levi A, Chao MV (1993) Differential expression of nerve growth factor receptors leads to altered binding affinity and neurotrophin responsiveness. Proc Natl Acad Sci U S A 90:7859-7863.

Bennett JL, Zeiler SR, Jones KR (1999) Patterned expression of BDNF and NT-3 in the retina and anterior segment of the developing mammalian eye. Invest Ophthalmol Vis Sci 40:2996-3005.

Benraiss A, Chmielnicki E, Lerner K, Roh D, Goldman SA (2001) Adenoviral brain-derived neurotrophic factor induces both neostriatal and olfactory neuronal recruitment from endogenous progenitor cells in the adult forebrain. J Neurosci 21:6718-6731.

Bentley CA, Lee KF (2000) p75 is important for axon growth and schwann cell migration during development. J Neurosci 20:7706-7715.

Berghuis P, Agerman K, Dobszay MB, Minichiello L, Harkany T, Ernfors P (2006) Brain-derived neurotrophic factor selectively regulates dendritogenesis of parvalbumin-containing interneurons in the main olfactory bulb through the PLCgamma pathway. J Neurobiol 66:1437-1451.

Bibel M, Hoppe E, Barde YA (1999) Biochemical and functional interactions between the neurotrophin receptors trk and p75NTR. Embo J 18:616-622.

Biffo S, Offenhauser N, Carter BD, Barde YA (1995) Selective binding and internalisation by truncated receptors restrict the availability of BDNF during development. Development 121:2461-2470.

Blum R, Konnerth A (2005) Neurotrophin-mediated rapid signaling in the central nervous system: mechanisms and functions. Physiology (Bethesda) 20:70-78.

Boeshore KL, Luckey CN, Zigmond RE, Large TH (1999) TrkB isoforms with distinct neurotrophin specificities are expressed in predominantly nonoverlapping populations of avian dorsal root ganglion neurons. J Neurosci 19:4739-4747.

Brockschnieder D, Pechmann Y, Sonnenberg-Riethmacher E, Riethmacher D (2006) An improved mouse line for Cre-induced cell ablation due to diphtheria toxin A, expressed from the Rosa26 locus. Genesis 44:322-327.

Buckland ME, Cunningham AM (1998) Alterations in the neurotrophic factors BDNF, GDNF and CNTF in the regenerating olfactory system. Ann N Y Acad Sci 855:260-265.

Bulfone A, Wang F, Hevner R, Anderson S, Cutforth T, Chen S, Meneses J, Pedersen R, Axel R, Rubenstein JL (1998) An olfactory sensory map develops in the absence of normal projection neurons or GABAergic interneurons. Neuron 21:1273-1282.

Burazin TC, Gundlach AL (1999) Localization of GDNF/neurturin receptor (c-ret, GFRalpha-1 and alpha-2) mRNAs in postnatal rat brain: differential regional and temporal expression in hippocampus, cortex and cerebellum. Brain Res Mol Brain Res 73:151-171.

Buszczak M, Spradling AC (2006) Searching chromatin for stem cell identity. Cell 125:233-236.

Calzá L, Giardino L, Pozza M, Bettelli C, Micera A, Aloe L (1998) Proliferation and phenotype regulation in the subventricular zone during experimental allergic encephalomyelitis: *In vivo* evidence of a role for nerve growth factor. ProcNatlAcadSciUSA 95:3209-3214.

Cameron HA, Wooley CS, McEwen BS, Gould E (1993) Differentiation of newly born neuron and glia in the dentate gyrus of the adult rat. Neuroscience 56:337-344.

Cao L, Dhilla A, Mukai J, Blazeski R, Lodovichi C, Mason CA, Gogos JA (2007) Genetic modulation of BDNF signaling affects the outcome of axonal competition in vivo. Curr Biol 17:911-921.

Capela A, Temple S (2002) LeX/ssea-1 is expressed by adult mouse CNS stem cells, identifying them as nonependymal. Neuron 35:865-875.

Carleton A, Petreanu LT, Lansford R, Alvarez-Buylla A, Lledo PM (2003) Becoming a new neuron in the adult olfactory bulb. Nat Neurosci 6:507-518.

Carrasco GA, Van de Kar LD (2003) Neuroendocrine pharmacology of stress. Eur J Pharmacol 463:235-272.

Castren E, Voikar V, Rantamaki T (2007) Role of neurotrophic factors in depression. Curr Opin Pharmacol 7:18-21.

Cecchi GA, Petreanu LT, Alvarez-Buylla A, Magnasco MO (2001) Unsupervised Learning and Adaptation in a Model of Adult Neurogenesis. J Comput Neurosci 11:175-182.

Chambers CB, Peng Y, Nguyen H, Gaiano N, Fishell G, Nye JS (2001) Spatiotemporal selectivity of response to Notch1 signals in mammalian forebrain precursors. Development 128:689-702.

Chao MV (2003) Neurotrophins and their receptors: a convergence point for many signalling pathways. Nat Rev Neurosci 4:299-309.

Chao MV, Bothwell MA, Ross AH, Koprowski H, Lanahan AA, Buck CR, Sehgal A (1986) Gene transfer and molecular cloning of the human NGF receptor. Science 232:518-521.

Chen KS, Nishimura MC, Armanini MP, Crowley C, Spencer SD, Phillips HS (1997) Disruption of a single allele of the nerve growth factor gene results in atrophy of basal forebrain cholinergic neurons and memory deficits. J Neurosci 17:7288-7296.

Chen WR, Xiong W, Shepherd GM (2000) Analysis of relations between NMDA receptors and GABA release at olfactory bulb reciprocal synapses. Neuron 25:625-633.

Chen ZY, Jing D, Bath KG, Ieraci A, Khan T, Siao CJ, Herrera DG, Toth M, Yang C, McEwen BS, Hempstead BL, Lee FS (2006) Genetic variant BDNF (Val66Met) polymorphism alters anxiety-related behavior. Science 314:140-143.

Cheng A, Wang S, Cai J, Rao MS, Mattson MP (2003) Nitric oxide acts in a positive feedback loop with BDNF to regulate neural progenitor cell proliferation and differentiation in the mammalian brain. Dev Biol 258:319-333.

Cheng A, Coksaygan T, Tang H, Khatri R, Balice-Gordon RJ, Rao MS, Mattson MP (2007) Truncated tyrosine kinase B brain-derived neurotrophic factor receptor

directs cortical neural stem cells to a glial cell fate by a novel signaling mechanism. J Neurochem 100:1515-1530.
Chiaramello S, Dalmasso G, Bezin L, Marcel D, Jourdan F, Peretto P, Fasolo A, De Marchis S (2007) BDNF/ TrkB interaction regulates migration of SVZ precursor cells via PI3-K and MAP-K signalling pathways. Eur J Neurosci 26:1780-1790.
Chiasson BJ, Tropepe V, Morshead CM, Van der Kooy D (1999) Adult Mammalian Forebrain Ependymal and Subependymal Cells Demonstrate Proliferative Potential, but only Subependymal Cells Have Neural Stem Cell Characteristics. JNeurosci 19:4462-4471.
Chittka A, Chao MV (1999) Identification of a zinc finger protein whose subcellular distribution is regulated by serum and nerve growth factor. Proc Natl Acad Sci U S A 96:10705-10710.
Chittka A, Arevalo JC, Rodriguez-Guzman M, Perez P, Chao MV, Sendtner M (2004) The p75NTR-interacting protein SC1 inhibits cell cycle progression by transcriptional repression of cyclin E. J Cell Biol 164:985-996.
Chmielnicki E, Benraiss A, Economides AN, Goldman SA (2004) Adenovirally expressed noggin and brain-derived neurotrophic factor cooperate to induce new medium spiny neurons from resident progenitor cells in the adult striatal ventricular zone. J Neurosci 24:2133-2142.
Christie BR, Cameron HA (2006) Neurogenesis in the adult hippocampus. Hippocampus 16:199-207.
Clary DO, Reichardt LF (1994) An alternatively spliced form of the nerve growth factor receptor TrkA confers an enhanced response to neurotrophin 3. Proc Natl Acad Sci U S A 91:11133-11137.
Cohen RI, Marmur R, Norton WT, Mehler MF, Kessler JA (1996) Nerve growth factor and neurotrophin-3 differentially regulate the proliferation and survival of developing rat brain oligodendrocytes. J Neurosci 16:6433-6442.
Cohen-Cory S (2002) The developing synapse: construction and modulation of synaptic structures and circuits. Science 298:770-776.
Committee TB (1970) Embryonic Vertebrate Central Nervous System: Revised Terminology. AnatRec 166:257-262.
Conner JM, Lauterborn JC, Yan Q, Gall CM, Varon S (1997) Distribution of brain-derived neurotrophic factor (BDNF) protein and mRNA in the normal adult rat CNS: evidence for anterograde axonal transport. J Neurosci 17:2295-2313.
Connor B, Dragunow M (1998) The role of neuronal growth factors in neurodegenerative disorders of the human brain. Brain Res Brain Res Rev 27:1-39.
Conover JC, Doetsch F, Garcia-Verdugo JM, Gale NW, Yancopoulos GD, Alvarez-Buylla A (2000) Disruption of Eph/ephrin signaling affects migration and proliferation in the adult subventricular zone. Nat Neurosci 3:1091-1097.
Conover JC, Erickson JT, Katz DM, Bianchi LM, Poueymirou WT, McClain J, Pan L, Helgren M, Ip NY, Boland P, Friedman B, Wiegand S, Vejsada R, Kato AC, DeChiara TM, Yancopoulos GD (1995) Neuronal deficits, not involving motor neurons, in mice lacking BDNF and/or NT4. Nature 375:235-238.
Coppola V, Kucera J, Palko ME, Martinez-De Velasco J, Lyons WE, Fritzsch B, Tessarollo L (2001) Dissection of NT3 functions in vivo by gene replacement strategy. Development 128:4315-4327.

Corbit KC, Aanstad P, Singla V, Norman AR, Stainier DY, Reiter JF (2005) Vertebrate Smoothened functions at the primary cilium. Nature 437:1018-1021.

Cordon-Cardo C, Tapley P, Jing SQ, Nanduri V, O'Rourke E, Lamballe F, Kovary K, Klein R, Jones KR, Reichardt LF, et al. (1991) The trk tyrosine protein kinase mediates the mitogenic properties of nerve growth factor and neurotrophin-3. Cell 66:173-183.

Cosgaya JM, Chan JR, Shooter EM (2002) The neurotrophin receptor p75NTR as a positive modulator of myelination. Science 298:1245-1248.

Craig CG, Tropepe V, Morshead CM, Reynolds BA, Weiss S, Van der Kooy D (1996) *In vivo* growth factor expansion of endogenous subependymal neural precursor cell populations in the adult mouse brain. JNeurosci 16:2649-2658.

Crowley C, Spencer SD, Nishimura MC, Chen KS, Pitts-Meek S, Armanini MP, Ling LH, McMahon SB, Shelton DL, Levinson AD, Phillips HS (1994) Mice lacking nerve growth factor display perinatal loss of sensory and sympathetic neurons yet develop basal forebrain cholinergic neurons. Cell 76:1001-1011.

Davies AM, Thoenen H, Barde YA (1986) The response of chick sensory neurons to brain-derived neurotrophic factor. J Neurosci 6:1897-1904.

Dayer AG, Cleaver KM, Abouantoun T, Cameron HA (2005) New GABAergic interneurons in the adult neocortex and striatum are generated from different precursors. J Cell Biol 168:415-427.

De Marchis S, Bovetti S, Carletti B, Hsieh YC, Garzotto D, Peretto P, Fasolo A, Puche AC, Rossi F (2007) Generation of distinct types of periglomerular olfactory bulb interneurons during development and in adult mice: implication for intrinsic properties of the subventricular zone progenitor population. J Neurosci 27:657-664.

Dechant G, Barde YA (1997) Signalling through the neurotrophin receptor p75NTR. Curr Opin Neurobiol 7:413-418.

Dechant G, Barde YA (2002) The neurotrophin receptor p75(NTR): novel functions and implications for diseases of the nervous system. Nat Neurosci 5:1131-1136.

Desai AR, McConnell SK (2000) Progressive restriction in fate potential by neural progenitors during cerebral cortical development. Development 127:2863-2872.

Doetsch F (2003) The glial identity of neural stem cells. Nat Neurosci 6:1127-1134.

Doetsch F, Alvarez-Buylla A (1996) Network of tangential pathways for neuronal migration in adult mammalian brain. ProcNatlAcadSciUSA 93:14895-14900.

Doetsch F, Garcia-Verdugo JM, Alvarez-Buylla A (1997) Cellular composition and three-dimensional organization of the subventricular germinal zone in the adult mammalian brain. JNeurosci 17:5046-5061.

Doetsch F, Garcia-Verdugo JM, Alvarez-Buylla A (1999a) Regeneration of a germinal layer in the adult mammalian brain. ProcNatlAcadSciUSA 96:11619-11624.

Doetsch F, Caille I, Lim DA, Garcia-Verdugo JM, Alvarez-Buylla A (1999b) Subventricular zone astrocytes are neural stem cells in the adult mammalian brain. Cell 97:703-716.

Doetsch F, Petreanu L, Caille I, Garcia-Verdugo JM, Alvarez-Buylla A (2002) EGF converts transit-amplifying neurogenic precursors in the adult brain into multipotent stem cells. Neuron 36:1021-1034.

Dorsey SG, Renn CL, Carim-Todd L, Barrick CA, Bambrick L, Krueger BK, Ward CW, Tessarollo L (2006) In vivo restoration of physiological levels of truncated TrkB.T1 receptor rescues neuronal cell death in a trisomic mouse model. Neuron 51:21-28.

Doxakis E, Wyatt S, Davies AM (2000) Depolarisation causes reciprocal changes in GFR(alpha)-1 and GFR(alpha)-2 receptor expression and shifts responsiveness to GDNF and neurturin in developing neurons. Development 127:1477-1487.

Dranovsky A, Hen R (2006) Hippocampal neurogenesis: regulation by stress and antidepressants. Biol Psychiatry 59:1136-1143.

Drew MR, Hen R (2007) Adult hippocampal neurogenesis as target for the treatment of depression. CNS Neurol Disord Drug Targets 6:205-218.

Du Y, Fischer TZ, Lee LN, Lercher LD, Dreyfus CF (2003) Regionally specific effects of BDNF on oligodendrocytes. Dev Neurosci 25:116-126.

Eberwine J, Yeh H, Miyashiro K, Cao Y, Nair S, Finnell R, Zettel M, Coleman P (1992) Analysis of gene expression in single live neurons. ProcNatlAcadSciUSA 89:3010-3014.

Egan MF, Kojima M, Callicott JH, Goldberg TE, Kolachana BS, Bertolino A, Zaitsev E, Gold B, Goldman D, Dean M, Lu B, Weinberger DR (2003) The BDNF val66met polymorphism affects activity-dependent secretion of BDNF and human memory and hippocampal function. Cell 112:257-269.

Eide FF, Vining ER, Eide BL, Zang K, Wang XY, Reichardt LF (1996) Naturally occurring truncated trkB receptors have dominant inhibitory effects on brain-derived neurotrophic factor signaling. J Neurosci 16:3123-3129.

Ekstrom S, Ericsson D, Onnerfjord P, Bengtsson M, Nilsson J, Marko-Varga G, Laurell T (2001) Signal amplification using "spot-on-a-chip" technology for the identification of proteins via MALDI-TOF MS. Anal Chem 73:214-219.

Emsley JG, Hagg T (2003) Endogenous and exogenous ciliary neurotrophic factor enhances forebrain neurogenesis in adult mice. Exp Neurol 183:298-310.

Enokido Y, Wyatt S, Davies AM (1999) Developmental changes in the response of trigeminal neurons to neurotrophins: influence of birthdate and the ganglion environment. Development 126:4365-4373.

Eriksson PS, Perfilieva E, Bjork-Eriksson T, Alborn A, Nordborg C, Peterson DA, Gage FH (1998) Neurogenesis in the adult human hippocampus. Nature Medicine 4:1313-1317.

Fallon J, Reid S, Kinyamu R, Opole I, Opole R, Baratta J, Korc M, Endo TL, Duong A, Nguyen G, Karkehabadhi M, Twardzik D, Loughlin S (2000) In vivo induction of massive proliferation, directed migration, and differentiation of neural cells in the adult mammalian brain. Proc Natl Acad Sci U S A 97:14686-14691.

Fan X, Xu H, Cai W, Yang Z, Zhang J (2003) Spatial and temporal patterns of expression of Noggin and BMP4 in embryonic and postnatal rat hippocampus. Brain Res Dev Brain Res 146:51-58.

Fan XT, Xu HW, Cai WQ, Yang H, Liu S (2004) Antisense Noggin oligodeoxynucleotide administration decreases cell proliferation in the dentate gyrus of adult rats. Neurosci Lett 366:107-111.

Farinas I, Yoshida CK, Backus C, Reichardt LF (1996) Lack of neurotrophin-3 results in death of spinal sensory neurons and premature differentiation of their precursors. Neuron 17:1065-1078.

Farinas I, Jones KR, Tessarollo L, Vigers AJ, Huang E, Kirstein M, de Caprona DC, Coppola V, Backus C, Reichardt LF, Fritzsch B (2001) Spatial shaping of cochlear innervation by temporally regulated neurotrophin expression. J Neurosci 21:6170-6180.

Ferri AL, Cavallaro M, Braida D, Di Cristofano A, Canta A, Vezzani A, Ottolenghi S, Pandolfi PP, Sala M, DeBiasi S, Nicolis SK (2004) Sox2 deficiency causes neurodegeneration and impaired neurogenesis in the adult mouse brain. Development 131:3805-3819.

Filippov V, Kronenberg G, Pivneva T, Reuter K, Steiner B, Wang LP, Yamaguchi M, Kettenmann H, Kempermann G (2003) Subpopulation of nestin-expressing progenitor cells in the adult murine hippocampus shows electrophysiological and morphological characteristics of astrocytes. Mol Cell Neurosci 23:373-382.

Fior R, Henrique D (2005) A novel hes5/hes6 circuitry of negative regulation controls Notch activity during neurogenesis. Dev Biol 281:318-333.

Fiore M, Amendola T, Triaca V, Alleva E, Aloe L (2005) Fighting in the aged male mouse increases the expression of TrkA and TrkB in the subventricular zone and in the hippocampus. Behav Brain Res 157:351-362.

Fiore M, Amendola T, Triaca V, Tirassa P, Alleva E, Aloe L (2003) Agonistic encounters in aged male mouse potentiate the expression of endogenous brain NGF and BDNF: possible implication for brain progenitor cells' activation. Eur J Neurosci 17:1455-1464.

Fragouli E (2007) Preimplantation genetic diagnosis: present and future. J Assist Reprod Genet 24:201-207.

Freeman ME, Kanyicska B, Lerant A, Nagy G (2000) Prolactin: structure, function, and regulation of secretion. Physiol Rev 80:1523-1631.

Friedrich RW, Laurent G (2001) Dynamic optimization of odor representations by slow temporal patterning of mitral cell activity. Science 291:889-894.

Fukuda S, Kato F, Tozuka Y, Yamaguchi M, Miyamoto Y, Hisatsune T (2003) Two distinct subpopulations of nestin-positive cells in adult mouse dentate gyrus. J Neurosci 23:9357-9366.

Fumagalli F, Racagni G, Riva MA (2006a) Shedding light into the role of BDNF in the pharmacotherapy of Parkinson's disease. Pharmacogenomics J 6:95-104.

Fumagalli F, Racagni G, Riva MA (2006b) The expanding role of BDNF: a therapeutic target for Alzheimer's disease? Pharmacogenomics J 6:8-15.

Gage FH (2000) Mammalian neural stem cells. Science 287:1433-1438.

Gage FH, Kempermann G, Palmer T, Peterson DA, Ray J (1998) Multipotent progenitor cells in the adult dentate gyrus. JNeurobiol 36:249-266.

Gaiano N, Fishell G (2002) The role of notch in promoting glial and neural stem cell fates. Annu Rev Neurosci 25:471-490.

Gaiano N, Nye JS, Fishell G (2000) Radial glial identity is promoted by notch1 signaling in the murine forebrain. Neuron 26:395-404.

Garces A, Haase G, Airaksinen MS, Livet J, Filippi P, deLapeyriere O (2000) GFRalpha 1 is required for development of distinct subpopulations of motoneuron. J Neurosci 20:4992-5000.

Garcia AD, Doan NB, Imura T, Bush TG, Sofroniew MV (2004) GFAP-expressing progenitors are the principal source of constitutive neurogenesis in adult mouse forebrain. Nat Neurosci 7:1233-1241.

Gascon E, Vutskits L, Jenny B, Durbec P, Kiss JZ (2007) PSA-NCAM in postnatally generated immature neurons of the olfactory bulb: a crucial role in regulating p75 expression and cell survival. Development 134:1181-1190.

Gascon E, Vutskits L, Zhang H, Barral-Moran MJ, Kiss PJ, Mas C, Kiss JZ (2005) Sequential activation of p75 and TrkB is involved in dendritic development of subventricular zone-derived neuronal progenitors in vitro. Eur J Neurosci 21:69-80.

Geetha T, Jiang J, Wooten MW (2005) Lysine 63 polyubiquitination of the nerve growth factor receptor TrkA directs internalization and signaling. Mol Cell 20:301-312.

Gheusi G, Cremer H, McLean H, Chazal G, Vincent JD, Lledo PM (2000) Importance of newly generated neurons in the adult olfactory bulb for odor discrimination. Proc Natl Acad Sci U S A 97:1823-1828.

Giuliani A, D'Intino G, Paradisi M, Giardino L, Calza L (2004) p75(NTR)-immunoreactivity in the subventricular zone of adult male rats: expression by cycling cells. J Mol Histol 35:749-758.

Givalois L, Naert G, Tapia-Arancibia L, Arancibia S (2006) Involvement of brain-derived neurotrophic factor in the regulation of hypothalamic somatostatin in vivo. J Endocrinol 188:425-433.

Givogri MI, de Planell M, Galbiati F, Superchi D, Gritti A, Vescovi A, de Vellis J, Bongarzone ER (2006) Notch signaling in astrocytes and neuroblasts of the adult subventricular zone in health and after cortical injury. Dev Neurosci 28:81-91.

Goldman SA, Nottebohm F (1983) Neuronal production, migration, and differentiation in a vocal control nucleus of the adult female canary brain. ProcNatlAcadSciUSA 80:2390-2394.

Gould E, Reeves AJ, Graziano MSA, Gross CG (1999) Neurogenesis in the neocortex of adult primates. Science 286:548-552.

Grewal SS, York RD, Stork PJ (1999) Extracellular-signal-regulated kinase signalling in neurons. Curr Opin Neurobiol 9:544-553.

Gritti A, Frolichsthal-Schoeller P, Galli R, Parati EA, Cova L, Pagano SF, Bjornson CRR, Vescovi AL (1999) Epidermal and fibroblast growth factors behave as mitogenic regulators for a single multipotent stem cell-like population from the subventricular region of the adult mouse forebrain. JNeurosci 19:3287-3297.

Guthrie KM, Wilson DA, Leon M (1990) Early unilateral deprivation modifies olfactory bulb function. J Neurosci 10:3402-3412.

Hack MA, Saghatelyan A, de Chevigny A, Pfeifer A, Ashery-Padan R, Lledo PM, Gotz M (2005) Neuronal fate determinants of adult olfactory bulb neurogenesis. Nat Neurosci.

Hadjantonakis AK, Gertsenstein M, Ikawa M, Okabe M, Nagy A (1998) Generating green fluorescent mice by germline transmission of green fluorescent ES cells. Mech Dev 76:79-90.

Hagg T (2005) Molecular regulation of adult CNS neurogenesis: an integrated view. Trends Neurosci 28:589-595.

Hamanoue M, Middleton G, Wyatt S, Jaffray E, Hay RT, Davies AM (1999) p75-mediated NF-kappaB activation enhances the survival response of developing sensory neurons to nerve growth factor. Mol Cell Neurosci 14:28-40.

Hartmann M, Brigadski T, Erdmann KS, Holtmann B, Sendtner M, Narz F, Lessmann V (2004) Truncated TrkB receptor-induced outgrowth of dendritic filopodia involves the p75 neurotrophin receptor. J Cell Sci 117:5803-5814.

Hashino E, Dolnick RY, Cohan CS (1999) Developing vestibular ganglion neurons switch trophic sensitivity from BDNF to GDNF after target innervation. J Neurobiol 38:414-427.

Henry RA, Hughes SM, Connor B (2007) AAV-mediated delivery of BDNF augments neurogenesis in the normal and quinolinic acid-lesioned adult rat brain. Eur J Neurosci 25:3513-3525.

Herrera DG, Garcia-Verdugo JM, Alvarez-Buylla A (1999) Adult-Derived Neural Precursors Transplanted into Multiple Regions in the Adult Brain. AnnNeurol 46:867-877.

Hertz L, Chen Y, Gibbs ME, Zang P, Peng L (2004) Astrocytic adrenoceptors: a major drug target in neurological and psychiatric disorders? Curr Drug Targets CNS Neurol Disord 3:239-267.

Higuchi R, Dollinger G, Walsh PS, Griffith R (1992) Simultaneous amplification and detection of specific DNA sequences. Biotechnology (N Y) 10:413-417.

Higuchi R, Fockler C, Dollinger G, Watson R (1993) Kinetic PCR analysis: real-time monitoring of DNA amplification reactions. Biotechnology (N Y) 11:1026-1030.

Hoglinger GU, Rizk P, Muriel MP, Duyckaerts C, Oertel WH (2004) Dopamine depletion impairs precursor cell proliferation in Parkinson disease. Nat Neurosci 7:726.

Holland EC, Varmus HE (1998) Basic fibroblast growth factor induces cell migration and proliferation after glia-specific gene transfer in mice. ProcNatlAcadSciUSA 95:1218-1223.

Holland PM, Abramson RD, Watson R, Gelfand DH (1991) Detection of specific polymerase chain reaction product by utilizing the 5'----3' exonuclease activity of Thermus aquaticus DNA polymerase. Proc Natl Acad Sci U S A 88:7276-7280.

Horner PJ, Palmer TD (2003) New roles for astrocytes: the nightlife of an 'astrocyte'. La vida loca! Trends Neurosci 26:597-603.

Huang EJ, Reichardt LF (2001) Neurotrophins: roles in neuronal development and function. Annu Rev Neurosci 24:677-736.

Huang EJ, Reichardt LF (2003) Trk receptors: roles in neuronal signal transduction. Annu Rev Biochem 72:609-642.

Huang EJ, Wilkinson GA, Farinas I, Backus C, Zang K, Wong SL, Reichardt LF (1999a) Expression of Trk receptors in the developing mouse trigeminal ganglion: in vivo evidence for NT-3 activation of TrkA and TrkB in addition to TrkC. Development 126:2191-2203.

Huang ZJ, Kirkwood A, Pizzorusso T, Porciatti V, Morales B, Bear MF, Maffei L, Tonegawa S (1999b) BDNF regulates the maturation of inhibition and the critical period of plasticity in mouse visual cortex. Cell 98:739-755.

Huangfu D, Anderson KV (2005) Cilia and Hedgehog responsiveness in the mouse. Proc Natl Acad Sci U S A 102:11325-11330.

Huangfu D, Liu A, Rakeman AS, Murcia NS, Niswander L, Anderson KV (2003) Hedgehog signalling in the mouse requires intraflagellar transport proteins. Nature 426:83-87.

Huber LJ, Chao MV (1995) Mesenchymal and neuronal cell expression of the p75 neurotrophin receptor gene occur by different mechanisms. Dev Biol 167:227-238.

Imura T, Kornblum HI, Sofroniew MV (2003) The Predominant Neural Stem Cell Isolated from Postnatal and Adult Forebrain But Not Early Embryonic Forebrain Expresses GFAP. J Neurosci 23:2824-2832.

Indo Y (2001) Molecular basis of congenital insensitivity to pain with anhidrosis (CIPA): mutations and polymorphisms in TRKA (NTRK1) gene encoding the receptor tyrosine kinase for nerve growth factor. Hum Mutat 18:462-471.

Irvin DK, Zurcher SD, Nguyen T, Weinmaster G, Kornblum HI (2001) Expression patterns of Notch1, Notch2, and Notch3 suggest multiple functional roles for the Notch-DSL signaling system during brain development. J Comp Neurol 436:167-181.

Isaacson JS, Strowbridge BW (1998) Olfactory reciprocal synapses: dendritic signaling in the CNS. Neuron 20:749-761.

Jackson EL, Garcia-Verdugo JM, Gil-Perotin S, Roy M, Quinones-Hinojosa A, Vandenberg S, Alvarez-Buylla A (2006) PDGFRalpha-Positive B Cells Are Neural Stem Cells in the Adult SVZ that Form Glioma-like Growths in Response to Increased PDGF Signaling. Neuron 51:187-199.

Janicki SM, Tsukamoto T, Salghetti SE, Tansey WP, Sachidanandam R, Prasanth KV, Ried T, Shav-Tal Y, Bertrand E, Singer RH, Spector DL (2004) From silencing to gene expression: real-time analysis in single cells. Cell 116:683-698.

Jankovski A, Sotelo C (1996) Subventricular zone-olfactory bulb migratory pathway in the adult mouse: Cellular composition and specificity as determined by heterochronic and heterotopic transplantation. JCompNeurol 371:376-396.

Johansson CB, Momma S, Clarke DL, Risling M, Lendahl U, Frisén J (1999) Identification of a Neural Stem Cell in the Adult Mammalian Central Nervous System. Cell 96:25-34.

Johnson D, Lanahan A, Buck CR, Sehgal A, Morgan C, Mercer E, Bothwell M, Chao M (1986) Expression and structure of the human NGF receptor. Cell 47:545-554.

Kaplan DR, Martin-Zanca D, Parada LF (1991a) Tyrosine phosphorylation and tyrosine kinase activity of the trk proto-oncogene product induced by NGF. Nature 350:158-160.

Kaplan DR, Hempstead BL, Martin-Zanca D, Chao MV, Parada LF (1991b) The trk proto-oncogene product: a signal transducing receptor for nerve growth factor. Science 252:554-558.

Kaplan MS, McNelly NA, Hinds JW (1985) Population Dynamics of adult-formed granule neurons of the rat olfactory bulb. JCompNeurol 239:117-125.

Kelsch W, Mosley CP, Lin CW, Lois C (2007) Distinct mammalian precursors are committed to generate neurons with defined dendritic projection patterns. PLoS Biol 5:e300.

Kempermann G (2002) Why new neurons? Possible functions for adult hippocampal neurogenesis. J Neurosci 22:635-638.
Kempermann G, Gage FH (2000) Neurogenesis in the adult hippocampus. Novartis Found Symp 231:220-235; discussion 235-241, 302-226.
Kernie SG, Liebl DJ, Parada LF (2000) BDNF regulates eating behavior and locomotor activity in mice. Embo J 19:1290-1300.
Kirschenbaum B, Goldman SA (1995) Brain-derived neurotrophic factor promotes the survival of neurons arising from the adult rat forebrain subependymal zone. ProcNatlAcadSciUSA 92:210-214.
Kiyatkin EA (2002) Dopamine in the nucleus accumbens: cellular actions, drug- and behavior-associated fluctuations, and a possible role in an organism's adaptive activity. Behav Brain Res 137:27-46.
Klein R, Parada LF, Coulier F, Barbacid M (1989) trkB, a novel tyrosine protein kinase receptor expressed during mouse neural development. Embo J 8:3701-3709.
Klein R, Conway D, Parada LF, Barbacid M (1990) The trkB tyrosine protein kinase gene codes for a second neurogenic receptor that lacks the catalytic kinase domain. Cell 61:647-656.
Klein R, Jing S, Nanduri V, O'Rourke E, Barbacid M (1991) The *trk* proto-oncogene encodes a receptor for nerve growth factor. Cell 65:189-197.
Knipper M, da Penha Berzaghi M, Blochl A, Breer H, Thoenen H, Lindholm D (1994) Positive feedback between acetylcholine and the neurotrophins nerve growth factor and brain-derived neurotrophic factor in the rat hippocampus. Eur J Neurosci 6:668-671.
Kohwi M, Osumi N, Rubenstein JL, Alvarez-Buylla A (2005) Pax6 is required for making specific subpopulations of granule and periglomerular neurons in the olfactory bulb. J Neurosci 25:6997-7003.
Kohwi M, Petryniak MA, Long JE, Ekker M, Obata K, Yanagawa Y, Rubenstein JL, Alvarez-Buylla A (2007) A subpopulation of olfactory bulb GABAergic interneurons is derived from Emx1- and Dlx5/6-expressing progenitors. J Neurosci 27:6878-6891.
Koketsu D, Mikami A, Miyamoto Y, Hisatsune T (2003) Nonrenewal of neurons in the cerebral neocortex of adult macaque monkeys. J Neurosci 23:937-942.
Kokoeva MV, Yin H, Flier JS (2005) Neurogenesis in the hypothalamus of adult mice: potential role in energy balance. Science 310:679-683.
Kornack DR, Rakic P (2001) Cell proliferation without neurogenesis in adult primate neocortex. Science 294:2127-2130.
Kosaka K, Kosaka T (2005) synaptic organization of the glomerulus in the main olfactory bulb: compartments of the glomerulus and heterogeneity of the periglomerular cells. Anat Sci Int 80:80-90.
Kosaka K, Aika Y, Toida K, Heizmann CW, Hunziker W, Jacobowitz DM, Nagatsu I, Streit P, Visser TJ, Kosaka T (1995) Chemically defined neuron groups and their subpopulations in the glomerular layer of the rat main olfactory bulb. NeurosciRes 23:73-88.
Kucera J, Ernfors P, Walro J, Jaenisch R (1995) Reduction in the number of spinal motor neurons in neurotrophin-3-deficient mice. Neuroscience 69:321-330.

Kuhn HG, Winkler J, Kempermann G, Thal LJ, Gage FH (1997) Epidermal growth factor and fibroblast growth factor-2 have different effects on neural progenitors in the adult rat brain. JNeurosci 17:5820-5829.

Kuipers SD, Bramham CR (2006) Brain-derived neurotrophic factor mechanisms and function in adult synaptic plasticity: new insights and implications for therapy. Curr Opin Drug Discov Devel 9:580-586.

Lai K, Kaspar BK, Gage FH, Schaffer DV (2003) Sonic hedgehog regulates adult neural progenitor proliferation in vitro and in vivo. Nat Neurosci 6:21-27.

Lamballe F, Klein R, Barbacid M (1991) trkC, a new member of the trk family of tyrosine protein kinases, is a receptor for neurotrophin-3. Cell 66:967-979.

Laurent G, Stopfer M, Friedrich RW, Rabinovich MI, Volkovskii A, Abarbanel HD (2001) Odor encoding as an active, dynamical process: experiments, computation, and theory. Annu Rev Neurosci 24:263-297.

Laywell ED, Rakic P, Kukekov VG, Holland EC, Steindler DA (2000) Identification of a multipotent astrocytic stem cell in the immature and adult mouse brain. Proc Natl Acad Sci U S A 97:13883-13888.

Lee KF, Davies AM, Jaenisch R (1994) p75-deficient embryonic dorsal root sensory and neonatal sympathetic neurons display a decreased sensitivity to NGF. Development 120:1027-1033.

Lee R, Kermani P, Teng KK, Hempstead BL (2001) Regulation of cell survival by secreted proneurotrophins. Science 294:1945-1948.

Lennington JB, Yang Z, Conover JC (2003) Neural stem cells and the regulation of adult neurogenesis. Reprod Biol Endocrinol 1:99.

Leventhal C, Rafii S, Rafii D, Shahar A, Goldman S (1999) Endothelial Trophic Support of Neuronal Production and Recruitment from the Adult Mammalian Subependyma. MolCellNeurosci 13:450-464.

Levi-Montalcini R (1987) The nerve growth factor 35 years later. Science 237:1154-1162.

Levison SW, Goldman JE (1993) Both oligodendrocytes and astrocytes develop from progenitors in the subventricular zone of postnatal rat forebrain. Neuron 10:201-212.

Levison SW, Chuang C, Abramson BJ, Goldman JE (1993) The migrational patterns and developmental fates of glial precursors in the rat subventricular zone are temporally regulated. Development 119:611-622.

Lewandoski M, Meyers EN, Martin GR (1997) Analysis of Fgf8 gene function in vertebrate development. Cold Spring Harb Symp Quant Biol 62:159-168.

Li X-C, Jarvis E, Alvarez-Borda B, Lim DA, Nottebohm F (2000) A relationship between behavior, neurotrophin expression, and new neuron survival. procNatacadsci 97:8584-8589.

Lie DC, Song H, Colamarino SA, Ming GL, Gage FH (2004) Neurogenesis in the adult brain: new strategies for central nervous system diseases. Annu Rev Pharmacol Toxicol 44:399-421.

Lie DC, Colamarino SA, Song HJ, Desire L, Mira H, Consiglio A, Lein ES, Jessberger S, Lansford H, Dearie AR, Gage FH (2005) Wnt signalling regulates adult hippocampal neurogenesis. Nature 437:1370-1375.

Lim DA, Alvarez-Buylla A (1999) Interaction between astrocytes and adult subventricular zone precursors stimulates neurogenesis. Proc Natl Acad Sci U S A 96. 96:7526-7531.

Lim DA, D. TA, Trevejo JM, Herrera DG, García-Verdugo JM, Alvarez-Buylla A (2000a) Noggin Antagonizes BMP Signaling to Create a Niche for Adult Neurogenesis. Neuron 28:713-726.

Lim DA, Tramontin AD, Trevejo JM, Herrera DG, Garcia-Verdugo JM, Alvarez-Buylla A (2000b) Noggin antagonizes BMP signaling to create a niche for adult neurogenesis. Neuron 28:713-726.

Lim DA, Suarez-Farinas M, Naef F, Hacker CR, Menn B, Takebayashi H, Magnasco M, Patil N, Alvarez-Buylla A (2006) In vivo transcriptional profile analysis reveals RNA splicing and chromatin remodeling as prominent processes for adult neurogenesis. Mol Cell Neurosci 31:131-148.

Lin LF, Doherty DH, Lile JD, Bektesh S, Collins F (1993) GDNF: a glial cell line-derived neurotrophic factor for midbrain dopaminergic neurons. Science 260:1130-1132.

Lindsay RM, Thoenen H, Barde YA (1985) Placode and neural crest-derived sensory neurons are responsive at early developmental stages to brain-derived neurotrophic factor. Dev Biol 112:319-328.

Linnarsson S, Willson CA, Ernfors P (2000) Cell death in regenerating populations of neurons in BDNF mutant mice. Brain Res Mol Brain Res 75:61-69.

Liu G, Rao Y (2003) Neuronal migration from the forebrain to the olfactory bulb requires a new attractant persistent in the olfactory bulb. J Neurosci 23:6651-6659.

Liu X, Wang Q, Haydar TF, Bordey A (2005) Nonsynaptic GABA signaling in postnatal subventricular zone controls proliferation of GFAP-expressing progenitors. Nat Neurosci 8:1179-1187.

Lois C, Alvarez-Buylla A (1994) Long-distance neuronal migration in the adult mammalian brain. Science 264:1145-1148.

Lois C, Garcia-Verdugo JM, Alvarez-Buylla A (1996) Chain migration of neuronal precursors. Science 271:978-981.

Lom B, Cogen J, Sanchez AL, Vu T, Cohen-Cory S (2002) Local and target-derived brain-derived neurotrophic factor exert opposing effects on the dendritic arborization of retinal ganglion cells in vivo. J Neurosci 22:7639-7649.

Long JE, Garel S, Alvarez-Dolado M, Yoshikawa K, Osumi N, Alvarez-Buylla A, Rubenstein JL (2007) Dlx-dependent and -independent regulation of olfactory bulb interneuron differentiation. J Neurosci 27:3230-3243.

Louissaint A, Jr., Rao S, Leventhal C, Goldman SA (2002) Coordinated interaction of neurogenesis and angiogenesis in the adult songbird brain. Neuron 34:945-960.

Luskin MB (1993) Restricted proliferation and migration of postnatally generated neurons derived from the forebrain subventricular zone. Neuron 11:173-189.

Luskin MB, McDermott K (1994) Divergent lineages for oligodendrocytes and astrocytes originating in the neonatal forebrain subventricular zone. Glia 11:211-226.

Machold R, Hayashi S, Rutlin M, Muzumdar MD, Nery S (2003) Sonic hedgehog is required for progenitor cell maintenance in telencephalic stem cell niches. Neuron 39:937.

MacLeod K, Backer A, Laurent G (1998) Who reads temporal information contained across synchronized and oscillatory spike trains? Nature 395:693-698.
Mak GK, Enwere EK, Gregg C, Pakarainen T, Poutanen M, Huhtaniemi I, Weiss S (2007) Male pheromone-stimulated neurogenesis in the adult female brain: possible role in mating behavior. Nat Neurosci 10:1003-1011.
Malatesta P, Hartfuss E, Gotz M (2000) Isolation of radial glial cells by fluorescent-activated cell sorting reveals a neuronal lineage. Development 127. 127:5253-5263-5253-5263.
Maroldt H, Kaplinovsky T, Cunningham AM (2005) Immunohistochemical expression of two members of the GDNF family of growth factors and their receptors in the olfactory system. J Neurocytol 34:241-255.
Marshall CJ (1995) Specificity of receptor tyrosine kinase signaling: transient versus sustained extracellular signal-regulated kinase activation. Cell 80:179-185.
Matsuo A, Nakamura S, Akiguchi I (2000) Immunohistochemical localization of glial cell line-derived neurotrophic factor family receptor alpha-1 in the rat brain: confirmation of expression in various neuronal systems. Brain Res 859:57-71.
McAllister AK (2001) Neurotrophins and neuronal differentiation in the central nervous system. Cell Mol Life Sci 58:1054-1060.
McAllister AK, Lo DC, Katz LC (1995) Neurotrophins regulate dendritic growth in developing visual cortex. Neuron 15:791-803.
McAllister AK, Katz LC, Lo DC (1999) Neurotrophins and synaptic plasticity. Annu Rev Neurosci 22:295-318.
McKerracher L, Winton MJ (2002) Nogo on the go. Neuron 36:345-348.
McLean JH, Darby-King A, Bonnell WS (2001) Neonatal olfactory sensory deprivation decreases BDNF in the olfactory bulb of the rat. Brain Res Dev Brain Res 128:17-24.
Meakin SO, MacDonald JI, Gryz EA, Kubu CJ, Verdi JM (1999) The signaling adapter FRS-2 competes with Shc for binding to the nerve growth factor receptor TrkA. A model for discriminating proliferation and differentiation. J Biol Chem 274:9861-9870.
Menezes JRL, Smith CM, Nelson KC, Luskin MB (1995) The division of neuronal progenitor cells during migration in the neonatal mammalian forebrain. MolCellNeurosci 6:496-508.
Menn B, Garcia-Verdugo JM, Yaschine C, Gonzalez-Perez O, Rowitch D, Alvarez-Buylla A (2006) Origin of oligodendrocytes in the subventricular zone of the adult brain. J Neurosci 26:7907-7918.
Merkle FT, Mirzadeh Z, Alvarez-Buylla A (2007) Mosaic organization of neural stem cells in the adult brain. Science 317:381-384.
Merkle FT, Tramontin AD, Garcia-Verdugo JM, Alvarez-Buylla A (2004) Radial glia give rise to adult neural stem cells in the subventricular zone. Proc Natl Acad Sci U S A 101:17528-17532.
Mi S, Lee X, Shao Z, Thill G, Ji B, Relton J, Levesque M, Allaire N, Perrin S, Sands B, Crowell T, Cate RL, McCoy JM, Pepinsky RB (2004) LINGO-1 is a component of the Nogo-66 receptor/p75 signaling complex. Nat Neurosci 7:221-228.

Middlemas DS, Lindberg RA, Hunter T (1991) trkB, a neural receptor protein-tyrosine kinase: evidence for a full-length and two truncated receptors. Mol Cell Biol 11:143-153.
Middleton G, Hamanoue M, Enokido Y, Wyatt S, Pennica D, Jaffray E, Hay RT, Davies AM (2000) Cytokine-induced nuclear factor kappa B activation promotes the survival of developing neurons. J Cell Biol 148:325-332.
Miklic S, Juric DM, Carman-Krzan M (2004) Differences in the regulation of BDNF and NGF synthesis in cultured neonatal rat astrocytes. Int J Dev Neurosci 22:119-130.
Ming GL, Song H (2005) Adult neurogenesis in the mammalian central nervous system. Annu Rev Neurosci 28:223-250.
Minichiello L, Klein R (1996) TrkB and TrkC neurotrophin receptors cooperate in promoting survival of hippocampal and cerebellar granule neurons. Genes Dev 10:2849-2858.
Minichiello L, Calella AM, Medina DL, Bonhoeffer T, Klein R, Korte M (2002) Mechanism of TrkB-mediated hippocampal long-term potentiation. Neuron 36:121-137.
Mirescu C, Gould E (2006) Stress and adult neurogenesis. Hippocampus 16:233-238.
Miyata T, Kawaguchi A, Okano H, Ogawa M (2001) Asymmetric inheritance of radial glial fibers by cortical neurons. Neuron 31:727-741.
Molliver DC, Wright DE, Leitner ML, Parsadanian AS, Doster K, Wen D, Yan Q, Snider WD (1997) IB4-binding DRG neurons switch from NGF to GDNF dependence in early postnatal life. Neuron 19:849-861.
Monti JM, Monti D (2007) The involvement of dopamine in the modulation of sleep and waking. Sleep Med Rev 11:113-133.
Mori K, Nagao H, Yoshihara Y (1999) The olfactory bulb: coding and processing of odor molecule information. Science 286:711-715.
Morshead CM, Van der Kooy D (1992) Postmitotic death is the fate of constitutively proliferating cells in the subependymal layer of the adult mouse brain. JNeurosci 12:249-256.
Morshead CM, Reynolds BA, Craig CG, McBurney MW, Staines WA, Morassutti D, Weiss S, van der Kooy D (1994) Neural stem cells in the adult mammalian forebrain: a relatively quiescent subpopulation of subependymal cells. Neuron 13:1071-1082.
Murase S, Horwitz AF (2002) Deleted in colorectal carcinoma and differentially expressed integrins mediate the directional migration of neural precursors in the rostral migratory stream. J Neurosci 22:3568-3579.
Murray M, Kim D, Liu Y, Tobias C, Tessler A, Fischer I (2002) Transplantation of genetically modified cells contributes to repair and recovery from spinal injury. Brain Res Brain Res Rev 40:292-300.
Nait-Oumesmar B, Decker L, Lachapelle F, Avellana-Adalid V, Bachelin C, Van Evercooren AB (1999) Progenitor cells of the adult mouse subventricular zone proliferate, migrate and differentiate into oligodendrocytes after demyelination. Eur J Neurosci 11. 11:4357-4366-4357-4366.
Najbauer J, Leon M (1995) Olfactory experience modulates apoptosis in the developing olfactory bulb. Brain Res 674:245-251.

Neet KE, Campenot RB (2001) Receptor binding, internalization, and retrograde transport of neurotrophic factors. Cell Mol Life Sci 58:1021-1035.

Ng KL, Li JD, Cheng MY, Leslie FM, Lee AG, Zhou QY (2005) Dependence of olfactory bulb neurogenesis on prokineticin 2 signaling. Science 308:1923-1927.

Nguyen L, Malgrange B, Breuskin I, Bettendorff L, Moonen G, Belachew S, Rigo JM (2003) Autocrine/paracrine activation of the GABA(A) receptor inhibits the proliferation of neurogenic polysialylated neural cell adhesion molecule-positive (PSA-NCAM+) precursor cells from postnatal striatum. J Neurosci 23:3278-3294.

Nicoll RA (1969) Inhibitory mechanisms in the rabbit olfactory bulb: dendrodendritic mechanisms. Brain Res 14:157-172.

Noctor SC, Martinez-Cerdeno V, Ivic L, Kriegstein AR (2004) Cortical neurons arise in symmetric and asymmetric division zones and migrate through specific phases. Nat Neurosci 7:136-144.

Noctor SC, Flint AC, Weissman TA, Dammerman RS, Kriegstein AR (2001) Neurons derived from radial glial cells establish radial units in neocortex. Nature 409:714-720.

Nonomura T, Hatanaka H (1992) Neurotrophic effect of brain-derived neurotrophic factor on basal forebrain cholinergic neurons in culture from postnatal rats. Neurosci Res 14:226-233.

Nottebohm F (1991) Reassessing the mechanisms and origins of vocal learning in birds. Trends Neurosci 14:206-211.

Nottebohm F (2002a) Neuronal replacement in adult brain. Brain Res Bull 57:737-749.

Nottebohm F (2002b) Why are some neurons replaced in adult brain? J Neurosci 22:624-628.

Nyfeler Y, Kirch RD, Mantei N, Leone DP, Radtke F, Suter U, Taylor V (2005) Jagged1 signals in the postnatal subventricular zone are required for neural stem cell self-renewal. Embo J 24:3504-3515.

Nykjaer A, Willnow TE, Petersen CM (2005) p75NTR--live or let die. Curr Opin Neurobiol 15:49-57.

Oppenheim RW, Houenou LJ, Parsadanian AS, Prevette D, Snider WD, Shen L (2000) Glial cell line-derived neurotrophic factor and developing mammalian motoneurons: regulation of programmed cell death among motoneuron subtypes. J Neurosci 20:5001-5011.

Oppenheim RW, Houenou LJ, Johnson JE, Lin LF, Li L, Lo AC, Newsome AL, Prevette DM, Wang S (1995) Developing motor neurons rescued from programmed and axotomy-induced cell death by GDNF. Nature 373:344-346.

Ormerod BK, Lee TT, Galea LA (2003) Estradiol initially enhances but subsequently suppresses (via adrenal steroids) granule cell proliferation in the dentate gyrus of adult female rats. J Neurobiol 55:247-260.

Orona E, Scott JW, Rainer EC (1983) Different granule cell populations innervate superficial and deep regions of the external plexiform layer in rat olfactory bulb. J Comp Neurol 217:227-237.

Packer MA, Stasiv Y, Benraiss A, Chmielnicki E, Grinberg A, Westphal H, Goldman SA, Enikolopov G (2003) Nitric oxide negatively regulates mammalian adult neurogenesis. Proc Natl Acad Sci U S A 100:9566-9571.

Palma V, Lim DA, Dahmane N, Sanchez P, Brionne TC, Herzberg CD, Gitton Y, Carleton A, Alvarez-Buylla A, Ruiz i Altaba A (2005) Sonic hedgehog controls stem cell behavior in the postnatal and adult brain. Development 132:335-344.

Palmer TD, Willhoite AR, Gage FH (2000) Vascular Niche for Adult Hippocampal Neurogenesis. Journal of Comparative Neurology 425:479-494.

Parras CM, Galli R, Britz O, Soares S, Galichet C, Battiste J, Johnson JE, Nakafuku M, Vescovi A, Guillemot F (2004) Mash1 specifies neurons and oligodendrocytes in the postnatal brain. Embo J 23:4495-4505.

Parrish-Aungst S, Shipley MT, Erdelyi F, Szabo G, Puche AC (2007) Quantitative analysis of neuronal diversity in the mouse olfactory bulb. J Comp Neurol 501:825-836.

Paton JA, Burd GD, Nottebohm F (1986) New neurons in an adult brain: Plasticity in an auditory-motor nucleus. In: The biology of change in otolaryngology (Ruben RW, al. e, eds), pp 201-210. Amsterdam: Elsevier Biomed.

Paul G, Davies AM (1995) Trigeminal sensory neurons require extrinsic signals to switch neurotrophin dependence during the early stages of target field innervation. Dev Biol 171:590-605.

Pearson BJ, Doe CQ (2004) Specification of temporal identity in the developing nervous system. Annu Rev Cell Dev Biol 20:619-647.

Pelleymounter MA, Cullen MJ, Wellman CL (1995) Characteristics of BDNF-induced weight loss. Exp Neurol 131:229-238.

Pencea V, Bingaman KD, Wiegand SJ, Luskin MB (2001) Infusion of brain-derived neurotrophic factor into the lateral ventricle of the adult rat leads to new neurons in the parenchyma of the striatum, septum, thalamus, and hypothalamus. J Neurosci 21:6706-6717.

Peretto P, Merighi A, Fasolo A, Bonfanti L (1997) Glial tubes in the rostral migratory stream of the adult rat. Brain ResBull 42:9-21.

Perez-Martin M, Azcoitia I, Trejo JL, Sierra A, Garcia-Segura LM (2003) An antagonist of estrogen receptors blocks the induction of adult neurogenesis by insulin-like growth factor-I in the dentate gyrus of adult female rat. Eur J Neurosci 18:923-930.

Petratos S, Gonzales MF, Azari MF, Marriott M, Minichiello RA, Shipham KA, Profyris C, Nicolaou A, Boyle K, Cheema SS, Kilpatrick TJ (2004) Expression of the low-affinity neurotrophin receptor, p75(NTR), is upregulated by oligodendroglial progenitors adjacent to the subventricular zone in response to demyelination. Glia 48:64-75.

Petreanu L, Alvarez-Buylla A (2002) Maturation and death of adult-born olfactory bulb granule neurons: role of olfaction. J Neurosci.

Philpot BD, Lim JH, Brunjes PC (1997) Activity-dependent regulation of calcium-binding proteins in the developing rat olfactory bulb. J Comp Neurol 387:12-26.

Picard-Riera N, Decker L, Delarasse C, Goude K, Nait-Oumesmar B, Liblau R, Pham-Dinh D, Evercooren AB (2002) Experimental autoimmune encephalomyelitis mobilizes neural progenitors from the subventricular zone to undergo oligodendrogenesis in adult mice. Proc Natl Acad Sci U S A 99:13211-13216.

Pinon LG, Minichiello L, Klein R, Davies AM (1996) Timing of neuronal death in trkA, trkB and trkC mutant embryos reveals developmental changes in sensory neuron dependence on Trk signalling. Development 122:3255-3261.
Platel JC, Dave KA, Bordey A (2008) Control of neuroblast production and migration by converging GABA and glutamate signals in the postnatal forebrain. J Physiol.
Privat A, Leblond CP (1972) The subependymal layer and neighboring region in the brain of the young rat. JCompNeurol 146:277-302.
Rakic P (1988) Specification of cerebral cortical areas. Science 241:170-176.
Rakic P (1995) Radial versus tangential migration of neuronal clones in the developing cerebral cortex. ProcNatlAcadSciUSA 92:11323-11327.
Rall W, Shepherd GM (1968) Theoretical reconstruction of field potentials and dendrodendritic synaptic interactions in olfactory bulb. J Neurophysiol 31:884-915.
Rall W, Shepherd GM, Reese TS, Brightman MW (1966) Dendrodendritic synaptic pathway for inhibitation in the olfactory bulb. ExpNeurol 14:44-56.
Rasika S, Nottebohm F, Alvarez-Buylla A (1994) Testosterone increases the recruitment and/or survival of new high vocal center neurons in adult female canaries. ProcNatlAcadSciUSA 91:7854-7858.
Rasika S, Alvarez-Buylla A, Nottebohm F (1999) BDNF mediates the effects of testosterone on the survival of new neurons in an adult brain. Neuron 22:53-62.
Redmond L, Hockfield S, Morabito MA (1996) The divergent homeobox gene *PBX1* is expressed in the postnatal subventricular zone and interneurons of the olfactory bulb. JNeurosci 16:2972-2982.
Reichardt LF (2006) Neurotrophin-regulated signalling pathways. Philos Trans R Soc Lond B Biol Sci 361:1545-1564.
Reya T, Duncan AW, Ailles L, Domen J, Scherer DC, Willert K, Hintz L, Nusse R, Weissman IL (2003) A role for Wnt signalling in self-renewal of haematopoietic stem cells. Nature 423:409-414.
Reynolds BA, Weiss S (1992) Generation of neurons and astrocytes from isolated cells of the adult mammalian central nervous system. Science 255:1707.
Rico B, Xu B, Reichardt LF (2002) TrkB receptor signaling is required for establishment of GABAergic synapses in the cerebellum. Nat Neurosci 5:225-233.
Rietze RL, Valcanis H, Brooker GF, Thomas T, Voss AK, Bartlett PF (2001) Purification of a pluripotent neural stem cell from the adult mouse brain. Nature 412:736-739.
Rochefort C, Gheusi G, Vincent JD, Lledo PM (2002) Enriched odor exposure increases the number of newborn neurons in the adult olfactory bulb and improves odor memory. J Neurosci 22:2679-2689.
Rogers JH (1992) Immunohistochemical markers in rat brain: colocalization of calretinin and calbindin-D28k with tyrosine hydroxylase. Brain Res 587:203-210.
Rose CR, Blum R, Pichler B, Lepier A, Kafitz KW, Konnerth A (2003) Truncated TrkB-T1 mediates neurotrophin-evoked calcium signalling in glia cells. Nature 426:74-78.
Roux PP, Barker PA (2002) Neurotrophin signaling through the p75 neurotrophin receptor. Prog Neurobiol 67:203-233.
Rowitch DH (2004) Glial specification in the vertebrate neural tube. Nat Rev Neurosci 5:409-419.

Rowitch DH, Lu QR, Kessaris N, Richardson WD (2002) An 'oligarchy' rules neural development. Trends Neurosci 25:417-422.
Ruvolo PP (2003) Intracellular signal transduction pathways activated by ceramide and its metabolites. Pharmacol Res 47:383-392.
Salehi AH, Roux PP, Kubu CJ, Zeindler C, Bhakar A, Tannis LL, Verdi JM, Barker PA (2000) NRAGE, a novel MAGE protein, interacts with the p75 neurotrophin receptor and facilitates nerve growth factor-dependent apoptosis. Neuron 27:279-288.
Sawamoto K, Wichterle H, Gonzalez-Perez O, Cholfin JA, Yamada M, Spassky N, Murcia NS, Garcia-Verdugo JM, Marin O, Rubenstein JL, Tessier-Lavigne M, Okano H, Alvarez-Buylla A (2006) New neurons follow the flow of cerebrospinal fluid in the adult brain. Science 311:629-632.
Scharff C, Kirn JR, Grossman M, Macklis JD, Nottebohm F (2000) Targeted neuronal death affects neuronal replacement and vocal behavior in adult songbirds [see comments]. Neuron 25. 25:481-492.
Scharfman H, Goodman J, Macleod A, Phani S, Antonelli C, Croll S (2005) Increased neurogenesis and the ectopic granule cells after intrahippocampal BDNF infusion in adult rats. Exp Neurol 192:348-356.
Schinder AF, Poo M (2000) The neurotrophin hypothesis for synaptic plasticity. Trends Neurosci 23:639-645.
Schmechel DE, Rakic P (1979) A Golgi study of radial glia cells in developing monkey telencephalon: Morphogenesis and transformation into astrocytes. AnatEmbryol 156:115-152.
Schmidt-Hieber C, Jonas P, Bischofberger J (2004) Enhanced synaptic plasticity in newly generated granule cells of the adult hippocampus. Nature 429:184.
Schoppa NE, Westbrook GL (1999) Regulation of synaptic timing in the olfactory bulb by an A-type potassium current. Nat Neurosci 2:1106-1113.
Schwartz PM, Borghesani PR, Levy RL, Pomeroy SL, Segal RA (1997) Abnormal cerebellar development and foliation in BDNF-/- mice reveals a role for neurotrophins in CNS patterning. Neuron 19:269-281.
Schweigreiter R (2006) The dual nature of neurotrophins. Bioessays 28:583-594.
Segal RA (2003) Selectivity in neurotrophin signaling: theme and variations. Annu Rev Neurosci 26:299-330.
Seri B, Garcia-Verdugo JM, McEwen BS, Alvarez-Buylla A (2001) Astrocytes give rise to new neurons in the adult mammalian hippocampus. J Neurosci 21:7153-7160.
Seroogy KB, Gall CM, Lee DC, Kornblum HI (1995) Proliferative zones of postnatal rat brain express epidermal growth factor receptor mRNA. Brain Res 670:157-164.
Seroogy KB, Lundgren KH, Lee DC, Guthrie KM, Gall CM (1993) Cellular localization of transforming growth factor-α mRNA in rat forebrain. Journal of Neurochemistry 60:1777-1782.
Sharp PJ (2005) Photoperiodic regulation of seasonal breeding in birds. Ann N Y Acad Sci 1040:189-199.
Shen Q, Wang Y, Dimos JT, Fasano CA, Phoenix TN, Lemischka IR, Ivanova NB, Stifani S, Morrisey EE, Temple S (2006) The timing of cortical neurogenesis is encoded within lineages of individual progenitor cells. Nat Neurosci 9:743-751.

Shepherd GM (1972) Synaptic organization of the mammalian olfactory bulb. Physiol Rev 52:864-917.
Shepherd GM, Greer CA (1998) Olfactory Bulb. In: The synaptic organization of the brain, fourth edition Edition (Shepherd GM, ed). New York: Oxford University Press, Inc.
Shingo T, Sorokan ST, Shimazaki T, Weiss S (2001) Erythropoietin regulates the in vitro and in vivo production of neuronal progenitors by mammalian forebrain neural stem cells. J Neurosci 21:9733-9743.
Shingo T, Gregg C, Enwere E, Fujikawa H, Hassam R, Geary C, Cross JC, Weiss S (2003) Pregnancy-stimulated neurogenesis in the adult female forebrain mediated by prolactin. Science 299:117-120.
Siuciak JA, Boylan C, Fritsche M, Altar CA, Lindsay RM (1996) BDNF increases monoaminergic activity in rat brain following intracerebroventricular or intraparenchymal administration. Brain Res 710:11-20.
Smeyne RJ, Klein R, Schnapp A, Long LK, Bryant S, Lewin A, Lira SA, Barbacid M (1994) Severe sensory and sympathetic neuropathies in mice carrying a disrupted Trk/NGF receptor gene. Nature 368:246-249.
Soria JM, Taglialatela P, Gil-Perotin S, Galli R, Gritti A, Verdugo JM, Bertuzzi S (2004) Defective postnatal neurogenesis and disorganization of the rostral migratory stream in absence of the Vax1 homeobox gene. J Neurosci 24:11171-11181.
Spassky N, Merkle FT, Flames N, Tramontin AD, Garcia-Verdugo JM, Alvarez-Buylla A (2005) Adult ependymal cells are postmitotic and are derived from radial glial cells during embryogenesis. J Neurosci 25:10-18.
Stenman J, Toresson H, Campbell K (2003) Identification of two distinct progenitor populations in the lateral ganglionic eminence: implications for striatal and olfactory bulb neurogenesis. J Neurosci 23:167-174.
Stewart RR, Hoge GJ, Zigova T, Luskin MB (2002) Neural progenitor cells of the neonatal rat anterior subventricular zone express functional GABA(A) receptors. J Neurobiol 50:305-322.
Stopfer M, Bhagavan S, Smith BH, Laurent G (1997) Impaired odour discrimination on desynchronization of odour-encoding neural assemblies. Nature 390:70-74.
Strohmaier C, Carter BD, Urfer R, Barde YA, Dechant G (1996) A splice variant of the neurotrophin receptor trkB with increased specificity for brain-derived neurotrophic factor. Embo J 15:3332-3337.
Stump G, Durrer A, Klein AL, Lutolf S, Suter U, Taylor V (2002) Notch1 and its ligands Delta-like and Jagged are expressed and active in distinct cell populations in the postnatal mouse brain. Mech Dev 114:153-159.
Tai YT, Svendsen CN (2004) Stem cells as a potential treatment of neurological disorders. Curr Opin Pharmacol 4:98-104.
Tamamaki N, Nakamura K, Okamoto K, Kaneko T (2001) Radial glia is a progenitor of neocortical neurons in the developing cerebral cortex. Neurosci Res 41:51-60.
Tanabe Y, Jessell TM (1996) Diversity and pattern in the developing spinal cord. Science 274:1115-1123.
Tanapat P, Hastings NB, Reeves AJ, Gould E (1999) Estrogen stimulates a transient increase in the number of new neurons in the dentate gyrus of the adult female rat. J Neurosci 19:5792-5801.

Tanis KQ, Newton SS, Duman RS (2007) Targeting neurotrophic/growth factor expression and signaling for antidepressant drug development. CNS Neurol Disord Drug Targets 6:151-160.

Tervonen TA, Ajamian F, De Wit J, Verhaagen J, Castren E, Castren M (2006) Overexpression of a truncated TrkB isoform increases the proliferation of neural progenitors. Eur J Neurosci 24:1277-1285.

Tokunaga A, Kohyama J, Yoshida T, Nakao K, Sawamoto K, Okano H (2004) Mapping spatio-temporal activation of Notch signaling during neurogenesis and gliogenesis in the developing mouse brain. J Neurochem 90:142-154.

Tomac A, Lindqvist E, Lin LF, Ogren SO, Young D, Hoffer BJ, Olson L (1995) Protection and repair of the nigrostriatal dopaminergic system by GDNF in vivo. Nature 373:335-339.

Torner L, Neumann ID (2002) The brain prolactin system: involvement in stress response adaptations in lactation. Stress 5:249-257.

Traiffort E, Charytoniuk D, Watroba L, Faure H, Sales N, Ruat M (1999) Discrete localizations of hedgehog signalling components in the developing and adult rat nervous system. Eur J Neurosci 11:3199-3214.

Tropepe V, Craig CG, Morshead CM, Van der Kooy D (1997) Transforming growth factor-α null and senescent mice show decreased neural progenitor cell proliferation in the forebrain subependyma. JNeurosci 17:7850-7859.

Tsoulfas P, Soppet D, Escandon E, Tessarollo L, Mendoza-Ramirez JL, Rosenthal A, Nikolics K, Parada LF (1993) The rat trkC locus encodes multiple neurogenic receptors that exhibit differential response to neurotrophin-3 in PC12 cells. Neuron 10:975-990.

Tsukamoto T, Hashiguchi N, Janicki SM, Tumbar T, Belmont AS, Spector DL (2000) Visualization of gene activity in living cells. Nat Cell Biol 2:871-878.

Ueki T, Tanaka M, Yamashita K, Mikawa S, Qiu Z (2003) A novel secretory factor, Neurogenesin-1, provides neurogenic environmental cues for neural stem cells in the adult hippocampus. J Neurosci 23:11732.

Valenzuela DM, Maisonpierre PC, Glass DJ, Rojas E, Nunez L, Kong Y, Gies DR, Stitt TN, Ip NY, Yancopoulos GD (1993) Alternative forms of rat TrkC with different functional capabilities. Neuron 10:963-974.

Van Gelder RN, von Zastrow ME, Yool A, Dement WC, Barchas JD, Eberwine JH (1990) Amplified RNA synthesized from limited quantities of heterogeneous cDNA. Proc Natl Acad Sci U S A 87:1663-1667.

van Praag H, Kempermann G, Gage FH (1999) Running increases cell proliferation and neurogenesis in the adult mouse dentate gyrus. Nat Neurosci 2:266-270.

Vilar M, Murillo-Carretero M, Mira H, Magnusson K, Besset V, Ibanez CF (2006) Bex1, a novel interactor of the p75 neurotrophin receptor, links neurotrophin signaling to the cell cycle. Embo J 25:1219-1230.

Voigt T (1989) Development of glial cells in the cerebral wall of ferrets: Direct tracing of their transformation from radial glia into astrocytes. JCompNeurol 289:74-88.

von Schack D, Casademunt E, Schweigreiter R, Meyer M, Bibel M, Dechant G (2001) Complete ablation of the neurotrophin receptor p75NTR causes defects both in the nervous and the vascular system. Nat Neurosci 4:977-978.

Waclaw RR, Allen ZJ, 2nd, Bell SM, Erdelyi F, Szabo G, Potter SS, Campbell K (2006) The zinc finger transcription factor Sp8 regulates the generation and diversity of olfactory bulb interneurons. Neuron 49:503-516.

Wang DD, Krueger DD, Bordey A (2003) GABA depolarizes neuronal progenitors of the postnatal subventricular zone via GABAA receptor activation. J Physiol 550:785-800.

Wang KC, Kim JA, Sivasankaran R, Segal R, He Z (2002) P75 interacts with the Nogo receptor as a co-receptor for Nogo, MAG and OMgp. Nature 420:74-78.

Ward NL, Hagg T (2000) BDNF is needed for postnatal maturation of basal forebrain and neostriatum cholinergic neurons in vivo. Exp Neurol 162:297-310.

Wegner M, Stolt CC (2005) From stem cells to neurons and glia: a Soxist's view of neural development. Trends Neurosci 28:583-588.

Weiss S, Reynolds BA, Vescovi AL, Morshead C, Craig CG, Van der Kooy D (1996) Is there a neural stem cell in the mammalian forebrain? Trends Neurosci 19:387-393.

Wen CJ, Xue B, Qin WX, Yu M, Zhang MY, Zhao DH, Gao X, Gu JR, Li CJ (2004) hNRAGE, a human neurotrophin receptor interacting MAGE homologue, regulates p53 transcriptional activity and inhibits cell proliferation. FEBS Lett 564:171-176.

Weskamp G, Reichardt LF (1991) Evidence that biological activity of NGF is mediated through a novel subclass of high affinity receptors. Neuron 6:649-663.

Wichterle H, Garcia-Verdugo JM, Alvarez-Buylla A (1997) Direct evidence for homotypic, glia-independent neuronal migration. Neuron 18:779-791.

Wilbrecht L, Kirn JR (2004) Neuron addition and loss in the song system: regulation and function. Ann N Y Acad Sci 1016:659-683.

Wilcox JN, Derynck R (1988) Localization of cells sythesizing transforming growth factor-Alpha mRNA in the Mouse brain. JNeurosci 8(6):1901-1904.

Willaime-Morawek S, Seaberg RM, Batista C, Labbe E, Attisano L, Gorski JA, Jones KR, Kam A, Morshead CM, van der Kooy D (2006) Embryonic cortical neural stem cells migrate ventrally and persist as postnatal striatal stem cells. J Cell Biol 175:159-168.

Winner B, Cooper-Kuhn CM, Aigner R, Winkler J, Kuhn HG (2002) Long-term survival and cell death of newly generated neurons in the adult rat olfactory bulb. Eur J Neurosci 16:1681-1689.

Wong ST, Henley JR, Kanning KC, Huang KH, Bothwell M, Poo MM (2002) A p75(NTR) and Nogo receptor complex mediates repulsive signaling by myelin-associated glycoprotein. Nat Neurosci 5:1302-1308.

Woo NH, Lu B (2006) Regulation of cortical interneurons by neurotrophins: from development to cognitive disorders. Neuroscientist 12:43-56.

Woolf TB, Shepherd GM, Greer CA (1991) Serial Reconstructions of Granule Cell Spines in the Mammalian Olfactory Bulb. Synapse 7:181-192.

Xiong H, Yamada K, Han D, Nabeshima T, Enikolopov G, Carnahan J, Nawa H (1999) Mutual regulation between the intercellular messengers nitric oxide and brain-derived neurotrophic factor in rodent neocortical neurons. Eur J Neurosci 11:1567-1576.

Xu B, Zang K, Ruff NL, Zhang YA, McConnell SK, Stryker MP, Reichardt LF (2000a) Cortical degeneration in the absence of neurotrophin signaling: dendritic retraction and neuronal loss after removal of the receptor TrkB. Neuron 26:233-245.

Xu B, Goulding EH, Zang K, Cepoi D, Cone RD, Jones KR, Tecott LH, Reichardt LF (2003) Brain-derived neurotrophic factor regulates energy balance downstream of melanocortin-4 receptor. Nat Neurosci 6:736-742.

Xu B, Gottschalk W, Chow A, Wilson RI, Schnell E, Zang K, Wang D, Nicoll RA, Lu B, Reichardt LF (2000b) The role of brain-derived neurotrophic factor receptors in the mature hippocampus: modulation of long-term potentiation through a presynaptic mechanism involving TrkB. J Neurosci 20:6888-6897.

Yacoubian TA, Lo DC (2000) Truncated and full-length TrkB receptors regulate distinct modes of dendritic growth. Nat Neurosci 3:342-349.

Yamashita T, Tohyama M (2003) The p75 receptor acts as a displacement factor that releases Rho from Rho-GDI. Nat Neurosci 6:461-467.

Yamashita T, Tucker KL, Barde YA (1999) Neurotrophin binding to the p75 receptor modulates Rho activity and axonal outgrowth. Neuron 24:585-593.

Yan Q, Matheson C, Sun J, Radeke MJ, Feinstein SC, Miller JA (1994) Distribution of intracerebral ventricularly administered neurotrophins in rat brain and its correlation with trk receptor expression. Exp Neurol 127:23-36.

Yan Q, Radeke MJ, Matheson CR, Talvenheimo J, Welcher AA, Feinstein SC (1997a) Immunocytochemical localization of TrkB in the central nervous system of the adult rat. J Comp Neurol 378:135-157.

Yan Q, Rosenfeld RD, Matheson CR, Hawkins N, Lopez OT, Bennett L, Welcher AA (1997b) Expression of brain-derived neurotrophic factor protein in the adult rat central nervous system. Neuroscience 78:431-448.

Yeo GS, Connie Hung CC, Rochford J, Keogh J, Gray J, Sivaramakrishnan S, O'Rahilly S, Farooqi IS (2004) A de novo mutation affecting human TrkB associated with severe obesity and developmental delay. Nat Neurosci 7:1187-1189.

Yokoi M, Mori K, Nakanishi S (1995) Refinement of odor molecule tuning by dendrodendritic synaptic inhibition in the olfactory bulb. Proc Natl Acad Sci U S A 92. 92:3371-3375.

Yoon SO, Casaccia-Bonnefil P, Carter B, Chao MV (1998) Competitive signaling between TrkA and p75 nerve growth factor receptors determines cell survival. J Neurosci 18:3273-3281.

Young KM, Merson TD, Sotthibundhu A, Coulson EJ, Bartlett PF (2007) p75 neurotrophin receptor expression defines a population of BDNF-responsive neurogenic precursor cells. J Neurosci 27:5146-5155.

Yu JM, Kim JH, Song GS, Jung JS (2006) Increase in proliferation and differentiation of neural progenitor cells isolated from postnatal and adult mice brain by Wnt-3a and Wnt-5a. Mol Cell Biochem 288:17-28.

Zafra F, Lindholm D, Castrén E, Hartikka J, Thoenen H (1992) Regulation of brain-derived neurotrophic factor and nerve growth factormRNA in primary cultures of hippocampal neurons and astrocytes. JNeurosci 12:4793-4799.

Zhang HT, Kacharmina JE, Miyashiro K, Greene MI, Eberwine J (2001) Protein quantification from complex protein mixtures using a proteomics methodology with single-cell resolution. Proc Natl Acad Sci U S A 98:5497-5502.

Zhang RL, Zhang ZG, Wang Y, LeTourneau Y, Liu XS, Zhang X, Gregg SR, Wang L, Chopp M (2007) Stroke induces ependymal cell transformation into radial glia in the subventricular zone of the adult rodent brain. J Cereb Blood Flow Metab 27:1201-1212.

Zheng W, Nowakowski RS, Vaccarino FM (2004) Fibroblast growth factor 2 is required for maintaining the neural stem cell pool in the mouse brain subventricular zone. Dev Neurosci 26:181-196.

Zhou X-F, Zettler C, Rush RA (1994) An improved procedure for the immunohistochemical localization of nerve growth factor-like immunoreactivity. JNeurosciMethods 54:95-102.

Zigova T, Pencea V, Wiegand SJ, Luskin MB (1998) Intraventricular administration of BDNF increases the number of newly generated neurons in the adult olfactory bulb. Molecular & Cellular Neurosciences 11:234-245.

Appendix: Protocols

A1 BrdU Labeling

1- Fix tissue (for cryostat sections; if starting with vibratome sections, re-fixing is not necessary) using 4% PFA 10 min at room temperature
2- Wash off fix 3x5 min in PBS
3- Incubate tissue in 2N HCl, 30 min at 37^{o}C (I place slides in a coplin jar with 2N HCl, then incubate in a 37^{o}C oven; for cell cultures I usually do 15min RT+15min at 37 ^{o}C)
4- Rinse 1x quickly in Boric Acid Buffer, then wash 1x10 min in Boric Acid Buffer
5- Wash 3x5-10 min in PBS
6- Block 1h at room temperature (I use 3%BSA+10% serum+0.1% Triton X100, but that is very flexible)
7- Incubate with anti-BrdU antibody O/N at 4^{o}C in a humidified chamber

Reagents
BrdU: 10 μM for culture, 50 mg/kg for live mice
Antibody: AbCam Rat anti-BrdU (# ab6326); use at 1:100

Boric Acid Buffer:
Stock A - 0.2M Boric Acid solution (7.44g in 600 ml distilled H2O)
Stock B - 0.05M Sodium Tetraborate (Borax) solution (9.5g in 500 ml distilled H2O)
Mix 550 ml Stock A + 450 ml Stock B, filter and pH to 8.4 with concentrated HCl
Notes: Borax is difficult to dissolve, so I recommend preparing that solution O/N (even warming up the solution it will take several hours).

If performing co-labeling with another antibody, I recommend doing the stainings sequentially, 1st using the other antibody (through 1ary Ab, 2ary Ab, all washes), then fixing at the end of the 1st immunostaining before starting the BrdU protocol from step 1. This will improve the quality of the non-BrdU immunostaining.

A2 In situ Hybridization

Day 1:

- Dry slides at R.T. for 10min, then fix 20min at R.T. (4% PFA)
- Wash 3x5min in DEPC-PBS
- Rinse in DEPC-H2O 3min
- Acetilation step (blocks binding of RNA probe to genomic DNA): place slides in freshly prepared acetylation solution (200ml DEPC-H2O + 3ml Triethanolamine, stirr), then add 0.5ml acetic anhydride
- Stirr 5min, then let sit another 5min
- Wash in DEPC-H2O 5min, then 3XSSC/50% formamide another 5min
- Prehybridization step: incubate slides with prehyb mix ~2h at R.T. (or at hybridization temperature if desired) in a humidified chamber containing 3XSSC/50% formamide
- Hybridization step: during the prehyb step, dilute DIG-RNA probes in hybridization mix and heat 5-10min at 70^{o}C to denature probes, then put on ice; add to slides and cover with coverslip
- Incubate 1-2 overnights at hybridization temperature (55-65 ^{o}C, depending on probe) in humidified chamber used for the prehyb step

Day 2:

- Wash 1x10min in 1xSSC/50% formamide (preheated to hybridization temperature) to remove coverslips, then 2x15min in same solution (use coplin jars for washes) in incubation oven
- Wash 2x15min in MABT at room temperature
- Block 2h at room temperature (20% sheep serum or normal goat serum + 2% Blocking Reagent in MABT)
- Incubate O/N at 4C with anti-DIG/AlkPhos antibody (Roche Cat#11 093 274 910; 1:2000 dilution)

Day 3:

- Wash 4-5x20min in MABT at room temperature
- Wash 2x10min in NTMT
- Incubate sections in staining solution (NTMT + NBT/BCIP) at 37C or room temperature (protect from light) (or use Fast Red from Roche)
- Stop reaction washing 2-3x10 min in PBS/10mM EDTA
- Mount in 90% glycerol + 10% PBS/10mM EDTA (brightfield) or AquaMount (fluorescence)

Prehybridization Mix	Stock
50% Formamide	100% Formamide (Molecular Biology grade)
5X DEPC-SSC	20X DEPC-SSC
40 ug/ml salmon sperm DNA	10mg/ml salmon sperm DNA
DEPC-H2O	

Hybridization Mix	Stock
50% Formamide	100% Formamide (Molecular Biology grade)
1X Denhardt's	50X Denhardt's (Sigma)
3X DEPC-SSC	20X DEPC-SSC
10mM DEPC-EDTA	0.5M DEPC-EDTA
10% Dextran Sulfate	50% Dextran Sulfate
0.5mg/ml yeast tRNA	10mg/ml yeast tRNA
0.5mg/ml salmon sperm DNA	10mg/ml salmon sperm DNA
DEPC-H2O	

MAB (5X)
Maleic acid 500mM
Set pH to 7.5
Add NaCl 750mM

MABT
1X MAB in H2O
Tween 0.1%

Blocking Reagent (#1 096 176, Roche)

NTMT
NaCl 100mM
Tris pH 9.5 50mM
MgCl2 100mM
Tween 20 0.1%
H2O

A3 Protein Electrophoresis and Western Blot

Protein collection

Will vary depending on source (cell culture, dissected tissue)

1) Add RIPA buffer to cells/tissue (volume will vary depending on amount of starting material)
2) Triturate using 27-gauge needle until no clumps are visible (as much as possible; can start with larger gauge needle if triturating large sample).
3) Freeze at -80^{o}C until ready to quantify protein (freezing helps tissue trituration)
4) Quantify protein content using Bradford reagent:
   a. Dilute Bradford Reagent 1:5 in ddH_20 and add 1 ml to each spectrophotometer cuvette
   b. Add 20, 17, 14, 10, 8, 4, 2 and 1 µl of a bovine serum albumin solution at 1 µg/µl (diluted in RIPA+Protease Inhibitors, just like the protein sample to be measured), or just RIPA+Protease Inhibitors for the blank.
   c. Measure absorbance of each standard dilution to make a calibration curve.
   d. Blank again and measure unknown samples in 1 ml Bradford reagent (measure 2 dilutions and average them out).

SDS-PAGE/Transfer

1) Using 7.5% Acrilamide gel (for larger proteins, higher for smaller proteins) with 15wells (15µl) of approx 0.75mm (BioRad 161-1118)
2) Add samples (10µg protein/well max) with 4x Loading Buffer after denaturating 5min@ 90ºC (Note: the sample with loading buffer can be mixed the day before and kept in freezer; protein ladder needn't be denatured, just add 5ul/well)
3) Run for about 2h at 100mV with running buffer 1x
4) Wash the gel with running buffer 1x.
5) Hydrate the PVDF membrane (0.2µm BioRad 162-0177) with MeOH
6) Assemble well the transfer system with pad, whatman, membrane, gel, whatman, pad. Gel on the **black** side
7) Transfer into a membrane at 300mA in transfer buffer (will vary;100mV is stable) for 2h in the cold room (use magnetic stir bar to circulate transfer buffer during transfer)
8) Rinse the membrane with TBS-T
9) Let it dry after hydrating again with MeOH (optional, if high background is a problem)

Immunoblot

1) Block membrane (optional 1h hydrate +) 1 hour in Blocking Buffer at room temperature or at 4ºC overnight. Incubate in primary antibody overnight at 4^{o}C in plastic pouch.
2) 3x10 minute washes in TBS-T
3) Secondary Antibody: anti-rabbit IgG HRP (1:5000) 1h at RT in plastic pouch
4) 3 x 10 minute washes TBS-T

5) HRP developing reagent (ECL, Amersham RPN2132): 2mL of solution A + 50ul of Solution B
6) Place membrane on saranwrap (or plastic cover) and cover with developing reagent freshly prepared
7) Carefully tip off reagent onto a paper towel
8) Cover membrane
9) Expose in dark for 30sec and 2 min.

Membrane Stripping

1) Rinse 2x the membrane with TBS-T.
2) Incubate with 20ml of stripping buffer in incubating chamber @ 55ºC for 30min.
3) Wash with TBS-T for 2x 10min.
4) Start next immunoblot

Running Buffer
1x SDS Running Buffer
10x 5L: 150g Tris
721g Glycine
50g SDS
add dH_20 up to 5L

Transfer Buffer (keep at 4°C, good for up to 2 weeks)
2L: 200ml 10x running buffer
400ml MeOH
1400ml dH_20

Washing Buffer
10x 5L: 170g Tris
400g NaCl
(adjust pH 7.0)
50ml Tween (add dH_20 up to 5L)

Stripping Buffer
2% SDS (5ml 10%SDS)
62.5M Tris pH6.8 (3.1ml 0.5M Tris pH6.8)
100mM BME (175µl BME; add fresh)
dH_2O (16.9ml dH_20)

Coomassie staining solution
2.50 g Coomassie Brilliant Blue R-250,
455 mL ethanol,
455 mL deionized / distilled water,
90 mL glacial acetic acid

1X RIPA Buffer (lasts long time at 4°C)
1 % Triton X100
0.1% SDS
5 mM EDTA
1% deoxycholic acid
add PBS up to final volume
Add protease inhib. immediately before use

4X Loading Buffer (one of many; store -20°C)
40% glycerol
9.2% SDS
20% BME
0.04% bromophenol blue
160 mM Tris pH 6.8

Blocking Buffer
50ml 1xTBS-T
2.5g Carnation Milk

Coomassie destaining solution
455 mL ethanol,
455 mL deionized / distilled water,
90 mL glacial acetic acid
(Can also be destained using only distilled water and heating, though at a much slower pace)

A4 Fluorescent TUNEL Labeling

1- Air-dry cryostat sections 10 min room temperature (RT)
2- Fix 20 min RT in 4% PFA
3- Wash 3x10 min in PBS
4- Transfer slides to Citrate buffer (trisodium salt citric acid 0.1M, pH 6.0 in H_20)
5- Microwave on high ~45 seconds, then cool rapidly on ice and adding H_20
6- Transfer slides to PBS
7- Block 30 min at RT (3% bovine serum albumin+20% normal goat serum in 0.1M Tris, pH 7.5)
8- Wash 2x5 min in PBS
9- Add TUNEL labeling mix to slides 1h at 37^{o}C in humidified chamber
10- Wash 3x10 min in PBS
11- Counterstain with DAPI and coverslip

TUNEL reagents from Roche kit Cat. #12 156 792 910
Always include negative and positive controls (see kit for details)

A5 Multiplex Single Cell RT-PCR

1- Put single cells into 9 ul DNAase solution, freeze immediately

DNAase Solution (per tube)

RNAsin	0.45 ul
DNAaseI, RNAase-free (10 U/ul)	0.018 ul
DTT	0.9 ul
DEPC-H_20	7.632 ul

2- Heat-inactivate DNAaseI 10 min at 94^{o}C (start from frozen samples, DNAaseI will digest genomic DNA while temperature rises, then becomes inactivated before degrading RNA; cells are lysed by osmotic shock in DNAase solution)

3- Run RT and 1st PCR reaction in same tube. During step 2, make RT-PCR mix, then add 40 ul of this mix to each tube containing cell and inactivated DNAaseI from step 2

RT-PCR Mix (per tube)

H_20	8 ul
2X Reaction Mix	25 ul
Primer Mix	6 ul (should not exceed 300 ng total; see below)
RT/Taq Mix	1 ul (OneStep Superscript II / Platinum Taq)
Template RNA	10 ul (from step 2)

(**Note:** Primer mix is a mix of all primers from all the genes to be analyzed; these are the "outside" primers in the multiplex PCR reaction. Because all primers are added together, the total amount/primer/reaction will vary depending on how many primer pairs are being used. No more than 300 ng total of primers should be added/reaction.)

RT-PCR Program

1. 42^{o}C	50 min
2. 94^{o}C	30 sec
3. 55^{o}C	30 sec
4. 72^{o}C	1.5 min
5. Back to step 2. (40 cycles total)	
6. 72^{o}C	5 min
7. 4^{o}C	Forever

4- Run 2nd PCR: use 2 ul of the RT-PCR reaction from step 3 to start new PCR using nested ("inside") primers. This time, 1 primer pair/reaction is used.

2nd PCR Mix (per tube)

H_20	39.3 ul
10X Buffer	5 ul
50mM MgCl2	1.5 ul
10mM dNTP mix	1 ul
Primer pair mix	1 ul (10 uM Fwd and Rev primer each, 1 gene/rx only)
Platinum Taq	0.2 ul
Template DNA	2 ul (from step 3)

2nd PCR Program

1. 94°C 5 min
2. 94°C 30 sec
3. 55°C 30 sec
4. 72°C 1.5 min
5. Back to step 2. (30 cycles total)
6. 72°C 10 min
7. 4°C Forever

A6 Single Cell RT-PCR With RNA Amplification

Cell Collection

- Make Cell Lysis buffer

Cell Lysis Buffer	**Vol/PCR tube**
H2O	2.75µl
5x 1st Strand Buffer	1µl
DTT (0.1M)	0.5µl
RNAsin (40U/µl)	0.25µl
NP40 (5%)	0.5µl
Total	5µl

- Dissect mouse tissue of interest and digest with Papain
- Remove Papain and triturate to single cell suspension in 1ml serum-containing medium
- Put cells through 22% Percoll (150mm radius, 500xg for 8min, accelerate 2, brake 0)
- Remove supernatant, ressuspend in medium suitable for FACS, add Propidium Iodide
- FACS-sort cell(s) into 5µl Cell Lysis buffer, agitate, centrifuge, keep on ice

1st Strand Synthesis (Round 1) *RNA-AMP1*

- Add all RT reagents to each tube (except enzymes) to a final volume of 9.25µl (5µl sample + 4.25µl RT reagents)

1st Strand Mix (Round 1)	**Vol/PCR tube**
H2O	1.75µl
5x 1st Strand buffer	1µl
DTT (0.1M)	0.5µl
SMART III Primer (100µM)	0.1µl
T7LD3' Primer (5µM stock)	0.4µl
dNTP Mix (10mM)	0.5µl
Total	4.25µl
RNAsin (40U/µl)	*a posteriori* (0.25µl)
PowerScript RT Enzyme	*a posteriori* (0.5µl)

- Heat 5min at 70°C, then 2min on ice, then 3min at 55°C, then slowly drop temperature (0.15°C/s) to 37°C. Keep at 37°C for 2min, then 42°C for 5min
- Add 0.25µl RNAsin (or 0.5µl if previous one is dead) + 0.5µl PowerScript RT enzyme (Clontech) (make a mix of both for all tubes) and incubate 1h at 42°C
- Add 0.4µl RNaseH/tube (1.5U/µl stock), incubate 10min at 37°C

2nd Strand Synthesis *RNA-AMP2*

- Use all 1st Strand product as template for this step: add 40µl PCR Mix to 10µl cDNA

2nd Strand PCR Mix	**Vol/PCR tube**
cDNA (from previous step)	(10µl)
H2O	32.8µl
10x Advantage 2 PCR Buffer	5µl
dNTP Mix (10mM)	1µl

5' PCR primer (100µM)	0.1µl
3' PCR primer (100µM)	0.1µl
Advantage 2 Polymerase Mix	1µl
Total	50µl

- Run PCR reaction as follows:

Temp.	**Time**
95°C	5min
95°C	15sec
68°C	6min
Back to step 2	19x
68°C	6min
4°C	Storage
End	(20 cycles total)

(protocol can be paused after this step)

ds-cDNA Purification *RNA-AMP3*

- DNA blunting: add 0.75ul T4 DNA Polymerase (Promega, 8U/ul; dilute 4x to 2U/ul) and incubate 15min at 37°C, then add 0.25ul mung bean nuclease (Promega, 95U/ul; dilute 20x to 4.75U/ul) + 5.1ul 10x mung bean buffer and incubate 15min at 37°C
- Add 50ul Proteinase K Solution [0.5ul Proteinase K (Roche, dilute 10x to 2ug/ul) + 50ul of 100mM Tris pH 8, 0.4% SDS, 20mM EDTA] to 50ul cDNA sample (final vol: 100ul at 50mM Tris pH 8, 0.2% SDS, 10mM EDTA). Incubate 15min at 55°C
- Assemble Micropure-EZ/Microcon YM-100 columns together (Millipore), dilute sample with DEPC-H2O to 250ul (max capacity of Micropure-EZ) and load all sample into Micropure-EZ enzyme removal column.
- Spin 15min at 500xg (room temp.) in a tabletop microcentrifuge. Discard flowthrough, add 500ul DEPC-H2O (max capacity of Microcon) and repeat spin 2x. After 3rd wash, invert column into new tube and spin 3 min at 1000xg (room temp.) to recover DNA (recovery volume depends on initial volume, temperature and spin time; aim for ~8ul)

aRNA Synthesis *RNA-AMP4*

- T7 Megascript kit: prepare a 20ul reaction using all the purified ds-cDNA from previous step (Keep reaction mix at RT to avoid precipitation of DNA with Reaction Buffer components). Incubate 5h at 37°C

Megascript Kit Component Mix	**Vol/PCR tube**
ATP Solution	2ul
CTP Solution	2ul
GTP Solution	2ul
UTP Solution	2ul
10x Reaction Buffer (keep at RT after thaw)	2ul
Enzyme Mix	2ul
(Ds-cDNA Template)	(8ul)
Total	20ul

aRNA Purification

- Dilute sample to larger volume in DEPC-H2O and Phenol/Chloroform extract twice
- Dilute sample to 500ul max with DEPC-H2O. Load all sample into Microcon YM-100 column and spin 15min at 500xg (room temp.) in a tabletop microcentrifuge.
- Discard flowthrough, add 500ul DEPC-H2O and repeat spin 2x to desalt. After 3rd wash, invert column into new tube and spin 3 min at 1000xg (room temp.) to recover RNA (recovery volume depends on initial volume, temperature and spin time; aim for ~10ul)

1st Strand Synthesis (Round 2) *RNA-AMP5*

- Use PowerScript RT again, but with random hexamers as primers. Add all reagents (minus enzymes) to each aRNA sample in PCR tubes. Denature 3min at 70°C, then put on ice. Add RNAsin and PowerScript RT enzymes, keep at room temp. 3 min, then incubate 1h at 42°C. Heat-inactivate the enzyme 10min at 95°C

1st Strand Mix (Round 2)	**Vol/PCR tube**
H2O	-
5x 1st Strand buffer	4ul
DTT (0.1M)	2ul
Random hexamers (Amersham, 1ug/ul)	0.1ul
dNTP Mix (10mM)	2ul
(aRNA template)	(10ul)
RNAsin (40U/µl)	*a posteriori* (1ul)
PowerScript RT Enzyme	*a posteriori* (1ul)
Total	20ul

- The sample is now ready for TaqMan PCR analysis

Primer Sequences

T7LD3′:
ATTCTAGAGGCCGAGGCGGCCGACATGTAATACGACTCACTATAGGGCG$(T)_{30}$VN
(V = A,G,C; N = A,G,C,T)
SMART III: AAGCAGTGGTATCAACGCAGAGTGGCCATTATGGCCGGG
5′PCR: AAGCAGTGGTATCAACGCAGAGTGGCCATTATGG
3′PCR: ATTCTAGAGGCCGAGGCGGCCGACATGTAATACGACTCACTATAGGGC

A7 RNA Isolation with Trizol Reagent

1- Homogenize dissected SVZ tissue in 1 ml of Trizol (Gibco, Cat. #15596-026) for every 50-100 mg of tissue by repeatedly aspirating through a small gauge needle and syringe.
2- Incubate the homogenized sample at room temperature for 5 min. to permit complete dissociation of nucleoprotein complexes. Add 2 ml chloroform, close tube and shake vigorously by hand for 15 sec. Incubate at room temperature for 2-3 min. Centrifuge samples at no more than 12000xg for 15 min. at 2-8^{o}C.
3- After centrifugation, the mixture separates into 3 phases. The RNA will be in the upper, aqueous phase (60% of the volume of the initial amount of Trizol used/tube). Collect upper aqueous phase into new tube.
4- Precipitate RNA mixing with isopropanol (0.5 ml for every 1 ml Trizol initially used). Incubate at room temperature for 10 min. Centrifuge samples at no more than 12000xg for 10 min. at 2-8^{o}C. The RNA will form a gel-like pellet at the bottom of the tube.
5- Remove the supernatant and wash the pellet once with 75% EtOH (1ml for 1 ml of Trizol initially used). Vortex sample and centrifuge at no more than 7500xg for 5 min. at 2-8^{o}C.
6- Remove supernatant and air-dry or vacuum-dry RNA pellet for 5-10 min. Do not use centrifuge under vaccum to dry and do not over-dry as this significantly reduces RNA solubility (partially-dissolved RNA samples have a A260/280 ratio <1.6).
7- Dissolve RNA in RNAase-free DEPC-treated water or 0.5% SDS solution (avoid SDS if using RNA for enzymatic reaction) by passing liquid through a pipette several times and incubating 10 min. at 55-60^{o}C. Store at -80 ^{o}C. For long-term storage, RNA can be dissolved in 100% Formamide at -80 ^{o}C.

A8 Beta-Galactosidase staining

1- Cut 50 μm sections (or 100-200 μm for electron microscopy) on vibratome
2- Collect into PBS (or PB for EM)
3- Transfer sections to X-Gal buffer
   A. 100 μl $MgCl_2$ (1M stock)
   B. 2.5 ml K3 Solution (1.646g K+Ferricyanide/50ml 0.1M PB; store at RT for months)
   C. 2.5 ml K4 Solution (2.112g K+Ferrocyanide/50ml 0.1M PB; store at RT for months)
   D. 0.6 ml X-Gal Solution (40mg X-Gal/1m dimethylformamide; store at -20^{o}C)
   E. Bring volume up to 50 ml with 0.1M PB

4- Incubate tissue in X-Gal buffer at 37^{o}C in the dark
5- Monitor staining (varies depending on tissue, can take minutes, hours, days)
6- Stop reaction washing with PB or PBS
7- Mount sections onto slides

A9 EM Inclusion for Pre-embedding Beta-Galactosidase Staining

Perfusion:

1. Prepare 500 ml of 2.5% Gluta / 2% Para (good for 3-4 weeks @ 4°C)
   Mix 10g paraformaldehyde in 200 ml DH_2O
   Heat mixture to ≤ 59°C with constant stirring
   Add 10N NaOH (no more than 3-4 drops) until para is completely dissolved
   Add 50 ml 0.2M monobasic PB
   Add 200 ml 0.2M dibasic PB
   Add 50 ml of 25% glutaraldehyde
2. Prepare 500 ml of 2.5% Gluta (good for 3-4 weeks @ 4°C)
   200 ml DH_2O
   50 ml 0.2M monobasic PB
   200 ml 0.2M dibasic PB
   50 ml of 25% glutaraldehyde
3. Infuse 0.9% saline with 1% heparine (RT) until drip clears
4. Infuse fixative (RT) for 5-10 min.
5. Decapitate
6. Postfix entire head for 30 min in 2.5% Gluta / 2% Para @ 4°C
7. Extract brain and postfix overnight in 2.5% Gluta @ 4°C

Cutting:

1. Rinse in PB (5×10 min) @ 4°C
2. Cut 50 μm slices into PB (use very clean glassware)
3. Perform β-Gal reaction (see Appendix A9 for details)
4. Store sections in PB in clean glass vial @ 4°C (Good for one week.)

Inclusion:

Prepare 1% Osmium (OsO_4) with 7% glucose in 0.1M PB. Keep in dark @ RT.
   0.25 ml 4% osmium
   0.50 ml 0.2M PB
   0.25 ml H_2O
   0.07 g glucose

8. Prepare maleic Acid (Good for 1 month @ 4°C)
   Component A recipe
      12.1 g TRIS
      11.6 g maleic acid
      500 ml DH_2O
   Component B recipe
      0.8 g NaOH
      100 ml DH_2O
   Mix 25 ml of component A + 27 ml component B + 48 ml DH_2O
   pH to 7.4 with HCl
9. Rinse sections in PB (2×10 min)
10. Transfer sections to OsO_4 for 1-2 hr in dark @ RT

11. Remove sections from OsO_4 when solution is wine-colored
12. Rinse in maleic acid @ 4°C (3×15 min)
13. While sections are rinsing, prepare araldite (Good for 2 weeks @ 4°C)
    Place 10 ml of araldite component A/M into a new specimen cup
    Add 10 ml of component B and shake well
    Add 0.4 ml of component D (stored @ 4°C) and shake well
    Add 0.4 ml of component C (stored @ 4°C) and shake well
    Place in vacuum chamber to remove air bubbles
14. Prepare 2% uranyl acetate (UA) in maleic acid (Good for 4 hr @ 4°C)
    Sonicate to mix and place immediately in 4°C
15. Incubate in maleic acid + 2% UA for 2.5-3.5 hr @ 4°C
16. While sections are rinsing, prepare aluminum foil cups.
17. While sections are rinsing, place araldite in foil cups on shaker for 1 hr.
    A. Place foil cups in plastic tissue dish
    B. Cover
    C. Check for leaks
18. Rinse in maleic acid @ 4°C (3×10 min)
19. Rinse sections in 25% EtOH for 5 min @ 4°C
20. Rinse sections in 50% EtOH for 5 min @ 4°C
21. Rinse sections in 70% EtOH for 5 min @ 4°C
22. Rinse sections in 95% EtOH (3×5 min @ 4°C)
23. Rinse sections in 100% EtOH (3×10 min @ 4°C)
24. Rinse sections in propylene oxide (2×2 min. @ RT)
25. Transfer sections to araldite on shaker overnight @ RT.
26. Prepare acetate "molds" for embedding

<u>Embedding:</u>

1. Put foil cups on slide warmer (5 min. @ 60°C)
2. Let araldite get runny
3. Put sections in acetate molds and cover in fresh araldite
4. Cover with acetate and place in over (60°C) for 2 hr
5. Place weight on top of molds
6. Let cook in oven for 3 days

A10 Tail DNA Extraction and PCR Genotyping

Tail DNA Extraction

1- Cut tip of tail with scissors (very small amount necessary) and place in eppendorf tube.
2- At this point, perform X-Gal staining or use fluorescent lamp to detect GFP, if necessary, before moving on to the next step.
3- Add 100 µl NaOH solution and 2 small drops of mineral oil.
4- Spin down tubes and heat at 100°C for 30-45 minutes.
5- Add 100 µl of Tris solution to neutralize NaOH solution, vortex briefly and spin down tube contents.
6- Use 1-2 µl for PCR reaction.

Note: this protocol is a fast and simple method to obtain DNA for PCR genotyping and works for most genotyping reactions, but it does not yield high quality, "clean" DNA. For some PCR reactions, a different protocol may be necessary to obtain better quality samples.

NaOH Solution
25 mM NaOH (0.1 g NaOH pellets)
2 mM EDTA (0.4 ml EDTA 0.5M)
Add H_20 to 100 ml

Tris Solution
40 mM Tris-HCl (pH 7.5-8.0)

PCR Genotyping

PCR Mix		*PCR (n2/C7/C8 primers)*	*PCR (Tau primers)*
H2O	13.4 µl	1- 94°C, 5 min	1- 94°C, 5 min
Buffer (10X)	2.0 µl	2- 94°C, 1 min	2- 94°C, 1 min
MgCl2 (25 mM)	2.0 µl	3- 55°C, 1.5 min	3- 63°C, 1.5 min
dNTP mix (10 mM)	0.4 µl	4- 72°C, 1.5 min	4- 72°C, 1.5 min
Fwd Primer (100 µM)	0.04 µl	5- Go to step 2 (39x)	5- Go to step 2 (34x)
Rev Primer (100 µM)	0.04 µl	6- 72°C, 7 min	6- 72°C, 7 min
AmpliTaq Gold	0.12 µl	7- 4°C, Forever	7- 4°C, Forever
Tail DNA	2.0 µl	8- End	8- End
Total vol.	20 µl		

A11 Alkaline Phosphatase Staining

Tissue preparation

1- Cut 50 μm sections (or 100-200 μm for electron microscopy) on vibratome.
2- Collect into PBS (or PB for EM).
3- Heat sections at 65^{o}C in oven for 1-1.5h to inactivate endogenous AP enzyme.
4- Change PBS solution to wash and cool sections.

Tissue staining

5- Transfer sections to AP buffer 10 min. at room temperature.
6- Incubate in active AP buffer in the dark at room temperature
7- Monitor staining (could take minutes/hours/overnight)
8- Stop reaction washing with PBS/EDTA (10 mM), counterstain (DAPI) and mount sections on slide; store in dark at 4^{o}C.

AP Buffer
100 mM $MgCl_2$
100 mM Tris pH 9.5
100 mM NaCl
Add H_20, pH to 9.5

Active AP Buffer
AP buffer
Add NBT/BCIP (Roche, #11681451001)
immediately before use

Note: The amount of $MgCl_2$ significantly changes the speed of the staining. Some people use 50 mM or even 5 mM $MgCl_2$, but I get good results with 100 mM $MgCl_2$, which is also faster.

A12 Microosmotic Pump Implant Surgery

Pump preparation

1- Assemble and fill pump at least 6h before surgery (usually the night before)
2- Cut pump cannula to desired length with electric saw
3- Cut plastic tube to 2.5 cm (mice) or 4 cm (rats) so that pump ends up between shoulder blades.
4- Insert piece containing cannula into one end of the plastic tube and the metal rod into the other end
5- Slowly fill pump reservoir with desired solution using a special needle leaving small drop of liquid protruding from top of pump.
6- Slowly fill plastic tube and attachments with desired solution (no bubbles should remain in the tube, though small bubbles usually do not prevent flow; vehicle solution is usually sterile 0.9% saline supplemented with 0.1% bovine serum albumin to prevent infused proteins from sticking to the inner tubing and metal of the pump).
7- Insert metal rod into pump reservoir.
8- Place entire device in sterile-filtered 0.9% saline solution at 37^{o}C (pump should be assembled and incubated at least 6h before surgery; usually this is done the night before the surgery)

Anesthesia and preparation

9- Weigh mouse or rat.
10- Inject anesthetic according to animal weight and species (will work for 30-45 min).
Mouse: Avertin (Tribromoethanol, 200-300 µg/g)
Rat: Ketamine (100 µg/g)/Xylazine (10 µg/g)
11- Wait ~5 minutes and check eyelid (reaction to touching eye) and pedal reflex (pinch paw); proceed only after animal no longer exhibits these reflexes (5-10 min.).
12- Shave top of head with electric shaver (from behind the ears to betweent the eyes).

Surgery

13- Secure animal's head between stereotaxic apparatus ear bars, placing them inside the ear canal and tightening just enough (head should feel stable, ear lobes symmetrical; for mice, a low popping sound from the eardrums is usually heard when ear bars are well placed)
14- Place animal's upper incisor teeth through the mouth-piece, making sure that the top of the head is leveled (parallel to the table).
15- Sterilize shaved area of the head (EtOH and Q-tips).
16- Make incision through the midline with scalpel blade (from between the eyes to behind the ears).
17- Remove all remaining membranes from the top of the skull with Q-tips and scraping.
18- Place "dummy" cannula on cannula holder held by stereotaxic apparatus vertically/directly over animal's head
19- Find Bregma, mark it with a needle tip and set all coordinates to zero over Bregma.
20- Move "dummy" cannula to the desired coordinates and mark location on skull.
21- Raise "dummy" cannula and drill skull until brain surface is visible or nearly visible.
22- Clear hole from remaining pieces of skull.

23- Insert scissors under skin, through back of head incision to form a space where the pump will be placed.
24- Insert pump reservoir under the skin on the animal's back until cannula is over the drilled hole.
25- Place pump cannula on cannula holder and re-zero at Bregma (often necessary).
26- Move cannula to the desired coordinates and lower slowly into brain until the base of the cannula is tightly pressed against skull.
27- Place dental cement all around base of cannula (the plastic grooved part).
28- When cement is dry, cut top peg of plastic cannula off with a hot scalpel blade.
29- Suture (mice) or staple (rats) incision over cannula and sterilize with Betadine.

Post-Surgery
30- Remove animal from stereotaxic apparatus.
31- Weigh animal once again and record that weight.
32- Inject analgesic intraperitoneally (Buprenorphine, 0.05-0.1 μg/g for mice, or 0.01-0.05 μg/g for rats) and return animal to cage.
33- Keep animal warm with latex glove filled with warm water and provide water and food inside cage. Monitor regularly over next 1-2 h.

Note: Cell transplantation (see Appendix A14 for details) and virus injections into adult mice/rats are similar, with the exception of points 1-8, 18, 23, 27, 28. All points using cannula holder are identical, but using the glass pipettes containing the cells/virus. Glass pipettes were made with a vertical pipette puller, then grinding the tip to make a bevelled opening (100 μl Drummond Wiretrol glass capillaries open to 100 μm diameter for cell delivery; 5 μl Drummond Wiretrol glass capillaries open to 20-40 μm for virus delivery).

A13 Fluorescence Immunohistochemistry

1- Air-dry slides 10 min. at room temperature (cryosections only, for vibratome sections proceed directly to step 4).
2- Post-fix cryosections on slide 10 min. with cold 4% paraformaldehyde.
3- Wash 3x5 min. in PBS.
4- Block sections in 3% bovine serum albumin + 10% normal serum (goat or donkey) + 0.1% Triton X100 (omit for certain antigens), 1h at room temperature.
5- Incubate sections overnight at 4^{o}C in 1^{ary} antibody diluted in block.
6- Wash 5x8 min. in PBS.
7- Incubate sections 1 hour at room temperature in 2^{ary} antibody diluted in block.
8- Wash 5x8 min. in PBS.
9- Incubate sections 1 hour at room temperature in Streptavidin/fluorophore conjugate diluted in block (optional, only when using a biotinilated 2^{ary} antibody for amplification).
10- Wash 5x8 min. in PBS.
11- Counterstain with DAPI (use at 100 ng/ml).
12- Check fluorescence staining under microscope, then coverslip with anti-fading mounting medium.
13- Store at 4^{o}C in the dark.

A14 Cell transplantation surgery

Injection pipet set up:
Pipette-puller set on 47/47 solenoid/heater – seems to change daily, so adjust accordingly.
Pipette used – 100 µl Drummond Wiretrol capillaries.
Pipette Goal: 1. 100 µm width (50µm also works, but has higher chance of clogging).
2. Pipet should taper quickly and have a long point.
3. Relatively short total length.
Wet the spin-plate with water and a little soap to clean. Mount injection pipet onto the stereotaxic holder and lower it until it touches the plate. Check under microscope to see opening size.

Genotyping and Dissection:
1- Cut tails of P0 newborn mice in the morning, labeling them with a pen.
2- Check for GFP and extract DNA.
3- Run genotyping PCR for TrkB locus.
4- Select TrkB-WT/GFP$^+$ and TrkB-KO/GFP$^+$ pups (usually I do it the day after PCR).
5- Collect brain and dissect SVZ into L15 Leibowitz medium on ice
6- Triturate SVZ from each dissected animal in eppendorf tube with 300 µl medium with DNAase solution using an L200 micropipette tip (aspirate ~20x until no clumps are visible).
7- Spin down cells (3 min. at 2000 rpm) and ressuspend in 5 µl.
8- Keep cells on ice until ready to do the graft (same day, the faster the better).

Surgical stage set up:
The stereotaxic stage should be at 90deg angle to the injection needle. Slide injection setup forward or backward to place the needle directly above the mouse brain.

Pipet fill:
1- Back-fill the pipet with a lot of mineral oil. Keep the pipet horizontal so there is always some oil at the back tip of the pipet. Tip the pipet back (with the back end down), so that some of the oil leaks out. Place the plunger in at an angle with ample oil surrounding it to prevent bubbles from forming during insertion. Insert plunger and push in until some of the oil comes out the pointed tip.
2- Make sure the injector is about half-way through the dial to give some room for releasing as well as aspirating.
3- Mount pipet onto stage and make sure the white holder for the plunger is a few mm above the back end of the pipet (prevents the plunger holder from pushing down on the whole pipet instead of just the plunger)
4- Fill tip with a little PBS to buffer between oil and cells. Pull up slowly to prevent bubbles.

Surgery:
1- Inject anesthetic according to mouse weight [Avertin (Tribromoethanol), 200-300 µg/g; will work for 30-45 min].
2- Load pipet with 5ul of cells.

3- Wait ~5 minutes and check eyelid (reaction to touching eye) and pedal reflex (pinch paw); proceed only after animal no longer exhibits these reflexes (5-10 min.).
4- Shave top of head with electric shaver (from behind the ears to betweent the eyes).
5- Secure animal's head between stereotaxic apparatus ear bars, placing them inside the ear canal and tightening just enough (head should feel stable, ear lobes symmetrical; a low popping sound from the eardrums is usually heard when ear bars are well placed)
6- Place animal's upper incisor teeth through the mouth-piece, making sure that the top of the head is leveled (parallel to the table).
7- Sterilize shaved area of the head (EtOH and Q-tips).
8- Make incision through the midline with scalpel blade (from between the eyes to behind the ears).
9- Remove all remaining membranes from the top of the skull with Q-tips and scraping.
10- Bring glass needle over mouse's head.
11- Find Bregma, mark it and set all coordinates to zero over Bregma.
12- Move needle to the desired coordinates and mark locations on skull.
13- Raise glass needle and drill skull until brain surface is visible or nearly visible.
14- Clear hole from remaining pieces of skull.
15- Re-zero needle at Bregma (often necessary).
16- Move needle to desired locations, zero depth coordinate at brain surface and lower to desired depth.
17- Inject cells slowly, checking that the meniscus is moving, wait and pull up needle.
18- Suture incision.

<u>Post-Surgery</u>
19- Remove animal from stereotaxic apparatus.
20- Weigh animal and record that weight.
21- Inject analgesic intraperitoneally (Buprenorphine, 0.05-0.1 µg/g for mice, or 0.01-0.05 µg/g for rats) and return animal to cage.
22- Keep animal warm with latex glove filled with warm water and provide water and food inside cage. Monitor regularly over next 1-2 h.

<u>Coordinates:</u>
1. 0.5mm Anterior to bregma, 1.1mm lateral, 1.7mm depth from brain surface
2. 1.0mm Anterior to bregma, 1.0mm lateral, 2.3 mm depth from brain surface
Make bilateral injections. Load new cells for each new mouse.